

2019

Improving Group Integrity of Tags in RFID Systems

Alkanhel, Reem

<http://hdl.handle.net/10026.1/15242>

<http://dx.doi.org/10.24382/1089>

University of Plymouth

All content in PEARL is protected by copyright law. Author manuscripts are made available in accordance with publisher policies. Please cite only the published version using the details provided on the item record or document. In the absence of an open licence (e.g. Creative Commons), permissions for further reuse of content should be sought from the publisher or author.

COPYRIGHT STATEMENT

This copy of the thesis has been supplied on condition that anyone who consults it is understood to recognise that its copyright rests with its author and that no quotation from the thesis and no information derived from it may be published without the author's prior consent.



UNIVERSITY OF
PLYMOUTH

Improving Group Integrity of Tags in RFID Systems

by

Reem Ibrahim AlKanhel

A thesis submitted to the University of Plymouth

in partial fulfilment for the degree of

DOCTOR OF PHILOSOPHY

School of Engineering, Computing and Mathematics

December 2019

Acknowledgements

I would like to express my deep and sincere gratitude to my Director of Studies, Dr. Marcel Adrian Ambroze. His professionalism, experience, logical way of thinking, and guidance has been invaluable during the course of my PhD.

I would also like to express my sincere gratitude to my other supervisors, Prof. Ingo Stengel, and Prof. Nathan Clarke, for their excellent advices, proof reading, and constructive comments that have been very useful to this study.

My thanks also go to Dr Jalal Almuhtadi for his advice during the course of my PhD.

Many thanks go to Ubaid Fayaz for his efforts with Matlab implementations.

Special thanks to my husband for all his advice, guidance and sacrifices that he has made. Without him, I will not be able to reach this far.

Special thanks also go to my best friend Eatedal for her support.

A great deal of appreciation goes to my beloved family members-my mother, daughters, son, sisters, and brothers for their love and support over the years. I am grateful that these people had faith in me and my abilities and have always been by my side throughout my studies.

Author's Declaration

At no time during the registration for the degree of Doctor of Philosophy has the author been registered for any other University award without prior agreement of the Doctoral College Quality Sub-Committee.

Work submitted for this research degree at the University of Plymouth has not formed part of any other degree either at the University of Plymouth or at another establishment.

This study was financed with the aid of a scholarship from Princess Nourah bint Abdulrahman University at the Kingdom of Saudi Arabia.

Relevant scientific seminars and conferences were attended at which work was often presented and several papers were published and prepared for publication.

Word count of main body of thesis: 48009 words

Signed:Reem.....

Date:1/12/2019.....

Abstract

Improving Group Integrity of Tags in RFID Systems

Reem Ibrahim AlKanhel

Checking the integrity of groups containing radio frequency identification (RFID) tagged objects or recovering the tag identifiers of missing objects is important in many activities. Several autonomous checking methods have been proposed for increasing the capability of recovering missing tag identifiers without external systems. This has been achieved by treating a group of tag identifiers (IDs) as packet symbols encoded and decoded in a way similar to that in binary erasure channels (BECs). Redundant data are required to be written into the limited memory space of RFID tags in order to enable the decoding process. In this thesis, the group integrity of passive tags in RFID systems is specifically targeted, with novel mechanisms being proposed to improve upon the current state of the art.

Due to the sparseness property of low density parity check (LDPC) codes and the mitigation of the progressive edge-growth (PEG) method for short cycles, the research is begun with the use of the PEG method in RFID systems to construct the parity check matrix of LDPC codes in order to increase the recovery capabilities with reduced memory consumption. It is shown that the PEG-based method achieves significant recovery enhancements compared to other methods with the same or less memory overheads. The decoding complexity of the PEG-based LDPC codes is optimised using an improved hybrid iterative/Gaussian decoding algorithm which includes an early stopping criterion. The relative complexities of the improved algorithm are extensively analysed and evaluated, both in terms of decoding time and the number of operations required. It is demonstrated that the improved algorithm considerably reduces the operational complexity and thus the time of the full Gaussian decoding algorithm for small to medium amounts of missing tags.

The joint use of the two decoding components is also adapted in order to avoid the iterative decoding when the missing amount is larger than a threshold. The optimum value of the threshold value is investigated through empirical analysis. It is shown that the adaptive algorithm is very efficient in decreasing the average decoding time of the improved algorithm for large amounts of missing tags where the iterative decoding fails to recover any missing tag. The recovery performances of various short-length irregular PEG-based LDPC codes constructed with different variable degree sequences are analysed and evaluated. It is demonstrated that the irregular codes exhibit significant recovery enhancements compared to

the regular ones in the region where the iterative decoding is successful. However, their performances are degraded in the region where the iterative decoding can recover some missing tags.

Finally, a novel protocol called the Redundant Information Collection (RIC) protocol is designed to filter and collect redundant tag information. It is based on a Bloom filter (BF) that efficiently filters the redundant tag information at the tag's side, thereby considerably decreasing the communication cost and consequently, the collection time. It is shown that the novel protocol outperforms existing possible solutions by saving from 37% to 84% of the collection time, which is nearly four times the lower bound. This characteristic makes the RIC protocol a promising candidate for collecting redundant tag information in the group integrity of tags in RFID systems and other similar ones.

Table of Contents

List of Figures	xi
List of Tables	xiv
List of Algorithms	xv
List of Acronyms	xvi
1 Introduction and Overview	1
1.1 Introduction	1
1.2 Aims and Objectives	7
1.3 Contributions to Knowledge	8
1.4 Methodology	10
2 An Overview of Group Integrity Methods in RFID Systems	12
2.1 Literature Review	12
2.2 Conclusions	20
3 RFID Systems	21
3.1 RFID System Components.....	21
3.1.1 RFID Tags	22
3.1.1.1 Types of RFID Tags	22
3.1.1.2 Types of Memory in RFID Tags	23
3.1.1.3 Classes of RFID Tags.....	25
3.1.2 RFID Readers	26
3.2 RFID Standards	27
3.3 Operating Frequencies.....	28
3.4 Data Coding.....	29
3.5 Multi-access Procedures (Anti-collision).....	30
3.5.1 Space Division Multiple Access Technique	30
3.5.2 Frequency Division Multiple Access Technique.....	31

3.5.3	Code Division Multiple Access Technique	31
3.5.4	Time Division Multiple Access Technique	31
3.5.4.1	Aloha-based Protocols.....	32
3.5.4.2	Tree-based Protocols	38
3.6	Conclusions	41
4	LDPC Codes.....	43
4.1	Preliminaries and Notations	44
4.2	Encoding Process	47
4.3	Decoding Algorithms	50
4.3.1	Iterative Decoding Algorithms	52
4.3.2	Maximum Likelihood Decoding Algorithms	54
4.3.3	Reduced Complexity Decoding Algorithms.....	57
4.4	Construction Methods for LDPC Codes	59
4.4.1	Random Constructions	59
4.4.1.1	Gallager Codes	59
4.4.1.2	MacKay Codes	61
4.4.1.3	Progressive Edge Growth (PEG) Methods	61
4.4.1.4	Approximate Cycle Extrinsic Message Degree (ACE) Methods.....	63
4.4.2	Algebraic Constructions	64
4.4.2.1	Quasi-Cyclic Codes.....	64
4.4.2.2	Euclidean Geometry Codes.....	65
4.4.2.3	Chinese Remainder Theorem (CRT) Methods.....	66
4.4.3	Main Comparisons of Construction Methods.....	67
4.5	Conclusions	68
5	Extended Grouping of RFID Tags Based on PEG Methods	70
5.1	System Model.....	70
5.2	Encoding Process	70
5.3	Decoding Process	72
5.4	Performance Evaluation	74
5.4.1	Using the GE and IT Decoding Algorithms	75
5.4.2	PEG-based vs CRT-based LDPC Codes	83

5.4.3	PEG-based vs ACE-based LDPC Codes	85
5.5	Conclusions	86
6	Improved Hybrid IT/GE Decoding Algorithm	87
6.1	Early Termination of the IT Decoding Algorithm	87
6.2	Missing Recovery Capability Analysis	92
6.3	Decoding Complexity Analysis	93
6.3.1	Decoding Time Analysis	93
6.3.2	Operational Complexity Analysis	97
6.3.2.1	IT Decoding Algorithm Analysis	97
6.3.2.2	GE Decoding Algorithm Analysis	97
6.3.2.3	Improved Hybrid Decoding Algorithm Analysis	99
6.4	Conclusions	101
7	Adaptive Hybrid Decoding Algorithm	103
7.1	Threshold Analysis	103
7.2	Irregular PEG-based LDPC Codes	106
7.3	Conclusions	112
8	Bloom Filters	114
8.1	Preliminaries of Bloom Filters	114
8.2	Bloom Filter Features	118
8.3	Bloom Filter Limitations	119
8.4	Bloom Filter Variants	120
8.4.1	Counting Bloom Filters	120
8.4.2	<i>d</i> -Left Counting Bloom Filters	121
8.4.3	Space Code Bloom Filters	122
8.4.4	Scalable Bloom Filters	122
8.4.5	Weighted Bloom Filters	123
8.5	Applications of Bloom Filters	123
8.5.1	Filtering Duplicate Data from RFID Data Streams	125
8.6	Conclusions	129

9	Efficient Redundant Information Collection Protocol.....	131
9.1	Tag Information Collection Protocols.....	132
9.2	System Model and Problem Statement	136
9.3	Performance Lower Bound	137
9.4	Possible Solutions	137
9.4.1	Baseline Collection Protocol	138
9.4.2	ID Collection Protocol.....	138
9.4.3	Multi-Hash Information Collection Protocol	139
9.5	Redundant Information Collection Protocol	140
9.5.1	Protocol Description	141
9.5.2	Performance Analysis.....	144
9.5.3	Cardinality Estimation.....	146
9.5.4	Hash Functions	147
9.6	Simulation Results.....	147
9.6.1	Simulation Settings.....	148
9.6.2	Collection Time Comparison Under Different Numbers of Tags and Information Lengths	148
9.6.3	Collection Time Comparison Under Different Settings of the False Positive Rate	
	151	
9.7	Conclusions	152
10	Conclusions and Future Work	153
10.1	Contributions and Achievements of the Research	153
10.2	Limitations of the Research.....	156
10.3	Further work.....	157
	References.....	159
	Appendices.....	175
	Appendix A-Some Source Codes of the Simulations	175
	Appendix B-Some Constructed LDPC-Based Codes	185

List of Figures

Figure 1.1: The main components of an RFID system (Jones and Chung, 2007)	1
Figure 1.2: Example scenario of a group integrity checking process (Sato <i>et al.</i> , 2012)	2
Figure 1.3: The three main phases of the complete system	7
Figure 2.1: A hierarchical structure of three tags (Ban [^] atre <i>et al.</i> , 2010)	12
Figure 2.2: Memory space organisation of the leaves (Sinha <i>et al.</i> , 2014).....	13
Figure 2.3: 4-regular graph representation of a group of eight tags (Glouche and Couderc, 2012)	14
Figure 2.4: Chain of tag IDs modelling (Sayers <i>et al.</i> , 2010).....	15
Figure 2.5: Group of pallets modelling (Sayers <i>et al.</i> , 2010)	16
Figure 2.6: Generation and distribution of a codeword for a group of tags (Chaves <i>et al.</i> , 2013)	16
Figure 2.7: Checking group integrity using ECCs (Chaves <i>et al.</i> , 2013)	17
Figure 3.1: RFID tags in various shapes and sizes (Coresonant, 2014)	22
Figure 3.2: RFID system standards and frequency bands (Knospe and Pohl, 2004).....	27
Figure 3.3: Data coding in RFID systems (Finkenzeller, 2010)	29
Figure 3.4: Collision behaviour of NRZ coding (Finkenzeller, 2010)	41
Figure 3.5: Collision behaviour of Manchester coding (Finkenzeller, 2010).....	41
Figure 4.1: The Tanner graph illustration of H in Equation (4.1) (Ryan, 2003)	46
Figure 4.2: The parity check matrix in the approximate lower-triangular form (Richardson and Urbanke, 2001).....	48
Figure 4.3: An example of a stopping set (Di <i>et al.</i> , 2002).....	54
Figure 4.4: Reduced complexity ML decoder on H_K (Paolini <i>et al.</i> , 2012)	56
Figure 5.1: An example of the encoding process and the information stored in RFID tags belonging to a group of 6 RFID tags	72
Figure 5.2: An example of the decoding process of a group of 6 RFID tags	73
Figure 5.3: The IT decoding algorithm in the group integrity of RFID tags	74
Figure 5.4: Flowchart of the simulation process.....	75
Figure 5.5: The average error rate of the identification of missing tag IDs from different group sizes: (a) $n = 25$; (b) $n = 49$; (c) $n = 121$; (d) $n = 169$, using the PEG-based LDPC codes with the IT and GE decoding algorithms.....	77

Figure 5.6: The average error rate of the identification of missing tag IDs from a group of size $n = 1000$ using the PEG-based codes with the IT decoding algorithm.....	80
Figure 5.7: The average error rate of the identification of missing tag IDs from a group of size $n = 1000$ using the PEG-based codes with the GE decoding algorithm	80
Figure 5.8: The histogram of unrecovered missing tag IDs of the (200, 3, 6) PEG-based LDPC codes with the GE decoding algorithm.....	81
Figure 5.9: The average error rate of the identification of missing tag IDs from a group of $n=169$, where $j=4$ and the related decoding time for both the IT and GE decoding algorithms	82
Figure 5.10: The average error rate of the identification of missing tag IDs from a group of size $n = 512$ using the PEG-based and CRT-based codes with the IT decoding algorithm.....	84
Figure 5.11: The average error rate of the identification of missing tag IDs from a group of size $n = 512$ using the PEG-based and CRT-based codes with the GE decoding algorithm...	84
Figure 5.12: The average error rate of the identification of missing tag IDs from a group of size $n = 502$ using the PEG-based and ACE-based codes with the IT and GE decoding algorithm	85
Figure 6.1: The iteration numbers required for decoding two group sizes: (a) $n = 49$; (b) $n = 169$, where $j = 3$, using the PEG-based LDPC codes	89
Figure 6.2: The enhanced iteration numbers required for decoding two group sizes: (a) $n = 49$; (b) $n = 169$, where $j = 3$, using the PEG-based LDPC codes	91
Figure 6.3: The average error rate of the identification of missing tag IDs from different group sizes: (a) $n = 25$; (b) $n = 49$ using the PEG-based LDPC codes with the GE and improved HB decoding algorithm	92
Figure 6.4: The average error rate of the identification of missing tag IDs from different group sizes: (a) $n = 121$; (b) $n = 169$ using the PEG-based LDPC codes with the GE and improved HB decoding algorithm	93
Figure 6.5: Histogram of the GE decoding time with respect to the simplified system size for a group of size $n = 169$, where $j = 3$, using the PEG-based LDPC codes.....	95
Figure 6.6: The average decoding time for recovering missing tag IDs from two group sizes: (a) $n = 49$ and (b) $n = 169$, where $j = 3$, using the PEG-based LDPC codes under the IT with early termination, the GE, and improved HB decoding algorithms	96
Figure 6.7: The average decoding time for recovering missing tag IDs from two group sizes: (a) $n = 49$ and (b) $n = 169$, where $j = 4$, using the PEG-based LDPC codes under the IT with early termination, the GE, and improved HB decoding algorithms	96

Figure 6.8: Operational complexity comparison between the IT, GE, and improved HB decoding algorithms for a group of $n=49$, where (a) $j=3$ and (b) $j=4$	101
Figure 6.9: Operational complexity comparison between the IT, GE, and improved HB decoding algorithms for a group of $n=169$, where (a) $j=3$ and (b) $j=4$	101
Figure 7.1: Reduction in the number of missing tags with iterations for $n=169$ tags, where $j=3$	104
Figure 7.2: The average decoding time for recovering missing tag IDs from two group sizes: (a) $n=49$ and (d) $n=169$, where $j=3$, using the PEG-based method under the IT with early termination, the GE, and improved HB decoding algorithms.....	105
Figure 7.3: The average error rate of the identification of missing tag IDs for irregular and regular PEG-based codes with $n=256$ under the IT decoding algorithm.....	107
Figure 7.4: The average error rate of the identification of missing tag IDs for irregular and regular PEG-based codes with $n=512$ under the IT decoding algorithm.....	108
Figure 7.5: Reduction in the number of missing tags with iterations for: (a) regular and (b) irregular PEG-based LDPC code with $n=256$	108
Figure 7.6: Influence of changing the fractions of low degree variable nodes on the performance of half rate short-length irregular PEG-based LDPC codes with $n=256$	109
Figure 7.7: Influence of changing high degree variable nodes on the performance of half rate short-length irregular PEG-based LDPC codes with $n=256$	110
Figure 7.8: Influence of changing the fractions of high degree variable nodes on the performance of half rate short-length irregular PEG-based LDPC codes with $n=256$	111
Figure 8.1: An example of a Bloom filter.....	115
Figure 8.2: An example of a CBF.....	121
Figure 8.3: Basic duplicate readings filtering (Yaacob and Mahdin, 2016).....	125
Figure 8.4: Duplicate filtering method of an RFID data stream (Kamaludin <i>et al.</i> , 2016)....	126
Figure 9.1: An example of the tag identification process with a BF in Yue <i>et al.</i> (2014).....	134
Figure 9.2: An illustrative example of the MIC protocol (Chen <i>et al.</i> , 2011).....	140

List of Tables

Table 3.1: RFID system features at available frequencies.....	28
Table 3.2: The number of tags versus the optimal frame size and the number of groups in the EDFSA (Lee <i>et al.</i> , 2005)	38
Table 4.1: the average number of recovered erasures for some analysed codes in Tomlinson <i>et al.</i> (2007).....	51
Table 5.1: Comparisons of the PEG-based LDPC codes with other LDPC-based codes.....	78
Table 5.2: Comparisons of the PEG-based and CRT-based LDPC codes.....	83
Table 5.3: Comparisons of the PEG-based and ACE-based LDPC codes	85
Table 6.1: Number of operations for the improved HB decoding algorithm.....	99
Table 7.1: The values of θ_{th} for different parameters of the PEG method	105
Table 7.2: Variable degree sequences for irregular codes in Figure 7.6.....	109
Table 7.3: Variable degree sequences for the irregular codes in Figure 7.7.....	110
Table 7.4: Variable degree sequences for the irregular codes in Figure 7.8.....	112
Table 9.1: Estimation time comparison (in second) under different group sizes	146
Table 9.2: Collection time comparison (in seconds) for different parity check values m	149
Table 9.3: Collection time comparison (in seconds) for the same parity check values m	150
Table 9.4: Collection time comparison (in second) under different values of P_{FP} , where $n = 2,000$	152

List of Algorithms

Algorithm 4.1: Construction of the parity check matrix using the PEG method.....	63
Algorithm 6.1: Improved IT Decoding.....	90
Algorithm 9.1: Constructing the BF	142
Algorithm 9.2: Membership testing	143
Algorithm 9.3: The RIC protocol.....	143

List of Acronyms

ACE	Approximate Cycle Extrinsic Message Degree
ACK	Acknowledgement
BC	Baseline Collection
BEC	Binary Erasure Channel
BER	Bit Error Rate
BF	Bloom Filter
BIC	Bloom-filter-based Information Collection
CBF	Counting Bloom Filter
CDMA	Code Division Multiple Access
CRT	Chinese Remainder Theorem
ECC	Error Correction Code
EDFSA	Enhanced Dynamic Framed Slotted Aloha
EG	Euclidean Geometry
EMD	Extrinsic Message Degree
EPC	Electronic Product Code
ETOP	Enhanced Tag Ordering Polling
FDMA	Frequency Domain Multiple Access
FER	Frame Error Rate
FSA	Framed Slotted Aloha
GE	Gaussian Elimination
GF	Galois Field
HB	Hybrid
HF	High Frequency

ID	Identifier
ISO	International Standard Organization
IT	Iterative
LDPC	Low Density Parity Check
LF	Low Frequency
LLR	Log-Likelihood Ratio
MF	Microwave Frequency
MIC	Multi-hash Information Collection
ML	Maximum Likelihood
ML-CCBF	Multi-Layer Compressed Counting Bloom Filter
NACK	Negative Acknowledgement
NRZ	Non-Return to Zero
P2P	Peer-to-Peer
PC	Physical Characteristic
PEG	Progressive Edge-Growth
PIC	Perfect-hashing-based Information Collection
RFID	Radio Frequency Identification
RHS	Right Hand Side
RIC	Redundant Information Collection
RS	Reed-Solomon
RTD	Resolvable Transversal Design
RTF	Reader-Talk-First
RZ	Return to Zero
SA	Slotted Aloha
SCBF	Space Code Bloom Filter
SDMA	Space Division Multiple Access

SIC	Single-hash Information Collection
SSF	Strongly Selective Family
TDMA	Time Domain Multiple Access
TOP	Tag Ordering Polling
TTF	Tag-Talk-First
UHF	Ultra-High Frequency
WAN	Wide Area Network

1 Introduction and Overview

1.1 Introduction

Radio frequency identification (RFID) is a technology that uses radio waves to identify and track objects automatically through radio waves. Typically, an RFID system is composed of tags, readers, and database servers. A tag is a small device that is attached to a physical object and stores information about the object in its user memory. In addition to the user memory, each tag has a special memory that stores the 96-bit tag identifier (ID), which uniquely identifies the physical object. The reader gathers information from multiple tags at a time through multiple access technique, then relaying them to the back-end database servers for further analysis and processing (Nambiar, 2009). A block diagram of such a system is shown in Figure 1.1. Tags come in three types, including passive, active, and semi-passive tags. Passive tags are cheaper, smaller in size, and have longer life than the other types of tags and hence, they are widely used in different applications. On the other hand, they have smaller memory size, only storing up to 1 kilobytes of information in commonly used models (Roberti, 2011).

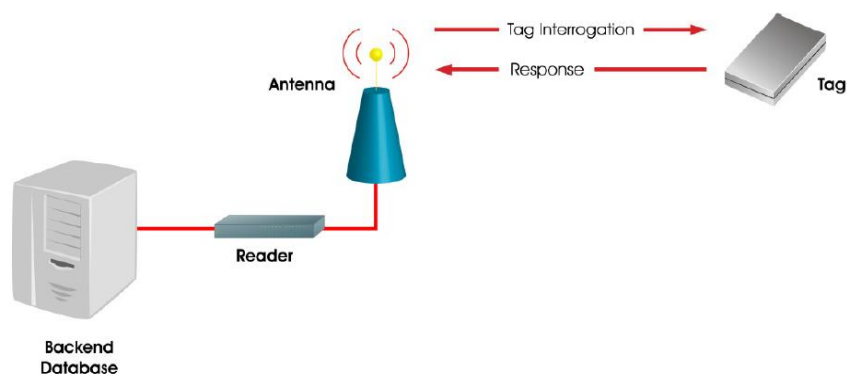


Figure 1.1: The main components of an RFID system (Jones and Chung, 2007)

RFID technology has been used in many application domains, including security, inventory, logistics, and public transportation. Many activities need the integrity verification of a set of objects in addition to individual object checking. The basic idea of a group integrity verification, is to check that a group of tagged objects, parts, animals, or people remains consistent during some process; whilst also determining the missing tag IDs, if they occur. In logistics, it is a common practice that items form a group and are handled together. It is also common to check personal belongings at airports to avoid loss or to prevent similar possessions being wrongly exchanged with those of someone else. A further example is when a group of children requires to be regularly checked during a school excursion to ensure that no child is missing. Figure 1.2 demonstrates an example scenario of such a process.

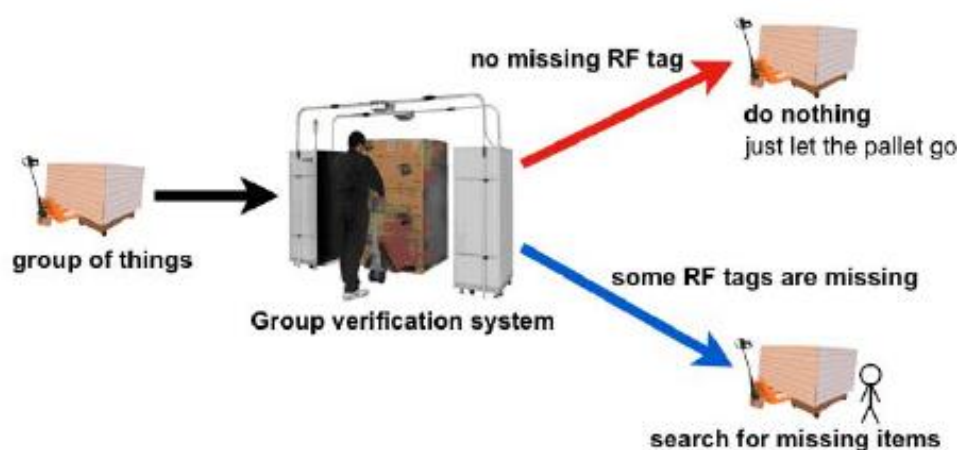


Figure 1.2: Example scenario of a group integrity checking process (Sato *et al.*, 2012)

Verifying the integrity of a received group of shipments, for example, is usually achieved by checking the shipment list, where the reader requires access to on-line databases. There are other methods for accomplishing verification of a group of tags. Juels (2004) studied the integrity of two RFID tags from the security perspective and presented yoking-proof, whereby a message authentication code is exchanged between the two tags and a verifier. This was enhanced and generalised for a group of tags in studies by Saito and Sakurai (2005),

Liu *et al.* (2013), Sundaresan *et al.* (2014), and Shen *et al.* (2015). Whilst all the proposed grouping-proofs provide integrity evidence for complete groups of tags, they do not address incomplete ones. Potdar *et al.* (2007) presented an integrity checking method which compares the total weight of a group of tags recorded in a database and their reading results.

Autonomous verification of a group of RFID tags without external systems is an essential feature in RFID systems, because it ensures standalone operations as well as scalability, privacy, and security. Banâtre *et al.* (2009) introduced the concept of “coupled objects” to describe groups of objects in autonomous group integrity checking, being a group of physical objects that represents a logical group. An essential characteristic of a coupled object is that the group information is self-contained within the objects, such that the group verification process is possible without using extra systems and hence, additional data are written into the user memory of RFID tags. A simple method to represent the coupled object or a group of objects would be to let each tag of a group store the set of IDs of all members. However, given that the tag ID is of size 96 bits and the passive tags have limited memory space, this approach is not scalable to large groups. Another method is to use a digest value to represent a group of tags (Banâtre *et al.*, 2009). For a group of n tags, group creation includes the following steps:

- 1) The reader collects the tag IDs denoted by $TID_1, TID_2, TID_3, \dots, TID_n$ from the group and orders them sequentially;
- 2) A hash function is applied to the collected tag IDs to obtain the digest value as hash $(TID_1, TID_2, TID_3, \dots, TID_n)$ and the resulting digest value is treated as a group ID;
- 3) The reader records the group ID in the user memory of the tags in the group.

Once a group is formed, group integrity checking includes the following steps:

- 1) The reader collects the tag IDs and the stored group IDs from a group of tags having the same group ID;

- 2) The collected tag IDs are ordered sequentially;
- 3) The same hash function of the group creation is applied over the collected tag IDs;
- 4) The computed hash value is compared with the stored group ID. If there is a mismatch, the group integrity is invalid, meaning that one or more tags are missing; otherwise, the group preserves its integrity.

Even though Banatre *et al.*'s method enables fully autonomous group integrity checking, it is not able to recover the missing tag IDs. A number of methods have been proposed to solve this issue by writing additional data into the user memory of the RFID tags, examples being, each tag in the group stores the tag IDs of some members that are arranged as chains (Sayers *et al.*, 2010), regular connected graphs (Glouche and Couderc, 2012), or tree structures (Sinha *et al.*, 2014). The robustness of these methods is strengthened by increasing the amount of redundant tag IDs stored among tags at the expense of memory costs. As a result, Sato, Igarashi, *et al.* (2012) presented another method in which a group of tag IDs is treated as packet symbols, which are encoded and decoded in a way similar to that of binary erasure channels (BECs). Due to the sparseness property of low density parity check (LDPC) codes as well as their good erasure recovery capabilities, the parity check matrix of LDPC codes is used as a group generator matrix to divide the main group into multiple overlapping subgroups virtually, henceforth referred to as the LDPC-based method. Each tag records all the parity check values in which they are involved. Therefore, tags of the same row of the matrix maintain the same set of information. The authors used the Gallager method (Gallager, 1962) to construct the parity check matrix and since the matrix is constructed randomly, two or more missing tags may have identical memberships. In other words, they belong to stopping sets, which degrades the performance of the method in recovering missing tag IDs with iterative decoding. To overcome this shortcoming, three nonrandom methods were utilised in the construction of the parity check matrices of the LDPC codes, aimed at increasing the recovery performance (Su *et al.*, 2013; Su and Tonguz, 2013; Su, 2014). The

performance of the existing LDPC-based methods can be increased by increasing the number of subgroups which each RFID tag belongs to, but at the expense of the tag's user memory. Su (2014) introduced a method to reduce the amount of information stored in a tag's user memory; however, it causes higher decoding complexity.

For the group integrity checking and decoding processes, the reader needs to collect the redundant information from all the tags in a group efficiently, because RFID systems have subsequent processes to perform. When the time is long, the task of collecting tag information may delay these processes of the system, which is undesirable, especially in large-RFID environments. Many existing RFID studies mainly focus on proposing ID collection protocols that collect tag IDs in the interrogation zone of the reader. These protocols are mainly classified into ALOHA-based (Cha and Kim, 2006; Vogt, 2002a) and tree-based (Law *et al.*, 2000; Hush and Wood, 1998) protocols. In ALOHA-based protocols, the reader sends a request message to the tags. Then, each tag transmits its ID to the reader at randomly chosen time slots. Consequently, more than one tag may possibly transmit their IDs at the same time slot; in this case, the time slot becomes a collision slot. On the other hand, if only one tag transmits its ID at a certain time, the tag is successfully identified. In tree-based protocols, collisions are reduced by building tree traversal approaches. When a collision occurs, the reader divides the tags into two subgroups and requests the subgroups with a smaller number of tags. The reader continues to divide the tags until all the tags are identified. Whilst the ID collection protocol can be used to collect tag information, the transmission overhead and time delay could be excessively high for redundant tag information.

In sensor-augmented RFID systems, tags are combined with miniaturised sensors to provide information about the surrounding environment. Collecting such information from tags with low communication costs and thus, short time spans, has inspired many studies in recent

years. Chen *et al.* (2011) proposed the Single-hash Information Collection (SIC) protocol and the improved version, the Multi-hash Information Collection (MIC) protocol, to periodically collect information from sensor-based RFID systems with a minimum collection time. By utilising several hash functions, the MIC protocol can resolve most hash collisions in a frame and thus, significantly enhance the protocol performance. Qiao *et al.* (2011; 2016) studied the same problem, but with respect to energy efficiency for active tags. The tag ordering polling protocol and the improved protocol were presented to read information from tags with the smallest amount of energy consumption. A follow-up work by Yue *et al.* (2012) complemented previous work with an additional protocol that is primarily designed to read sensor-produced information from RFID tags with multiple readers. The extended study in Yue *et al.* (2014) targeted an unknown subset of tags with one reader. The proposed protocols utilised Bloom filters that are distributively built and transferred from the tags to the reader to identify the target tags efficiently. The reader can then build a hash vector from a frame of time slots to link each identified tag to each slot in order to send its information. In sensor-based RFID systems, the tags have no knowledge about the information the reader has and should send all their information.

Many methods in the literature filter out the duplicate information in RFID systems (Mahdin and Abawajy, 2011; Jiang *et al.*, 2012; Mezzi and Akaichi, 2013). Duplicate data are produced because an RFID reader reads the same tag multiple times, or the same tag is read by multiple readers. All these methods concentrated on filtering duplicate information at the reader's side before the information is transmitted to back-end database servers for processing, which causes communication overheads between the reader and the tags. The majority of the proposed methods are based on Bloom filters. Generally, the received data are maintained in Bloom filters to eliminate duplicates and thus, reduce memory and communication consumptions.

Motivated by the need to increase the missing recovery capabilities of the checking methods with low memory and decoding overheads; and to read redundant tag information from a group of tags with low communication overheads, several methods are designed in this thesis aimed at increasing the functionality of the complete system of group integrity application in resource constrained environments of RFID systems. Figure 1.3 shows the three main phases of the complete system.

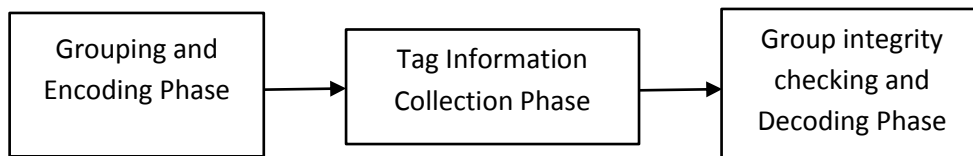


Figure 1.3: The three main phases of the complete system

1.2 Aims and Objectives

This research is devoted to the development of group integrity application in RFID systems. The aim is to propose novel mechanisms to improve the performance in recovering missing tag IDs with low memory consumptions and decoding complexity, whilst also collecting redundant tag information from a group of tags with low communication overheads. In order to achieve these, the following research objectives are established:

- 1) To review existing autonomous group integrity checking methods and define their limitations;
- 2) To investigate RFID systems with a focus on important features directly related to the thesis;
- 3) To investigate LDPC codes in BECs with special attention to their construction methods and decoding algorithms;
- 4) To design and evaluate a new method, with the aim of increasing the missing recovery capabilities with low memory overheads;

-
- 5) To design, analyse, and evaluate an optimised decoding algorithm, with the aim of achieving high recovery performance with low decoding complexity;
 - 6) To review existing tag information filtering and collection protocols, with a focus on their designs and limitations;
 - 7) To investigate a Bloom filter with a focus on its features, limitations, and the ways in which the Bloom filter has been utilised in some systems, especially in RFID ones;
 - 8) To design and evaluate a novel tag information collection protocol that is used to collect redundant tag information from a group of tags in a group integrity application with low communication overheads.

1.3 Contributions to Knowledge

The following list summarise the main contributions made by the thesis.

- 1) Using the progressive edge-growth (PEG) method to increase the recovery capability of missing tags in group integrity applications of RFID systems. It has been found that the recovery performance of the method outperforms existing methods, with either the same or less memory overheads.
- 2) Optimising the decoding complexity using an improved hybrid decoding algorithm which includes an early stopping criterion to avoid unnecessary iterations of iterative decoding for undecodable blocks, thus saving decoding time. This improved algorithm has achieved the optimal missing recovery capabilities of the full Gaussian elimination decoding algorithm.
- 3) Conducting extensive analysis and evaluations of the improved hybrid decoding complexity, both in terms of the number of operations required and the decoding time. It has been found that the improved hybrid decoding algorithm considerably reduces the operational complexity and also the time of the full Gaussian decoding algorithm for

small to medium amounts of missing tags up to a certain threshold value, which depends on the missing recovery capabilities of the iterative decoding algorithm.

- 4) Designing an adaptive algorithm to avoid the iterative decoding when the missing amount is larger than a threshold. It has been found that the adaptive decoding algorithm is very efficient in decreasing the average decoding time of the improved hybrid decoding, thus saving more decoding time of up to 10% for large amounts of missing tags, where the iterative decoding fails to recover any missing tags.
- 5) Conducting numerous simulations to analyse and evaluate the missing recovery performance of various half rate short-length irregular PEG-based LDPC codes constructed with different variable degree sequences. It has been found that the irregular codes achieve better missing recovery than regular codes only in the region where the iterative decoding is successful and the density evolution method is good for the irregular PEG construction.
- 6) Designing a novel tag information collection protocol based on a Bloom filter to filter redundant tag information at the tag's side efficiently and thus, saving collection time. The designed protocol includes a method for estimating the number of the target parity check values. The performance of the designed protocol outperforms the existing solutions by saving from 37% to 84% of the collection time.

Several papers have been published and submitted for publication, including:

- 1) Alkanhel, R., Ambroze, M. (2016). 'Extended Grouping of RFID Tags Based on Progressive Edge-Growth Methods', in 5th International Conference on Electronic Devices, Systems and Applications (ICEDSA). Ras Al Khaimah, UAE 6–8 December. IEEE, pp. 1–5, DOI: 10.1109/ICEDSA.2016.7818544.

- 2) Alkanhel, R., Ambroze, M. (2017). ‘Optimizing the Decoding Complexity of PEG-based Methods with an Improved Hybrid Iterative/Gaussian Elimination Decoding Algorithm’, *Advances in Science, Technology and Engineering Systems Journal*, 2(3), pp. 578–586, DOI: 10.25046/aj020374.
- 3) Alkanhel, R., Ambroze, M. (2017). ‘Decoding Complexity Analyses of PEG-based Methods with the Improved Hybrid Iterative/Gaussian Elimination Decoding Algorithm’, in *International Conference on Electrical and Computing Technologies and Applications (ICECTA)*. Ras Al Khaimah, UAE 21–23 November. IEEE, pp. 239–243, DOI: 10.1109/ICECTA.2017.8251925.
- 4) Alkanhel, R., Ambroze, M. (2018). ‘An Efficient Redundant Information Collection Protocol for the Group Integrity of Tags in RFID Systems’, *International Journal of Future Generation Communication and Networking* (submitted).

1.4 Methodology

A schematic diagram of the research methodology is presented in Figure 1.4 to show its phases for achieving the thesis objectives and the relationships between these objectives and the chapters. The thesis is organised into ten chapters. References are located at the end of this thesis, together with two appendices containing some source codes of the simulations and some constructed LDPC-based codes.

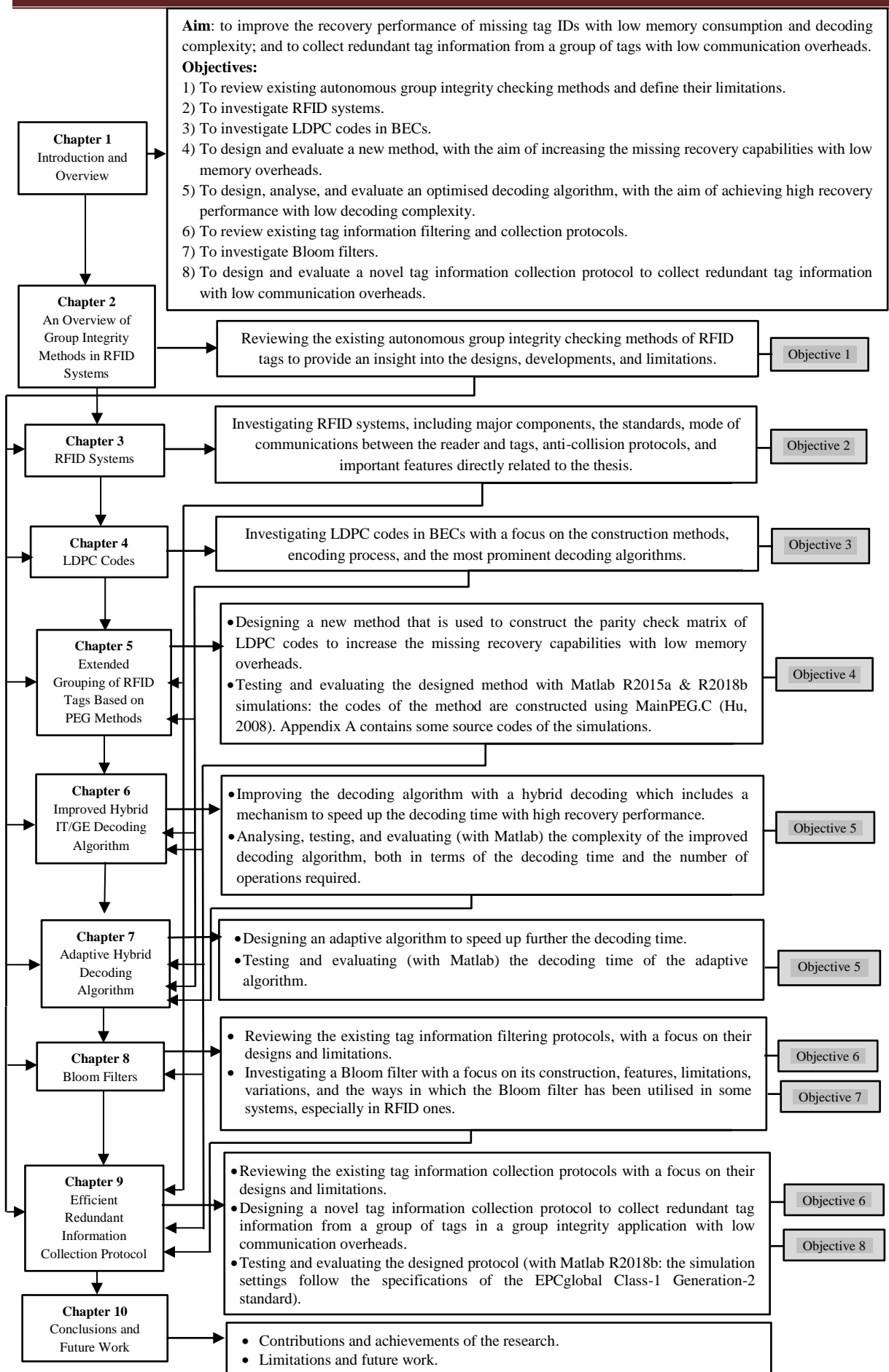


Figure 1.4: A schematic diagram of the research methodology

2 An Overview of Group Integrity Methods in RFID Systems

A number of researchers have proposed autonomous methods for group integrity checking without external systems, by writing additional data into the limited memory space of RFID tags. These data reference other tags or represent their membership in the group. This chapter provides a literature review of different autonomous group integrity checking methods of RFID tags, with a focus on their design and limitations.

2.1 Literature Review

Banâtre *et al.* (2009) used a digest value to represent a group of tags logically, as presented in Chapter 1. Later, in 2010 and 2011, the authors extended the basic principle to have objects belonging to several groups in a hierarchical structure. Instead of having a flat addressing scheme where all tags are present at the same level, hierarchical data structures or coupled object trees allow for the independent checking of each tree or subtree. Each tagged object stores the hash value that corresponds to the group or the level to which the object belongs. Figure 2.1 represents two groups O_1 and O_2 , where O_1 consists of two tags $f1$ and $f2$, whereas O_2 consists of the group $O_1 = \{f1, f2\}$ and the tag $f3$.

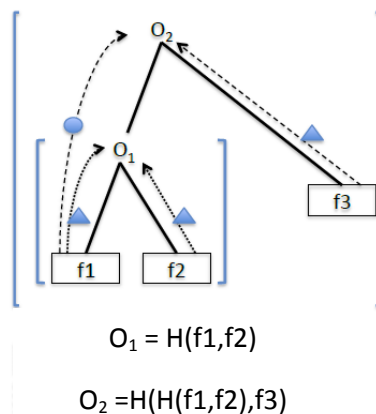


Figure 2.1: A hierarchical structure of three tags (Banâtre *et al.*, 2010)

Whilst Banatre *et al.*'s method enables autonomous group integrity checking, it cannot recover the missing tag IDs and for this reason, some methods have been proposed to overcome this. Sinha *et al.* (2014) utilised a tree structure to check the integrity of composite objects, with hierarchical representation of the tree being distributed among its leaf nodes. In other words, the data about internal nodes are stored on an RFID tag's memory attached to the leaf. Figure 2.2 shows an example of Sinha *et al.*'s model, where each leaf node records three types of information, including its sibling IDs, its parent ID, its ancestor node ID, and associated child IDs. The distributed information forms a logical link between leaves, which helps to assemble the composite object, check the integrity of the structure, and identify missing tags. When missing all leaves belonging to any subtree, Sinha *et al.*'s model is not able to identify missing tags, because each leaf node stores two sets of data only. One set is associated with its siblings and is used to identify missing siblings, whilst the other is related to its ancestor subtree and is used to construct the tree. The robustness of the method can be increased by increasing the redundancy of the information stored in the tags at the expense of memory costs.

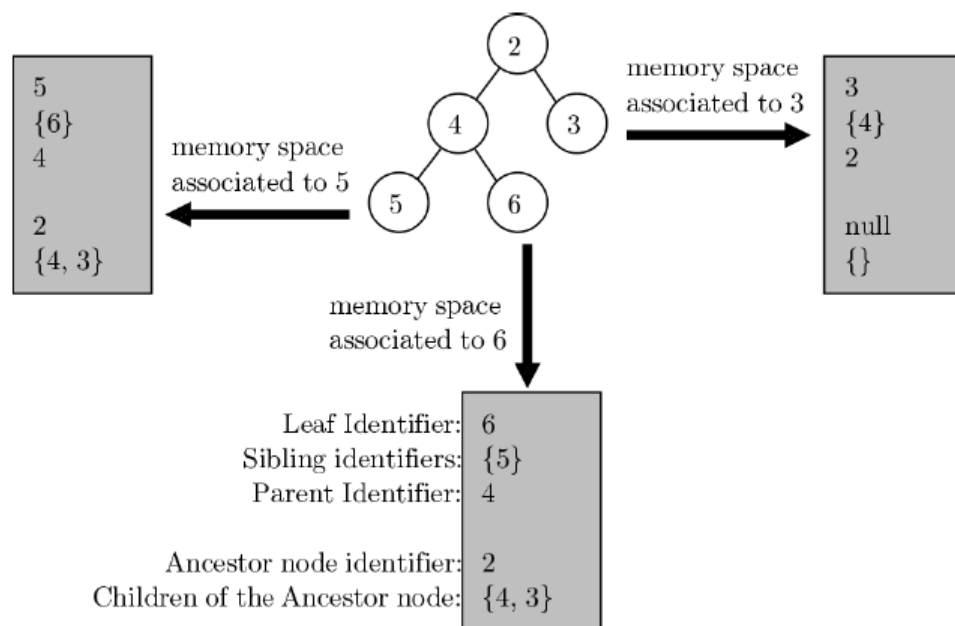


Figure 2.2: Memory space organisation of the leaves (Sinha *et al.*, 2014)

Glouche and Couderc (2012) proposed a different method in which a set of tags is arranged as a regular connected graph. Each vertex of the graph is represented by a tag, which records the graph structure, that is, the IDs of its neighbours as shown in Figure 2.3. The presence of each tag is evenly recorded on the other tags so the same amount of memory is consumed in each. When a tag is missing, it can be recovered using the information stored in its neighbours. In a k -regular graph, each tag stores the IDs of its k neighbours. When, at most, k tags are missing, the structure guarantees that the IDs of all the missing tags will be recovered. However, when more than k tags are missing, only k of them can be recovered. The amount of memory required to record the IDs of the neighbours is a multiple of k and is proportionally increased when k increases. The amount of missing tags that can be recovered is increased by increasing the degree of the graph, which affects the number of IDs to be recorded on tags. The authors, interestingly, make the following comment in their paper:

“Unfortunately, as RFID tags provide very limited memory capacity, it is difficult to implement redundant storage and robust data structures distributed over a set of RFID tags”

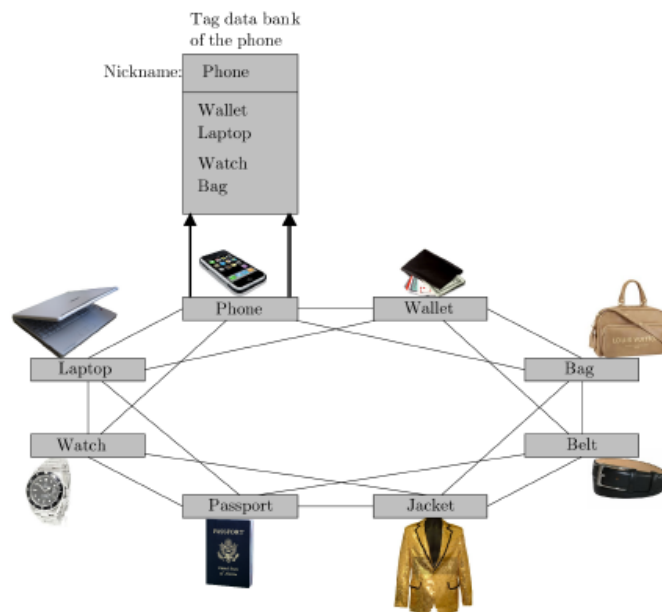


Figure 2.3: 4-regular graph representation of a group of eight tags (Glouche and Couderc, 2012)

Sayers *et al.*, (2010) proposed a chain of IDs to check the integrity of a group of tags on a pallet. For a group of tags, each stores the IDs of the next two tags in the sequence. This ensures the redundancy of the IDs, which helps to recover missing tags. For example, the ID of tag C in Figure 2.4 is redundantly stored in the previous two tags, that is, tag A and tag B. In order to enable the system to differentiate between real missing items and those that are present, but cannot be read while the items are on the pallet, the physical characteristics (PC), such as the weight or total number of items are also stored on the tags and pallets. For example, the weight of the pallet is compared with either PC_p stored on tag D or stored on tag P. If there is a mismatch, this guarantees that one or more tags are missing. In addition, the physical characteristics can be used for an individual tag to verify its authenticity. A disadvantage of this method is that when more than two consecutive tags are missing, it cannot detect and recover some missing tag IDs.

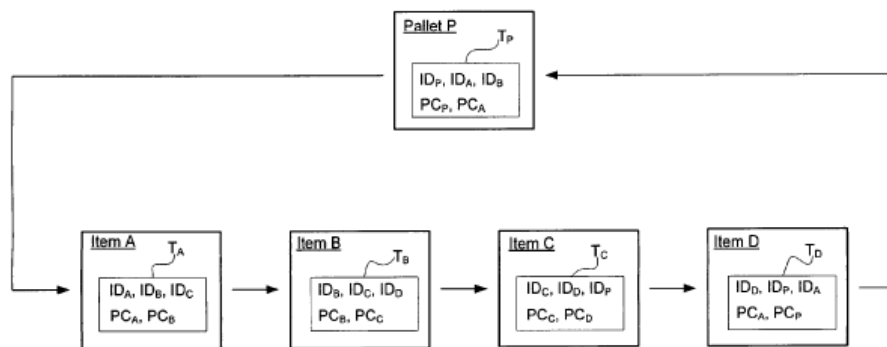


Figure 2.4: Chain of tag IDs modelling (Sayers *et al.*, 2010)

To increase the robustness of the system, Sayers *et al.* (2010) also stored the IDs of a given pallet across multiple pallets, as illustrated in Figure 2.5, where ID_{PA} , for example, indicates the IDs for all the tags on pallet A. The robustness of the method depends on the amount of the redundant data as this consumes more memory spaces especially with a large group of tags.

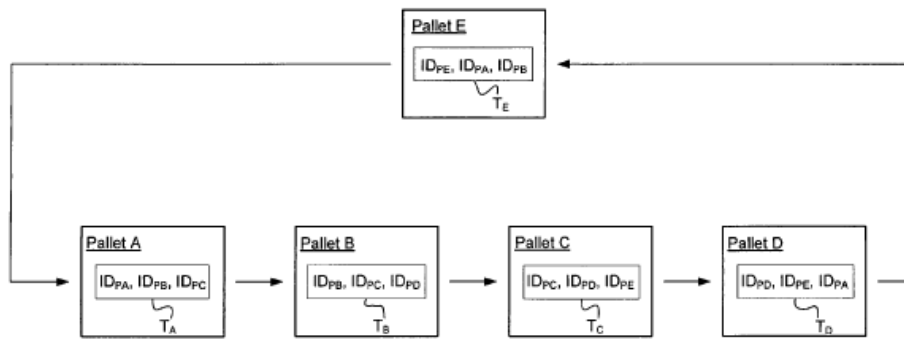


Figure 2.5: Group of pallets modelling (Sayers *et al.*, 2010)

Chaves *et al.*, (2013) proposed another method using Error Correction Codes (ECCs) applied to a group of tag IDs. In a set of tags, all the IDs are assembled to a message that is encoded using an ECC and then, the codeword is split up into a number of parts. Each part is stored on each tag in the group. The codeword is stored with an address to ensure that is assembled in a specific order, as shown in Figure 2.6. The EPC in the figure is an abbreviation for “The Electronic Product Code”, which is equivalent to the tag ID used in this thesis.

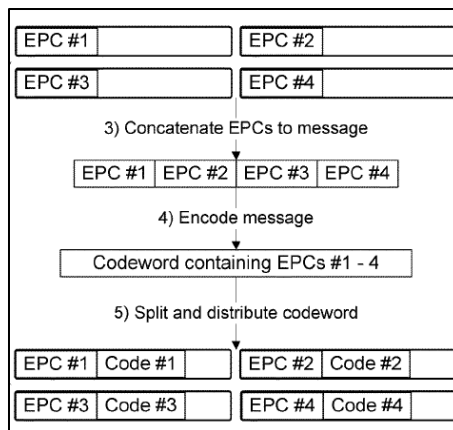


Figure 2.6: Generation and distribution of a codeword for a group of tags (Chaves *et al.*, 2013)

In a checking process, all available portions of the codeword are assembled based on their addresses. The recovery of the missing portions depends on the remaining parts and the type of ECC used, with Figure 2.7 depicting an example of the checking process. Whilst Chaves *et al.*'s method presents a compact representation of the redundancy, missing a chain of consecutive tags may become an obstacle to the recovery process.

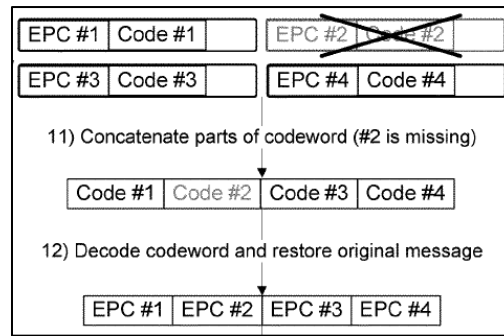


Figure 2.7: Checking group integrity using ECCs (Chaves *et al.*, 2013)

Another direction of the research in this field was proposed in Sato *et al.* (2011; 2012), in which a group of tag IDs is treated as packet symbols and encoded and decoded in a way similar to that of binary erasure channels (BECs). Due to the sparseness property of low density parity check (LDPC) codes as well as their good erasure recovery capabilities, the parity check matrix of LDPC codes is constructed with the Gallager method and then used as a group generator matrix to divide the main group into multiple overlapping subgroups virtually. For a group of tags, the group ID is calculated as the bitwise exclusive or XOR of the hashed tag IDs. In addition to the group ID, each tag stores all subgroup IDs, that is, the parity check values to which it belongs. Subgroup IDs are calculated in the same way as the group ID. The number of missing IDs is estimated as the rank of a matrix containing missing tag IDs. Then, Sato, Igarashi, *et al.* (2012) extended the previous method to recover the IDs of missing tags. In the extended method, also called extended grouping, extra information is added to the tag's memory in addition to subgroup IDs. The subgroup IDs are computed as the XOR of tag IDs, and therefore, the bit length of the subgroup IDs is equal to the bit length of the tag IDs, i.e. 96 bits. In addition, a short ID that is a portion of the tag ID is assigned to each tag. The bit length of each short ID is set to the minimum number of bits necessary to distinguish a group of tags. For example, a short ID of 8 bits is enough for a group less than

256 tags. Each tag stores all short IDs of other tags belonging to the same subgroup (parity check constraint). The short IDs are used to re-establish the Tanner graph during the decoding process and thus, recover the IDs of the missing tags. During the decoding process, missing tag IDs are computed as the XOR of the subgroup IDs and the known IDs of all tags belonging to the same subgroup. It has been assumed that a situation where all the tags belonging to one subgroup are missing does not occur. The procedure of the group decoding is similar to the iterative decoding algorithm in the BEC. The properties of the matrices used for the encoding, including the way of division, the number of subgroups which each tag belongs to, and the number of tags in each subgroup, are important, because they have a direct relationship with the recovery performance and the amount of information stored in the tag's memory. Because the Gallager's parity check matrix is constructed randomly, the method fails to resolve the exact amount of missing tags and recover some missing tag IDs when they belong to stopping sets. This degrades the performance of the method in resolving the accurate amount of missing tags or recovering missing tag IDs with the iterative decoding.

To overcome the above shortcoming, three nonrandom methods were utilised in the construction of the parity check matrices of LDPC codes, aiming to maximise the performance in resolving the accurate number of missing IDs or recovering more. Su *et al.* (2013) constructed the matrices based on the properties of strongly selective families (SSFs) whereas Su and Tonguz (2013) utilised the redundancy property of the remainder presentation in the Chinese remainder theorem (CRT). Su (2014) also used resolvable transversal designs (RTDs) to construct the matrices. The author introduced a method called group splitting, which splits rows of the parity check matrix into smaller ones to improve the recovery performance of the proposed method and to reduce the amount of information stored in the tag's memory. However, group splitting causes higher decoding complexity. The performance of the aforementioned LDPC-based methods can be enhanced by increasing

the number of subgroups that each RFID tag belongs to (i.e. the column weight of the parity check matrix), but at the expense of the tag's memory, as concluded by their authors. For example, the SSF-based method can recover up to five missing tag IDs by writing 528-bit additional information into the user memory of each tag in a group of 121. Increasing the memory overhead to 704-bit, the largest number of missing tag IDs that can be recovered by the method is increased to 13.

All the LDPC-based methods aim to provide equal missing protection for all tags in a group, as each tag is included in the same number of subgroups. However, there are some cases where not all tags need the same protection level. For instance, when tracking laundry with RFID tags, expensive clothes are considered to be more important than others. This application requires unequal missing protections amongst the tags. Accordingly, Su and Wang (2015) and Su *et al.* (2015) introduced the concept of unequal missing protection for the design of grouping of RFID tags. The design is based on joining some group generator matrices with equal missing protection. The amount of protection levels that the new matrix offers depends on the joint sub-matrices and the number of overlapping columns. Only the tags associated with the overlapping columns have the highest protection levels with additional stored information and thus, more memory overheads.

From the security perspective, Juels (2004) presented a yoking-proof protocol of two RFID tags, which verifies the simultaneous presence of two tags. A message authentication is exchanged between the two tags and a verifier. Saito and Sakurai (2005) developed an improved version to overcome the vulnerability of replay attack. They also generalised the problem of the yoking-proof to a grouping-proof, which verifies the presence of a group of tags in the range of a reader. Later, several protocols were presented aiming to improve the security of grouping-proof protocols (Liu *et al.*, 2013; Sundaresan *et al.*, 2014; Shen *et al.*, 2015), which use an off-line or on-line verifier to generate a proof. However, tags and

verifiers must previously share a secret key. Despite all the proposed grouping-proofs providing integrity evidence for complete groups of tags, they do not address incomplete ones. In particular, they do not give any information about missing tags. Following the same principles of Sato, Igarashi, *et al.* (2012), Burmester and Munilla (2016) utilised Reed-Solomon (RS) erasure codes to identify the missing tags with a grouping-proof protocol. More precisely, they used $RS(n, k)$ code to encode the IDs of a group of tags. The concatenation of tag IDs is rearranged into blocks and then encoded to get an RS codeword, which is then split into blocks and stored in the memory of each tag in the group. RS decoding can only be performed, if the scanned blocks are ordered correctly with gaps for the missing blocks. For this purpose, control information is needed to ensure the order of tag IDs at the time of encoding. The authors highlighted how the optimal code is costly when the group of tags is large. Therefore, the number of tags and missing tags is assumed to be small.

2.2 Conclusions

It can be seen that many autonomous methods have been proposed for checking the integrity of a group of tags in RFID systems without external systems. The compact representation of group members in LDPC-based methods is of significant importance to accommodate the limited memory space of passive RFID tags. The performance of the methods in recovering missing tag IDs can be enhanced by increasing the amount of redundant information at the expense of memory costs. Even though there is an effort to reduce memory consumption, the decoding complexity is increased accordingly. Having the same memory consumptions, the performance of the existing LDPC-based methods is mainly affected by the structure of the parity check matrix used for the encoding. More precisely, the presence of stopping sets limits the recovery capability of the iterative decoding.

3 RFID Systems

RFID is an automatic technology that enables the identification and tracking of objects through radio waves (Bolic *et al.*, 2010). It has been successfully used in different applications, including supply chain management, objects tracking management, production process control, agriculture management, transportation, healthcare and medicine, and services to name a few. The main advantage of RFID systems is the automated identification and data capture, which has brought significant improvements to resource optimisation, end-user enhancements, and process efficiency across a wide range of business activities (Jia *et al.*, 2012). This chapter presents an overview of RFID systems, including major the components, its standards, mode of communications between the readers and the tags, anti-collision protocols, and important features directly related to the thesis.

3.1 RFID System Components

A typical RFID system consists of three main components: RFID tags, readers, back-end database servers. The tag is a small device that is attached to an object as the identifier of the object. It stores and transmits information to readers through radio waves. The reader generates magnetic fields that enable the RFID system to locate tagged objects that are within its field. The reader gathers information from multiple tags and relays them to the back-end database servers for further analysis and processing (Nambiar, 2009). The back-end database server is used to store and process the information centrally. The back-end database server uses the gathered information in the field by the readers to perform different functions, such as verifying identities and granting authorisation, keeping inventories, alerting suppliers when new inventories are required, tracking the movement of items, and redirecting them (Hunt *et al.*, 2007). Unlike typical RFID systems, the autonomous group integrity verification of this

thesis eliminates the use of the back-end database servers to ensure standalone operations as well as scalability, privacy, and security.

3.1.1 RFID Tags

An RFID tag, also known as a transponder, is composed of an antenna, a microchip that gives the tag some limited functionality, and a substrate or printed circuit board. Information is received and transmitted by the antenna, while the chip stores and processes the information. The printed circuit board holds the tag parts together. Generally, the chip is used to store data about an object the tag is attached to. The object is provided with a unique identification number, which, along with other related information, such as product type and manufacturing date are stored in the chip (Brown, 2007). The size of the tags is determined by the size of their antenna since the microchip is usually very small in size. Tags are available in many different shapes, sizes, and protective housings depending on the application and the environment in which they will be used. Figure 3.1 demonstrates the different shapes and sizes of RFID tags.



Figure 3.1: RFID tags in various shapes and sizes (Coresonant, 2014)

3.1.1.1 Types of RFID Tags

Three types of RFID tags are in use, including active, passive and semi-passive ones, which are described below (Ahson and Ilyas, 2008).

Active tag: It contains its own power source in the form of a battery or a solar cell, which is used to power up its microchip and transmits the signal to the RFID reader. The active tag has a larger memory up to 128 kilobytes (Roberti, 2011), longer read range up to 100 metres, and greater processing power than other types of tags. On the other hand, the larger size and higher cost limit their popularity. These tags can be ideal for asset management in large systems.

Passive tag: It does not need any power source. It derives the power from the signal transmitted by the RFID reader and thus, there is a constraint on the read range of passive tags to receive a strong signal from the reader. The read range of passive tags is limited to 7 metres and typically, they can store from 64 bits to 1 kilobyte of data (Roberti, 2011). However, new passive tags can store up to 64 kilobytes of data in new Fujitsu models (Fujitsu, 2014). Passive tags are less expensive, smaller in size, and have a longer life than active ones and therefore, they are widely used in different applications. The focus of this research is devoted to this type of tag, where the limited memory space is of high consideration.

Semi-passive tag: It can also be called a semi-active tag and has a power source similar to active ones. This power source is used to power up the circuit on its microchip only. Semi-passive tags transmit the signal using the same way as that of passive tags, but at a higher rate. The overall features of semi-passive tags are located in between those of passive and active ones.

3.1.1.2 Types of Memory in RFID Tags

Tags come in different types based on their memory capabilities as follows (Finkenzeller, 2010).

Read-only tag: The information is permanently stored on the tags during manufacture or at the user's site. The communication between the tag and the reader is unidirectional from the former. If a read-only tag is placed in the reader region, the tag starts to broadcast its ID continuously. It is important to ensure that there is only one tag in the reader region, otherwise two or more tags will send their IDs simultaneously, which results in a collision and thus, the tags are unidentified by the reader. Despite this limitation, this type of tag is generally inexpensive and consumes low power. It also suits some applications where one tag ID is transmitted such as the identification of pallets, containers or animals. Read-only tags can operate at all frequencies of RFID systems.

Read-write tag: It is occupied by a writable memory, such as an electrically erasable programmable read-only memory (EEPROM) for passive tags and static random-access memory (SRAM) for active ones. The user can change the tag ID and add additional information to the tag's memory by the reader. This gives the user the flexibility to store and process information and therefore, eliminates the requirement for the back-end database server which is applicable for the autonomous operation of group integrity application. Read-write tags can process reader commands as well as support anti-collision and cryptological procedures. Similar to read-only tags, they can operate at all frequencies of RFID systems. However, they are more expensive and consume more power than read-only tags.

The RFID tags have four memory banks, as described in the EPCglobal Class-1 Generation-2 standard (EPCglobal, 2015):

Reserved memory: It stores the access and kill password and cannot store data besides these two passwords. The role of the 32-bit access password is to enable and disable the tag's write capabilities, whereas the 32-bit kill password permanently disables the tag. This memory bank is read and write protected, only being writable if a certain password needs to be specified.

EPC memory: It has a minimum of 96 bits of writable memory and it stores the 96-bit tag ID called the EPC, which uniquely identifies the physical object. The EPC memory also stores a 16-bit cyclic redundancy check code computed over the contents of the EPC code, and some control bits.

Tag manufacture information memory: It stores the information that describes the tag itself, including the manufacturer ID and a code that specifies the tag model. It may also contain information that describes tag capabilities.

User memory: It comes blank from the manufacturer and enables users to store additional data of different sizes based on the type of the tags (see subsection 3.1.1.1). This area of memory is used to store the information needed by the autonomous group integrity verification of this thesis.

3.1.1.3 Classes of RFID Tags

RFID Tags are constructed to comply with a specification called a class. The EPCglobal organisation describes six tag classes ranging from 0 to 5 that increasingly have greater capabilities and more features. These classes are grouped into generations. Generation-1 includes classes 0 and 1 and defines the physical and logical requirements for read-only passive tags. Generation-2 defines the physical and logical requirements for RFID system operating in the 860–960 MHz frequency range and includes classes 1–5. A general description of these classes is as follows (EPCglobal, 2015):

Class-0 and class-1 Generation-1: Provide the basic identification capability for read-only passive tags. Class 0 is for factory programmed tags, whereas class 1 is for user-programmable tags after manufacture;

Class-1 Generation-2: Defines read-write passive tags. The simulation settings in Chapter 9 follow the specifications of this class;

Class-2: Additional functionalities are added to read-write passive tags, including encryption and access control. It is not yet completed;

Class-3: Provides longer range and broadband communications for semi-passive tags that are powered by on-board batteries. It is not yet fully defined;

Class-4: Provides peer-to-peer communications and additional sensing for active tags. It is still in the early definition stage;

Class-5: Defines active tags that contain enough power to activate other tags and communicates with devices other than readers. It is also still in the early definition stage.

3.1.2 RFID Readers

An RFID reader is also called an interrogator since it queries the tags when they enter its range. It is an electronic device that can be used as a standalone or be integrated with other devices. The reader consists of a high frequency (HF) interface that has a transmitter and receiver, control unit, and one or more antennas. The antenna can be integrated into the reader, or it can be a separate device. Larger systems usually separate the antennas from the reader, whereas handheld units combine the two. The HF interface generates power to activate the tag, and sends and receives information from it. The control unit codes and decodes the signal received from the tag. It also uses a microprocessor to control the communication with the tag (Finkenzeller, 2010). In more complex RFID systems, the control unit usually performs some complex processes, including the execution of an anti-collision scheme, encryption and decryption of the transmitted data as well as authentication between tags and readers (Jia *et al.*, 2012). In addition, the control unit of this research needs to perform the decoding and filtering processes. The reader may be self-contained and store

the data internally or it may be a part of other systems such as a Wide Area Network (WAN). There is also a middleware, which controls the reader as well as the information from the tags. It forwards the gathered data to the database systems. It performs basic processes including integration, filtering, and controlling of the reader (Hunt *et al.*, 2007).

3.2 RFID Standards

RFID systems have a significant number of associated standards, with Figure 3.2 demonstrating the most relevant ones. The majority are defined by the International Standard Organisations (ISO) and the EPCglobal organisation. The standards cover three key areas of RFID applications and uses, including:

- 1) Air interface;
- 2) Conformance and interoperability between applications and RFID systems;
- 3) Data encoding and contents.

The purpose of RFID standards is to create a level of product consistency in the RFID industry and thus, enhance the efficiency of RFID systems, make the system more cost effective, and lead to industry development (Hunt *et al.*, 2007). The simulation settings in Chapter 9 follow the specifications of the EPCglobal standard.

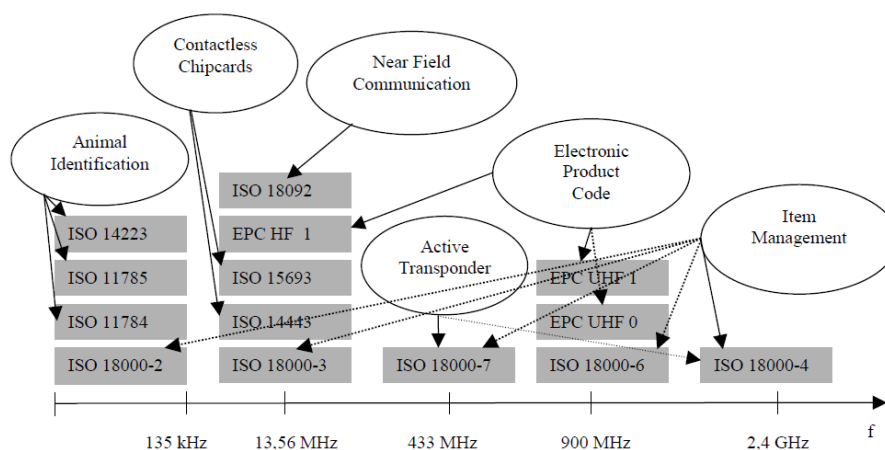


Figure 3.2: RFID system standards and frequency bands (Knospe and Pohl, 2004)

3.3 Operating Frequencies

A range of frequencies exists for the use of RFID systems and each of them has different capabilities. The use of tags, the read range needed, the material of the tagged item, and the type of surrounding environment determine the frequency required. Table 3.1 summarises the operating frequencies and their characteristics (Ward and Kranenburg, 2006; Hunt *et al.*, 2007; Datta, 2016). Whilst the protocols for the communications at UHF are defined in the EPCglobal standard, as used for the current research, other frequencies are also applicable for autonomous group integrity verification.

Criterion	Low Frequency (LF)	High Frequency (HF)	Ultra-High Frequency (UHF)	Microwave Frequency (MF)
Frequency range	125–134 KHz	13.56 MHz	860-960 MHz	2.45 or 5.8 GHz
Type of tag	Passive	Passive	Active and passive	Active and passive
Approximate read range	1–50cm	1.5m	4–7m for passive tags 100m for active tags	1m for passive tags 100m for active tags
Data transfer rate	< 10kbits/s	< 100kbits/s	< 100kbits/s	< 200kbits/s
Tag cost	High	Lower than LF tags	Lowest	Highest
Typical RFID applications	Access control, animal and vehicle identification	Smart cards, baggage handling, item tracking, and libraries	Toll collection, pallet tracking, baggage handling, warehouse management, and supply chain management	Toll collection and real time item tracking
Performance near metal or wet surface	Best ←—————→ Worst			
Number of tags read per second	Lowest ←—————→ Highest			
Power consumption	Lowest ←—————→ Highest			
Passive tag size	Largest ←—————→ Smallest			

Table 3.1: RFID system features at available frequencies

3.4 Data Coding

Data encoding is the process of interpreting binary data that are transferred between the tags and readers as line codes or a stream of symbols. Different coding schemes of data are used in RFID systems, as shown in Figure 3.3 The coding schemes can be classified into two main types as follows (Chabanne *et al.*, 2011):

Level coding: The logic value relates to the voltage level of the signal. The non-return to zero (NRZ) coding is an example of this type. In NRZ coding, a logic value 1 is coded by a high signal and a logic value 0 is coded by a low one;

Transition coding: The logic value relates to the difference between the two voltage levels of the signal. Manchester coding, the most commonly used coding scheme, generates a transition at the centre of the bit. It uses a positive transition to represent a logic value 0 and a negative transition to represent a logic value 1.

RFID systems usually use a different coding scheme for tag to reader communications than for reader to tag ones. The coding scheme should be selected with various considerations, including power sources of tags, bandwidth available, and collision detection ability. In the EPCglobal standard, UHF passive tags encode the data using FM0 or Miller coding whereas the reader uses Manchester coding.

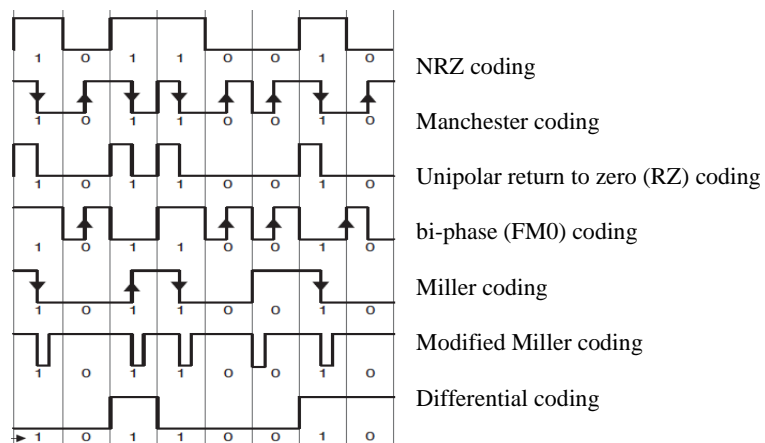


Figure 3.3: Data coding in RFID systems (Finkenzeller, 2010)

3.5 Multi-access Procedures (Anti-collision)

The operation of RFID systems usually involves reading multiple tags simultaneously, such as identifying the entire contents of a pallet at once for a group integrity checking process. A reader issues signals to interrogate the tag IDs or the information stored in them. This mode of communication is called multi-access and it is one of the key features of RFID systems. The communication channel between the reader and the tags has a certain capacity and it is specified by the data rate. The shared capacity must be divided between the tags in a way that their signals are transmitted to a single reader without collisions. Collisions occur when two or more tags transmit at the same time. Anti-collision protocols are of great importance to the performance of RFID systems in this research, because without them the tags have to retransmit their data when collisions occur, which consumes time and power. The existing anti-collision protocols are generally categorised into four techniques, including Space Division Multiple Access (SDMA), Frequency Domain Multiple Access (FDMA), Time Domain Multiple Access (TDMA) and Code Division Multiple Access (CDMA) techniques. The objective of these techniques is to receive a tag ID with low complexity, transmission power, and time delay (Shih *et al.*, 2006).

3.5.1 Space Division Multiple Access Technique

SDMA divides the channel into spatially separated domains. It can be implemented using multiple directive antennas and readers to reduce their reading range and to form an array of ranges in the space. Another way of implementing this technique is to use an electronically controlled directional antenna. The directional beam can be directed to a tag and thus, different tags can be distinguished by their angular location in the range of the reader. This multi-access technique is expensive and hence, is limited to a few particular applications (Finkenzeller, 2010).

3.5.2 Frequency Division Multiple Access Technique

FDMA allows different communication channels to work together simultaneously using different operating frequencies. This technique is implemented using tags with an adjustable communication frequency. A tag can receive any signal at the optimally suited reader frequency and then, respond to one of its available operation frequencies. For example, the communication channel from the reader to the tag operates on 135 KHz, whereas that from the tag to the reader operates in the range 860-960 MHz. A disadvantage of this technique is the cost since one reader must be available for each communication channel and therefore, it is limited to a few particular applications (Finkenzeller, 2010).

3.5.3 Code Division Multiple Access Technique

There are different variants of the CDMA technique based on how the spreading is done, but generally, each tag is assigned a different pseudo random binary sequence to spread its data over the entire spectrum. It provides multiple simultaneous communications using the same frequency operation and the reader is able to differentiate each signal from the others by their signatures. CDMA brings significant benefit in anti-collision for security purposes. However, it needs a very complicated system, which has restrained its adaption for RFID systems (Karmakar, 2010).

3.5.4 Time Division Multiple Access Technique

Most of the RFID communication systems use the TDMA technique, which allocates the available channel capacity to readers and tags with respect to time. Communications between the reader and the tags can be Tag-Talk-First (TTF) or Reader-Talks-First (RTF). TTF modes are very slow and inflexible and thus most applications use RTF modes. Generally, the signal from the reader synchronises the clocks of the tags. A reader starts each cycle of communication by transmitting commands and parameters in a time slot to select an

individual from a large group of tags. Then, the communication is established between the selected tag and the reader, with the selected tag subsequently responding. After reception of the tag's message, it can be muted or its transmission rate can be minimised. The RFID tag anti-collision protocols using TDMA techniques are mainly classified into Aloha-based and tree-based protocols (Sarangan *et al.*, 2008). In the next subsections, some of the more frequently used anti-collision protocols are presented. The protocols are briefed to a certain extent where the operational principle of the protocol can be understood without complications.

3.5.4.1 Aloha-based Protocols

The basic idea of ALOHA-based protocols is that the reader broadcasts a query request to the tags and then, each transmits its ID to the reader at the randomly generated time slots. Consequently, there is a certain possibility that more than one tag may transmit their IDs during the same time slot and in this case, the time slot turns out to be a collision one. On the other hand, if only one tag transmits its ID in a certain time, then the tag is successfully identified and will not participate in the subsequent process. ALOHA-based protocols are widely used in RFID systems. They are simple, have moderate performance, consume low power, and promise dynamic adaptability to different loads of RFID tags. However, they experience the problem of tag starvation, whereby a tag may never be identified because its signals collide every time (Shih *et al.*, 2006). In the following, some common ALOHA-based protocols are presented.

Pure Aloha Protocol: This protocol is the simplest of all the TDMA protocols. It is used exclusively with read-only tags, for which they send their tag IDs only. These data are transmitted to the reader in a cyclical communication. After receiving the reader's signal, the tag replies with its ID at a random time. Then, the tag waits for the reader's reply, which could be a positive acknowledgment (ACK), meaning the transmission was successful, or a negative acknowledgment (NACK), indicating the existence of a collision, in which case the

tag needs to retransmit the same information. Since the tags transmit their IDs randomly when signaled by the reader, without any control, collisions are inevitable. The efficiency of this protocol is degraded when reading a large group of tags (Liu and Lai, 2006).

Slotted Aloha (SA) Protocol: This protocol is an enhancement to the pure ALOHA protocol. In this protocol, the time is divided into a number of synchronous time slots and the reader controls this number. The transmission time of the tag's message is equal to the size of the slot. Each tag sends its ID in a predefined time slot. If collisions occur, tags retransmit their messages in other time slots after a random waiting time. The synchronisation among the tags is controlled by the reader. The synchronisation between the tags and the reader as well as the response to the tag at a predefined time decrease the probability of the collisions and therefore increase the performance of the protocol. However, it still has insufficient performance when the amount of tags is large (Liu and Lai, 2006).

Framed Slotted Aloha (FSA) Protocol: It is an improvement of the SA protocol where a tag is allowed to send only once in a frame. It contains frames and read cycles as well as the slots. A frame contains a number of time slots and a read cycle involves a frame to read the tag IDs or identify the tags. The frame size is fixed during the identification process. The reader starts each cycle of the reading with a request message containing the frame size and a random number. Then, each tag uses the random number to select a slot in the subsequent frame and replies in that slot. If no tag responds in the slot, the slot is said to be empty. If one tag responds, the slot is treated as a singleton slot, whilst if two or more tags respond, the slot turns out to be a collision one. Singleton or collision slots can also be called nonempty slots. The unidentified tags must respond in the next read cycle and this process is repeated until all the tags have transmitted their message successfully (Zhen *et al.*, 2005). Because of the fixed frame size of the FSA protocol, its performance degrades when there is unexpected variation

in the amount of tags. Moreover, additional delay will result when a large frame size is used with fewer tags (Liu and Lai, 2006).

Dynamic Frame Slotted Aloha (DFSA) Protocol: In the DFSA protocol, the reader can adjust the frame size in each read cycle of the communication between the reader and the tags. The frame size is determined by collecting the information about the previous read cycle, including the number of singleton (C_1), empty (C_0) and collision (C_k) slots. This information is used to estimate the number of tags for the current round and thus, adapt the frame size accordingly (Huang and Le, 2007). Generally, when the number of tags is large, the probability of collisions is minimised by increasing the frame size. On the other hand, when the number of tags is small, the frame size is decreased. The performance of this protocol is better than that of the FSA protocol since setting the frame size to the number of tags will achieve the lowest identification delay. However, if the number of tags increases its performance degrades, because the frame size cannot be increased indefinitely beyond 256 for the accuracy of the estimation techniques. Hence, this protocol performs well when the number of tags is quite small (Vogt, 2002b; Kaewsirisin *et al.*, 2008). The DFSA algorithm has several versions, depending on the estimation technique that change the frame size. The main difference amongst these techniques is how and what they estimate. Accuracy is the primary requirement of a tag estimation technique, for inaccurate ones cause empty or collided slots, which consumes time and power. The popular and most accurate tag estimation functions, as evaluated by (Klair *et al.*, 2007) are briefly explained below.

Vogt (2002a; 2002b) proposed two estimation techniques. One is based on a simple assumption that at least two tags can cause a collision. The number of estimated tag n_{est} is calculated in each read cycle, as:

$$n_{est} = C_1 + 2C_k \quad (3.1)$$

The second technique is based on the Chebyshev inequality principle, which aims to reduce the distance between the actual read result vector $\langle C_0, C_1, C_k \rangle$ and the theoretical calculated result vector $\langle E_0^{f,n}, E_1^{f,n}, E_k^{f,n} \rangle$, as:

$$n_{est} = \min \left| \begin{pmatrix} E_0^{f,n} \\ E_1^{f,n} \\ E_k^{f,n} \end{pmatrix} - \begin{pmatrix} C_0 \\ C_1 \\ C_k \end{pmatrix} \right| \quad (3.2)$$

where, f is the current frame size, n is the number of tags, $E_0^{f,n}$ represents the expected number of empty slots, $E_1^{f,n}$ is the expected number of singleton slots, and $E_k^{f,n}$ is the expected number of collision slots. The probability that r tags reply in one slot is a binomial distribution, as:

$$p(y = r) = \binom{n}{r} p^r (1 - p)^{n-r} \quad (3.3)$$

where, p is success probability and y is a random variable. Since each slot in the frame has equal probability, Equation (3.3) can be written, as:

$$p(r) = \binom{n}{r} \left(\frac{1}{f}\right)^r \left(1 - \frac{1}{f}\right)^{n-r} \quad (3.4)$$

Therefore, the expected number of slots filled with r responding tags out of n is given by:

$$E_r^{f,n} = f \binom{n}{r} \left(\frac{1}{f}\right)^r \left(1 - \frac{1}{f}\right)^{n-r} \quad (3.5)$$

From Equation (3.5), the values of $E_0^{f,n}$, $E_1^{f,n}$, and $E_k^{f,n}$ can be calculated, as:

$$E_0^{f,n} = f \left(1 - \frac{1}{f}\right)^n \quad (3.6)$$

$$E_1^{f,n} = n \left(1 - \frac{1}{f}\right)^{n-1} \quad (3.7)$$

$$E_k^{f,n} = f - E_0^{f,n} - E_1^{f,n} \quad (3.8)$$

Cha and Kim (2006) also proposed two tag estimation techniques. The first simply estimates the number of tags, as:

$$n_{est} = C_1 + 2.39C_k \quad (3.9)$$

The second estimation technique is based on the calculation of the ratio of the number of collided slots to the frame size, as:

$$C_{ratio} = \frac{C_k}{f} \quad (3.10)$$

By substituting the value of C_{ratio} into the following equation:

$$C_{ratio} = 1 - \left(1 - \frac{1}{f}\right)^{n_{est}} \left(1 + \frac{1}{f}\right) \quad (3.11)$$

the value of n_{est} can be calculated after each read cycle.

The aforementioned simple techniques are easier to implement and have low computational overheads. They are more accurate for low amounts of tags. However, their accuracy decreases when the number of tags is increased due to the usage of the constant multiplier, which does not take into account the collisions of a large number of tags in a slot. On the other hand, the second techniques are more robust for a large number of tags, because they use the read results after each cycle and the theoretical calculated values at the expense of computation overheads (Klair *et al.*, 2007).

EPCglobal has also developed a tag estimation algorithm called Q -algorithm which is specified in the standard. The algorithm needs the reader to increase or decrease the frame size with a constant. First, the reader broadcasts a request message containing a slot counter Q and a frame of size $2Q$, where Q is an integer in the range $0 \leq Q \leq 8$. Each tag selects a slot randomly in the range $[0 - (2Q-1)]$. In the case of a collision slot, the reader increases Q by a constant c where $0.1 \leq c \leq 0.5$. For an idle slot, it decrements the value of Q by c . A slot that has a single response does not change the value of Q . The frame size of the next round is then set based on the resulting value of Q . This algorithm can enhance the read performance when the number of tags is much larger or smaller than the frame size (Chen and Kao, 2011).

Enhanced Dynamic Frame Slotted Aloha (EDFSA) Protocol: To solve the problem of identifying large numbers of tags, Lee *et al.* (2005) proposed the EDFSA protocol by restricting the number of responding tags to nearly equal to the frame size to achieve optimal system efficiency. When the number of responding tags exceeds the maximum frame size

(i.e. 256), the tags are split into a number of groups in order to achieve optimal system efficiency. In each read cycle, the number of unread tags is estimated using Equation (3.). If the estimated number of unread tags is much larger than the maximum frame size that gives the optimal system efficiency, those unread ones are split into a number of groups. Only one group of unread tags is allowed to reply to the reader. The number of groups M is computed, as:

$$M = \left\lceil \frac{\text{The number of estimated tags}}{\text{the maximum frame size}} \right\rceil \quad (3.12)$$

and the system efficiency is calculated, as:

$$\text{System Efficiency} = \frac{\text{The number of singleton slots}}{\text{the current frame size}} \quad (3.13)$$

Then, the reader sends a request including the number of groups and a random number to the tags. The tags receiving the request message use the random number and their tag IDs to generate a new number and then, divide it by the number of groups. Only the tags that have a zero remainder reply to the reader. When the number of estimated tags is much smaller than the maximum frame size, the reader reduces the frame size without grouping and in this case it sends a request message with the number of groups equal to 1. The reader estimates the number of unread tags and adapts the frame size after each read cycle. This process is repeated until all the tags have been read. Table 3.2 illustrates the values of M for different tag ranges. The authors also proposed the optimal frame sizes for various tag ranges to achieve optimal system efficiency. When the number of unread tags is less than 355, the value of M is one which allows every unread tag to respond. On the other hand, when the number of unread tags increases, the group of tags is divided into M groups and thus, the reader read tags on a group basis. This type of protocol is one of the existing solutions that is implemented and compared with the designed protocol in Chapter 9.

The number of unread tags	Frame size	The number of groups M
1 – 11	8	1
12 – 19	16	1
20 – 40	32	1
41 – 81	64	1
82 – 176	128	1
177 – 354	256	1
355 – 707	256	2
708 – 1416	256	4
1417 – 2831	256	8

Table 3.2: The number of tags versus the optimal frame size and the number of groups in the EDFSA (Lee *et al.*, 2005)

3.5.4.2 Tree-based Protocols

In tree-based protocols, collisions are reduced by building tree traversing approaches. When a collision occurs, the reader divides the tags into two subgroups and queries that with fewer tags. The reader continues to divide the tags until all the tags have been successfully identified (Capetanakis, 1979). A weak point of these protocols is that they must restart the reading process when new tags enter the reader's range while other tags are being read. In addition, they are complex and require more time to identify tags than that for the ALOHA-based protocols. However, they are free of the tag starvation problem (Shih *et al.*, 2006). The tags get divided into subgroups based on different algorithms. In the following, some common algorithms are introduced.

Tree Splitting Algorithm: This algorithm operates by splitting collided tags into b subgroups using a b random number generator and these subgroups become smaller until they contain just one tag. Each tag has a counter to maintain its position in the tree and when its value is zero, the tag enters the transmit mode. Otherwise, the tag enters the sleep or wait mode. In the case of a collision, the tag in the transmit mode generates a random number and adds it to the value of its counter, whilst tags in the wait mode increment their counter by one. When the

reader receives a single reply, the tags in the wait mode decrease their counter by one. All tags enter the sleep mode after being identified (Hush and Wood, 1998).

Query Tree Algorithm: In this algorithm, the reader broadcasts a prefix to all tags in its region. Then, a tag the ID of which matches the prefix replies to the reader. When a collision occurs, the reader appends the prefix with a binary 0 or 1 until none exists. Once a tag is identified, the reading cycle is terminated and a new one is issued with a new prefix (Law *et al.*, 2000). Some extensions to the query tree have been proposed in Law *et al.* (2000) to enhance the performance of the original algorithm, as follows:

- 1) *Shortcutting:* The reader appends the prefix with the binary 0 and 1, subsequently pushing the two new prefixes onto the stack. The reader then transmits one of the prefixes. If there is no reply, this means that two or more tags have the second new prefix. In this case, if the reader sends the second new prefix, a collision will exist. Thus, it removes the second new prefix from the stack and appends it with the binary 0 or 1 and then, pushes them onto the stack instead.
- 2) *Aggressive advancement:* The reader appends the prefix with multiple bits instead of just one.
- 3) *Categorisation:* If a group of tag IDs has the same prefix, the identification process can be enhanced by identifying each group independently.
- 4) *Incremental matching:* This algorithm minimises the length of the transmitted prefix by requiring the tags to store the last prefix. Therefore, instead of sending the same prefix appended with the binary 0 or 1, the reader sends only bit 0 or 1 in the next read cycle.

Binary Search Algorithm: In this algorithm, the reader recognises the position of the collided bit by using Manchester coding. When a collision occurs, the reader divides tags into subgroups based on the collided bits. To show the benefit of using this coding in tracing out the collided bit, its collision behaviour is compared with NRZ coding. If at a time at least one

tag sends a signal, the reader interprets the received signal using the NRZ coding as a high signal and decodes it as logic value 1, as shown in Figure 3.4. In this case, the reader cannot trace back the decoded signal and decide whether it is from one tag or many tags. The transmission error in the data block can be detected by using the block checksum. On the other hand, when two or more tags send different data simultaneously, the positive transitions cancel the negative transitions using the Manchester code. If there is no transition, it is interpreted as a collision having occurred between at least two tags, as depicted in Figure 3.5. In both coding schemes, when two or more tags send identical data simultaneously, they successfully received and interpreted by the reader. This feature is utilised to read redundant tag information in the designed protocol in Chapter 9.

The binary search algorithm divides the collided tags into two groups. Those that have first collided bit 0 are allowed to send in the subsequent request, whilst the tags with first collided bit 1 are not allowed to do so. Assume that there are four tags and their tag IDs are of 8-bits. Initially, the reader sends a request message asking all tags that have IDs less than or equal to 11111111 to reply. All tags will reply with their tag IDs to the reader, thus resulting in collisions in some bits. Assume collisions occurred in the received tag ID at bit 0, bit 3 and bit 5, then clearly bit 5 is the highest collided bit. This indicates that there is at least one tag the ID of which is less than 11011111. The reader sends a new request message asking tags that have IDs less than or equal to 11011111 to reply in the next read cycle. Now assume that the received tag IDs have collisions at bit 4. Again, the reader sends a request message to the tags that have the tag IDs less than or equal to 11001111 to reply in the next read cycle. Tag 2 only replies in this round and is thus, identified by the reader. By repeating these procedures, all tags are identified (Finkenzeller, 2010).

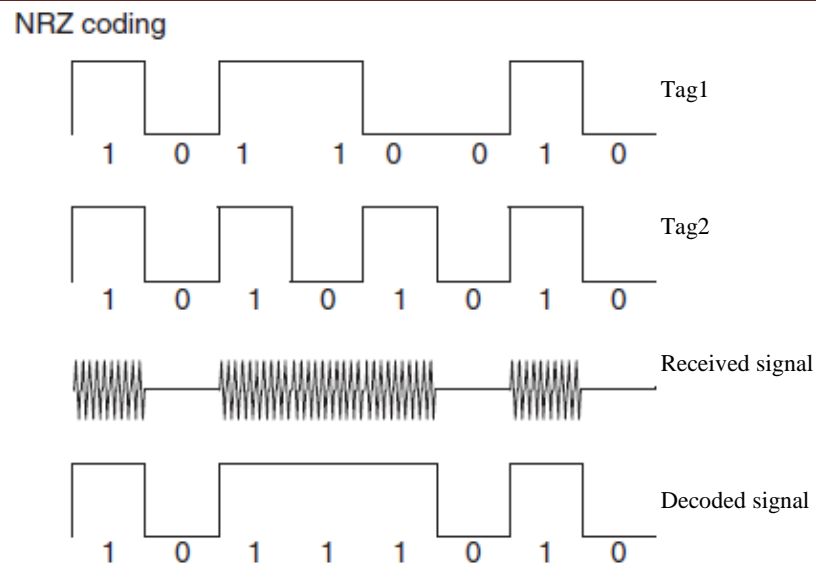


Figure 3.4: Collision behaviour of NRZ coding (Finkenzeller, 2010)

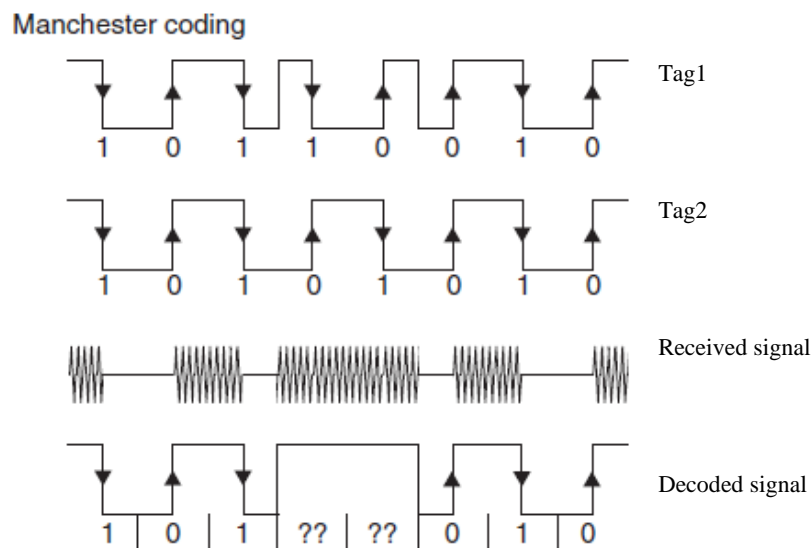


Figure 3.5: Collision behaviour of Manchester coding (Finkenzeller, 2010)

3.6 Conclusions

An overview of RFID systems has been presented in this chapter, providing all the necessary and important bases for the thesis. Specifically, there has been explanation of the main system components, the standards, and the operating frequencies. The different types of tags have been reviewed, concentrating on their important features directly in relation to the

thesis, including the types of memory. There has also been coverage of the differences between ALOHA-based and tree-based anti-collision protocols, including a detailed explanation to help understand how the protocols work. Their advantages and limitations have been highlighted as well.

4 LDPC Codes

In modern communication systems, transmissions can be affected by data loss caused by router congestion, intermittent connectivity, or poor channel situations. In such cases, erasure codes represent the main solution. They are a type of forward error correction codes for the BEC that has been used for modelling the transmission of data over the Internet (Ryan and Lin, 2009). This channel was introduced by Elias in 1955 (Elias, 1955). A transmitted bit is either completely erased with probability p or correctly received with probability $1 - p$. Elias proved that there exist codes of rate R for any $R < 1 - p$ that can be used to transmit over channels of capacity $1 - p$. Erasure codes rely on augmenting the transmitted message bits with some redundant information called parity check bits and the resulting message is called a codeword. The parity check bits are inserted in such a way that each codeword is adequately distinct from one another and thus, allowing receivers to recover the original message (Huffman and Pless, 2003). Among the different classes of erasure codes, the attention in this thesis is limited to LDPC codes, because of their sparseness, which suits the limited memory space of passive tags. In addition, they exhibit good erasure recovery capabilities and comparably low decoding complexity (Liva *et al.*, 2009). This chapter provides a comprehensive overview of LDPC codes in the BEC with a focus on the encoding process, the most prominent decoding algorithms, and various construction techniques. This chapter provides sufficient relevant preliminary information for comprehending the subsequent ones.

4.1 Preliminaries and Notations

LDPC codes were first introduced by Gallager in 1962 (Gallager, 1962). They are codes the parity check matrices of which, as the name implies, are sparse. In other words, the parity check matrix H of an LDPC consists of low density of “1” entries and this characteristic suits the limited memory space of passive tags. Each column of H relates to a bit in the codeword and each row to a parity check equation. The parity check matrix H is of size $m \times n$, where m is the number of parity check bits and n is the length of the codeword. A parity check matrix is said to be regular when every column of H has the same weight j (the number of “1” entries in each column) and every row has the same weight l (the number of “1” entries in each row), where $l = j \times (n/m)$ and $j < l$. If the number of “1” entries in each column or row is not constant, then the code is an irregular LDPC one (Shedsale and Sarwade, 2012). LDPC codes are usually represented as (n, j, l) LDPC code or as (n, k) LDPC code, where k is the number of message bits.

The theory of LDPC codes is connected to a field of mathematics called graph theory and some basic notations and definitions used in it are briefly presented in what follows (Tomlinson *et al.*, 2017).

Definition 1: (*Node, Edge, Neighbouring*) A graph, represented by $P(V, E)$, contains an ordered set of nodes and edges.

- A **node** (or a **vertex**) is usually represented as a dot. The set $V(P)$ contains nodes of $P(V, E)$. If v is a node of $P(V, E)$, it is represented as $v \in V(P)$. The notation $|V(P)|$ denotes the cardinality of the nodes.
- An **edge** (u, v) joins two nodes $u \in V(P)$ and $v \in V(P)$ and it is represented as a line joining the two. The set $E(P)$ consists of two nodes of $V(P)$.

- If $(u, v) \in E(P)$, then $u \in V(P)$ and $v \in V(P)$ are **neighbouring** nodes of $P(V, E)$. In the same way, the two nodes are connected to the edge (u, v) .

Definition 2: The **degree** of a node $v \in V(P)$ is the number of edges that are connected to it.

Definition 3: The **Bipartite** or **Tanner graph** $P(V, E)$ contains two disjoint sets of nodes, $V_v(P)$ and $V_c(P)$, such that $V(P) = V_v(P) \cup V_c(P)$, and every edge $(v_i, c_j) \in E(P)$, such that $v_i \in V_v(P)$ and $c_j \in V_c(P)$ for some integers i and j .

The matrix defined in (4.1) is an example of a 5×10 parity check matrix for the regular $(10, 2, 4)$ LDPC code.

$$H = \begin{matrix} & v_1 & v_2 & v_3 & v_4 & v_5 & v_6 & v_7 & v_8 & v_9 & v_{10} \\ \left. \begin{matrix} 1 & 1 & 1 & 1 & 0 & 0 & 0 & 0 & 0 & 0 \\ 1 & 0 & 0 & 0 & 1 & 1 & 1 & 0 & 0 & 0 \\ 0 & 1 & 0 & 0 & 1 & 0 & 0 & 1 & 1 & 0 \\ 0 & 0 & 1 & 0 & 0 & 1 & 0 & 1 & 0 & 1 \\ 0 & 0 & 0 & 1 & 0 & 0 & 1 & 0 & 1 & 1 \end{matrix} \right\} & \begin{matrix} c_1 \\ c_2 \\ c_3 \\ c_4 \\ c_5 \end{matrix} \end{matrix} \quad (4.1)$$

LDPC codes are usually exemplified in graphical ways using a Tanner graph (Tanner, 1981). It gives a complete illustration of the code and it helps in the explanation of the decoding process. The Tanner graph contains two groups of nodes, which are n variable nodes for the codeword bits, and m parity check nodes for the parity check equations. An edge connects a variable node to a parity check node, if that variable node is contained in the related parity check equation. Therefore, the number of edges in the Tanner graph is equivalent to the number of “1” entries in H (Richardson and Urbanke, 2001).

Definition 4: A **cycle** in a Tanner graph is a sequence of joined nodes that starts and ends at the same node, which contains other nodes no more than once. The length of a cycle is the number of edges it includes.

Definition 5: The **girth** of a Tanner graph is the minimum cycle length of the graph. The **local girth** of a node $v \in V(P)$ is the length of the shortest cycle that passes through that node.

Since the Tanner graph is bipartite, the minimum length of a cycle is four. Short cycles, especially of length 4 degrade the iterative decoding performance of LDPC codes as will be explained in subsection 4.3.1 (Ryan, 2003). Figure 4.1 shows the Tanner graph of H defined in Equation (4.1). The variable nodes are represented by circles while the parity check nodes are squares and a cycle of length 6 is exemplified by the bold edges.

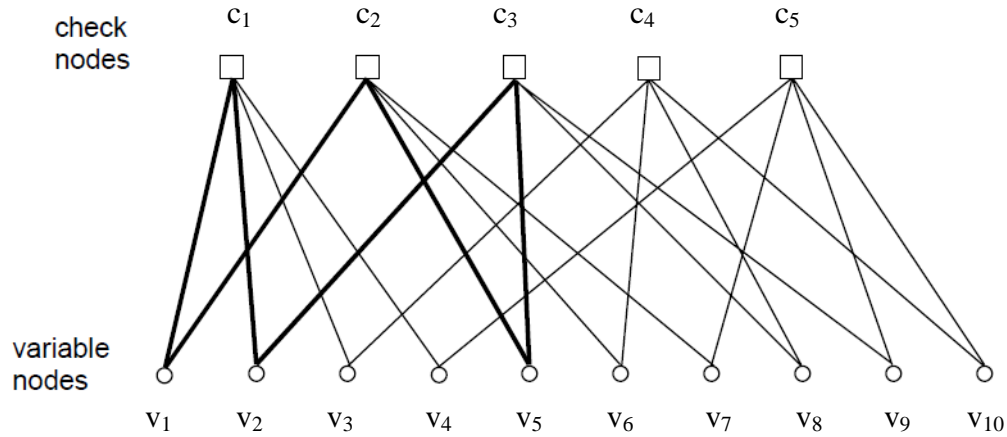


Figure 4.1: The Tanner graph illustration of H in Equation (4.1) (Ryan, 2003)

For an irregular LDPC code, the variable and parity check node degree sequences are used to represent the code. The polynomials:

$$\Lambda_{\lambda}(x) = \sum_{i \geq 1} \lambda_i x^i \quad (4.2)$$

and

$$\Lambda_{\rho}(x) = \sum_{i \geq 1} \rho_i x^i \quad (4.3)$$

specify the variable and parity check degree sequence, respectively, where λ_i and ρ_i are the fractions of nodes of degree i (Tjhai, 2007). Degree sequences should satisfy:

$$\sum_{i \geq 1} \lambda_i = 1 \quad (4.4)$$

and

$$\sum_{i \geq 1} \rho_i = 1 \quad (4.5)$$

For example,

$$\Lambda_\lambda(x) = 0.4x^2 + 0.27x^3 + 0.24x^6 + 0.09x^9 \quad (4.6)$$

means that 40%, 27%, 24%, and 9% of the columns have weights of 2, 3, 6, and 9, respectively, whereas,

$$\Lambda_\rho(x) = 0.70x^{13} + 0.30x^{14} \quad (4.7)$$

means that 70% and 30% of the rows have weights of 13 and 14, respectively. Another representation considers the fraction of edges that are linked to the nodes of degree i . The former representation is used throughout this thesis.

4.2 Encoding Process

A message of k bits can be encoded using a generator matrix G . The encoding process introduces redundancy of size m bits, where $m = n - k$. If the k message bits are represented by the vector $u = [u_1, u_2, \dots, u_k]$, the codeword x of a binary message u can be generated using:

$$x = uG \quad (4.8)$$

where the operation is carried out under modulo-2 arithmetic. The ratio k/n is the rate of the code which represents the amount of redundancy introduced by the code, where higher rate means smaller m and vice versa. For a regular code, the rate can also be expressed as $1 - j/l$, since $m \times l = j \times n$. Generally, a code can have any values of m , however, only $n - k$ of them will be linearly independent and thus, the rank of H is equal to $n - k$. The generator matrix is usually constructed by performing the Gauss-Jordan elimination on H to transform it into:

$$H = [-P, I_m] \quad (4.9)$$

where P is an $m \times k$ matrix and I_m is the identity matrix. The identity matrix, I_m , is an $m \times m$ matrix with “1” entries on the diagonal from the top left corner to the bottom right corner and “0” entries elsewhere. The generator is then formed, as:

$$G = [I_k, P^T] \quad (4.10)$$

where, $(.)^T$ denotes the transpose of its argument. A code is called systematic, if the first k codeword bits represent the message bits. In this case the first k columns of the generator matrix represent the $k \times k$ identity matrix, otherwise, it is called non-systematic code (Gravano, 2001). Transforming H into the desired form as in Equation (4.10) needs $O(n^3)$ operations. The limitation of encoding through G is that the submatrix P^T is not sparse and thus, the encoding complexity is $O(n^2)$ (Ryan and Lin 2009). Therefore, Richardson and Urbanke (2001) proposed an effective encoding method that takes advantage of the parity check matrix sparseness. The encoding overhead can be minimised to, at most, $O(n + g^2)$, where g is a small constant, and in the worst circumstances as a small fraction of n . The columns and rows of H are, firstly, permuted into an approximate lower-triangular form, as shown in Figure 4.2.

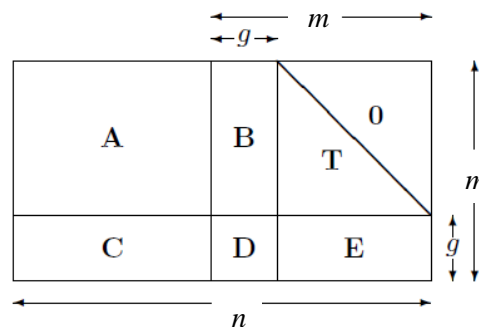


Figure 4.2: The parity check matrix in the approximate lower-triangular form (Richardson and Urbanke, 2001)

The five matrices A , B , C , D , and E are sparse, whereas the matrix T is in a lower triangular form which has “1” entries on the diagonal. The result can be written, as:

$$H = \begin{pmatrix} A & B & T \\ C & D & E \end{pmatrix} \quad (4.11)$$

Then, GE is applied to E to zero out the matrix which is similar to multiplying Equation (4.11) by:

$$\begin{pmatrix} I & 0 \\ ET^{-1} & I \end{pmatrix} \quad (4.12)$$

To get:

$$\begin{pmatrix} A & B & T \\ -ET^{-1}A + C & -ET^{-1}B + D & 0 \end{pmatrix} \quad (4.13)$$

The source vector u of length k can be encoded as $c = [u, p_1, p_2]$, where p_1 and p_2 denote the parity part of length g and $m-g$, respectively. More precisely, p_1 and p_2 are calculated so that the codeword c must satisfy Equations (4.14) and (4.15), as:

$$Au^T + Bp_1^T + Tp_2^T = 0 \quad (4.14)$$

$$(-ET^{-1}A + C)u^T + (-ET^{-1}B + D)p_1^T = 0 \quad (4.15)$$

Following the same interest, Mackay (2005) proposed the staircase codes, where the parity check matrix is divided into two submatrices. The left submatrix H_1 is an $m \times k$ submatrix, the columns of which, relate to message bits. The right submatrix H_2 is an $m \times m$ submatrix with columns relating to parity check bits of weight 2 or less arranged in a staircase structure, as:

$$H = \left[\begin{array}{cccccc|ccccc} 0 & 1 & 1 & 0 & 1 & 0 & 1 & 0 & 0 & 0 & 0 & 0 \\ 1 & 0 & 0 & 1 & 1 & 0 & 1 & 1 & 0 & 0 & 0 & 0 \\ 0 & 1 & 0 & 1 & 0 & 1 & 0 & 1 & 1 & 0 & 0 & 0 \\ 1 & 0 & 1 & 0 & 0 & 1 & 0 & 0 & 1 & 1 & 0 & 0 \\ 0 & 0 & 1 & 0 & 1 & 1 & 0 & 0 & 0 & 1 & 1 & 0 \\ 1 & 1 & 0 & 1 & 0 & 0 & 0 & 0 & 0 & 0 & 1 & 1 \end{array} \right] \quad (4.16)$$

The staircase structure converts the codes into systematic forms and thus, it can be easily encoded in a linear time. If the data u are loaded into the first k bits of the codeword, then the m parity bits $p_1 \dots p_m$ can be calculated one at a time from left to right in a linear time, using only the message bits and the previously computed parity check bit, as:

$$\begin{aligned}
P_1 &= \sum_{n=1}^k H_{1n} u_n \\
P_2 &= P_1 + \sum_{n=1}^k H_{2n} u_n \\
P_3 &= P_2 + \sum_{n=1}^k H_{3n} u_n \\
&\vdots \\
P_m &= P_{m-1} + \sum_{n=1}^k H_{mn} u_n
\end{aligned} \tag{4.17}$$

The encoding overhead is $O(n)$, if the sparsity of the matrix H is exploited when calculating the sums in Equation (4.17). Unlike encoding in the BEC, the autonomous group integrity verification utilises an $m \times n$ parity check matrix of an LDPC code as a group generator matrix to encode a group of tag IDs of size n . Further details are given in Chapter 5.

4.3 Decoding Algorithms

A received codeword y , is said to be valid, if it satisfies:

$$Hy^T = 0 \tag{4.18}$$

Denoting the number of erasures by $n_e \in \{1, 2, \dots, n\}$, the received codeword with erasures can be represented, as:

$$H_k y_k^T = H_k y_k^T \tag{4.19}$$

where, y_k means the set of loss bits of length n_e of the codeword, and y_k refers to the set of known bits of length $n_e = n - n_e$. Similarly, H_k is the matrix containing the columns of H related to y_k , whereas H_k is the matrix containing the columns of H related to y_k . The capability of a code to recover erasures is measured by the minimum Hamming distance d_{min} of the code. The Hamming distance between two codewords is the number of bit positions in which they differ, whereas the d_{min} represents the smallest Hamming distance between any pair of the codeword. A code has a good distance, if d_{min}/n tends to a constant greater than zero. Gallager (1962) found that a typical (n, j, k) LDPC code with a fixed $j \geq 3$ has a d_{min} that grows linearly with n . Column weight j has also been proven to affect the d_{min} . Increasing only the column weight j or increasing it together with row weight l will increase the value of m and thus, decrease the rate. However, the d_{min} is increased accordingly. A code of minimum

distance d_{min} can recover, at most, $d_{min} - 1$ erasures. If the code can recover from any set of k coordinates of the codeword, that is, if $d_{min} - 1 = n - k$, the code is optimal with respect to recovering erasures (Luby *et al.*, 2001a; Ryan and Lin, 2009). On the other hand, analysis conducted by Tomlinson *et al.* (2007) of the erasure recovering performance of linear binary codes has proven that many (n, k) codes, such as the extended Bose, Chaudhuri, and Hocquenghem (BCH) codes and extended quadratic residue codes, can recover, on average, nearly $n - k$ erasures. It is also been proven that codes designed with iterative decoding, including the turbo and LDPC codes, exhibit weak performance compared to algebraic codes designed for maximum d_{min} . Table 4.1 illustrates the average number of recovered erasures for some analysed codes.

The performance of LDPC codes under any decoding algorithm over the BEC is usually described by plotting the Frame-Error-Rate (FER) or the Bit-Error-Rate (BER) curve as a function of the erasure probability. The behaviour of the curve typically consists of three regions. The first, known as the error floor region, occurs at smaller values of erasure probability and it shows the decoding failure to recover some erasures. As the erasure probability is increased, the error rate starts to increase rapidly forming a waterfall region. The dramatic change in the error rate with the increase of erasure probability depends on the type of the decoding algorithm. The third region, known as the erroneous region, occurs at higher values of erasure probability and it shows the inability of the decoder to recover nearly all of the erasures. In the next subsections, the most prominent decoding algorithms over the BEC that employed in this research are presented.

(n, k, d_{min}) Code	Average number of recovered erasures
(128, 99, 10) Extended BCH Code	27.44
(256, 207, 14) Extended BCH Code	47.4
(512, 457, 14) Extended BCH Code	53.4
(200, 100, 32) Extended Quadratic Residue	98.4
(200, 100, 10) PEG-LDPC Code	93.19
(240, 120, 16) Turbo Code	116.5

Table 4.1: the average number of recovered erasures for some analysed codes in Tomlinson *et al.* (2007)

4.3.1 Iterative Decoding Algorithms

Luby *et al.* (2001a) were the first who successfully applied iterative (IT) decoding algorithms for LDPC codes over the BEC. The IT decoding is also known as a message-passing algorithm and is equivalent to Gallager's soft decoding algorithm (Gallager, 1962). Whilst the IT decoding is suboptimal in recovering erasures, it has the advantage of demonstrating a linear decoding complexity of $O(n)$ (Richardson and Urbanke, 2008). The IT decoding algorithm recovers erasures by recursively exchanging messages along the edges of a Tanner graph between variable nodes and parity check nodes. Firstly, all parity check equations having only one erased bit are found and the erased bits are recovered. Then, new equations that have only one erased bit may be formed and used to recover further erased bits. The decoding process can be simplified as follows (Johnson, 2009):

- 1) Each variable node v_i sends the same message $M_{v_i} \in \{0, 1, e\}$, where e denotes the erased bit, to each of its connected parity check nodes;
- 2) If a parity check node receives only one e , it replaces the erased bit with the XOR of the known bits in its check equation;
- 3) Each parity check node c_j sends different messages $E_{c_j v_i} \in \{0, 1, e\}$ to each of its connected variable nodes v_i . These messages represent the results of the previous step;
- 4) If the variable node of an erased bit receives $E_{c_j v_i} \in \{0, 1\}$, the variable node updates its value to the value of $E_{c_j v_i}$.

The IT decoding algorithm iterates the above process until all the erasure bits have been recovered successfully or a predetermined maximum number of iterations I_{max} has passed without successful decoding due to the existence of stopping sets (Di *et al.*, 2002). A stopping set is a set of variable nodes, such that all parity check nodes (neighbours) of the set are connected to the set at least twice. It is also a set of linearly dependent columns of H . In

general, a stopping set consists of multiple cycles and the only stopping set that contains a single cycle is one that contains all degree-2 variable nodes (Tian *et al.*, 2003). Figure 4.3 shows an example of a stopping set containing variable nodes v_7 , v_8 , v_9 , and v_{10} and marked by bold lines. The size of a stopping set is the number of variable nodes it contains. They play a vital role in the IT decoding algorithm of LDPC codes over the BEC. If all stopping set symbols are erased, none of them can be recovered. The minimum stopping set size of a code identifies the minimum number of erasures causing a decoding failure (Di *et al.*, 2002), which is termed the stopping distance, d_{stop} . Generally, the performance of the IT decoding algorithm is limited by the number and size of the minimum stopping sets. Hence, a good LDPC code must have no or very few small stopping sets. Orlistky *et al.* (2002; 2005) proved that the sizes of minimum stopping sets of regular (n, j, l) LDPC codes with girths 4, 6, and 8, are 2, $j + 1$, and $2 \times j$, respectively. Tian *et al.* (2003) proved that a code that has a d_{min} includes at least one small stopping set of size d_{min} . Therefore, avoiding all small stopping sets of size $d_{stop} \leq t$ guarantees that $d_{min} > t$. Since a stopping set contains cycles, removing short cycles decreases the probability of small stopping sets. Di *et al.* (2002) showed that in the BECs the remaining set of unrecovered erasures after the IT decoding is equal to the maximum size stopping set. The distribution of the stopping set in LDPC codes defines the erasure patterns for which the IT decoding will not succeed on the BEC. Finding the stopping set distribution of any parity check matrix is a difficult process. However, the average stopping set distribution can be found instead. This process is known as a finite-length analysis. It involves computing the exact average bit and error probabilities for any regular LDPC codes.

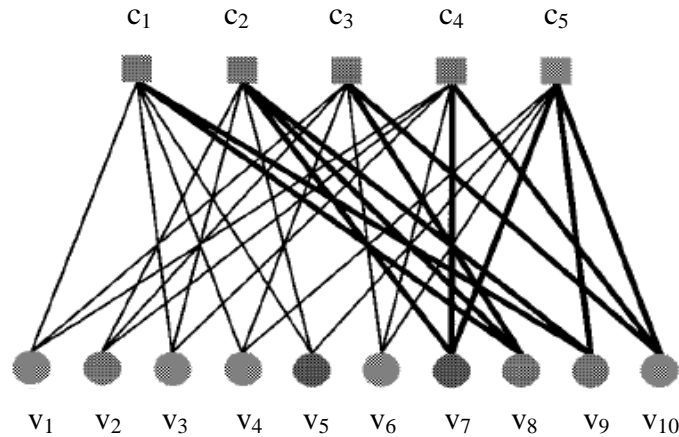


Figure 4.3: An example of a stopping set (Di *et al.*, 2002)

4.3.2 Maximum Likelihood Decoding Algorithms

Maximum likelihood (ML) decoding algorithms on the BEC turn into solving the system of m linear equations and finding n_e unknowns (erasures) in Equation (4.19). According to Di *et al.*, (2002), optimal decoding is possible, if Equation (4.19) has a unique solution. The system of linear equations has a unique solution, if and only if, the columns of H_k are linearly independent or the matrix H_k has full column rank, that is, $\text{rank}(H_k) = n_e$. Since H_k has m rows, its columns can be linearly independent only, if $|y_k| \leq m$. In addition, since any $d_{\min} - 1$ columns of H and thus, columns of H_k are linearly independent, the system of linear equations is solvable whenever $|y_k| < d_{\min}$ (Ryan and Lin, 2009). For solving a system of linear equations, three classes of algorithms were proposed. The first, contains the conjugate gradient and Lanczos methods. These two algorithms are the variant of the standard conjugate gradient and Lanczos algorithms for solving a system of linear equations over real entities (Odlyzko, 1985; Coppersmith *et al.*, 1986). A drawback of this class of algorithm is that it is not guaranteed to derive a solution when the system of linear equations is solvable (Odlyzko, 1985; Teitelbaum, 1998). Hence, Teitelbaum (1998) improved Lanczos algorithms

in order to avoid this shortcoming. Both algorithms need about $O(n^2)$ operations. The second class is the Wiedemann method and its derivatives (Wiedemann, 1986). This algorithm employs the Berlekamp-Massey algorithm and guarantees deriving a solution in about $O(n^2)$ operations, but it is complicated to program (LaMacchia and Odlyzko, 1990). The third class is structured Gaussian elimination (GE) algorithms, also called intelligent GE algorithms, which were introduced by Odlyzko (1985). The classical GE algorithm needs a row permutation process and then, an equation solving one. Employing the classical GE algorithm or GE for short, on the matrix H_k in Equation (4.19) has a complexity scaling as $O(n^3)$ and therefore, ML decoding becomes impractical for long block lengths. On the other hand, the structured GE algorithm converts a system of sparse linear equations into a non-sparse system with smaller dimensions of the unknown. Such unknowns are called pivots or reference variables (Liva *et al.*, 2009). The purpose of the structured GE algorithm is to limit the average number of pivots from which the remaining unknowns can be recovered using back substitution operations, while the pivots are solved using the GE algorithm. LaMacchia and Odlyzko (1990) analysed the performance of different algorithms using problems of discrete logarithm calculations and integer factorisations. The authors concluded that a very large sparse system can be solved efficiently by using structured GE algorithms. Burshtein and Miller (2004) proposed a practical decoding algorithm similar to the structured GE algorithm to decode LDPC codes over the BEC efficiently. They exploited the sparseness of the matrix H_k to reduce the decoding complexity of the GE algorithm and thus to enable the ML decoding for long block lengths. The description of the algorithm is as follows.

- 1) The columns of H are first permuted so that the left part contains all the columns corresponding to known variables in H_k , while the right part contains all those corresponding to the erased variables in H_k .
- 2) H_k is transformed into an approximate triangular matrix, as proposed by Richardson and Urbanke (2001). This means searching for degree-1 rows in H_k , then performing row and

column permutations to bring the found “1” entries into a diagonal form. The results are the submatrices C , T which is in a lower triangular form, whilst R_U and R_L have columns that cannot be put into lower triangular form. The α variables related to the columns of R_U and R_L form the pivots. The matrices C , R_U , and R_L are sparse, as illustrated in Figure 4.4(a).

- 3) Perform row additions on C repeatedly to zero out the matrix. The matrix T is also transformed into an identity matrix by row additions. Both R_U and R_L become dense due to the row additions, as illustrated in Figure 4.4(b).
- 4) Recover the α pivots by applying the GE algorithm only on the rows of the equations corresponding to the columns of R_L . If all pivots are recovered, then the remaining $e - \alpha$ unknowns can be obtained using back substitution operations.

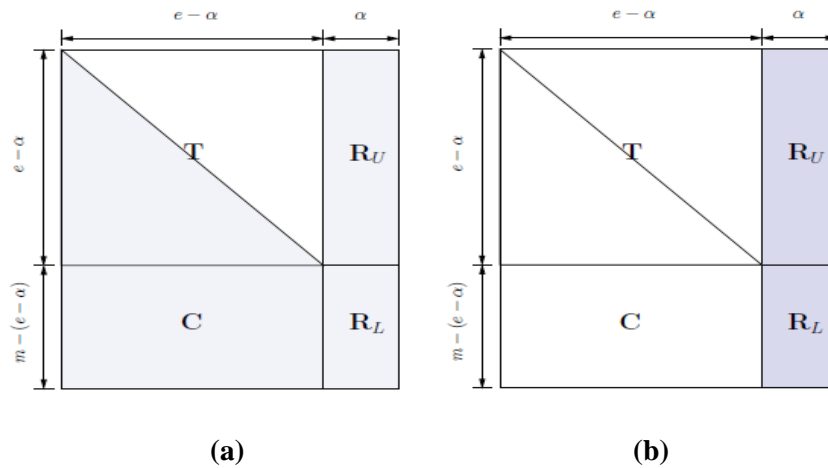


Figure 4.4: Reduced complexity ML decoder on H_k (Paolini *et al.*, 2012)

This decoding algorithm succeeds, if the rank $(R_L) \geq \alpha$ after the zero matrix step. During the triangulation and zero matrix steps, all operations are performed also in parallel on $H_k y_k^T$. The main advantage of this algorithm is that the GE algorithm is employed only on R_L and not on the whole set of unknowns. The GE step is the critical step of Burshtein and Miller’s algorithm and has a complexity of $O(\alpha^3)$. However, this can be considerably decreased, if the number of pivots is very small and hence, it is important to keep the size of R_L as small as

possible. This can be achieved by using one of the sophisticated methods for choosing the pivots presented by Burshtein and Miller (2004) and improved by Liva *et al.* (2009).

Eliminating the permutation process can also reduce the computational complexity of the GE algorithm, as proposed by Tomlinson *et al.* (2004). The proposed “In-Place” algorithm consists of two processes, including: a polynomial update process and back filling process. At the beginning of the algorithm, the erasure bits are substituted in the matrix H . Then, the first process marks the first equation containing the first erased bit. This equation is subtracted from all other equations having the same erased bit and not yet marked to generate a new group of equations. The process repeats until either no marked equations exist having the same erased bit or no erased bits exist that are not in marked equations. Having a set of erasure bits in the last marked equations, the second process begins with the last row of equations and solves the erasures backwards. Compared with the GE algorithm, the complexity of Tomlinson *et al.*’s algorithm remains $O(n^3)$, however, the multiplicative constant is significantly decreased.

4.3.3 Reduced Complexity Decoding Algorithms

Reduced complexity decoding algorithms for LDPC codes over the BEC can be implemented as Hybrid (HB) decoding algorithms. These algorithms combine different decoding algorithms with the aim of improving erasures recovery performance or decoding complexity over the BECs. A number of HB decoding algorithms have been proposed in the literature for different LDPC codes in the BECs. In four independent studies by Cunche and Roca (2008), Paolini *et al.* (2008), Yang *et al.* (2008), and Huang *et al.* (2011), HB IT/ML decoding algorithms were proposed, with the basic idea of employing the IT decoding first. If this decoding fails to recover all the erased bits due to the existence of stopping sets, the ML decoding is activated to complete the decoding process and resolve a simplified system. The ML decoding algorithm can fully recover the erasures in the simplified system, if the

columns of the decoding matrix containing erasures are linearly independent. It has been shown that implementing HB decoding on LDPC-triangle and LDPC-staircase codes achieves a high performance in terms of erasure recovery capabilities similar to that of the ML decoding as well as decoding speeds close to that of an ideal code, even with small block sizes (Cunche and Roca, 2008). The same conclusion has been drawn for generalised irregular repeat accumulate codes (Paolini *et al.*, 2008), for turbo Gallager codes (Yang *et al.*, 2008), and for fountain codes in the BEC (Huang *et al.*, 2011). Mattoussi and Roca (2012) proposed a variant HB decoder that combines four types of decoding algorithms, including IT, Reed Solomon, binary and non-binary GE decoding algorithms. The proposed HB decoding was used to decode the generalised LDPC-staircase code for the BEC which is constructed by extending LDPC-staircase codes through Reed-Solomon codes using “quasi” Hankel matrices. Even though the HB decoding utilises a non-binary GE decoder that is more complex, the system on which it is applied is simplified by the previous three decoders. This allows for reaching the maximum recovery capabilities of the code. Decoding succeeds, if one or some of these decoding algorithms succeed. Recently, Bocharova *et al.* (2018) proposed a reduced complexity near-ML decoding algorithm for very long quasi-cyclic LDPC codes over the BEC. The proposed algorithm is a HB decoding that combines the IT decoding of the quasi-cyclic LDPC code and a sliding-window of the ML decoding. The second component is applied “quasi-cyclically” to a quite short sliding window of the ML decoding of a zero-tail terminated LDPC convolutional code. The complexity of the proposed algorithm is polynomial in the window length. On the other hand, it is linear in the length of the code.

Besides the HB decoding algorithms, the reduced complexity suboptimal decoding algorithms for LDPC codes over the BEC are generally based on appending redundant rows to the parity check matrix and employing post-processing of variable guessing when the IT decoding is not successful. Enhancing the performance of the IT decoding of linear codes

over the BECs by employing redundant parity check matrices has been studied, such as in Sankaranarayanan and Vasić (2005), Schwartz and Vardy (2006) and recently considered by Bocharova *et al.* (2017). A predetermined number of dual codewords is appended to the parity check matrix of an LDPC code, which can later be used by the IT decoder instead of the original matrix. The dual codewords are appended in ascending order of their weights, such that $d_{stop} = d_{min}$. The proposed method can be applied to short LDPC codes since finding low weight dual codewords needs complex operations. Employing post-processing of variable guessing was first studied in Pishro-Nik and Fekri (2004) for short-length LDPC codes, where the complexity is quite small. The proposed method needs a minimum number of trials of the IT decoding equal to a polynomial function of the number of bit guesses. The complexity of the decoder increases exponentially with the number of guessed variables. An improved version in Vellambi and Fekri (2007) is based on the observation that a significant fraction of unsatisfied neighbours of a stopping set are of weight 2. This observation is exploited to simplify the decoding process by replacing the related pairs of variable nodes by one variable node. In Olmos *et al.* (2010), the method is improved for finite length codes. It eliminates parity check and variable nodes and thus, its complexity is identical to the IT decoding algorithm.

4.4 Construction Methods for LDPC Codes

This section presents some of the methods for constructing LDPC codes with special attention to the PEG algorithm on which the current research is based.

4.4.1 Random Constructions

4.4.1.1 Gallager Codes

In the original paper of Gallager (1962), the rows of H are divided into j submatrices with m / j rows in each. The first submatrix of independent rows includes l consecutive “1” entries ordered from left to right through the columns. That is, for $i \leq m / j$, the i -th row contains ones

in columns $(i - 1) \times l + 1$ through $i \times l$ and zeros elsewhere. The other submatrices of rows are simply random column permutations of the first submatrix. Hence, each column of H has a “1” entry once in every one of the j submatrices. Due to the random nature of Gallager’s LDPC code, the absence of short cycles especially of length 4, is not guaranteed (Ryan and Lin, 2009). The following is the parity check matrix of the (20, 3, 4) Gallager-LDPC code.

$$H = \begin{bmatrix} 1 & 1 & 1 & 1 & 0 & 0 & 0 & 0 & 0 & 0 & 0 & 0 & 0 & 0 & 0 & 0 & 0 & 0 & 0 & 0 \\ 0 & 0 & 0 & 0 & 1 & 1 & 1 & 1 & 0 & 0 & 0 & 0 & 0 & 0 & 0 & 0 & 0 & 0 & 0 & 0 \\ 0 & 0 & 0 & 0 & 0 & 0 & 0 & 0 & 1 & 1 & 1 & 1 & 0 & 0 & 0 & 0 & 0 & 0 & 0 & 0 \\ 0 & 0 & 0 & 0 & 0 & 0 & 0 & 0 & 0 & 0 & 0 & 0 & 1 & 1 & 1 & 1 & 0 & 0 & 0 & 0 \\ 0 & 0 & 0 & 0 & 0 & 0 & 0 & 0 & 0 & 0 & 0 & 0 & 0 & 0 & 0 & 0 & 1 & 1 & 1 & 1 \\ \hline 1 & 0 & 0 & 0 & 1 & 0 & 0 & 0 & 1 & 0 & 0 & 0 & 1 & 0 & 0 & 0 & 0 & 0 & 0 & 0 \\ 0 & 1 & 0 & 0 & 0 & 1 & 0 & 0 & 0 & 1 & 0 & 0 & 0 & 0 & 0 & 0 & 0 & 1 & 0 & 0 \\ 0 & 0 & 1 & 0 & 0 & 0 & 1 & 0 & 0 & 0 & 0 & 0 & 0 & 1 & 0 & 0 & 0 & 1 & 0 & 0 \\ 0 & 0 & 0 & 1 & 0 & 0 & 0 & 0 & 0 & 0 & 1 & 0 & 0 & 0 & 1 & 0 & 0 & 0 & 1 & 0 \\ 0 & 0 & 0 & 0 & 0 & 0 & 0 & 1 & 0 & 0 & 0 & 1 & 0 & 0 & 0 & 1 & 0 & 0 & 0 & 1 \\ \hline 1 & 0 & 0 & 0 & 1 & 0 & 0 & 0 & 0 & 0 & 0 & 1 & 0 & 0 & 0 & 0 & 0 & 1 & 0 & 0 \\ 0 & 1 & 0 & 0 & 0 & 0 & 1 & 0 & 0 & 0 & 1 & 0 & 0 & 0 & 0 & 1 & 0 & 0 & 0 & 0 \\ 0 & 0 & 1 & 0 & 0 & 0 & 0 & 1 & 0 & 0 & 0 & 0 & 1 & 0 & 0 & 0 & 0 & 0 & 1 & 0 \\ 0 & 0 & 0 & 1 & 0 & 0 & 0 & 0 & 1 & 0 & 0 & 0 & 0 & 1 & 0 & 0 & 1 & 0 & 0 & 0 \\ 0 & 0 & 0 & 0 & 1 & 0 & 0 & 0 & 0 & 1 & 0 & 0 & 0 & 0 & 1 & 0 & 0 & 0 & 0 & 1 \end{bmatrix} \quad (4.20)$$

Many studies have been focused on enhancing the performance of the LDPC codes. The irregular LDPC code introduced by Luby *et al.* (2001b) is one example that exhibits a significant enhancement compared to regular codes. Variable nodes as well as parity check nodes have different degrees and thus, the level of missing protection differs over a codeword. The columns of the matrix H that have greater numbers of “1” entries, provide higher missing protection levels than those with fewer of these entries. During the IT decoding process, erasures whose columns of H have a greater number of “1” entries require a few iterations to be recovered. Therefore, in the successive iterations, the recovered erasures will then be used to recover the remaining ones. To design good irregular degree distribution pairs, Richardson *et al.* (2001) proposed a density evolution method. This method is used to determine the maximum level of channel noise, called the threshold, where the IT decoding can recover erasures and to optimise degree distributions. Whilst Chung *et al.*, (2001) used a Gaussian approximation to simplify the analysis of the decoding algorithm and to estimate the threshold. These two approaches are based on a cycle-free assumption, which

is only valid for infinite length LDPC codes. However, there are different methods for designing good finite length LDPC codes, as presented below.

4.4.1.2 MacKay Codes

MacKay (1999) provided algorithms to generate semi-randomly sparse parity check matrices and consequently decrease short cycles in the Tanner graphs of Gallager codes. Some of them that are free of length 4 cycles are listed below:

- 1) H is constructed by randomly generating columns of weight j while row weight is kept to being as uniform as possible. The number of overlapping “1” entries between any two rows is less than 2;
- 2) H is constructed as above, except there are no two columns having overlap larger than one;
- 3) H is constructed as above. A small number of columns are also deleted to avoid short cycles.

One limitation of the MacKay codes is that their structure is inefficient to enable low encoding complexity (Ryan, 2003).

4.4.1.3 Progressive Edge Growth (PEG) Methods

Hu *et al.* (2001; 2005) proposed the PEG method to avoid short cycles and thus, minimum stopping sets in the Tanner graph. The PEG method has good performance even for large block lengths (Shedsale and Sarwade, 2012). The method constructs Tanner graphs in an edge-by-edge or progressive manner with large local girths at variable nodes. When the cycles are long, the IT decoding algorithm iterates several times and thus, the recovery performance increases. The PEG method is initialised by three parameters, including the number of variable nodes (n), the number of parity check nodes (m), and the variable node degree sequence (D_v), which represents the list of degrees for each of the variable nodes. The

method starts with the lowest degree variable nodes and proceeds to those of higher degrees, with the aim of maximising the local girth of every variable node. The method does not progress to the next variable node until all of the edges of the present variable node have been connected.

For a given variable node, the first edge links it to a lowest degree parity check node under the current setting of the graph. Following edges of the variable node are linked in a way that either no cycle is generated or, when this is inevitable, that generated has the largest local girth possible under the current graph setting. Hence, if the current state of the graph shows that one or more parity check nodes are unreachable from the current variable node by traversing the linked edges, the new edge links an unreachable parity check node and thus, no cycle is generated. If all parity check nodes are reachable from the current variable node, the new edge should be linked to the parity check node with the lowest degree that generates the maximum local girth. Multiple choices may exist to choose the parity check node from the set of those available. That is, all choices result in the same local girth under the current graph setting. This issue can be solved by either choosing the first parity check node or randomly selecting any parity check node from the set. Both choices result in the same performance.

Denote the set of parity check nodes by $C = \{c_1, c_2, \dots, c_m\}$, the set of variable nodes by $V = \{v_1, v_2, \dots, v_n\}$, and the set of edges by E , where $E \subseteq C \times V$. An edge $(c_i, v_j) \in E$, if and only if, $h_{i,j} = 1$, where $h_{i,j} \in H$, $1 \leq i \leq m$, $1 \leq j \leq n$. Also, let $D_v = \{d_{v_1}, d_{v_2}, \dots, d_{v_n}\}$ represent the variable node degree sequence in ascending order, where d_{v_j} is the degree of variable node v_j . Similarly, let $D_c = \{d_{c_1}, d_{c_2}, \dots, d_{c_m}\}$ represent the parity check node degree sequence in ascending order, where d_{c_j} is the degree of parity check node c_j . Let $N_{v_j}^t$ represent the set of parity check nodes that are connected to v_j within depth t , whereas $\setminus N_{v_j}^t$ denotes the complement of the set. Finally, let $E_{v_j}^z$ represent the z^{th} edge linked to v_j , where $1 \leq z \leq d_{v_j}$.

Algorithm 4.1 shows the details of the PEG method (Hu *et al.*, 2001), which is employed to improve the autonomous group integrity verification in this research.

Algorithm 4.1: Construction of the parity check matrix using the PEG method

Input: (n, m, D_v)

Output: H

1: for $j = 1$ to n do

2: for $y = 1$ to d_{v_j} do

3: if $y = 1$ then

$E_{v_j}^1 \leftarrow \text{edge}(c_i, v_j)$, where $E_{v_j}^1$ is the first edge connected to v_j , and c_i

has the minimum degree in the current graph state $E_{v_1} \cup E_{v_2} \cup \dots \cup E_{v_j}$.

4: else

Extend a tree from v_j up to depth z , such that $'N_{v_j}^z \neq \emptyset$ but $'N_{v_j}^{z+1} = \emptyset$, or

the number of elements in $N_{v_j}^z$ is not increasing, but is less than m . Then,

$E_{v_j}^y \leftarrow \text{edge}(c_i, v_j)$, where c_i is selected from $'N_{v_j}^z$ and has the minimum

degree.

5: end if

6: end for

7: end for

4.4.1.4 Approximate Cycle Extrinsic Message Degree (ACE) Methods

The approximate cycle extrinsic message degree (ACE) method proposed by Tian *et al.* (2003; 2004) is another method that accounts for cycles, especially the overlapping of multiple cycles in the Tanner graph of an LDPC code. The method prevents stopping sets of small sizes by maximising the connections between the variable nodes within a short cycle and parity check nodes outside the cycle. Consequently, useful information can flow from outside the cycle into the cycle. An extrinsic check node of variable nodes in a cycle is one

that is connected to the cycle only once. The extrinsic message degree (EMD) for a cycle is the number of these extrinsic check nodes connected to the cycle. The approximate cycle EMD (ACE) for a cycle of length 2α is the maximum possible EMD for the cycle. Since a variable node with degree j in a cycle can be linked to, at most, $j-2$ extrinsic parity check nodes, the ACE for a cycle of length 2α is $\sum_{i=1}^{\alpha} j_i - 2$. The proposed method constructs a Tanner graph or parity check matrix in such a way that short cycles have large EMD values. This has the effect of increasing the size of the smallest stopping set as the EMD of a stopping set is zero. The method produces an (α, c_{ACE}) LDPC code, with cycles of length 2α or less having ACE values of at least c_{ACE} . The method starts with the lowest weight column of the parity check matrix and proceeds to columns of higher weight. If the ACE value of a cycle is at least c_{ACE} , the candidate column for the parity check matrix is added. There is a tradeoff between α and c_{ACE} , such that increasing one parameter unavoidably causes the other parameter more difficult to implement. For $\alpha = 6, 7, 9, 10, 13$, the maximum c_{ACE} values that can be achieved are 7, 5, 4, 3, 2, respectively. The constructed code with the ACE method is always irregular (Tian *et al.*, 2004), which may prove to be an obstacle for the group integrity application of RFID systems. Xiao and Banihashemi (2004) combined the ACE and PEG algorithms to obtain a hybrid ACE-PEG one, which results in codes with good iterative decoding performance. In Chapter 5, the performances of the PEG-based LDPC codes in recovering missing tag IDs in the autonomous group integrity verification are compared with those of the ACE-based LDPC codes.

4.4.2 Algebraic Constructions

4.4.2.1 Quasi-Cyclic Codes

Lan *et al.* (2007) proposed quasi-cyclic codes. A code is called as such, if for any σ cyclic shifts of a codeword, this results in another codeword. A cyclic code is also a quasi-cyclic with $\sigma = 1$. The simplest form of quasi-cyclic codes is row circulant codes, as:

$$H = [A_1, A_2, \dots, A_q] \quad (4.21)$$

where, A_1, A_2, \dots, A_q are binary $j \times j$ circulant matrices. Having one invertible circulant matrices, for example A_q , G can be built in systematic form, as:

$$G = \left[I_{j(q-1)} \left| \begin{array}{c} (A_q^{-1}A_1)^T \\ (A_q^{-1}A_2)^T \\ \vdots \\ (A_q^{-1}A_{q-1})^T \end{array} \right. \right] \quad (4.22)$$

The resulted quasi-cyclic code is of length $j \times q$ and dimension $j \times (q - 1)$. The algebra of $j \times j$ binary circulant matrices is similar to that of polynomials modulo $x^j - 1$ over Galois Field (2) or GF(2) for short. In this case, the codeword is encoded as $c(x) = [i(x), p(x)]$, where $i(x)$ describes k message bits and $p(x)$ is given by:

$$p(x) = \sum_{l=1}^{q-1} i_l(x) \times (a_q^{-1}(x) \times a_l(x))^T \quad (4.23)$$

Quasi-cyclic codes possess structures that are free of length 4 cycles as well as allowing low decoding complexity at the cost of poor performances for large n . Cunche *et al.* (2010) showed that a class of quasi-cyclic LDPC codes can be used to decrease the complexity of ML decoding significantly in the implementation of HB decoding. This is accomplished by a number of row and column permutations, scaled as $k\sqrt{k}$, which transform a quasi-cyclic parity check matrix into a pseudo-band form. This method can be effectively used to decode quasi-cyclic LDPC codes of medium and short lengths or of high rates as well.

4.4.2.2 Euclidean Geometry Codes

Kou *et al.* (2001) constructed Euclidean geometry (EG) codes using points and lines of Euclidean geometries over finite fields. The following simply explains the fundamental construction of EG codes. Let EG with n points and m lines have four structural properties, as follows:

- 1) Every line contains p points;
- 2) Any two points are linked by one and only one line;

- 3) Every point is intersected by l lines;
- 4) Any two lines are either parallel or they intersect at one and only one point.

An $m \times n$ parity check matrix is formed where rows and columns relate to the lines and points of the EG, respectively. $h_{i,j} = 1$, if and only if the i -th line of EG contains the j -th point of EG. A row in the parity check matrix represents the points on a specific line of EG and has weight p , whereas a column represents the lines that intersect at a certain point in EG and has weight l . The parity check matrix can be simply seen as the incidence matrix of the lines over the points in EG. The Tanner graphs of these types of codes have girth 6. However, the values of j and l are relatively large, which is undesirable in some applications, including the autonomous group integrity application. In addition, there is no flexibility in the choice of the length and rate of the code (Ryan, 2003).

4.4.2.3 Chinese Remainder Theorem (CRT) Methods

To overcome the random nature of the Gallager LDPC codes, Su and Tonguz (2013) utilised the redundancy property of the remainder presentation in the Chinese remainder theorem (CRT) to construct the parity check matrix of LDPC codes. Let a_1, a_2, \dots, a_w be any w integers and b_1, b_2, \dots, b_w be positive integers that are pairwise relatively prime, where $\gcd(b_p, b_q) = 1, \forall p \neq q, 1 \leq p, \text{ and } q \leq w$. According to the theorem, the system of congruences:

$$x \equiv a_i \pmod{b_i} \quad \text{for } i=1, 2, \dots, w \quad (4.24)$$

has a unique solution module $\prod_{i=1}^w b_i$ (Ding *et al.*, 1996). A positive integer x is uniquely identified by the residues a_1, a_2, \dots, a_w of x module b_1, b_2, \dots, b_w . Thus, having $j \geq w$ integers that are relatively prime in pairs $b_1 < b_2 < \dots < b_w$, where $x < \prod_{i=1}^w b_i$, the residues of x module b_1, b_2, \dots, b_w are a redundant representation of x . The feature that allows for the building of the parity check matrix is that by choosing $j \geq w$ integers that are relatively prime in pairs $b_1 < b_2 < \dots < b_w$, any two positive integers $x_1, x_2 < \prod_{i=1}^w b_i$ disagree on at least $j - x$

+1 residues module b_1, b_2, \dots, b_w (Goldreich *et al.*, 2000). The CRT algorithm proposed by Su and Tonguz (2013) builds the parity check matrix H of LDPC codes by, firstly, identifying three parameters, including the length of the codeword n , the column weight j , and a positive integer $w \leq j$ subsequently, performing the following procedure.

- 1) Choose j positive integers $b_1 < b_2 < \dots < b_j$ that are relatively prime in pairs, where,

$$b_j \leq \frac{n}{2} \quad (4.25)$$

$$\prod_{i=1}^w b_i \geq n \quad (4.26)$$

- 2) For each b_i , where $1 \leq i \leq j$, build a parity check matrix $H(i)$ of size $b_i \times n$, where the (p, q) th entry is set to 1, if,

$$q - 1 \equiv p - 1 \pmod{b_i} \quad (4.27)$$

is true, otherwise, it is set to 0.

- 3) The submatrices $H(i)$ are concatenated to build the main parity check matrix $H(n, j, w)$ of size $m \times n$, where $m = \sum_{i=1}^j d_i$, as:

$$H = \begin{bmatrix} H(1) \\ H(2) \\ \dots \\ H(j) \end{bmatrix} \quad (4.28)$$

The constructed CRT-based LDPC code is always irregular and there is no flexibility in the choice of its rate. Whilst, Su and Tonguz (2013) employed this method to improve autonomous group integrity verification, these drawbacks eliminate deriving a realistic baseline performance comparison with other codes. The performances of the CRT-based LDPC codes in recovering missing tag IDs in autonomous group integrity verification are compared with those of the PEG-based LDPC codes in Chapter 5.

4.4.3 Main Comparisons of Construction Methods

In general, long random codes perform better in the waterfall region than algebraic codes of the same parameters. The encoding process of the random codes involves implementing the GE process first and then storing the result matrix in a memory. On the other hand, algebraic

codes usually have a lower error floor. Codes with large minimum Hamming distances can be constructed more easily than random ones. Furthermore, since algebraic codes, such as quasi-cyclic codes can be defined using polynomials, the encoding process may be simplified using a linear-feedback shift-register circuit where the memory overhead is least. They also have advantages in integrated circuits decoder implementation, because of their cyclic symmetry, which results in simple modular structure and regular wiring (Lan *et al.*, 2007).

4.5 Conclusions

In the family of erasure codes over the BECs, a significant role is played by LDPC codes, because of their good performance and their comparably low decoding complexity. Their parity check matrices are characterised by a low density of “1” entries, which suits the limited memory space of passive tags. A message is encoded using a generator matrix that is formed from the parity check matrix. The performance of LDPC codes, both in terms of erasure recovery capabilities and decoding speeds, is largely dependent on the decoding algorithm used. The two most prominent decoding algorithms to recover erasures over the BECs are the IT and ML decoding algorithms. The IT decoding algorithm features a linear decoding complexity, but it remains suboptimal in recovering erasures, as it is affected by the existence of stopping sets. On the other hand, the ML decoding algorithm for the BEC, which can be implemented as the GE algorithm, provides the optimum decoding in terms of erasure recovery capabilities, but at the price of high decoding complexity. A good decoding strategy may consist of combining the IT and ML decoding algorithms. This hybrid IT/ML decoding algorithm allows for a compromise between performance and complexity. Different methods exist in the literature for constructing LDPC codes. Mitigating short cycles and thus, stopping sets are of primary concern when constructing LDPC codes for the autonomous group integrity verification of tags to enable linear time decoding with high recovery capabilities. Hence, the PEG method is used to construct the parity check matrix of LDPC codes in this

research. The GE decoding algorithm is deployed to represent the ML decoding throughout this thesis.

5 Extended Grouping of RFID Tags Based on PEG Methods

In this chapter, extended grouping of RFID tags is improved in terms of missing recovery capabilities. Due to the sparseness property of LDPC codes and the mitigation of the PEG method for short cycles, this method is used to construct the parity check matrix H of LDPC codes in order to increase the performance of the code in recovering missing tag IDs with low memory consumptions. The recovery performance of PEG-based LDPC codes is analysed and assessed under the IT and GE decoding algorithms. The properties of the constructed PEG Tanner graphs are also analysed and compared with the Tanner graphs of other codes.

5.1 System Model

Consider an RFID system with one reader and many passive tags. On the basis of the EPCglobal Class-1 Generation-2 standard, each tag stores the 96-bit ID that uniquely identifies the tagged object. Tags can perform some calculations, such as hashing. They have special memories, as presented in subsection 3.1.1.2 of Chapter 3, in addition to the user memory which enables users to store additional information. The communication between the reader and the tags uses a framed, slotted Aloha protocol, which follows the RTF mode. The signal from the reader synchronises the clocks of the tags. In each cycle of communication, a reader broadcasts a request in a time slot and then, multiple tags reply in the following slotted frame. As stated in the standard, the transmission rate between the reader and the tags is asymmetric and subject to the environment.

5.2 Encoding Process

Algorithm 4.1 of the PEG method, which is described in subsection 4.4.1.3 of Chapter 4, is used to construct the parity check matrix H of LDPC codes. The algorithm is initialised with

three parameters, including the number n of tag IDs, the number m of subgroups, and the variable node degree sequence. Then, a group of n RFID tag IDs denoted by $TID_1, TID_2, TID_3, \dots, TID_n$ is encoded using the constructed H of size $m \times n$, as:

$$\begin{Bmatrix} c_1 \\ c_2 \\ \cdot \\ \cdot \\ \cdot \\ c_m \end{Bmatrix} = H \cdot \begin{Bmatrix} TID_1 \\ TID_2 \\ \cdot \\ \cdot \\ \cdot \\ TID_n \end{Bmatrix} \quad (5.1)$$

to generate m subgroup IDs, where $c_i, i \in \{1..m\}$ is the subgroup ID of the i -th subgroup. As represented in coding theory, the resultant codeword block length denoted by x is of size $n + m$. c_i is computed as the XOR (denoted by \oplus) of the IDs of the tags belonging to the same subgroup. The set of information needed to be recorded in the memory of each RFID tag in a group is calculated based on the number of subgroups in which the tag is involved (the column weight j of H) and the number of short IDs of other tags belonging to the same subgroup (the row weight l of H). The bit length of each short ID s_i is set to the minimum number of bits that are necessary to distinguish a group of tags. For example, a short ID of 8 bits is enough for a group of less than 256 tags. Note that the short ID of each tag is not needed to be recorded in its memory. Hence, the set of information needed to be recorded for each subgroup is a 96-bit subgroup ID c_i in addition to $s_i \times (l - 1)$. Therefore, the total length of information recorded by each tag in its memory is equal to:

$$j \times (c_i + s_i \times (l - 1)) \quad (5.2)$$

Figure 5.1 shows an example of the encoding process of 6 tag IDs denoted by $TID_1, TID_2, \dots, TID_6$ and all the information recorded in these tags. Since, Tag_1 is involved in the parity check value c_1 with Tag_4 and Tag_5 , it records c_1 as well as s_4 and s_5 .

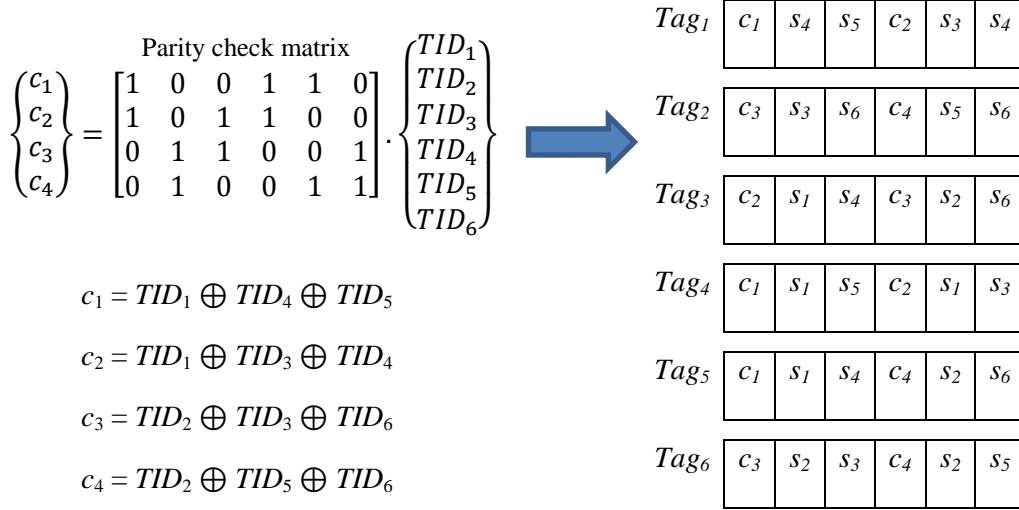


Figure 5.1: An example of the encoding process and the information stored in RFID tags belonging to a group of 6 RFID tags

5.3 Decoding Process

During the decoding process, the interrogator obtains tag IDs, parity check values, and short IDs from the available tags, then checks the integrity of each subgroup. Based on the results of the checking process, Equation (5.1) can be rearranged into the following form:

$$H_k y_k^T = C^T \oplus H_k y_k^T \quad (5.3)$$

where, y_k and y_k are the arrays of lost and known tag IDs, respectively. Further, C represents the set of subgroup IDs. The interrogator can obtain H_k from the short IDs of missing tags. Figure 5.2 shows the decoding process for the example presented in Figure 5.1, where TID_3 and TID_6 are missing. Equation (5.3) represents a set of linear equations with only y_k^T as the unknown and it also describes a Tanner graph containing two groups of nodes. One group

represents the tag IDs and the other, the subgroup IDs. An edge links a tag node to a subgroup node, if the tag is part of the subgroup. The missing tag IDs in Equation (5.3) can be recovered using the IT decoding or GE decoding algorithms, each with different performance and complexity. Figure 5.3 illustrates the IT decoding algorithm for the example presented in Figure 5.2. The Tanner graph is initialised as presented in part (a), where the dark squares denote the missing tag IDs. Bold and thin lines represent identified and unidentified edges, respectively. Known variables (tag IDs) are passed to subgroup IDs as in part (b). Then, missing tag IDs (TID_3 and TID_6) are recovered in part (c). The second iteration of variable passing illustrated in part (d) confirms that the recovered tag IDs satisfy the parity check constraint c_3 . In the remainder of the thesis, for simplicity, the term “parity check values” is used to represent “subgroup IDs” and the term “parity check constraints” to represent “subgroups”.

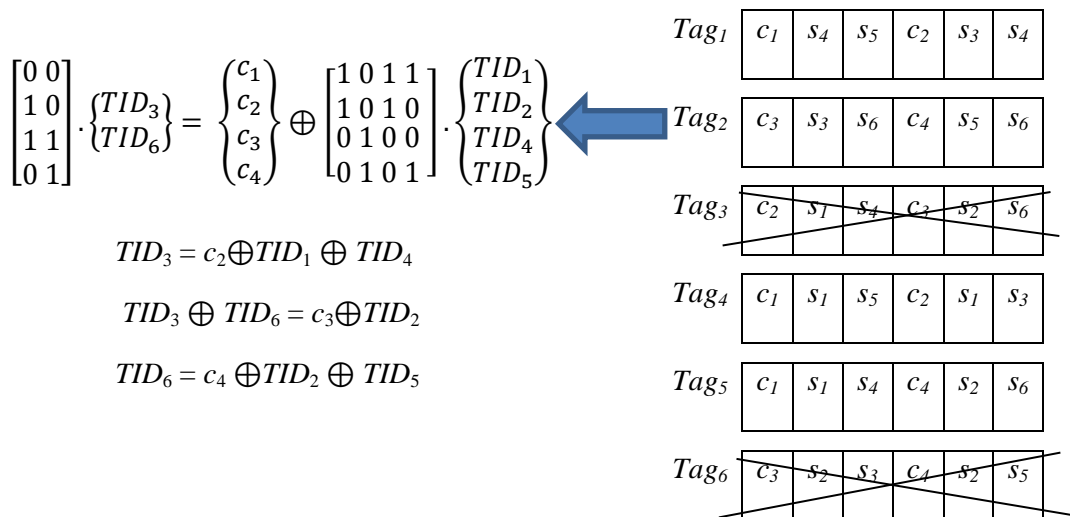


Figure 5.2: An example of the decoding process of a group of 6 RFID tags

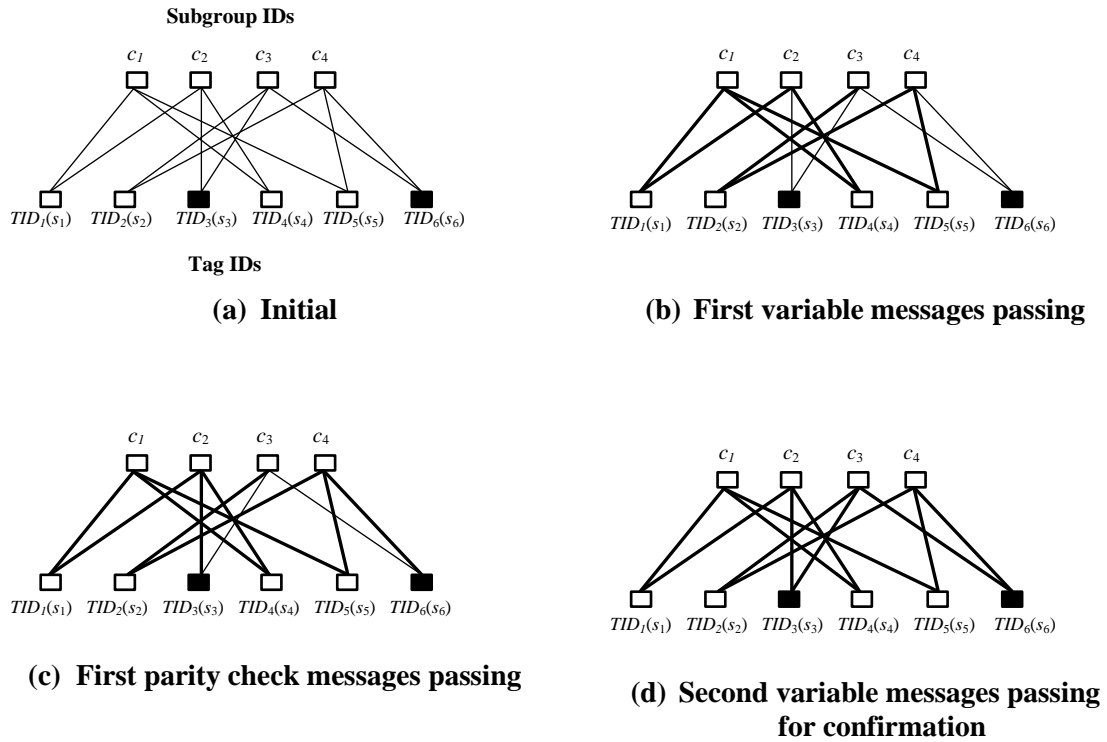


Figure 5.3: The IT decoding algorithm in the group integrity of RFID tags

5.4 Performance Evaluation

This section evaluates the missing recovery capability of the PEG-based LDPC codes with Matlab R2015a and R2018b simulations. Different parity check matrices are constructed using MainPEG.C (Hu, 2008), which outputs different matrices for different parameters, including n , m , and j . Generally, the procedures of the simulation can be applied to test the performance of any LDPC-based code in the research. In the following, the process of the simulation is summarised and the related flowchart is shown in Figure 5.4.

- 1) The simulator generates n random 96-bit $TIDs$;
- 2) The simulator performs the encoding algorithm on the group of n $TIDs$ in order to obtain m parity check values c_i ;

- 3) The simulator removes r TIDs from the group of n (not including the parity check values), where r varies from 1 to $n-1$. Missing tag IDs are chosen randomly and uniformly from the main group;
- 4) The simulator applies the decoding algorithm to known tag IDs and parity check values in order to recover the missing tag IDs. If the result of the decoding algorithm is different from the missing tag IDs, it is treated as an error;
- 5) The simulator repeats the above two processes 10^5 times for each value of r and then, computes the average error rate as the mean value of errors existing in the 10^5 rounds in order to obtain an accurate value of the statistics.

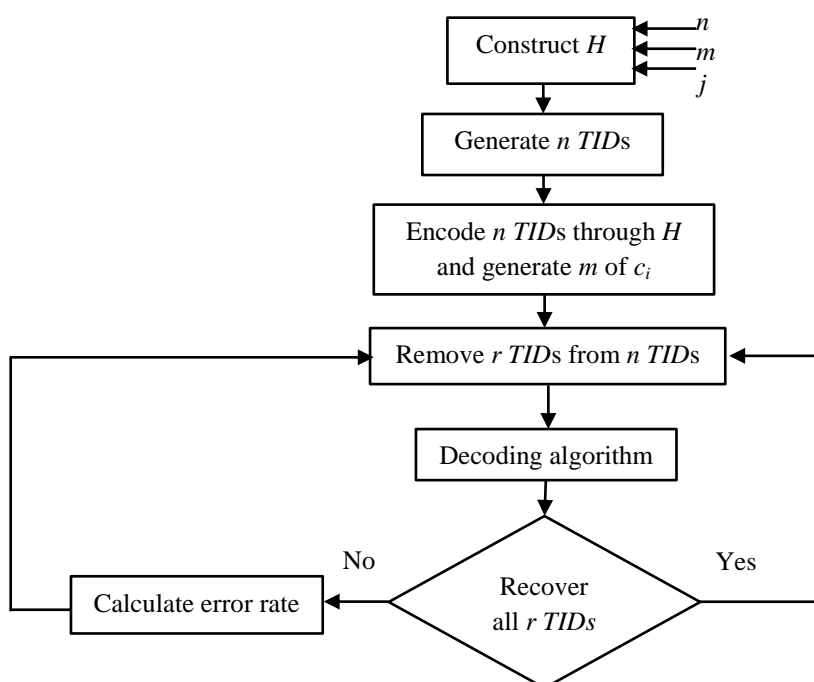


Figure 5.4: Flowchart of the simulation process

5.4.1 Using the GE and IT Decoding Algorithms

The performances of the PEG-based LDPC codes are examined under the GE and IT decoding algorithms. For comparison with other LDPC-based methods presented in Chapter 2, which are based on encoding using the parity check matrices of LDPC codes, the same parameters are used in the construction of the parity check matrices. The size of the tested group of RFID tags is assumed to be equal to $n = 25, 49, 121, \text{ and } 169$. Since the aim of the

autonomous group integrity verification in RFID systems is to minimise the memory consumption, only a small value of j is considered. The column weight, j , varies between 3 and 4 whereas the row weight, l , is fixed for each group. It is important to highlight that some constructed matrices using the PEG method are nearly regular with minor rows have different weights. Appendix B presents some of the constructed matrices. Figure 5.5 depicts the performance of the PEG-based LDPC codes in recovering missing tag IDs with the IT and GE decoding algorithms for different values of n . Two performance criteria are considered, including error rates and memory costs. The error rate is the percentage that the decoder cannot recover missing RFID tags. The memory cost represents the information needed to be recorded in the memory of each tag, which can be calculated using Equation (5.2). For example, using (25, 3, 5) code, each tag needs to store an amount of information equal to $3 \times (96 + 8 \times (5 - 1)) = 384$ bits, where the length of the short ID s_i is 8 bits. The results in the figure show that the recovery capabilities for both decoding algorithms increase with increasing j . The main reason for this behaviour is that increasing j increases the value of m and so too, the d_{min} of the code, which results in increasing the value of d_{stop} and the rank of the matrix H_k . However, the amount of memory consumption increases as a consequence. Table 5.1 illustrates the comparison of the PEG-based method with other extended grouping LDPC-based methods. The performance of the other methods is obtained from Su and Tonguz (2013). It is clearly shown that the aforementioned finding is true for all methods. For example, if 10 tags are missing from a group of $n = 49$, all of their IDs can be recovered with at least $j = 3$, using the PEG-based methods under the IT decoding algorithm. In this case, each tag records 432-bit, additional information. However, if 13 IDs are missing, each tag is required to store 576-bit additional information in order to achieve 100% reliable recovery (zero average error rate). If the reliability can be reduced to 95%, the consumed memory spaces can be decreased to 432-bit where the IT and GE decoding algorithms cannot recover some missing tag IDs. As the number of missing tags increases, the performance of the two

decoding algorithms decreases. For example, when the number of missing tags is 20, the average error rate for the IT decoding algorithm is 0.8, meaning that a few number of missing IDs is recovered.

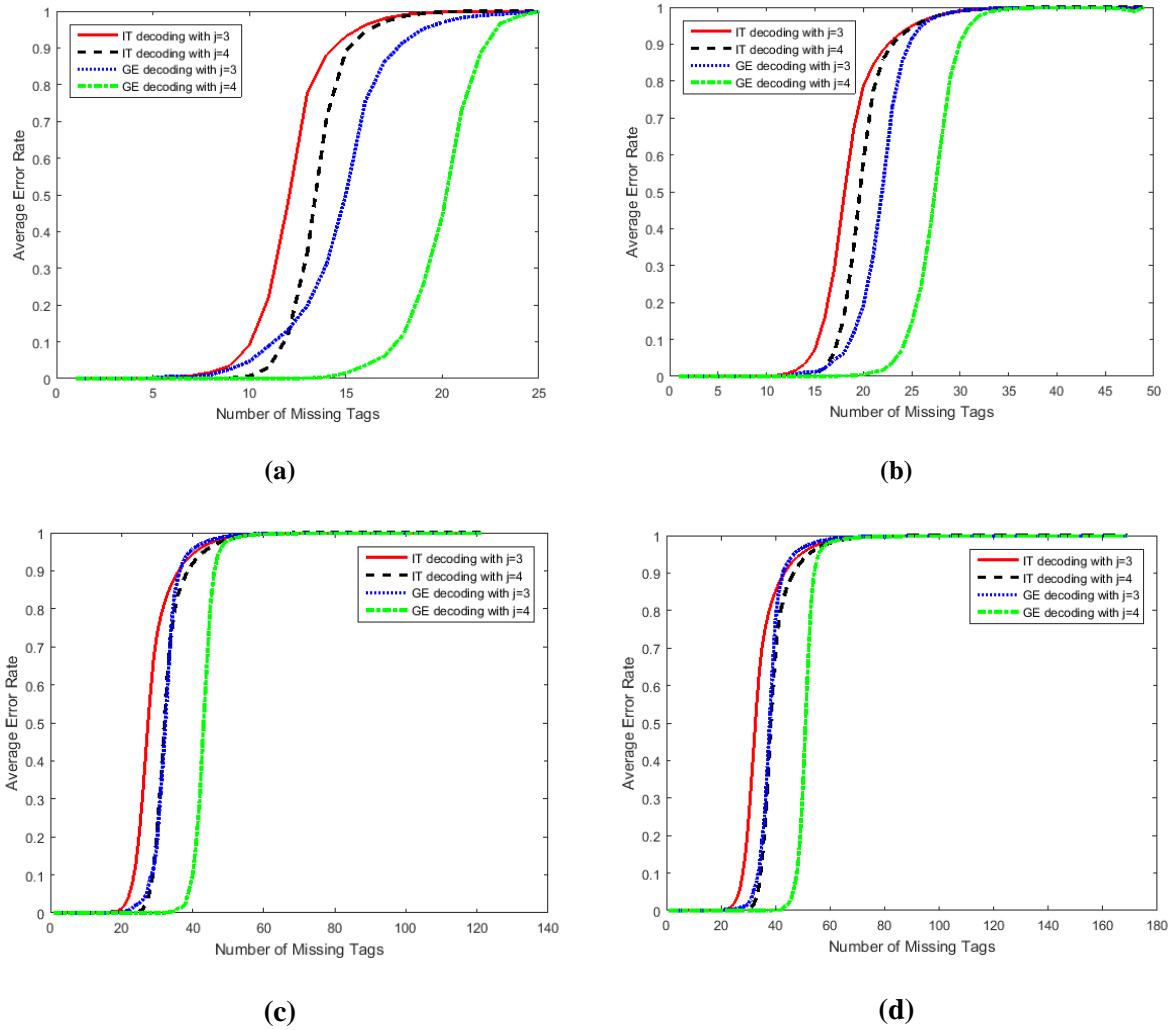


Figure 5.5: The average error rate of the identification of missing tag IDs from different group sizes: (a) $n = 25$; (b) $n = 49$; (c) $n = 121$; (d) $n = 169$, using the PEG-based LDPC codes with the IT and GE decoding algorithms

It is also clear that the selection of tags for subgroups needs to be carried out in a systematic way. Table 5.1 shows that, with the same memory consumption, the PEG-based LDPC code achieves greater improvement in recovering missing tag IDs compared to the other codes. The simulation reveals that the PEG-based LDPC code under the IT decoding algorithm can recover up to 13 missing tag IDs with a 0% error rate by writing 576-bit additional information to each tag in a group of 49 tags. Lowering the memory overhead to 432-bit, the largest number of missing IDs that can be recovered by the code without any error is 10,

which is still higher than that provided by other codes. This reduction in memory overhead can save 25% of each tag's memory while outperforming the performance of other methods.

Parameters (n, j, l)	LDPC Codes	Maximum number of missing tags that can be identified within a specified tolerance of error rate		m	Tag memory consumption in bits
		0%	5%		
(25, 3, 5)	Gallager-based	3	8	15	384
	SSF-based	5	9		
	CRT-based	5	11		
	RTD-based	5	9		
	PEG-based under IT	5	10		
	PEG-based under GE	7	11		
(25, 4, 5)	Gallager-based	5	11	20	512
	SSF-based	7	11		
	CRT-based	9	15		
	PEG-based with IT	9	12		
	PEG-based with GE	12	18		
(49, 3, 7)	Gallager-based	1	9	21	432
	SSF-based	5	12		
	CRT-based	5	15		
	PEG-based with IT	10	15		
	PEG-based with GE	13	18		
(49, 4, 7)	Gallager-based	3	16	28	576
	SSF-based	7	16		
	CRT-based	8	21		
	PEG-based with IT	13	17		
	PEG-based with GE	16	24		
(121, 3, 11)	Gallager-based	1	13	33	528
	SSF-based	5	20		
	CRT-based	5	23		
	RTD-based	5	20		
	PEG-based with IT	16	23		
	PEG-based with GE	20	28		
(121, 4, 11)	Gallager-based	6	27	44	704
	SSF-based	13	27		
	CRT-based	15	33		
	PEG-based with IT	23	28		
	PEG-based with GE	30	40		
(169, 3, 13)	Gallager-based	1	13	39	576
	SSF-based	5	24		
	CRT-based	5	27		
	PEG-based with IT	17	27		
	PEG-based with GE	19	32		
(169, 4, 13)	Gallager-based	1	31	52	768
	SSF-based	9	32		
	CRT-based	16	37		
	PEG-based with IT	28	34		
	PEG-based with GE	31	45		

Table 5.1: Comparisons of the PEG-based LDPC codes with other LDPC-based codes

The results of Table 5.1 also depict that the performance of the PEG-based LDPC code degrades with the IT decoding algorithm compared with its performance with the GE decoding algorithm. This is caused by the presence of small size of stopping sets, which are phenomena of the IT decoding only. The simulation reveals that when applying the PEG method to a group of 169 tags, the largest number of missing tag IDs that can be recovered without any error is 28 with the IT decoding algorithm. On the other hand, applying the GE decoding algorithm causes a noticeable improvement of up to 31 using the same parameters, where $j = 4$.

The simulation also reveals the advantages of using the PEG method with larger groups of tags. Applying the PEG method to a group of $n = 121$ and 169 tags results in dramatic recoveries with a 0% error rate, which is not the case with other LDPC-based codes. With the same memory consumption, the PEG-based code can recover up to 17 missing tag IDs from a group of 169 tags, where $j=3$, using the IT decoding algorithm, which is three times the performance of the CRT-based code. This results from the fact that the PEG method accounts for small stopping sets in Tanner graphs by maximising the girth, which is more achievable when the group size is large. The Tanner graph of the (169, 3, 13) PEG-based LDPC code has a girth of 6 and by maximising the length of the code, the girth is also increased. For example, the (512, 3, 6) PEG-based LDPC code has a girth of 8 and further increasing the length of the code can cause an increase in the girth to 10, such as for the (1000, 3, 5) PEG-based LDPC code.

The effects of changing l on the performance of the IT and GE decoding algorithms with long length codes, such as $n = 1000$, are shown in Figure 5.6 and Figure 5.7, respectively. The results of the IT decoding clearly reveal that although the (1000, 4, 5) code where $m=800$, has a girth of 8, smaller than the girth of the (1000, 3, 5) code with $m=600$, which is 10, it achieves higher performance, as with shorter length codes that are examined above, due to the larger

value of m and also, its bigger d_{min} it has. On the other hand, decreasing the l of the code from 8 to 6 with the same $m=500$ and girth=8 enhances the IT performance. The same conclusion can also be drawn for the performance of the GE decoding, but with an improvement of the (1000, 4, 8) code over the (1000, 3, 6) code when recovering less than 500 missing tag IDs.

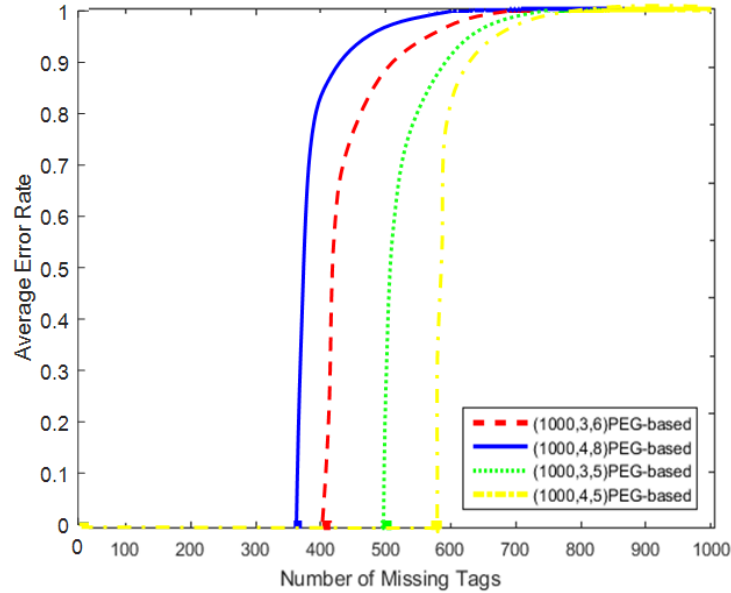


Figure 5.6: The average error rate of the identification of missing tag IDs from a group of size $n = 1000$ using the PEG-based codes with the IT decoding algorithm

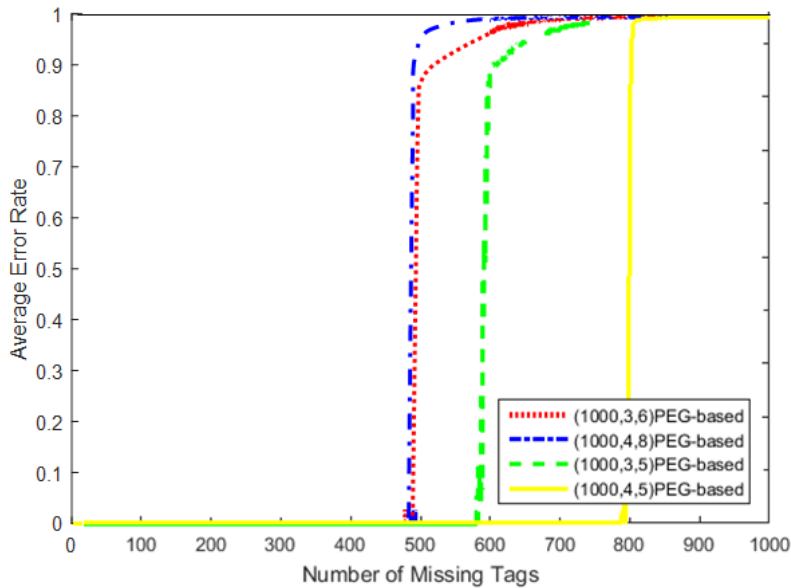


Figure 5.7: The average error rate of the identification of missing tag IDs from a group of size $n = 1000$ using the PEG-based codes with the GE decoding algorithm

To confirm the performance of the PEG-based LDPC codes with that of Tomlinson *et al.* (2007), the (200, 3, 6) PEG-based LDPC code is constructed with $n=200$, $m=100$, and $j=3$ and then tested with the GE decoding algorithm. The constructed code has a girth equal to 10 and a group of 200 tag IDs is encoded through the constructed matrix to generate a codeword x of length 300. Figure 5.8 shows the histogram of the unrecovered missing RFID tag IDs, with the average number of recovered missing tag IDs being 96.59. When a group of 100 tag IDs is encoded to generate a codeword x of length 200, as normally done in the BEC, the average number of recovered erasures is 96.64. This discloses an interesting finding that for (200, 3, 6) PEG-based LDPC codes, the average number of recovered erasures is nearly equal to m , which is higher than the finding of Tomlinson *et al.* (2007) of 93.19. Appendix B presents the constructed (200, 3, 6) PEG-based LDPC matrix.

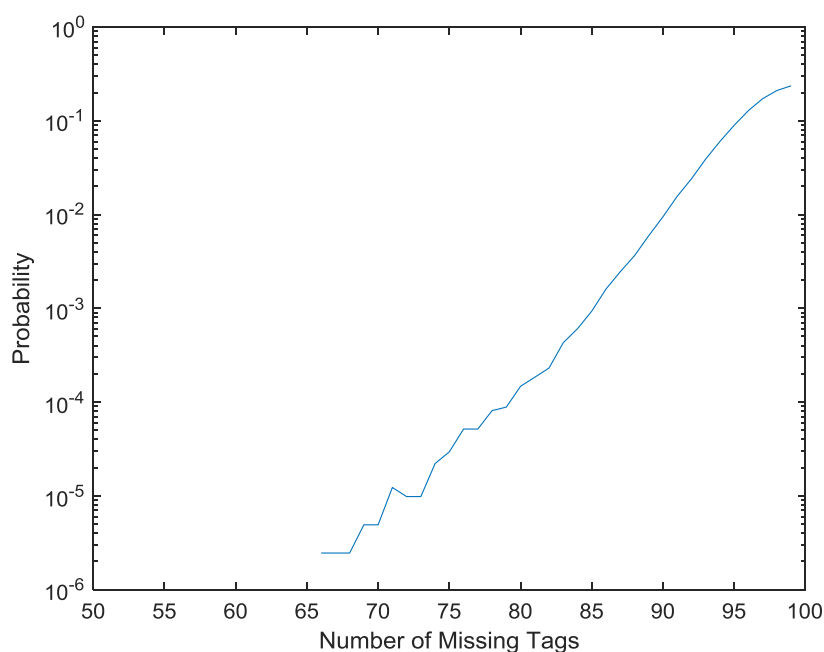


Figure 5.8: The histogram of unrecovered missing tag IDs of the (200, 3, 6) PEG-based LDPC codes with the GE decoding algorithm

To provide a preliminary comparison between the complexity and the time of the GE and IT decoding algorithms, the running time of decoding the PEG-based LDPC codes is measured

on a 2.6 GHz Intel i7-6600U processor. For (49, 3, 7) PEG-based LDPC codes, the GE and IT decoding algorithms take about 0.63 and 0.021 milliseconds (ms), on average, respectively, to recover 15 missing tags. Increasing j causes an increase in the average running time of the GE decoding to 0.96 ms and in the IT decoding to 0.052 ms. On the other hand, increasing the group size to 169, where $j = 3$, causes a large increase in the average time, especially for the GE decoding, to 4.6 ms, in order to recover 25 missing tag IDs, whilst the IT decoding only requires 0.084 ms. Figure 5.9 shows the average error rate of the identification of missing tag IDs from a group of $n=169$, where $j=4$ and the related decoding time for both the IT and GE decoding algorithms. It is clearly shown that the latter can recover more missing tag IDs than the former. However, its decoding time is higher due to the fact that the IT decoding algorithm has a linear decoding complexity of $O(x)$, whereas the GE has a complexity of $O(x^3)$, where x is the codeword block length. Generally, the GE decoding algorithm provides the optimum decoding in terms of missing recovery capabilities. However, the complexity and thus, the time needed for the decoding procedure could make it impractical in real RFID systems, especially for a large group of tags. Thus, a good decoding strategy may combine the GE and IT decoding algorithms in order to make a compromise between the performance and complexity.

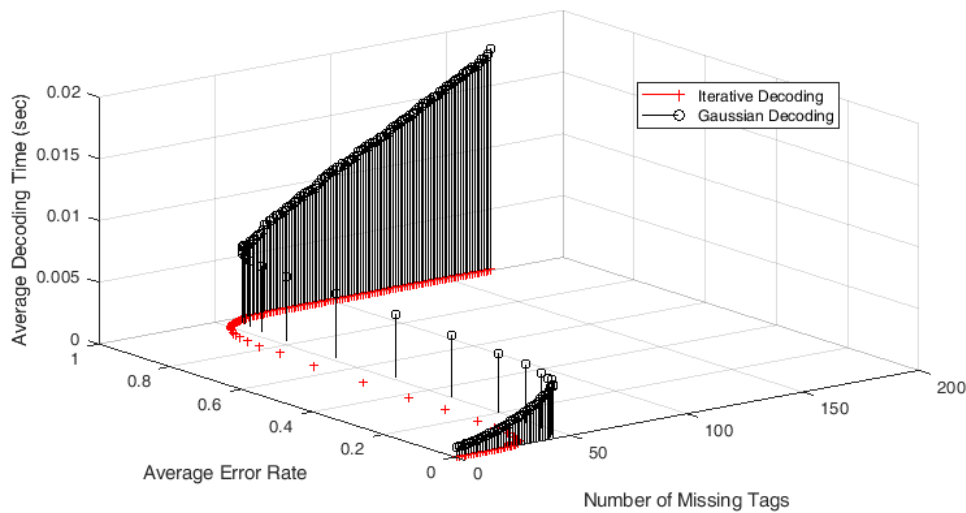


Figure 5.9: The average error rate of the identification of missing tag IDs from a group of $n=169$, where $j=4$ and the related decoding time for both the IT and GE decoding algorithms

5.4.2 PEG-based vs CRT-based LDPC Codes

This subsection evaluates the performance of the (n, j, l) PEG-based and (n, j, w) CRT-based LDPC codes with large group sizes with the IT and GE decoding algorithms. In order to derive a realistic baseline performance comparison, the same group size n and column weight j are used to build the matrices of the two codes. Table 5.2 compares the girth as well as the memory consumption of the PEG-based and CRT-based codes. Clearly, according to the results, the PEG-based codes outperform their counterpart by having larger girths and low memory consumption. Even though the $(512, 3, 19)$ and $(1024, 3, 29)$ PEG-based codes have girths similar to the CRT-based codes, each tag needs to record only 828-bit and 1245-bit, respectively, of additional information which is smaller than those of the CRT-based codes. The large number of parity check values m in the PEG-based codes may affect the decoding complexity. However, this can be simplified by using the improved hybrid decoding algorithm designed in the next chapter. Increasing the group size also increases the girth of the PEG-based codes to 10, while that of the CRT-based one remains stable. For the CRT-based codes, increasing w from 2 to 3 degrades the girth to 4 and increases the memory consumption. Figure 5.10 and Figure 5.11 show the performance of these codes in recovering missing tag IDs with the IT and GE decoding algorithms, respectively. It is clear that the PEG-based codes have advantages over the CRT-based codes in preventing small stopping sets with low memory consumption. Appendix B contains the constructed $(512, 3, 2)$ and $(512, 3, 3)$ CRT-based LDPC matrices as well as the $(512, 3, 6)$ and $(512, 3, 19)$ PEG-based LDPC matrices.

Codes	Girth	m	Tag memory consumption in bits
$(512, 3, 2)$ CRT-based	6	82	948
$(512, 3, 3)$ CRT-based	4	30	2478
$(512, 3, 6)$ PEG-based	8	256	438
$(512, 3, 19)$ PEG-based	6	82	828
$(1024, 3, 2)$ CRT-based	6	106	1377
$(1024, 3, 3)$ CRT-based	4	38	3357
$(1024, 3, 6)$ PEG-based	10	512	486
$(1024, 3, 29)$ PEG-based	6	106	1245

Table 5.2: Comparisons of the PEG-based and CRT-based LDPC codes

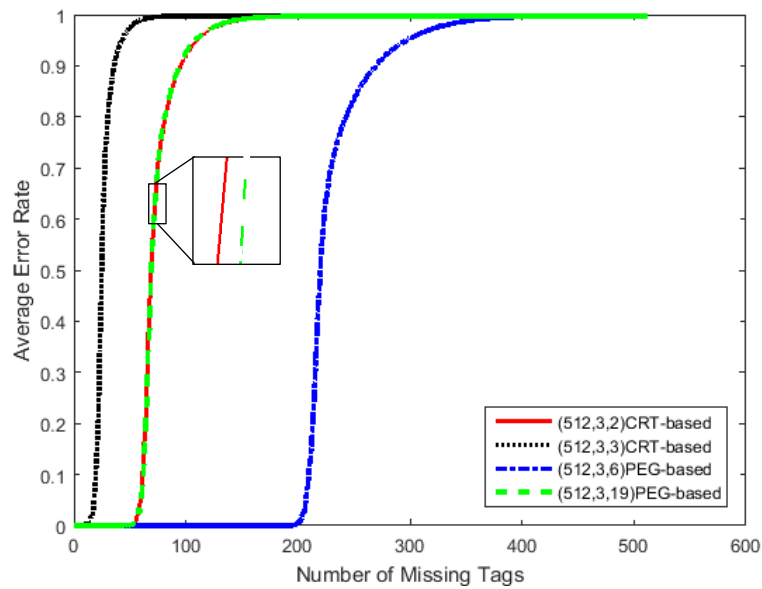


Figure 5.10: The average error rate of the identification of missing tag IDs from a group of size $n = 512$ using the PEG-based and CRT-based codes with the IT decoding algorithm

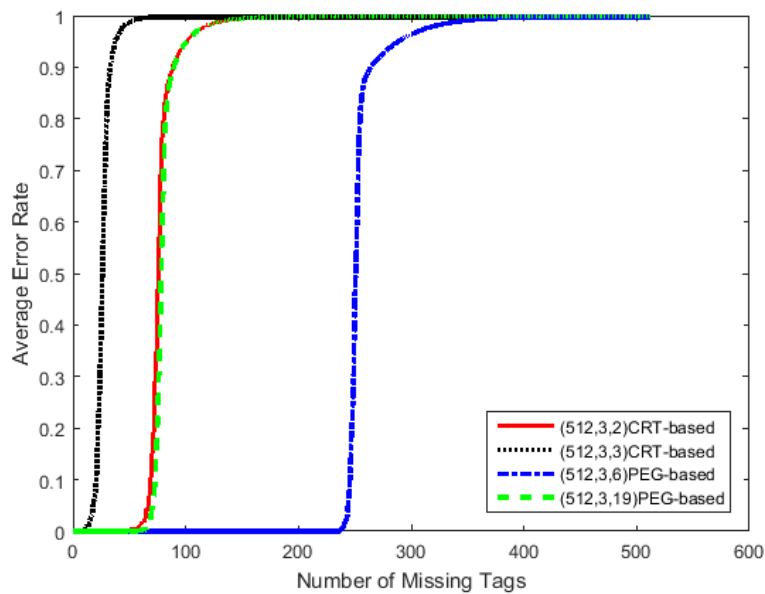


Figure 5.11: The average error rate of the identification of missing tag IDs from a group of size $n = 512$ using the PEG-based and CRT-based codes with the GE decoding algorithm

5.4.3 PEG-based vs ACE-based LDPC Codes

The performance of the PEG-based and ACE-based LDPC codes with different group sizes are evaluated under the IT and GE decoding algorithms. The two codes are constructed using the same parameters, including n , m , and j . Table 5.3 compares the girths as well as the memory consumptions of the PEG-based and ACE-based codes. The PEG-based codes outperform their counterpart by consuming lower memory overheads. Figure 5.12 shows the performance of the codes with the IT and GE decoding algorithms. It can be concluded that the PEG-based codes have advantages over the ACE-based ones in preventing small stopping sets with low memory consumption for low to medium amounts of missing tags. However, the ACE codes outperform their counterparts for high amounts of missing tags. Appendix B presents the constructed (502, 3) PEG-based and ACE-based LDPC matrices.

(n, j) Codes		Girth	m	Tag memory consumption in bits
(256, 3)	ACE-based	4	128	558
	PEG-based	8		423
(502, 3)	ACE-based	4	251	612
	PEG-based	8		423

Table 5.3: Comparisons of the PEG-based and ACE-based LDPC codes

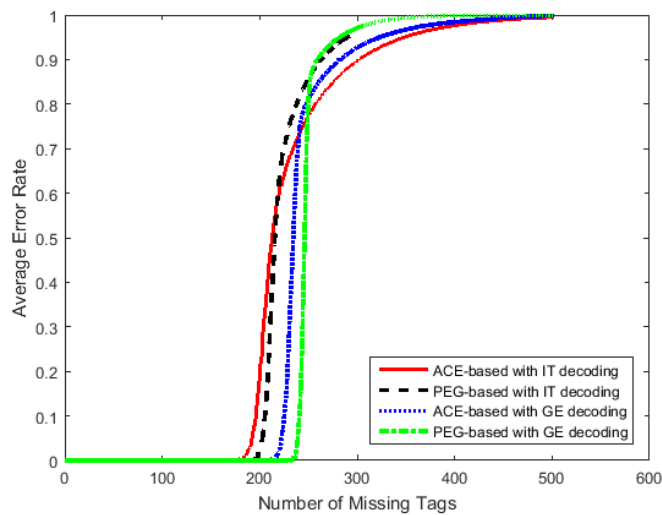


Figure 5.12: The average error rate of the identification of missing tag IDs from a group of size $n = 502$ using the PEG-based and ACE-based codes with the IT and GE decoding algorithm

5.5 Conclusions

This chapter has presented the PEG-based LDPC codes for improving the recovery performance of missing RFID tag IDs in the extended grouping of group integrity application. A group of RFID tag IDs has been treated as packet symbols and encoded and decoded in a way similar to that of the BECs. Due to the mitigation of the PEG method for small stopping sets, it has been used to construct the parity check matrix H of LDPC codes of size $m \times n$. Then, the matrix H was utilised as a generator matrix to encode a group of n RFID tag IDs and generate m parity check values. The missing recovery performance of the constructed codes has been tested and evaluated with the IT decoding and GE decoding algorithms. The properties of the constructed PEG Tanner graphs have also been analysed and compared with the Tanner graphs of other codes. The simulation results show that the PEG-based LDPC codes can provide significant missing recovery enhancement with the same or less memory overheads compared to other existing LDPC-based codes.

6 Improved Hybrid IT/GE Decoding Algorithm

This chapter focuses on optimising the decoding complexity of the PEG-based LDPC code for the extended grouping of RFID tags using a hybrid (HB) decoding algorithm. It combines the IT with the GE decoding algorithms, with the basic idea of employing the IT decoding first. If it fails to recover all the erased symbols, the GE decoding is activated to complete the decoding process and resolve the simplified system. This HB decoding is improved by including an early stopping criterion to avoid unnecessary iterations of the IT decoding algorithm for undecodable blocks, thus saving decoding time. Extensive simulations have been carried out to analyse and assess the performance achieved with decoding the PEG-based LDPC codes under the improved HB decoding algorithm, both in terms of missing recovery capabilities and decoding complexities.

6.1 Early Termination of the IT Decoding Algorithm

Early termination of the IT decoding algorithm has been widely researched within correcting errors introduced by channels. In each iteration, the algorithm detects decodable blocks by checking the parity check constraints. If all parity check constraints are satisfied, the decoding terminates, otherwise, the decoding always completes I_{\max} iterations for undecodable blocks. The decoding time increases linearly with the number of decoding iterations. To avoid unnecessary decoding iterations when processing undecodable blocks, an effective stopping criterion is required to terminate the decoding process early and hence, save decoding time and tag power consumption (Mohsenin *et al.*, 2011). Different early stopping criteria have been proposed for the IT decoding algorithm, aiming to detect undecodable blocks and to stop the decoding process in its early stage. These criteria can be divided into two types as follows.

- One type utilises log-likelihood ratios (LLRs), for example the criterion presented by Kienle and Wehn (2005). It identifies undecodable blocks using variable node reliability, which is the addition of the absolute values of all variable node LLRs. The decoding process is stopped, if the variable node reliability remains unchanged or is decreased within two consecutive iterations. This is a consequence of the observation that there is a consistent increase of the variable node reliability from a decodable block. Similar criteria have been proposed by Li *et al.* (2006), Cai *et al.* (2008), and Chen (2012), which monitor the convergence of the mean magnitude of the LLRs at the end of each iteration to identify undecodable blocks.
- The other types of criteria are those that observe the numbers of satisfied or unsatisfied parity check constraints. For example, the criterion in Shin *et al.* (2007) and the improved version in Alleyne and Sodha (2008) compare the numbers of satisfied parity check constraints in two consecutive iterations. If they are equal, the decoding process is halted. On the other hand, the criteria in Han and Liu (2010) and Mohsenin *et al.* (2011) use the number of unsatisfied parity check constraints to detect undecodable blocks.

During the HB decoding process of the PEG-based codes, the decoding time of the IT decoding for undecodable blocks becomes longer as the decoding iterates for I_{max} . Figure 6.1 shows the number of iterations as a function of the missing tags for two variants of group sizes, including 49 and 169 tags, where $j=3$. I_{max} is set to 50 and 150, respectively. It is explicit that as the number of missing tags increases, iteration for I_{max} starts to occur due to the existence of undecodable blocks. This can clearly be seen in the region where the IT decoding has failed, for example, when recovering more than 10 and 17 missing tags from a group of 49 and 169, respectively. Therefore, taking into account an early stopping criterion, which adaptively adjusts the number of decoding iterations, arises as an attractive solution to avoid unnecessary iterations and thus, save decoding time. Since the main advantage of the HB decoding is to reduce the GE decoding complexity, the frequency of its usage should be

as small as possible even for a large number of missing tags. In addition, when GE decoding is utilised, the size of the simplified system should be as small as possible. This suggests a stopping criterion for the PEG-based LDPC code that permits partial decoding of undecodable blocks up to a point where the IT decoding algorithm cannot recover any further missing tag IDs. The proposed criterion can distinguish between decodable and undecodable blocks. It does not cause any computation overheads, as it utilises the information available during the decoding process. Algorithm 6.1 outlines the improved IT decoding algorithm with the early termination criterion. Let v_j denote the set of variables in the j^{th} check equation of the code, and E_{c_j, v_i} is the outgoing message from the check node j to the variable node i . The improved algorithm is based on the observation of the amount of erasures n_e^I at the end of each iteration I . It halts the decoding process, if the amount remains unchanged or does not decrease within two consecutive decoding iterations, as in Step 24. This is as a result of the observation that the decodable blocks exhibit a consistent decrease in the amount of erasures.

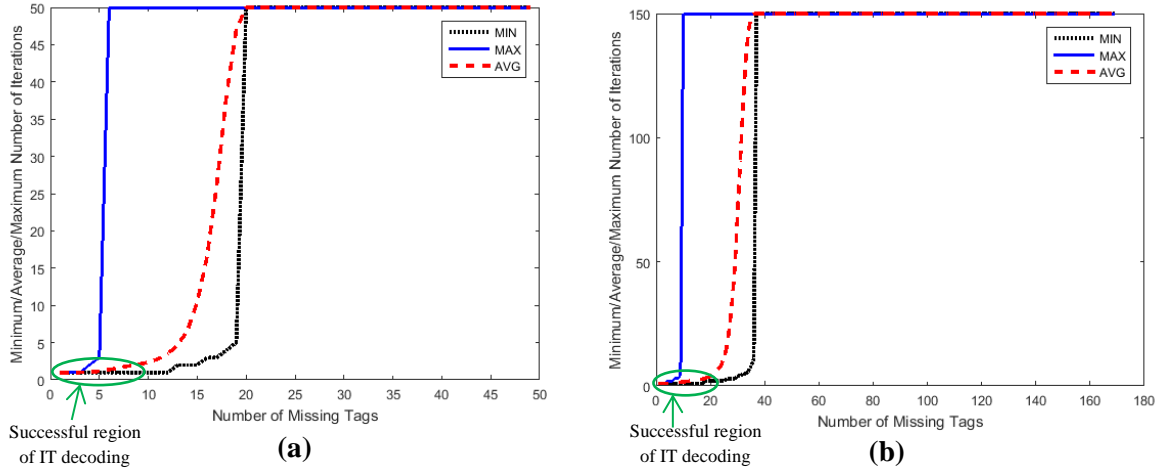


Figure 6.1: The iteration numbers required for decoding two group sizes: (a) $n = 49$; (b) $n = 169$, where $j = 3$, using the PEG-based LDPC codes

Algorithm 6.1: Improved IT Decoding**Input:** the received codeword y **Output:** $M = [M_1, \dots, M_n]$ where $M_i \in \{0, 1, e\}$

```

1:  $I = 1$  › Initialisation
2:  $n_e^{I-1} = n_e$ 
3: for  $i = 1$  to  $n$  do
4:    $M_i = y_i$ 
5: end for
6: repeat
7:   for  $j = 1$  to  $m$  do
8:     for all  $i \in v_j$  do
9:       if a check node  $j$  receives only one  $M_i = 'e'$  then
10:         $E_{c_j v_i} = \sum_{\tilde{i} \in v_j, \tilde{i} \neq i} M_{\tilde{i}} \oplus c_j$  › Calculating check nodes messages
11:       else
12:         $E_{c_j v_i} = 'e'$ 
13:       end if
14:     end for
15:   end for
16:   for  $i = 1$  to  $n$  do
17:     If  $M_i = 'e'$  then
18:       If there is at least one  $E_{c_j v_i} = 0$  or  $1$  then
19:         $M_i = E_{c_j v_i}$  › Recovering missing tag ID using incoming messages
20:       end if
21:     end if
22:   end for

```

- 23: $n_e^l = \text{count 'e' in } M_i \forall i = 1 \dots n$
- 24: **if** ($M_i \neq 'e' \forall i = 1 \dots n$) or ($I = I_{max}$) or ($n_e^{l-1} = n_e^l$) **then**
- 25: Terminate the IT decoding and start the GE decoding
- 26: **else**
- 27: Increment I
- 28: $n_e^{l-1} = n_e^l$
- 29: **end if**
- 30: **until** terminated

To illustrate the impact of the early stopping criterion on decoding time, Figure 6.2 shows iteration numbers taken for various missing amounts to be compared with those of the conventional IT decoding, as depicted in Figure 6.1. One can observe that the stopping criterion greatly reduces the average number of iterations in the region where the IT decoding is not successful. Figure 6.2 shows that undecodable blocks need, at most, 16 and 22 iterations, respectively, when recovering more than 10 and 17 missing tags.

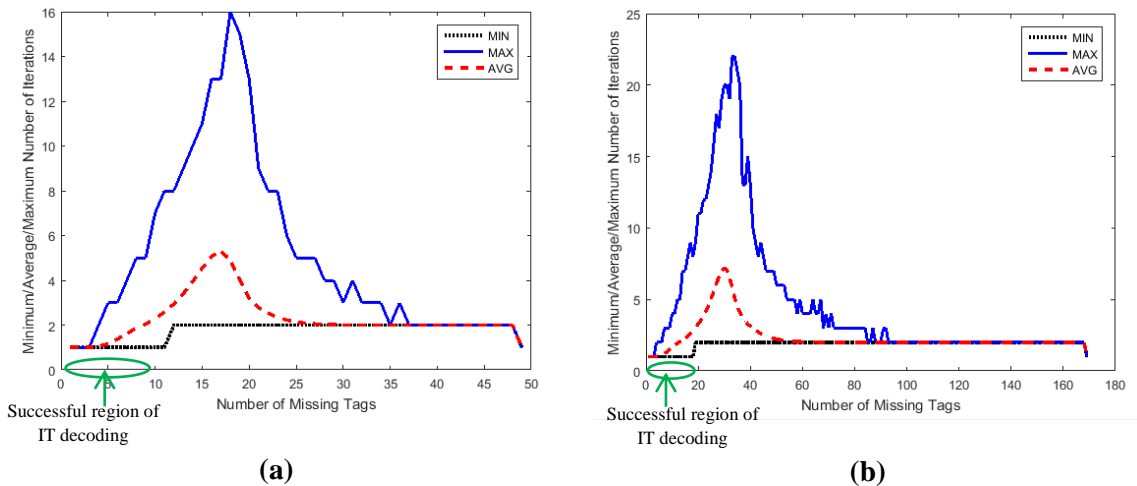


Figure 6.2: The enhanced iteration numbers required for decoding two group sizes: (a) $n = 49$; (b) $n = 169$, where $j = 3$, using the PEG-based LDPC codes

6.2 Missing Recovery Capability Analysis

To illustrate the performance of the improved HB decoding algorithm in recovering missing tag IDs, Figure 6.3 and Figure 6.4 show the average error rate as a function of the number of missing tags under the improved HB and GE decoding algorithms for the same parameters in Table 5.1. It is clear that the performance of the two decoding algorithms is identical, which means that the improved HB algorithm achieves the optimal missing recovery capabilities of the full GE decoding algorithm, since the remaining systems of the IT decoding are solved with this algorithm. Similar to the performance of the IT and GE decoding algorithms, in subsection 5.4.1 of Chapter 5, increasing j increases the value of m and thus, the d_{min} of the code, which results in increasing the value of d_{stop} and the rank of the matrix H_k . However, the amount of memory consumption increases as a consequence. For example, if 13 tags are missing from a group of $n = 49$, all their IDs can be recovered with at least $j = 3$ under the improved HB decoding. In this case, each tag records 432-bit additional information. However, if 16 IDs are missing, the column weight needs to be adjusted to 4 in order to achieve 100% reliable recovery (zero average error rate) and thus, each tag is required to store 576-bit additional information.

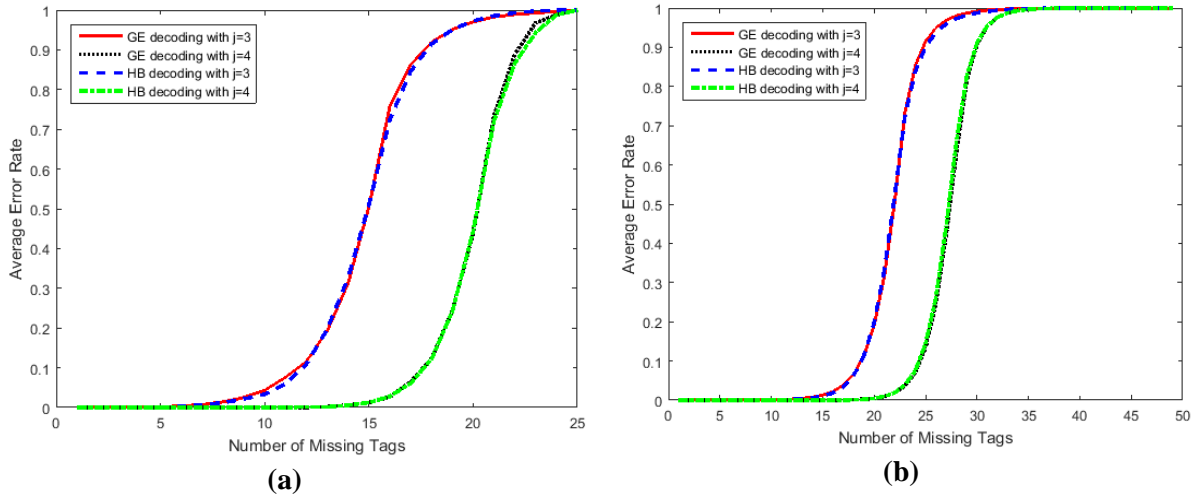


Figure 6.3: The average error rate of the identification of missing tag IDs from different group sizes: (a) $n = 25$; (b) $n = 49$ using the PEG-based LDPC codes with the GE and improved HB decoding algorithm

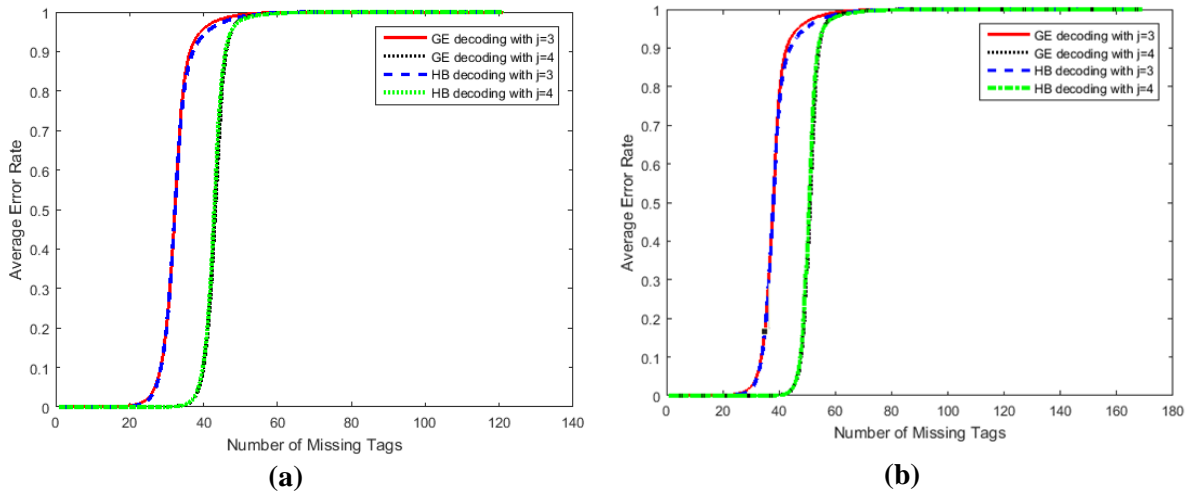


Figure 6.4: The average error rate of the identification of missing tag IDs from different group sizes: (a) $n = 121$; (b) $n = 169$ using the PEG-based LDPC codes with the GE and improved HB decoding algorithm

6.3 Decoding Complexity Analysis

The relative complexities of the improved HB decoding algorithm are analysed in terms of decoding time and the number of operations required. The entire decoding complexity is equal to the complexity of the IT decoding plus that of the GE decoding, if stopping sets exist. This is mainly determined by the efficiency of the first stage of the IT decoding; the better its performance, the less the complexity and thus, the time of the improved HB decoding.

6.3.1 Decoding Time Analysis

Two experiments are conducted:

- 1) Decoding time measurements when the IT decoding fails and thus, the GE decoding is required. This is the worst case from a decoding point of view;

- 2) Decoding time measurements as a function of the number of missing tags to compare two cases, one where the IT decoding is successful and the other where the IT decoding fails and the GE decoding is needed. This experiment is more illustrative of real situations.

Decoding Time when the GE Decoding is Required (Worst Case): Figure 6.5 illustrates the decoding time during the GE decoding process of the improved HB decoding for a group of 169 tags, where $j = 3$. By changing the number of missing tags, the resulting average simplified system size changes, which affects the decoding time. The figure illustrates this time as a function of the simplified system size and the related result. The systems size is equal to the number of unrecovered missing tag IDs after the IT decoding phase. The region where the IT decoding recovers some missing tag IDs is only considered in this analysis. In the second region, where the IT decoding cannot recover any missing tag IDs, the GE decoding time is equal to that of the full systems. The improved HB decoding algorithm efficiently decreases the average decoding time of the GE decoding, because the complex GE decoding is only utilised when required over a simplified system resulting from the IT decoding. The histogram demonstrates that all simplified systems have an average decoding time close to their minimum, which indicates that most systems have a decoding time below their average. It can clearly be seen that the maximum average decoding time remains nearly below 0.004 s related to a maximum decoding time of 0.004 s. In contrast, the GE decoding on the full systems is slower, especially for a large group of tags. When the system size increases, the GE decoding time also increases, following an $O(x^3)$ law. This is confirmed in Figure 6.6 part (b) presented in the next section. For a group of size 169, where $j = 3$, it is evident that the decoding time lasts, on average, 0.006 s.

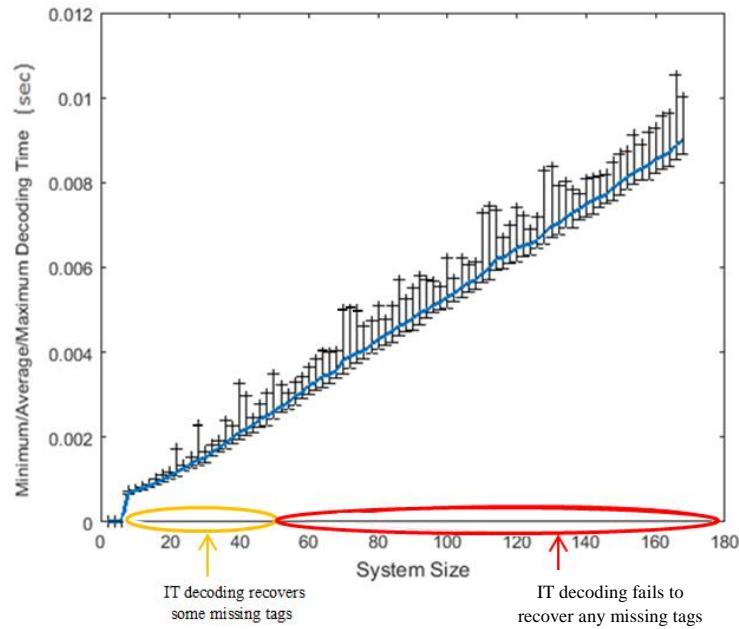


Figure 6.5: Histogram of the GE decoding time with respect to the simplified system size for a group of size $n = 169$, where $j = 3$, using the PEG-based LDPC codes

Decoding Time of the Improved Hybrid Decoding: Figure 6.6 and Figure 6.7 show the average decoding time as a function of the number of missing tags under the IT with early termination, the GE, and improved HB decoding algorithms. It is evident that the decoding time depends on the missing amounts experienced. With small numbers of missing tags, the decoding time of the improved HB decoding is fast and is similar to that of the IT decoding. This is clear in the first region, where the IT decoding is successful. After this, the decoding time of the improved HB decoding progressively increases since the IT decoding turns out to be ineffective in recovering some missing tags and thus, the size of the simplified system, which is solved by the GE decoding, starts to increase. On the other hand, due to the stopping criterion, the IT decoding still continues, trying to decode missing tags as much as possible, as shown on the figure. Then, above a certain threshold which depends on the missing recovery capabilities of the IT decoding, the decoding time of the improved HB decoding gradually approaches the full GE decoding as shown in the third region. It is clear that the n and j parameters also have major impacts on the decoding time. As n or j increases,

the improved HB decoding time increases too. This is due to the increasing in the number of operations required by the IT and GE decoding algorithms, as seen in the next subsection. If the HB decoding time is compared with the GE decoding time for the full system, it can be concluded that this decoding is faster for small to medium numbers of missing tags, even when the GE decoding is required.

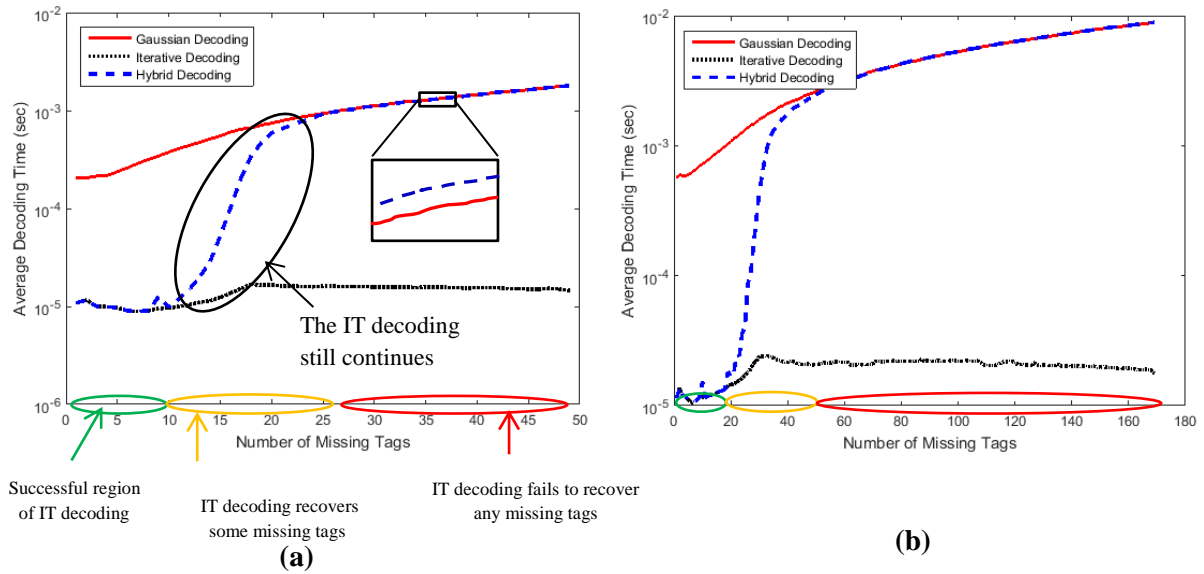


Figure 6.6: The average decoding time for recovering missing tag IDs from two group sizes: (a) $n = 49$ and (b) $n = 169$, where $j = 3$, using the PEG-based LDPC codes under the IT with early termination, the GE, and improved HB decoding algorithms

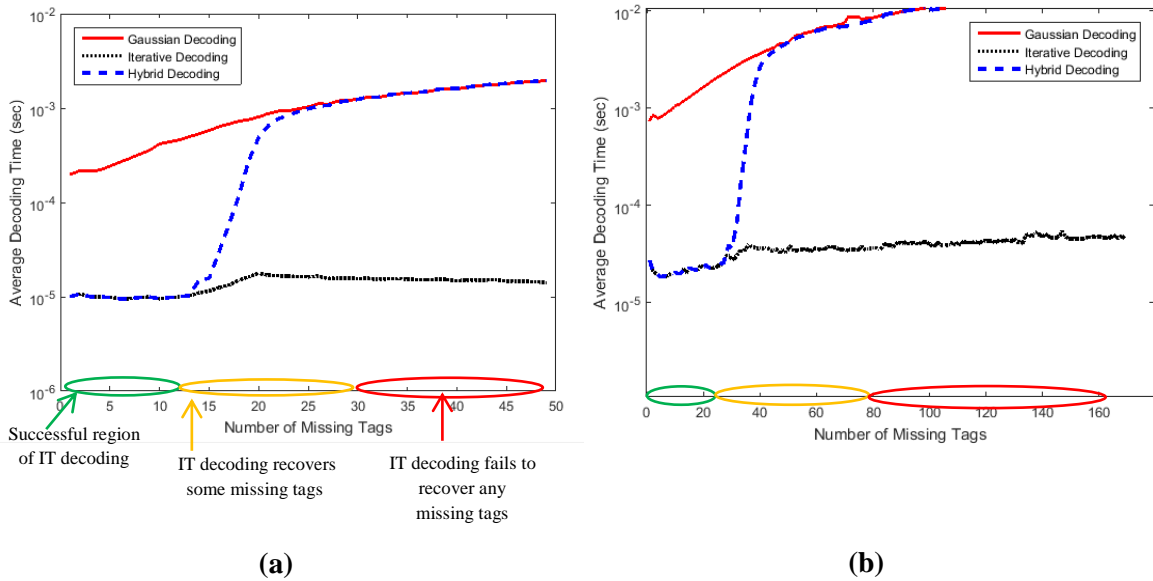


Figure 6.7: The average decoding time for recovering missing tag IDs from two group sizes: (a) $n = 49$ and (b) $n = 169$, where $j = 4$, using the PEG-based LDPC codes under the IT with early termination, the GE, and improved HB decoding algorithms

6.3.2 Operational Complexity Analysis

This subsection focuses on analysing the operational complexity of decoding the PEG-based LDPC codes with the improved HB decoding algorithm.

6.3.2.1 IT Decoding Algorithm Analysis

During the IT decoding process, if at row i of H there exists more than one erasure, then there is insufficient information to decode each erasure. Thus, these rows are not calculated during the operational complexity analysis, except for counting the number of bit operations. A bit operation is a test operation on a single bit variable. The search for erasures on the i -th row needs n bit operations and for all m rows, $m \times n$ bit operations are needed. In each iteration of the IT decoding algorithm, the number of erasures n_e is reduced. The IT decoding begins with the parity check equation with a single erasure. For each equation having only a single erasure, the single recovery process needs $n-1$ multiplications and $n-1$ XOR operations. Therefore, the required number of operations for the IT decoding algorithm (N_o^{IT}) in terms of n_e erasures with I_{max} iterations is:

$$N_o^{IT} = \sum_{l=2}^{I_{max}} ((n_e^{l-1} - n_e^l) (2n-2) + m n) \quad (6.1)$$

6.3.2.2 GE Decoding Algorithm Analysis

The GE decoding algorithm solves Equation (5.3), by reducing H_k to the row echelon form. The process of the algorithm is composed of two phases: The forward elimination phase to find n_e independent equations and an equation-solving phase to solve the set of n_e linearly independent equations. The forward elimination phase first reduces the system into an upper triangular form, which can be done using elementary row operations, as follows: Starting from $i = 0$, search for a nonzero entry in column i , the pivot, with row $j \geq i$. Rearrange rows i and j and then, add the row i to all the rows having nonzero elements of column i . At the

same time, the same process is performed on the simplified right-hand side (RHS) of the system, that is, the right entry of the i -th row is added to right entries of related rows. The search for the first 1 on the i -th column needs a maximum of m bit operations and for all n_e columns, $m \times n_e$ bit operations are needed. Once a "1" entry is found in row j , test whether $H_{k_{ib}} = 1$ for $b = 1, 2, \dots, j-1, j+1, \dots, m$, and then, add row j to row b . This phase needs a single bit operation, which checks whether $H_{k_{ib}} = 1$ and $n_e + 1$ operations for the addition of row j to row b . Since these operations have to be performed for $b = 1, 2, \dots, j-1, j+1, \dots, m$ and $i = 1, 2, \dots, n_e$, a total of $n_e(m-1)(2+n_e)$ operations is needed. Hence, the total number of operations needed by the GE decoding algorithm to triangulate an $m \times n_e$ matrix is:

$$(m \times n_e) + n_e(m-1)(2+n_e) \quad (6.2)$$

$$mn_e^2 + 3mn_e - n_e^2 - 2n_e \quad (6.3)$$

The algorithm continues with a backward substitution phase, recursively resolving erased symbols until the solution is found. The last symbol of an upper triangular matrix gives the value of the symbol on the RHS. Then, this value is replaced in all the equations in which it is included. With n_e equations to be solved in a linear system, the calculated value of each decoded bit requires n_e multiplications and $n_e - 1$ XOR operations. Thus, the required number of operations for the second phase is:

$$n_e(2n_e - 1) \quad (6.4)$$

$$2n_e^2 - n_e \quad (6.5)$$

For the RHS of the system, it needs n_e multiplications and n_e XOR operations, where n_e is the number of known tag IDs. Therefore, the required number of operations to simplify the RHS of the system is:

$$2n_e \cdot m \quad (6.6)$$

For a complete GE decoding algorithm, the required number of operations (N_o^{GE}) is obtained by adding Equations (6.3), (6.5), and (6.6) to get:

$$N_o^{GE} = 3n_e(m-1) + n_e^2(m+1) + 2mn_e \quad (6.7)$$

6.3.2.3 Improved Hybrid Decoding Algorithm Analysis

The improved HB decoding algorithm first employs IT decoding with an early stopping criterion. If this fails to recover all the erased symbols owing to the existence of stopping sets, GE decoding is activated to complete the decoding process and to resolve the simplified system. Since the improved HB decoding algorithm combines the IT decoding and GE decoding algorithms, the entire decoding complexity is equal to the complexity of IT decoding plus that of GE decoding to solve the simplified system. Three cases are considered here relating to the behaviour of the IT decoding algorithm.

- The first case is when the IT decoding algorithm successfully recovers all missing tag IDs and the complexity in this case includes only that of this algorithm.
- The next case is when the IT decoding algorithm fails to recover some missing tag IDs and the complexity here includes the IT decoding computations and GE computations for the unrecovered missing IDs after the IT decoding algorithm.
- The final case is when the IT decoding algorithm fails to recover any missing tag IDs, and the GE computations on the full system are only considered here. The complexity of the improved HB decoding algorithm is illustrated in Table 6.1, where n_{e^*} is the number of unrecovered missing tag IDs after the IT decoding phase.

Case	Number of Operations
First Case	N_o^{IT}
Second Case	$N_o^{IT} + 3n_{e^*}(m-1) + n_{e^*}^2(m+1) + 2mn_{e^*}$
Third Case	N_o^{GE}

Table 6.1: Number of operations for the improved HB decoding algorithm

Figure 6.8 and Figure 6.9 depict a comparison of the operational complexity between the IT, GE, and improved HB decoding algorithms for two group sizes, including 49 and 169, where j varies between 3 and 4. It is clear that the decoding complexity depends on the missing amounts n_e . For a small amount of n_e where IT decoding is successful, the complexity of the improved HB decoding is similar to that of IT decoding, such as when n_e is below 10 for a group of 49 tags and $j = 3$. For a medium amount of n_e where IT decoding fails to recover some missing tag IDs, the complexity of IT decoding starts to decrease due to the stopping criterion, whereas the complexity of the improved HB decoding gradually approaches that of the full GE decoding, because the latter is required more often. Then, above a threshold where IT fails to recover any missing tag IDs, the complexity of the improved HB decoding is equal to that of the full GE decoding algorithm. It is clear that the PEG method parameters also affect the decoding complexity. As a group size n or column weight j increases, the improved HB decoding complexity also increases as shown in the black ovals on the y-axis. This can be attributed to particular phenomena. The complexity of the IT decoding also depends on the number of XOR and multiplication operations, which is determined by the number of variables in each parity check constraint, whereas the complexity of GE decoding mainly depends on the number of linear equations and the number of variables. Therefore, by increasing n or j , the number of operations required by the IT and GE decoding algorithms is increased accordingly.

It can be concluded that the improved HB decoding considerably reduces the decoding complexity and thus the time of the full GE decoding for small and medium amounts of missing tags, which are proportional to the total number of tags in a group. For example, missing a medium amount of tags from a group of 49 tags would be considered as a small amount for a group of 169 tags. The improved HB decoding could enhance the group integrity applications, such as grouping or categorising animals, based on certain features, to produce different food in a factory.

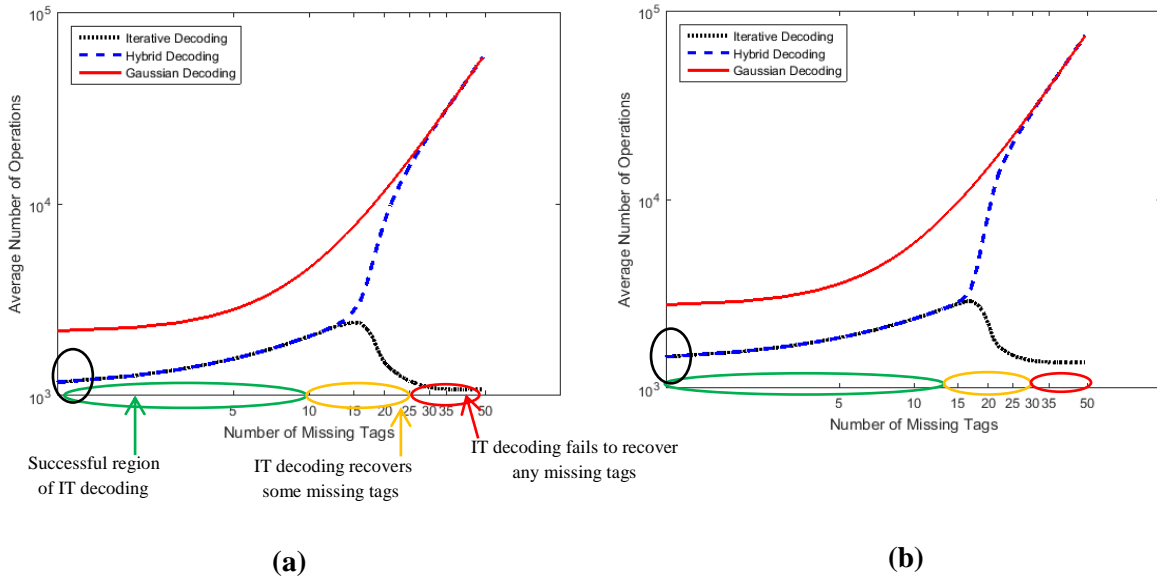


Figure 6.8: Operational complexity comparison between the IT, GE, and improved HB decoding algorithms for a group of $n=49$, where (a) $j=3$ and (b) $j=4$

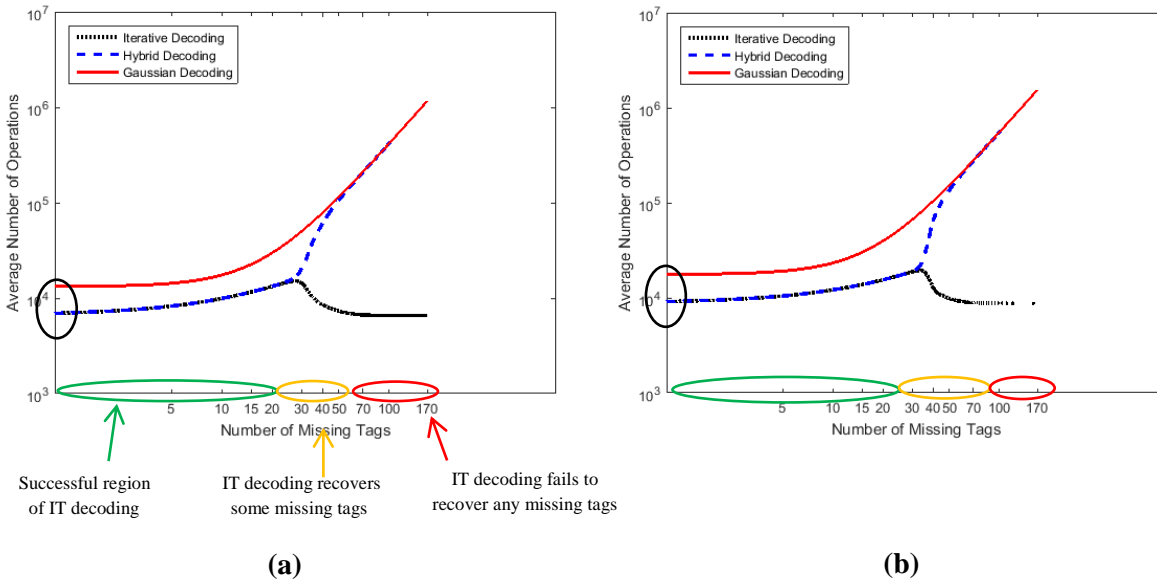


Figure 6.9: Operational complexity comparison between the IT, GE, and improved HB decoding algorithms for a group of $n=169$, where (a) $j=3$ and (b) $j=4$

6.4 Conclusions

The decoding complexity of the PEG-based LDPC codes has been optimised using an improved HB IT/GE decoding algorithm. This improved HB decoding includes an early

stopping criterion to avoid unnecessary iterations of IT decoding for undecodable blocks and thus, saving decoding time. The stopping criterion greatly reduces the average number of decoding iterations for undecodable blocks and therefore, reduces decoding time when compared to the conventional IT decoding algorithm. It has been shown that the improved HB decoding algorithm achieves the optimal missing recovery capabilities of the full GE decoding, since the remaining systems of IT decoding are solved with the GE decoding algorithm. The relative complexities of the improved HB decoding algorithm have been analysed both in terms of decoding time and the number of operations required. Simulation results have been presented demonstrating that the improved HB decoding algorithm considerably reduces the operational complexity and thus, the time of the full GE decoding for small to medium amounts of missing RFID tags, up to a certain threshold value, which depends on the missing recovery capabilities of IT decoding. This makes the improved HB decoding algorithm a promising candidate for decoding the PEG-based LDPC codes in the extended grouping of group integrity application in RFID systems.

7 Adaptive Hybrid Decoding Algorithm

In this chapter, the joint use of the two decoding components of the improved HB decoding algorithm is adapted based on the missing amounts of RFID tags in order to avoid the IT decoding when the missing amount is larger than a threshold and thus, save more decoding time. The optimum value of the threshold value has been investigated for different missing amounts of tags and different parameters of the PEG method through empirical analysis. Various simulations have been conducted in order to analyse and evaluate the impact of the threshold value on the improved HB decoding time. This chapter also analyses and assesses the missing recovery performance of various short-length irregular PEG-based LDPC codes constructed with different variable degree sequences.

7.1 Threshold Analysis

The improved HB decoding algorithm can be easily tailored to avoid the IT decoding phase and thus, save more decoding time when the number of missing tags exceeds a threshold (θ_{th}). This threshold represents the capability of the IT decoding algorithm to recover missing tag IDs, which depends on the missing amounts n_e and the parameters of the PEG method, including n and j . The optimum value for θ_{th} is obtained by empirical analysis. The simulation is implemented with different parameters of the PEG method over a range of the numbers of missing tags in the region where the IT decoding recovers some missing tag IDs. Figure 7.1 demonstrates the reduction in the number of missing tags across iterations without the stopping criterion for a group of 169 tags, where $j = 3$. It can clearly be seen from part (a) of the figure, that for values of $n_e \leq 40$, the number of missing tags decreases, but for values of $n_e \geq 70$, the number of missing tags does not, even as $I \rightarrow I_{max}$. The transition value of n_e between these two results is called the θ_{th} value. To close in on θ_{th} further, the simulation is applied to

a range of numbers of missing tags between these two values. Part (b) shows that, for values of $n_e \geq 58$, the number of missing tags does not decrease by one, even as I gets very large, but for values of $n_e \leq 47$, this decreases by at least two missing tags. To close in on θ_{th} even further, the simulation is applied between these two values as in Part (c) and therefore, it can be concluded that the value of θ_{th} is in the range 50–53. Even though the value of θ_{th} is larger than the amount of the parity check values, the GE decoding phase of the HB decoding can still recover some missing tag IDs, as depicted in Figure 5.5 of Chapter 5. Table 7.1 illustrates the values of θ_{th} for different parameters of the PEG method. The results reveal that this value increases by increasing n or j . This is because larger LDPC codes built with the PEG methods have elegant properties in regard to their girth.

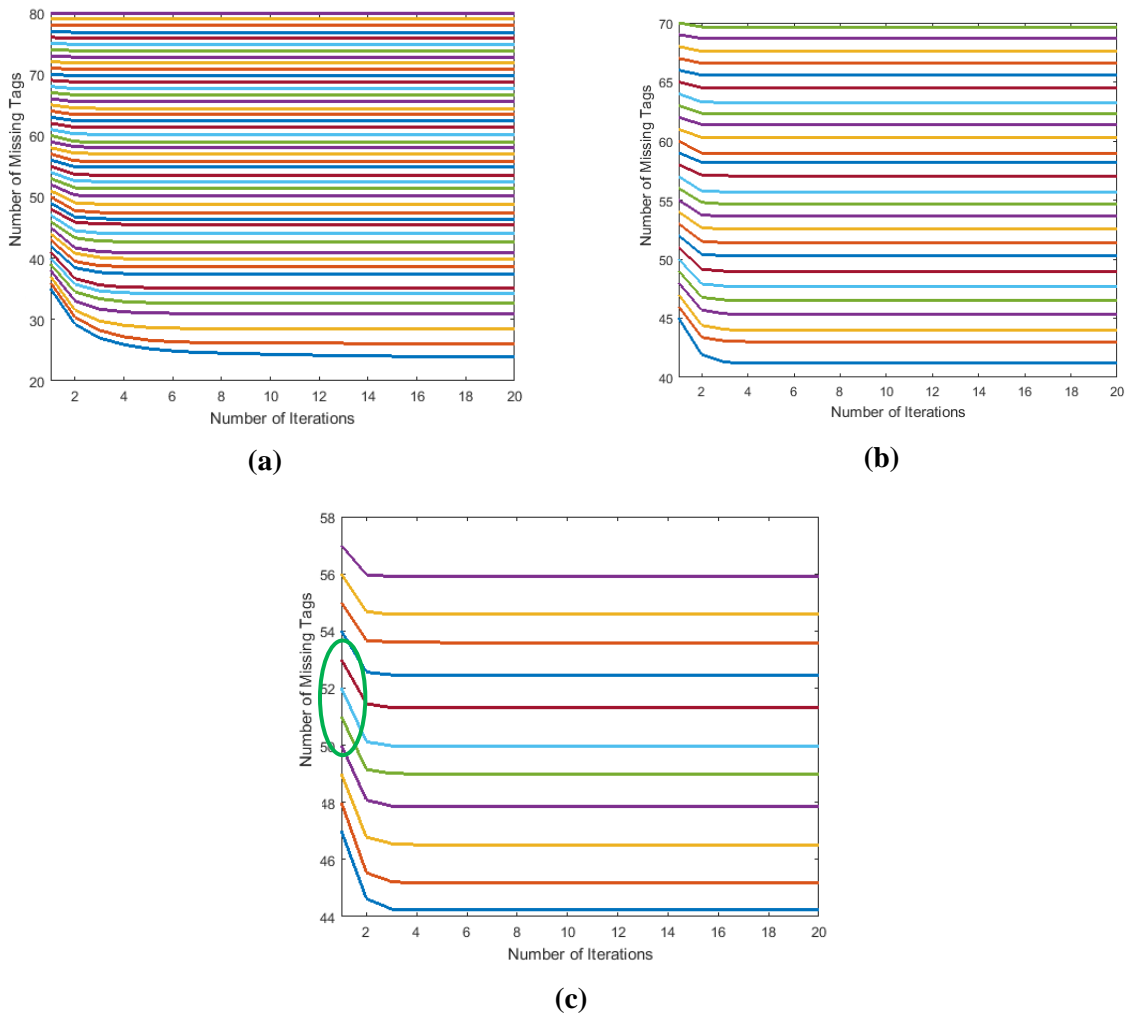


Figure 7.1: Reduction in the number of missing tags with iterations for $n=169$ tags, where $j=3$

Parameters (n, j, l)	The value of θ_{th}
(25, 3, 5)	9-11
(25, 4, 5)	11-13
(49, 3, 7)	22-24
(49, 4, 7)	23-25
(121, 3, 11)	40-43
(121, 4, 11)	42-45
(169, 3, 13)	50-53
(169, 4, 13)	54-57

Table 7.1: The values of θ_{th} for different parameters of the PEG method

To illustrate the impact of θ_{th} on the improved HB decoding time, Figure 7.2 shows a plot of the average decoding time of the adaptive algorithm for a group of 49 and 169, where $j = 3$. The process of the simulation is repeated for each value of θ_{th} in the range depicted in Table 7.1 in order to achieve an optimum time. Compared with the results obtained in Figure 6.6, the results shown in Figure 7.2 indicate that the adaptive decoding algorithm is very efficient in decreasing the average decoding time of the improved HB decoding and thus, save more decoding time of up to 10% for large amounts of missing RFID tags where the IT decoding fails to recover any missing tags.

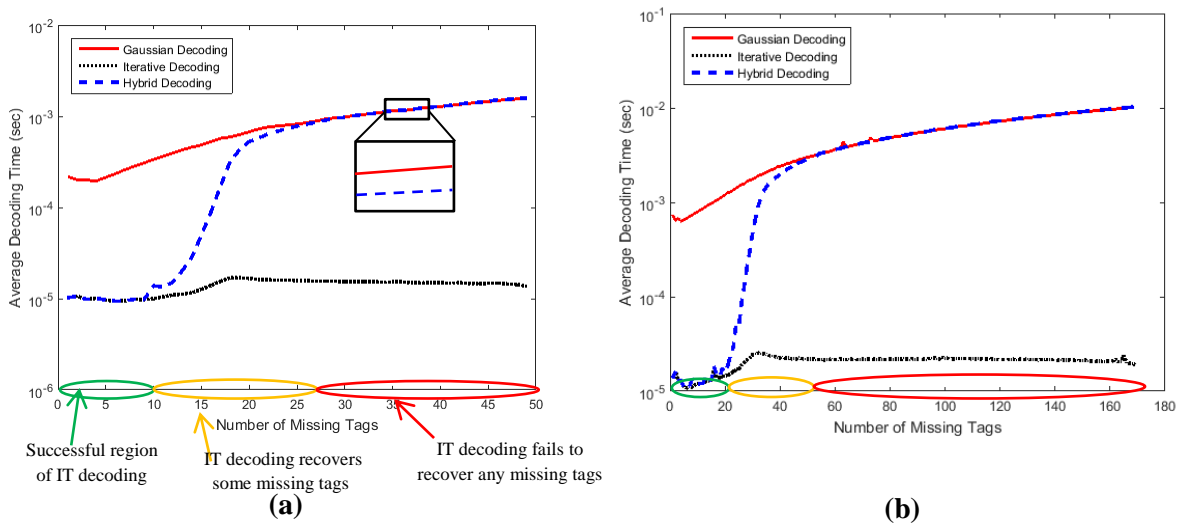


Figure 7.2: The average decoding time for recovering missing tag IDs from two group sizes: (a) $n = 49$ and (b) $n = 169$, where $j = 3$, using the PEG-based method under the IT with early termination, the GE, and improved HB decoding algorithms

7.2 Irregular PEG-based LDPC Codes

Grouping RFID tags with regular codes provides an equal missing protection level for all the members since each tag is involved in the same number of parity check constraints (or subgroups). On the other hand, there are applications where not all the members need the same missing protection level. For example, in the application of tracking personal luggage at the airport, some bags are regarded as more important than others, because they contain valuable items. Therefore, the important tagged objects should have higher missing protection levels, such that they are more likely to be recovered. Since variable nodes of higher degrees in irregular codes converge faster (Luby *et al.*, 2001b), they are assigned to valuable tagged objects.

Hu *et al.* (2002; 2005) built irregular LDPC codes using the PEG method, where IT decoding exhibits a significant performance compared with randomly constructed codes. This performance is not surprising in the light of a study rigorously accentuating the power of irregular graphs in designing erasure correcting codes conducted by Luby *et al.* (2001b). Some studies have been dedicated to examining the convergence thresholds for regular and irregular LDPC codes, such as those by Luby *et al.* (1997) and Richardson *et al.* (2001). The results show that the thresholds of irregular LDPC codes generally outperform regular codes. This section investigates the performance of half rate short-length irregular PEG-based LDPC codes constructed from different variable node degree sequences, where $n = 256$. In the PEG construction, the variable node distribution is only considered and the parity check node distribution is kept to be as uniform as possible (Hu *et al.*, 2001). The half rate irregular PEG-based codes are constructed based on the optimised degree distribution given in Table I and II of Richardson *et al.* (2001), with maximum variable node degrees 5, 8, 11, 15, and 20. On the other hand, five regular codes are constructed with the same parameters (with $n=256$, $m=128$, and $j=3$), but with different seeds in order to get different distributions. It has been remarked

that the simulated performance for the five (256, 3, 6) regular codes exhibits identical behaviour and for this reason only one code is presented in the plot. Figure 7.3 shows the performance of the constructed codes, where it is clear that the performance of the irregular codes outperforms the regular one in the first regions where IT decoding is successful. This discloses that for short block lengths, the density evolution is an effective method for the designing of good irregular PEG-based LDPC codes. However, their performances are lower than the regular code in the second region, where the IT decoding recovers some missing tag IDs, as clearly illustrated inside the orange oval. Among the constructed irregular codes, the one with the maximum variable degrees of 8 achieves the best performance in the first region. The performance of the regular code versus the irregular codes is also clear when increasing n to 512, as illustrated in Figure 7.4.

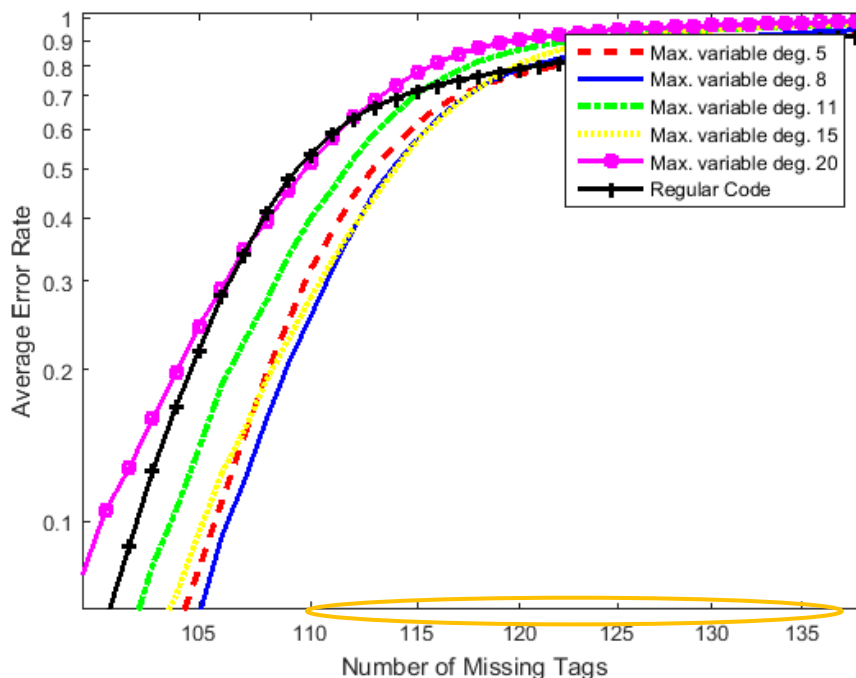


Figure 7.3: The average error rate of the identification of missing tag IDs for irregular and regular PEG-based codes with $n=256$ under the IT decoding algorithm

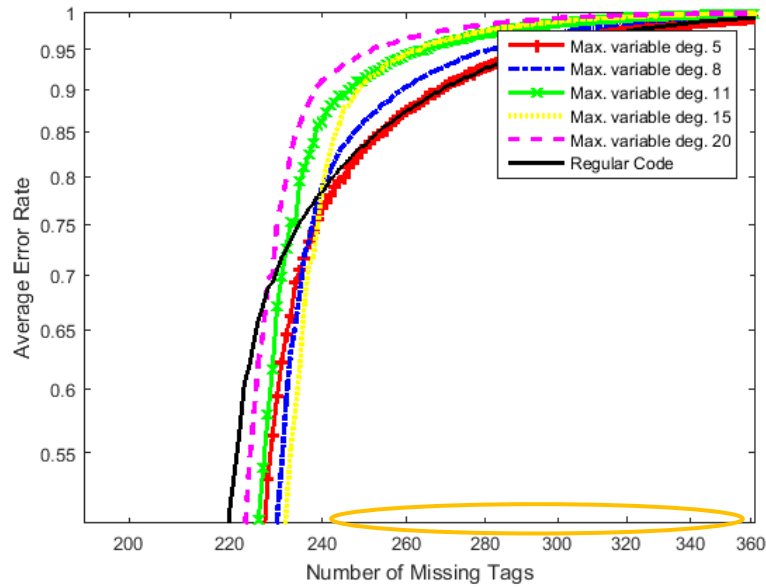


Figure 7.4: The average error rate of the identification of missing tag IDs for irregular and regular PEG-based codes with $n=512$ under the IT decoding algorithm

To gain a clear insight into the second region where the IT decoding fails to recover some missing tag IDs, especially inside the orange oval, the previous empirical threshold analysis conducted in section 7.1 is extended to compare the performance of the irregular code with maximum variable degrees of 8 and the regular one. From Figure 7.5, one can observe that the capability of the regular code in recovering missing tag IDs in the second region exceeds that of the irregular one and thus, its θ_{th} value is larger as marked by the green oval.

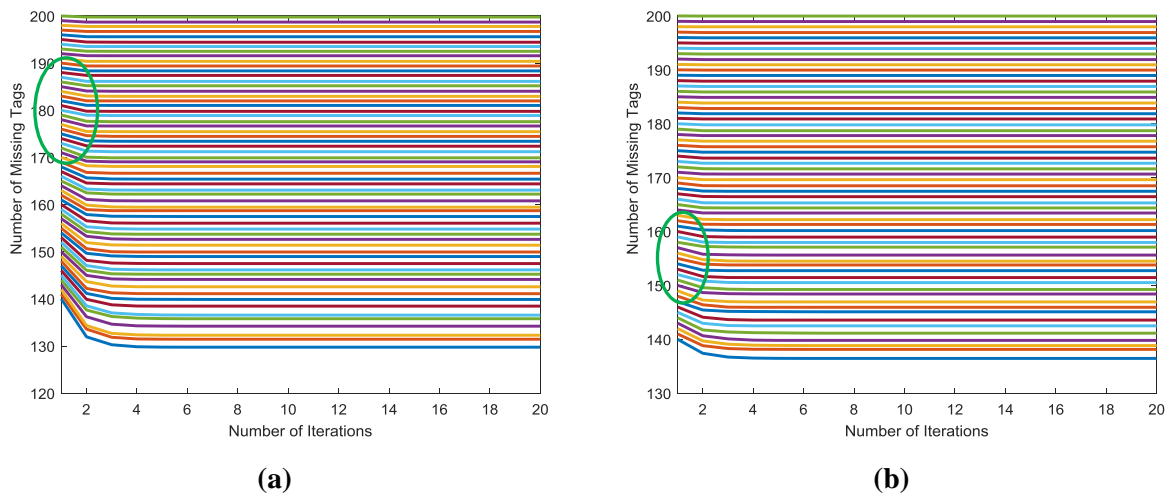


Figure 7.5: Reduction in the number of missing tags with iterations for: (a) regular and (b) irregular PEG-based LDPC code with $n=256$

Figure 7.6 shows the influence of changing the fractions of low degree variable nodes, particularly λ_2 and λ_3 , on the performance of half rate short-length irregular codes, while the fractions of high degree variable nodes are kept the same. Table 7.2 shows the variable degree sequences of the simulated irregular codes based on table 2.4 of Tjhai (2007). The results show that as the fraction of low degree variable nodes increases, the performance of the IT decoding in recovering missing tag IDs also increases in the two regions, as demonstrated by Code 3, Code 4, Code 5, and Code 6. The main reason for this behaviour is that these irregular codes with a high fraction of low degree variable nodes have a higher minimum Hamming distance d_{min} and a lower amount of short cycles. Among all of these codes, Code 6 achieves the best performance.

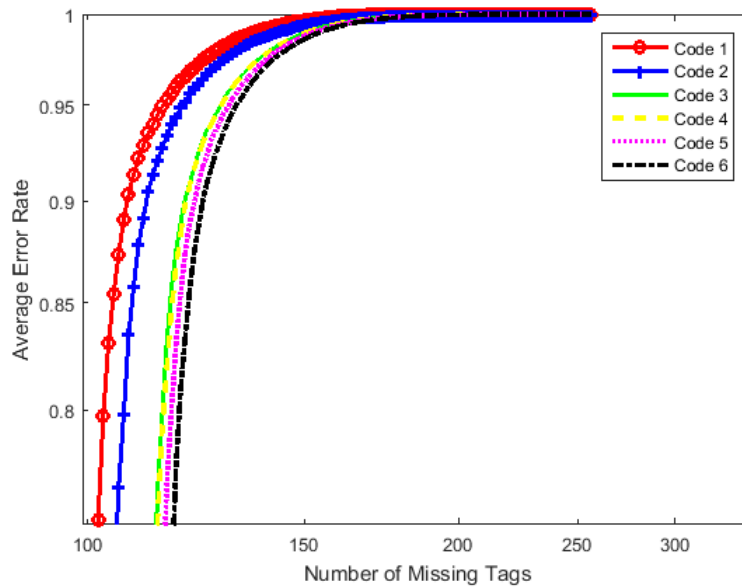


Figure 7.6: Influence of changing the fractions of low degree variable nodes on the performance of half rate short-length irregular PEG-based LDPC codes with $n=256$

Code	λ_2	λ_3	λ_4	λ_5	λ_{14}
Code 1	0.200	0.100	0.550	0.050	0.100
Code 2	0.250	0.200	0.400	0.050	0.100
Code 3	0.350	0.400	0.100	0.050	0.100
Code 4	0.450	0.200	0.200	0.050	0.100
Code 5	0.500	0.175	0.175	0.050	0.100
Code 6	0.550	0.150	0.150	0.050	0.100

Table 7.2: Variable degree sequences for irregular codes in Figure 7.6

Figure 7.7 illustrates the influence of changing the high degree variable nodes of half rate short-length codes on the performance of recovering missing tag IDs. Table 7.3 shows the variable degree sequences of the simulated irregular PEG-based LDPC codes. These irregular codes have the same degree sequences except for their maximum variable node degree. It is evident that the recovery performance of the irregular code that has a maximum variable node degree of 7 outperforms other simulated irregular codes in both regions. On the other hand, the recovery performance degrades as the irregular code has a higher maximum variable node degree, as demonstrated by Code 11. This is due to a specific phenomenon. Increasing the maximum variable node degree causes an increase in the amount of short cycles.

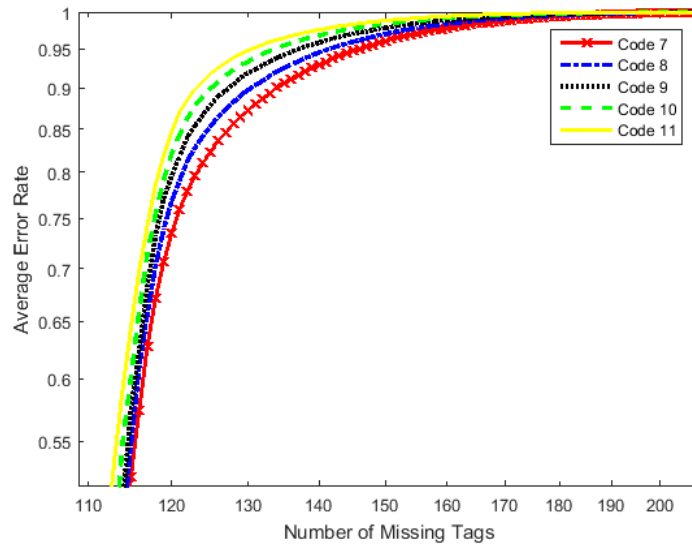


Figure 7.7: Influence of changing high degree variable nodes on the performance of half rate short-length irregular PEG-based LDPC codes with $n=256$

Code	λ_2	λ_3	λ_4	λ_5	λ_7	λ_9	λ_{11}	λ_{13}	λ_{15}
Code 7	0.550	0.150	0.150	0.050	0.100				
Code 8	0.550	0.150	0.150	0.050		0.100			
Code 9	0.550	0.150	0.150	0.050			0.100		
Code 10	0.550	0.150	0.150	0.050				0.100	
Code 11	0.550	0.150	0.150	0.050					0.100

Table 7.3: Variable degree sequences for the irregular codes in Figure 7.7

Opposite to Figure 7.6, Figure 7.8 illustrates the influence of changing the fractions of high degree variable nodes on the recovery performance of half rate short-length irregular PEG-

based LDPC codes, while the fractions of low degree variable nodes are kept the same. Table 7.4 shows the variable degree sequences of the simulated irregular codes. In contrast to the findings of Tjhai (2007) on additive white Gaussian noise (AWGN) channels, the results show that increasing the fraction of the high degree variable nodes degrades the recovery performance in the two regions, as demonstrated by the performance of Code 14, Code 18, and Code 22. On the other hand, Code 13, Code 17, and Code 21, which have the smallest fraction of high degree variable nodes achieve the best performance among other simulated irregular codes in their group.

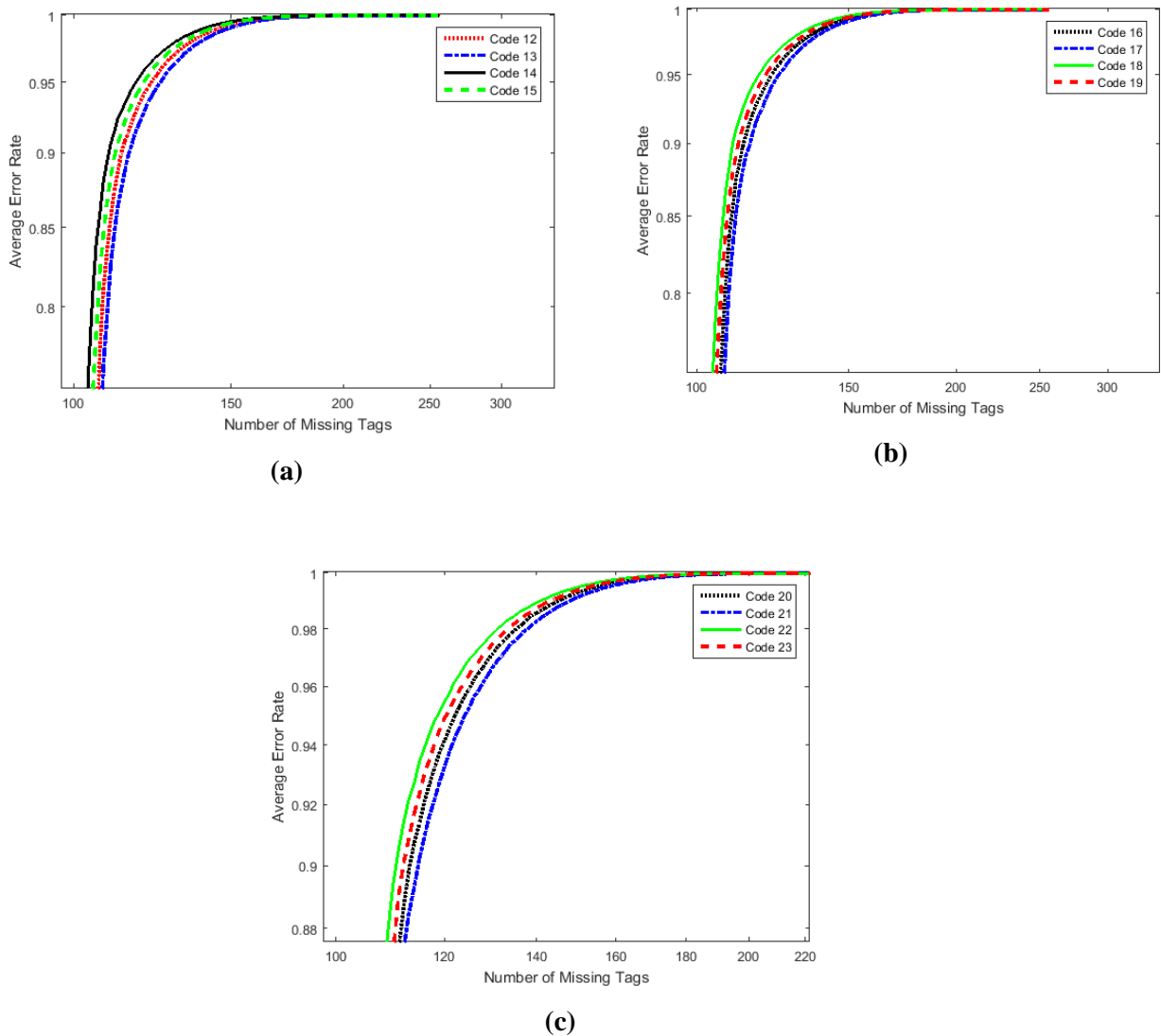


Figure 7.8: Influence of changing the fractions of high degree variable nodes on the performance of half rate short-length irregular PEG-based LDPC codes with $n=256$

Code	λ_2	λ_3	λ_4	λ_5	λ_{12}
Code 12	0.250	0.200	0.400	0.050	0.100
Code 13	0.250	0.215	0.400	0.050	0.085
Code 14	0.250	0.171	0.400	0.050	0.129
Code 15	0.250	0.186	0.400	0.050	0.114
Code 16	0.250	0.200	0.400	0.050	0.100
Code 17	0.250	0.200	0.415	0.050	0.085
Code 18	0.250	0.200	0.371	0.050	0.129
Code 19	0.250	0.200	0.386	0.050	0.114
Code 20	0.250	0.200	0.400	0.050	0.100
Code 21	0.250	0.200	0.400	0.065	0.085
Code 22	0.250	0.200	0.400	0.021	0.129
Code 23	0.250	0.200	0.400	0.036	0.114

Table 7.4: Variable degree sequences for the irregular codes in Figure 7.8

7.3 Conclusions

The joint use of the two decoding components of the improved HB decoding algorithm is adapted based on the missing amounts of RFID tags in order to avoid IT decoding when the missing amount is larger than a threshold and thus, save more decoding time. The optimum value of the threshold value has been investigated for different missing amounts of tags and different parameters of the PEG method through empirical analysis. It has been shown that the adaptive decoding algorithm is very efficient in decreasing the average decoding time of the improved HB decoding for large amounts of missing RFID tags where IT decoding fails to recover any missing tags. More simulations have been conducted to analyse and evaluate the missing recovery performance of various short-length irregular PEG-based LDPC codes constructed with different variable degree sequences. It has been demonstrated that the irregular PEG-based LDPC codes exhibit noticeable missing recovery enhancements compared to the regular PEG-based LDPC codes in the region where IT decoding is successful. However, their performances are degraded in the second region where IT decoding can recover some missing tag IDs. It has been empirically found that for half rate

short block lengths, the density evolution method is good for irregular PEG construction. Simulation results have also shown that as the fraction of low degree variable nodes increases, the performance of IT decoding in recovering missing tag IDs also increases in the two regions. On the other hand, increasing the fraction of the high degree variable nodes degrades the recovery performance in the two regions. In addition, the recovery performance of the code that has a maximum variable node degree of 7 outperforms other simulated codes with maximum variable node degrees of 9, 11, 13, and 15 in both regions.

8 Bloom Filters

A Bloom filter (BF) is a simple data structure that can store the items of a set in a space efficient way and support membership queries that ask: “Is element a in set B ?”. Burton Bloom presented BFs in 1970 (Bloom, 1970). Since that time, BFs have received increased attention and been extensively employed in various systems due to their space efficiency. This has been reflected in the latest studies and numerous new proposed algorithms that are directly or indirectly based on BFs, as shown in the existing surveys targeted different systems other than RFID systems and accomplished by Broder and Mitzenmacher (2004), Tarkoma *et al.* (2012); Geravand and Ahmadi (2013), Saravanan and Senthilkumar (2015), and Luo *et al.* (2018). Despite BFs enabling false positives, the space optimisation always outweighs this limitation in most practical applications as long as the probability of the false positive is sufficiently small and controlled. This chapter provides an overview of BFs with a focus on their construction, features, limitations, variations, and the ways in which they have been utilised in some systems, especially in RFID ones. This review gives preliminary information relevant to the designing of the novel redundant tag information collection protocol presented in the next chapter.

8.1 Preliminaries of Bloom Filters

A BF of a set $W = \{w_1, w_2, \dots, w_y\}$ containing y elements is described by a hashed Boolean vector of b bits, all initialised to 0. A BF uses k independent hash functions h_1, \dots, h_k , which map each element $w \in W$ to the bits $h_z(w) \in \{1, 2, \dots, b\}$ for $1 \leq z \leq k$ that are set to 1. For ideal performance, each of the k hash functions should be a part of the class of universal hash functions. In other words, it should hash each item to a uniform random number. In order to check whether an item $q \in W$, a k hash function is applied to q and whether all $h_z(q)$ have

been set to 1 is checked, otherwise, $q \notin W$. Testing a membership using a BF may yield a false positive due to hash collisions. That is, it suggests that an item $q \in W$, but it is not when all indexed bits were previously set to 1 by other items. Figure 8.1 illustrates an example of a BF, where the filter is initialised with zeros. Each item w_i in the set is hashed k times and each hash result represents a bit location which is set to 1. To test whether an element q_i is a member in the set, it is hashed k times and the related bits in the filter are checked. The element q_1 is definitely not a member because one of the related bits is 0. On the other hand, the element q_2 is either a member or the related bits have by chance been set to 1 during the insertion of other elements.

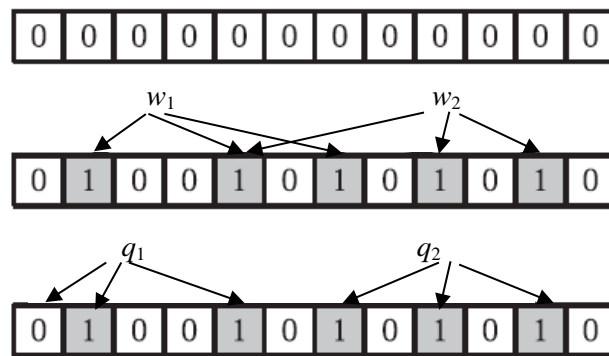


Figure 8.1: An example of a Bloom filter

As abovementioned, even though the BF allows false positives, for many applications in practical situations the space savings always outweigh this limitation when the false positive rate is controlled to be adequately small (Broder and Mitzenmacher, 2004). According to Bloom (1970), the probability of a false positive for an element not in the set or the false positive rate P_{FP} of the BF constructed from m elements is derived as follows. By assuming that a hash function chooses each position in the BF with equal probability, the probability that a certain bit is not set to 1 by a hash function when adding an element to the filter is:

$$1 - \frac{1}{b} \quad (8.1)$$

With k hash functions, the probability that none of them are set a certain bit to 1 is:

$$\left(1 - \frac{1}{b}\right)^k \quad (8.2)$$

The probability that a given bit is remain 0 after adding m elements to the BF is:

$$\left(1 - \frac{1}{b}\right)^{mk} \quad (8.3)$$

Therefore, the probability that the bit is 1 is:

$$1 - \left(1 - \frac{1}{b}\right)^{mk} \quad (8.4)$$

During membership testing, an element is said to be a member of a set, if all of the k positions in the BF are set to 1. Consequently, the probability of this occurring when the element is not a member can be represented as:

$$P_{FP} = \left(1 - \left(1 - \frac{1}{b}\right)^{mk}\right)^k \quad (8.5)$$

From the Taylor series expansion, the value of $1 - 1/b$ is almost the same as $e^{-\frac{1}{b}}$ and thus:

$$P_{FP} \approx \left(1 - e^{-\frac{mk}{b}}\right)^k \quad (8.6)$$

P_{FP} can be reduced by reducing the value of the right-hand side of Equation (8.5). The minimum value of P_{FP} can be found by taking the derivative of Equation (8.5) with respect to k as:

$$\frac{dP_{FP}}{dk} = 0 \quad (8.7)$$

which gives the optimal value of k as:

$$k = \frac{b}{m} \times \ln 2 \quad (8.8)$$

and thus, the minimum value of P_{FP} is $0.61285^{b/m}$. At this point, the BF achieves a balanced configuration in which nearly half of the bits are set to 0 and half are set to 1. The more elements that are added to the set, the higher the probability of false positives. Therefore,

with the given k , to have a fixed false positive probability, the value of b must increase linearly with the number of elements added to the BF. As stated in Gremillion (1982) and Mullin (1983), the probability of the false positive in practice is larger than the value given by Equation (8.5). Theoretically, Bose *et al.* (2008) showed that Equation (8.5) offers a lower bound of the false positive rate. Given a desired P_{FP} and the number of elements m , the optimal length of the BF can be computed as:

$$b = -\frac{m \times \ln P_{FP}}{(\ln 2)^2} \quad (8.9)$$

For example, if the desired P_{FP} is 0.0001, signifying accuracy of 99.99 %, the optimal length of the BF is around $19.2 \times m$ bits. In practice, the probability of a false positive P_{FP} of a BF depends on three parameters, including the number of elements added to the set m , which is application dependable and cannot be controlled, the number of bits b or the length of the BF, and the number of hash functions k . To meet the accuracy requirement, the value of b should be optimised. There is a trade-off between the probability of the false positive and the length of the BF. A lower P_{FP} requires a larger value of b , which may increase the communication overheads of transmitting the BF between the reader and tags or the memory spaces to store the BF. Hence, for applications where the time or the space is critical, additional strategies may be required to remedy misjudged elements. However, the simulation results in subsection 9.6.3 of Chapter 9 show that the designed protocol is faster than other collection protocols even with the lowest tested value of P_{FP} . As k is proportional to b , increasing the latter causes an increase in the former. Implementing k hash functions on tags may cause processing overheads, because each tag needs to perform the calculations independently by using its limited resources. On the other hand, the implementation of hash functions can be simplified to decrease the complexity of a tag's circuit, as presented in subsection 9.5.4 of Chapter 9.

8.2 Bloom Filter Features

BFs exhibit the following features, which attract the designing of the novel redundant tag information collection protocol in this research.

Space efficient: BFs can considerably compress elements at the cost of a small false positive rate. The set of elements is compressed into a b bit vector, regardless of the size of the elements in bits. The resulting space cost only relates to the number of encoded elements m and not the size of the elements in bits (Bloom, 1970). For example, a BF with P_{FP} is equal to 0.0001 and an accuracy of 99.99 %, needs only around 19.2 bits per element to compress a set of parity check values each of size 96 bits. Having a set of 500 parity check values, the BF can save 80% of the bits needed. As a result, the BF is space efficient for compressing aggregated parity check values between the reader and the tags, which is the main reason why it has been included in the design of the novel redundant tag information collection protocol in this research.

Constant time of insertion and querying: The time complexity of inserting as well as querying an element in the BF is $O(k)$, which is less than that of trees, that is, $O(\log m)$. In addition, it is less than the time needed by lists or tables, which is equal to $O(m)$ (Guo *et al.*, 2010).

One inevitable error: Despite a BF suffering from inevitable false positives, it is free of false negatives. When a BF states that an element is not a member in a set, there is no doubt about the decision. In contrast, when a BF states that an element is a member of a set, there is a probability that the decision is incorrect (Broder and Mitzenmacher, 2004).

8.3 Bloom Filter Limitations

Even though BFs provide a compact structure for representing a set and supporting membership queries, they do experience some limitations and they are considered in the design of the redundant information collection protocols in this research. These limitations are in the following (Luo *et al.*, 2018):

False positives: The false positive rate can be decreased by extending the length of the BF. However, the misleading membership may cause some influences on the applications, which should be considered.

Adaptability: The three parameters of the BF are defined before deployment. Any bit is not allowed to be altered once it has been set to the binary 1. In addition, a BF is only representing a static set. That is, the encoded elements cannot be changed or deleted. Once implemented, the length of the BF and the employed hash functions cannot be altered.

Functionality: BFs support only membership queries, that is, additional operations, such as deletion and multiplicity queries, are not supported. When an element is deleted from the BF, the indexed bits cannot be set to 0, because they may affect another element and thus, label it as not a member of the BF, which leads to a false negative. This limitation will not affect the current state of the designed protocol.

Implementation: Whilst BFs are easy to implement, some requirements such as filter access, space optimisation, and cost calculation may cause some difficulties for the applications. In addition, implementing high performance hash functions requires complex operations, which may not suit lightweight hardware. The aforementioned requirements get even worse when there is a large amount of elements to be encoded. However, the implementation of hash functions can be simplified to decrease the complexity of a tag's circuit. For example, a pre-

stored logical ring of random numbers may be used to produce hash values, as described in subsection 9.5.4 of Chapter 9.

Despite these limitations, in particular, the false positives, the compact structure for representing a set of parity check values with a BF and thus, the reduced time to send these values between the reader and tags outweighs them, as long as the probability of the false positives is sufficiently small and controlled in the designed protocol in the next chapter.

8.4 Bloom Filter Variants

Several modifications and developments have been made over the standard BF from different aspects to overcome its limitations. In fact, the BF variants introduced below are the results of improving various systems. In this section, some important and commonly used variants are presented.

8.4.1 Counting Bloom Filters

The standard BF only allows for the insertion of elements into a BF. To enable the deletion of elements, a counting Bloom filter (CBF) was proposed by Fan *et al.* (2000), which replaces a vector of bits with one of counters. The CBF has d counters along with the d bits. When an element is inserted into or removed from the CBF, the related counters are increased or decreased respectively. Figure 8.2 demonstrates an example, where the counter values relate to the number of elements linked to the counter. The length of the counter should be sufficiently large enough to prevent counter overflow. In the analysis accomplished by the authors, it is concluded that a counter of 3 or 4 bits should suffice for most applications. CBFs have the same properties as BFs, at the expense of 3 or 4 times memory space cost. Ficara *et al.* (2008) proposed an enhanced structure called a Multi-Layer Compressed Counting Bloom Filter (ML-CCBF). The structure uses a hierarchy of hash-based filters in addition to CBFs in order to provide space to counters and thus to avoid overflows. Huffman

coding is also used to compress counter values even further. However, the costs of addition and deletion are increased accordingly. Rothenberg *et al.* (2010) improved upon the deletion process in terms of memory space, with an enhanced method that splits the filter into r regions. The collision information is represented by a compact representation composed of a bitmap of size r that sets to 0 when the region is free of collisions and thus, the deletions are permitted, otherwise, it is set to 1.

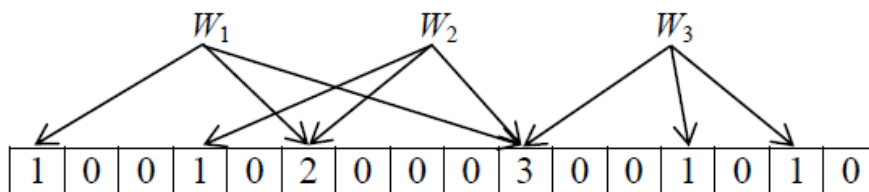


Figure 8.2: An example of a CBF

8.4.2 d -Left Counting Bloom Filters

Bonomi *et al.* (2006) proposed a data structure that utilises d -left hashing and fingerprints. It works in a way similar to that of a CBF, but with a less memory space. The d -left hashing method splits a hash table into d sub-tables with equal sizes. Each sub-table has r/d segments, where r is the total number of segments. Each segment contains a number of cells of fixed size and each cell maintains a counter and a fingerprint of the element. If an element is added to the table, d segments are selected by calculating d independent hash values of the element. Parallel search of the d sub-tables is used by element lookups to get the related fingerprint and counter. If an element is deleted, the counter is decreased by one. The counters of this type of filter are much smaller than those in the CBF owing to the utilisation of the d -left hashing and fingerprints that generate a smaller amount of collisions.

8.4.3 Space Code Bloom Filters

Kumar *et al.* (2006) proposed space code Bloom filters (SCBFs) to encode a multiset and to manipulate the number of existence of an element in the multiset. Typically, a group of standard BFs is used and a maximum likelihood estimation method to measure the existence of an element in the multiset. To add an element in the SCBF, the element is hashed using one set of randomly chosen hash functions and then, the related bits in the filter are set to 1. To perform a membership query for an element, the number of sets that the element matches is counted and this number is utilised to approximate multiplicity of the element in the multiset.

8.4.4 Scalable Bloom Filters

One limitation of a BF is to set the filter length d in advance based on the number of elements m and the desired value of P_{FP} . When the number of elements is unavailable, the filter length may be over-estimated and consequently, will consume memory spaces. Hence, Almeida *et al.* (2007) proposed a scalable BF to adapt the filter length to the number of elements added dynamically. The authors constructed a sequence of heterogeneous BFs in an incremental way. When a BF reaches its limit with respect to the false positive probability, a new one is inserted. Each BF uses different lengths and hash functions, which results in large overheads when performing membership queries. Later, in 2010, Guo *et al.* enhanced dynamic set representations with homogenous BFs structured in a dynamic matrix, the rows of which are related to the BFs. The matrix initially contains one active BF and the elements of the set are added to it. When the BF reaches the limit of its false positive probability, it is stored and set to be inactive and a new one is built and set to be active. The membership query process is similar to that of a standard BF, whereas deletion of an element is implemented in a way similar to that of CBFs. Despite the proposed structure enabling the representation of a dynamic set, the false positive probability may become too large and thus, it is necessary to

occasionally rebuild the whole structure. In addition, the upper bound on the number of elements m must be set in advance (Guo *et al.*, 2010).

8.4.5 Weighted Bloom Filters

The weighted BF, as proposed by Bruck *et al.* (2006), uses the number of queries to assign weights for the elements in BFs. The elements that have high frequencies of queries are allocated a high amount of hash functions in order to minimise the occurrence of false positives. The false positive probability differs for each input and the average false positive probability is calculated based on the frequencies of all the elements in the filter. This type of BF accomplishes a high level of optimisation for real time applications.

8.5 Applications of Bloom Filters

Originally, a BF was employed in dictionaries to search words and to support spell check operations in text editors, such as UNIX spell-checkers (Mullin and Margoliash, 1990). Instead of storing the whole dictionary, a compact representation of a BF is stored. If a false positive occurs, the text editor will spell the word incorrectly and in this case, it can be ignored. In distributed databases, rather than exchanging lists of information between hosts holding part of the database, BFs of these lists are sent to decrease communication overheads between hosts (Mullin, 1990). In Peer-to-Peer (P2P) networks, Guo and Li (2013) and Skachek and Rabbat (2014) employed BFs to find the set difference in order to solve the problems of approximate set reconciliation with minimum amount of information transmitted between two peers. Approximate set reconciliation is a common and fundamental task in P2P systems, where each member of a node pair wants to send its set of unique items to another member. For example, suppose there are two sets of items Set_x and Set_y , relating to two peers, x and y , respectively. An application requires to recognise those items that exist in set x , but not in set y , that is, items in $Set_x - Set_y$. A typical approach is to have y send a BF of its items

to x . Then, x will check all its items against the BF and transmit items that are not members of it. Due to the false positive probabilities, not all items in $\text{Set}_x - \text{Set}_y$ will be transmitted, but most will.

Luo *et al.* (2017) extended the set reconciliation to multisets reconciliation in which each set of items allows an item to appear multiple times, that is, the multiplicity of each item can be greater than one. Hence, each cell of the constructed BF includes two fields that store the IDs and the number of items linked to it in order to identify different items and differences in the multiplicities of these between the two multisets. Chen *et al.* (2012) used BFs in a similar fashion as employed in approximate set reconciliation problems, except that their goal was to find the set intersection and union instead of the set difference in multi-keyword search to decrease the transmission overheads. To find the set intersection, that is, $\text{Set}_x \cap \text{Set}_y$, y sends a BF of its items to x . Then, x will check all its items against the BF and transmits items that are members of it. False positives may be eliminated by recalculating the intersection operation of y and the result set. For the union operation, that is, $\text{Set}_x \cup \text{Set}_y$, the process is similar to the intersection operation except that the results set is obtained by choosing the items that are not in y by testing those in x using the BF. Finding the set difference between two pairs using the BF has inspired the designing of the novel redundant tag information collection protocol in this research.

In RFID systems, the literature contains a wealth of material based on the BF and its variants to solve various issues, including filtering duplicate data, as presented below, searching for a group of tags (Chen *et al.*, 2016), unknown tag scanning (Qian *et al.*, 2016), missing tag detection (Yu *et al.*, 2017), grouping (Liu *et al.*, 2016), and estimating the number of tags (Li *et al.*, 2015). Generally, BFs have been employed to compact the transmitted tag IDs between the reader and tags in order to reduce transmission overheads and the parameters of the BFs are set based on the predefined false positive rate requirement.

8.5.1 Filtering Duplicate Data from RFID Data Streams

RFID systems naturally produce a large amount of duplicate readings. Duplicate readings are produced because an RFID reader reads the same tag multiple times or the same tag is read by multiple readers due to their overlapped regions. Any reading is treated as a duplicate when it is recurrent and does not provide new information to the system. Duplicate readings need to be removed, because they waste memory and processing resources as well as causing communication overheads in RFID systems (Bashir *et al.*, 2013). Figure 8.3 shows the basic filtering concept of duplicate readings.

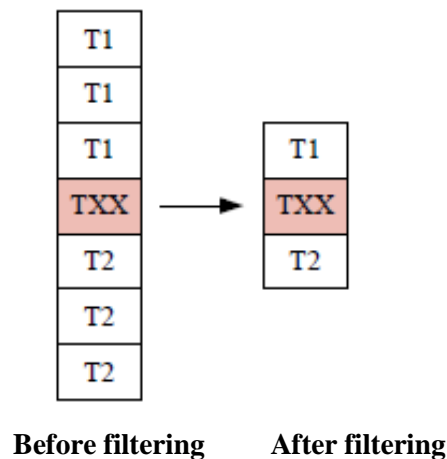


Figure 8.3: Basic duplicate readings filtering (Yaacob and Mahdin, 2016)

Various BF-based approaches have been proposed in the literature to detect and filter duplicate readings from an RFID data stream. Typically, these approaches consider filtering tag readings that take place in readers (local filtering) or middleware (global filtering) or both, after the data are received from the tags and before being forwarded to the backend database servers for subsequent processing, as shown in Figure 8.4. The region of an RFID reader is generally divided into major and minor regions, where the latter represents the overlapping region. Wang *et al.* (2008) proposed eager and lazy methods that employ the

standard a BF to filter duplicate data. When new data arrive at a local reader, it is added to the BF, then, the BF is transmitted to the middleware for the update. The middleware manages readings from readers under its network before forwarding them to the backend database server. In the eager method, a copy of the BF is transmitted to every reader in order to eliminate reading duplicate data again. However, it is costly to inform all the readers about a new reading every time it arrives. In the lazy method, only a reader that transmits new data has a copy of the BF from the middleware. This method needs to update the middleware each time a new reading is coming in, which may result in wasting lots of bandwidth.

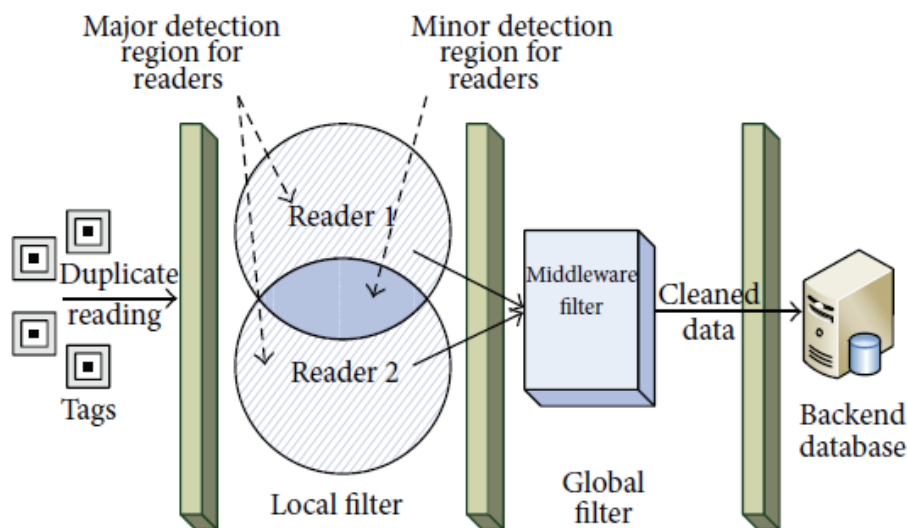


Figure 8.4: Duplicate filtering method of an RFID data stream (Kamaludin *et al.*, 2016)

To support deletion of old readings, Mahdin and Abawajy (2011) introduce the decaying BF. Even though the CBF supports deletion of elements, it does not have any way of knowing which counters represent the elements in its filter. The decaying BF can delete old readings by including sliding windows in its filter. The counters in the filter are initialised to the sliding window size and are decreased by one when a new reading is inserted. If the reading already exists, all the relevant counters are set to the sliding window size again. When there is no reading coming in from a tag, which means that the tagged object has left the reader region,

the reading will be removed from the filter as a result of the decreasing process. A false positive happens, if all the counters are not set to 0 for a non-member element. The probability of one is increased when the BF is full, when all or nearly all the counters have been utilised to represent the elements. For this reason, the length of the BF should be long enough to accommodate the number of incremented elements and the old elements should be deleted to decrease the false positive probability. In addition, in the same context, Lee and Chung (2011) proposed time BFs, where the filtering process takes place at the middleware's side. The time BF uses the time information to test whether the reading is duplicated or not. The filter uses an integer array in place of a bit one, where each entry is set to the identified time of a tag. If the entries are already set to the time of the previous reading, they will be overwritten with the time of the new reading. To test whether an element is a duplicate or not, all the related k entries are checked. If there is at least one entry where the result of the subtraction of its time from that of the tested element is larger than a threshold, this means that the tested element is not a duplicate. Due to the transmission of duplicates to the middleware, a lot of bandwidth is wasted and consequently, a bottleneck exists on the middleware's side. Mezzi and Akaichi (2013) discussed the same idea, but with some differences. They proposed a method based on the difference of the time of the current and the previous flow. Jiang *et al.* (2012) stressed the importance of eliminating duplicates as early as possible in order to decrease network bandwidth. For this reason, they proposed two layers of filtering methods. The first is at the reader's side, where a BF is used to filter local duplicates. The other filtering method is employed at the middleware's side, where a distributed time BF is utilised to filter global duplicates. The two layers filtering process generates a small false positive rate and causes latency at the reader's side as well, because it requires filtering the duplicate data before forwarding them to the middleware. Following the same concept, Kamaludin *et al.* (2016) modified the BF and used only a single hash function to reduce the complexity and thus speed up the filtering process. The authors employed two

filters in addition to the landmark window to allow for the deletion of old elements. The proposed method tests the time to delete the reading and if the condition is met, all the counters are reset to 0. Every incoming reading is hashed using a single hash function, with the result of the hashing being treated as the counter index in the two arrays. The algorithm first tests whether the reading is duplicated or not and if so, the reading will be rejected. Then, if the first array index at the counter is empty, then that index will record the tag ID, or else, if the second array index at that counter is empty, then that index will record the tag ID. If not, the reading is a false positive. Yongsheng and Zhijun (2013) combined CBFs with dynamic chain lists to detect and filter duplicate readings produced from reading the same tag multiple times. The dynamic chain is implemented as a linked list and the CBF is constructed from an array of times to enable the deletion of old data. The counter is increased and decreased when an element is inserted into and removed from the filter, respectively. The cell is set when the counter is changed from 0 to 1. This method has some limitations such as the reader producing a large volume of data. In addition, when a duplicate is found, the reader has to search for a match in the double linked list, which causes latency. Dutta *et al.* (2013) constructed a BF that is able to store elements from multiple sets. Each element of the stream is hashed to a p -bit fingerprint using Rabin's method (Rabin, 1981) and the results of the hashing are considered as the input to the filter. Therefore, the addition of an element involves the addition of its hash value and conversely removing one involves the removing of its hash value. The authors also proposed a dynamic filter to handle the variations in the stream behaviour, which is constructed from an array of pointers. When an element is to be added to the filter, a bucket is dynamically allocated and is linked to the pointer in the related index of the vector. On the other hand, removal of an element involves the deletion of the bucket in which the hash of the element was recorded and then, the free cells are added to the main pool of free spaces. Membership testing requires checking the buckets linked to the pointer of the array index in which the element is hashed.

A study by Guoqiong *et al.* (2016) supported filtering of RFID data streams in mobile environments. The proposed filtering method considers both the time and location information of readings. The single vector of a BF is extended to a vector of two dimensions with one dimension recording reader IDs, whilst the other records the time of the detection event. The filter is initialised with all bits being set to 0. When a new reading x is received, it is encoded using the k hash functions and the indexes are set to the related reader ID and time. If one of the times of the resulting indexes is equal to 0 this means that the reading is for non-redundant data. If all the time values of the k indexes are not equal to 0, but there is one entry having the same reader ID, this indicates that the location of the tag has been changed and also, a non-redundant data. The authors also adopted a random decay method for the removal of old data by randomly selecting a number of cells in the filter to decrease their time by 1. This results from the fact that, if the time of a cell has not been changed for a long period, it reaches 0 after a number of decreasing processes, which is identical to the process of removing the item of the cell. In 2017, Guoqiong *et al.* studied filtering redundant data for uncertain RFID data streams gathered from areas far away from the reader. The proposed BF consists of four tuples $\langle p, et, f, r \rangle$ to store the existential probability of the tag, the latest time, the sum of the decay weights, and the location. Each hash function relates to a different counter. The minimum existential probability is obtained by comparing the existential probabilities of all the k counters and then, comparing these with the minimum probability threshold. If it is larger than the threshold, the location entry is different from that of the reading, and the time difference is less than a threshold, then this indicates that the reading is a non-duplicate.

8.6 Conclusions

A BF is a simple data structure that can store the items of a set in a space efficient way and support membership queries. Due to its space efficiency, it has been widely employed in various systems. Regarding RFID systems, the literature contains a wealth of proposed

methods based on the BF to solve various issues including filtering duplicate data from RFID data streams. However, all the methods concentrate on filtering duplicate data at the reader or the middleware's side after they are received from the tags and before being forwarded to the backend database servers for processing, which results in communication overheads between the reader and the tags. The main limitation of using the BF is that it enables false positives. However, the space optimisation and thus, the reduced time to send the BF between the reader and tags outweighs this limitation, as long as the probability of the false positives is sufficiently small and controlled, as in the designed protocol. This chapter has provided an overview of the BF with a focus on its construction, features, limitations, variations, and the ways in which it has been utilised in some systems, especially RFID ones. This review has provided preliminary information relevant to the designing of the novel redundant tag information collection protocol presented in the next chapter.

9 Efficient Redundant Information Collection Protocol

The extant autonomous group integrity methods in RFID systems write redundant data into the memory of RFID tags. These data reference other tags or represent their membership in the group. In LDPC-based methods, parity check values and short IDs are written into the memory of RFID tags, as shown in Figure 5.1 of Chapter 5. For the group integrity checking and decoding processes, the reader needs to collect the parity check values and their short IDs from the available tags. Designing an efficient collection protocol is needed for reading such redundant information from the tags in RFID systems. The key performance measure for the protocol is time efficiency, because RFID systems have subsequent processes to perform, including integrity checking and decoding processes. When the time is long, the task of collecting tag information may delay these processes of the system, which is undesirable, especially in large-RFID environments. The study in this chapter is aimed at efficiently collecting such redundant information from a group of tags, thus enhancing the complete system of group integrity applications. Whilst there are many methods in the literature that filter out duplicate information in RFID systems, as presented in subsection 8.5.1 of Chapter 8, all these concentrate on filtering duplicate information at the reader or the middleware's side after the information is received from the tags and before being transmitted to the backend database servers for processing. This causes communication overheads between the reader and the tags. Existing possible solutions are also not efficient in solving the problem since they do not distinguish redundancy among tags, which result in long collection times. To achieve time efficiency, a novel protocol called the Redundant Information Collection (RIC) protocol is designed. It is based on a BF that efficiently filters redundant tag information at the tag's side. Extensive simulations have been carried out to analyse and assess the performance achieved with the designed protocol.

9.1 Tag Information Collection Protocols

In sensor-augmented RFID systems, tags are combined with miniaturised sensors to provide information about the surrounding environment for example humidity and temperature. Collecting such information from tags with low communication costs and thus, short time spans, has inspired many studies in recent years. Chen *et al.* (2011) proposed the Single-hash Information Collection (SIC) protocol and the improved version, the Multi-hash Information Collection (MIC) protocol, to periodically collect information from sensor-augmented RFID systems with a minimum execution time. By utilising several hash functions, the MIC protocol can resolve most hash collisions in a time slotted frame and thus, significantly enhance the protocol performance compared to the SIC protocol (more details are given below in section 9.4.3). Qiao *et al.* (2011; 2016) studied the same problem from the aspect of energy efficiency for active tags. The Tag Ordering Polling (TOP) protocol and the enhanced version (ETOP) were proposed to read information from a group of tags in large RFID systems with minimum energy consumption. The information here contains that of the sensor information as well as the link between the information and the tag so that the reader can correctly link sensor information to the related object. In an earlier version presented in 2011, the reader sends a vector instead of tag IDs. Each tag ID in the group is mapped to a bit in the vector using a hash function and the corresponding bit in the vector is set to 1. The vector is divided into segments of size 96 bits to send each segment in one time slot of the current frame. Each tag only requires checking a specific bit in the vector at a location specified by the hash of its ID. Only a tag that finds its value in the vector is 1 will stay active and report its information to the reader in the subsequent time slotted frame. The vector also identifies the order in which the polled tags will report their information in order to eliminate collisions. If a tag finds that there are i 1s in the vector preceding its bit, it determines that its order is $(i + 1)$ when sending its information to the reader.

In the enhanced version presented in 2016, the vector is implemented as a partitioned BF to reduce the occurrence of false positives. Each segment is evenly split into k partitions. For each tag in the group, the reader hashes its ID to get some hash bits. It uses these bits to link each tag to its related segment, and then deploys k hash bits to link further each tag to one related bit in each partition of the segment. The partitioned BF allocates k bits for each hashed tag which is similar to a standard BF; however, it spreads the k related bits in k partitions. The reader broadcasts each segment with the total number of tags x encoded in all the preceding segments. Upon receiving its segment, a tag performs the k hash bits to check its membership. Then, it calculates its location in the reporting order by adding the value of x to the number of 1s preceding its bit in the partition that has the largest number of 1s.

A follow-up work by Yue *et al.* (2012) complements previous work with a new protocol primarily designed to read sensor-produced information from RFID tags with multiple readers. The extended study in Yue *et al.* (2014) targets an unknown subset of tag IDs with one reader. They proposed the Bloom-filter-based Information Collection (BIC) protocol, in which tags build their BF and transfer them simultaneously to the reader in order to identify the target tags efficiently. Different from the existing protocols, in that of Yue *et al.*, the reader has no knowledge about the target tag IDs from which it collects information. Therefore, the reader, first, is required to identify the tags in its region in order to gather information from them. Figure 9.1 illustrates a simple example of the protocol in identifying the interrogated tags. The reader sends a request message, including the length of the BF b and the number of hash functions k , as in part (a). Upon receiving the reader's message, each tag constructs its BF using the reader's parameters. Then, it encodes its ID into the filter and sends this to the reader. All the interrogated tags send their BF simultaneously as in part (b). In the physical layer, an idle carrier represents a logic value 0 and a busy one, a logic value 1. For each received signal at the reader's side, if the channel is idle, the received signal is set to 0. If the channel is busy, which indicates that at least one tag is sending, the received signal is

set to 1. After the transmissions of all the BF from the tags, the reader can create a new BF that represents all tags, as in part (c). The reader uses the new BF to filter the interrogated tag set from a set of all tag IDs stored in the back-end database server. Then, can start collecting information from the interrogated tag set by sending an ordering vector to schedule the tags' transmissions, as in the TOP protocol. The authors set the parameters of the BF, including its length b and its hash functions k , according to the size of the set to be encoded and the desired false positive rate (i.e. 1×10^{-4}), as discussed in section 8.1 of Chapter 8.

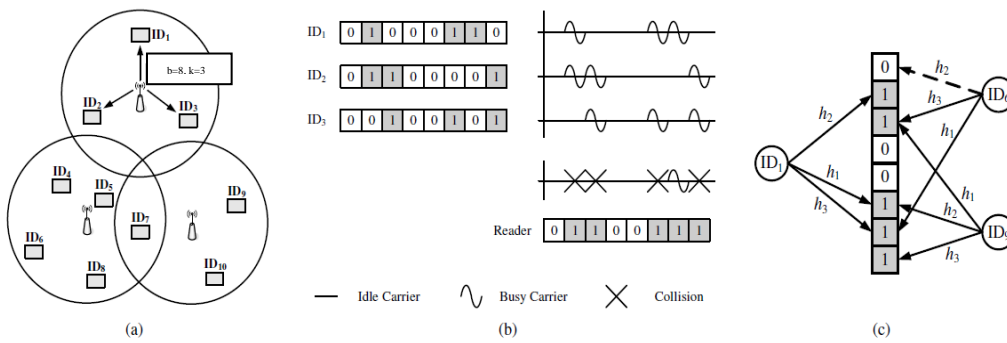


Figure 9.1: An example of the tag identification process with a BF in Yue *et al.* (2014)

To increase the frame utilisation, Xie *et al.* (2017) proposed a protocol called the minimal Perfect hashing-based Information Collection (PIC) protocol that establishes a one-to-one mapping between target tags and slots. To eliminate target tag collisions, the protocol starts with the assignment process, which allocates target tags to successive indices. The assignment process contains a number of rounds and in each round, the reader sends an order vector to allocate a portion of target tags to their indices. Upon receiving the order vector, each tag will check its related bit. If it is 1, the tag will be allocated to a slot at index $(n + y)$, where n represents the number of target tags that have been allocated in the preceding rounds, and y is the number of 1s preceding this bit. In order to filter out the non-target tags and thus, preventing them from interfering with the target tags, an improved BF is employed. It

consists of b items and each of them is a k bit fingerprint of the related target tag. Each fingerprint is calculated based on the target tag ID. The reader transmits each fingerprint in a slot of the next time frame. Each tag aiming to respond in the i -th slot and finding that the i -th fingerprint is not identical to its fingerprint will keep silent. The transmission order of the fingerprints is based on the slot indices allocated to target tags in the assignment process. Since the reader has the knowledge of the tag IDs and the hashing parameters used in the filtering phase, the error of the false positives can be solved by broadcasting the non-target tag IDs that pass the membership test in order to deactivate them.

Another direction of the research was proposed recently in Liu *et al.* (2017), who studied category information collection problems in multi-category RFID systems. In such systems, the tag ID consists of a category ID, which specifies the category that a tag is a member in; and a member ID, which indicates a certain tag in the category. All tags belonging to the same category store the same category information and hence, there is no need to collect category information from all tags in the same category; one tag's response is enough to satisfy the requirement. The proposed protocol consists of two phases. The first phase aims to separate a category from others, while the second attempts to poll one tag in a category according to the geometry distribution of tag IDs by using a 4-bit index. The reader first broadcasts a request message, including the frame size f and a random seed r . Upon receiving the message, each tag randomly selects a slot in the frame at the index $h(r, CID)$, where $h(\cdot)$ is a hash function shared by all tags with range $[0, \dots, f-1]$ and CID is a category ID. As each tag takes its CID as the hash seed, the tags from the same category choose the same slot. The reader can know which slots in the frame are selected by tags belonging to the same category from the receiving category IDs and in this case, these are called useful slots, otherwise, they are called useless ones. The reader then broadcasts an ordering vector, as in the TOP protocol of Qiao *et al.* (2011; 2016). Each bit in the vector relates to a slot in the frame and is set to 0 to represent a useless slot or 1 to represent a useful one. If the vector is too long to fit into one

time slot, it is split into segments of size 96 bits. In order to single out a tag in an efficient way, each selects an index $R(h(TID, r) \bmod 2^X)$, where X is a constant and $R(\cdot)$ is the location of the right-most bit of 1 in the input. Since the reader has the knowledge of tag IDs, it knows the hashing result of each tag. The reader then sends a frame of slots, where each slot contains a $\log_2 X$ -bit index to pull a single tag from a category, while other tags in the category will keep silent. In all the work presented above, it has been assumed that the reader has the knowledge of the tag IDs presented in the system by being connected to a back-end database server that stores the IDs of all the tags.

9.2 System Model and Problem Statement

The underlying RFID system here is the same as that in section 5.1 of Chapter 5. Consider a group of RFID tag IDs denoted as $ID = \{ID_1, ID_2, ID_3, \dots, ID_n\}$ corresponding to a group of passive tags represented as $TAG = \{tag_1, tag_2, tag_3, \dots, tag_n\}$, where n is the number of tags in the group. These tag IDs are encoded using a parity check matrix of size $m \times n$, which is constructed using the PEG method to generate a set of parity check values of size m denoted by $C = \{c_1, c_2, c_3, \dots, c_m\}$. The bit length of each c_i is equal to that of the tag ID, that is, 96 bits. To enable autonomous integrity checking without using external systems, each tag stores its parity check values (c_i), as well as a set of short IDs (s_i) referring to other tags belonging to the same row of the parity check matrix. For the group integrity checking and decoding processes, the reader needs to collect the parity check values and their short IDs from available tags. Designing a fast collection protocol to read such redundant information from the tags is needed in order not to delay these processes. The goal of the designed protocol is to collect all c_i efficiently and their s_i in the interrogation zone of the reader within a desired false positive rate. More precisely, the design should consider the redundancy among tags and collect each c_i and its s_i only once. Hence, the complete system, which includes the three main phases, as shown in Figure 1.3 of Chapter 1 is enhanced. In this study, for the purpose

of collecting redundant tag information, a group of tags belonging to the same row of the parity check matrix maintains the same order of short IDs and consequently, the short ID of the tag needs to be recorded in its memory.

9.3 Performance Lower Bound

Let t_{bit} denote the time needed to send one bit. In group integrity application, the information related to one parity check value and its short IDs is denoted by $c_i+s_i \times l$ and can be expressed as x , where l represents the row weights of the parity check matrix used for the encoding. All the tags contain the same amounts of parity check information, which are denoted by $j \times (c_i+s_i \times l)$ and can be expressed as $j \times x$, where j is the column weights of the parity check matrix. Therefore, each tag needs a time, the length of which is equal to $x \times t_{bit}$ in order to send one piece of parity check information. For collecting all tag information, the lower bound on the collection time for a group of n tags is $n \times j \times x \times t_{bit}$. For collecting redundant information, the lower bound is much less than $n \times j \times x \times t_{bit}$. The reader needs to collect each c_i and its s_i only once. Thus, the lower bound on the collection time is $m \times x \times t_{bit}$. It is unlikely that this lower bound is achievable, because the reader requires extra time to transmit its request and coordinate the protocol process. Despite this, it provides a benchmark for assessing the performance of the designed protocol.

9.4 Possible Solutions

In this section, three existing solutions to general and different problems that could be applied to collect redundant tag information are examined, and these are simply called possible solutions. None of them is efficient in solving the redundant information collection problem since they do not distinguish redundancy among tags, which results in long collection times. This gives clear knowledge about the solution of the redundant tag information collection problem, which motivates the designing of the novel protocol presented in section 9.5.

9.4.1 Baseline Collection Protocol

A baseline collection (BC) protocol for collecting tag information is to let the RFID reader broadcast the ID of one tag. Then, it receives the information of the related tag and the reader repeats this process until it gets all the information needed. As regard to collecting redundant information, the tag does not have knowledge of the information that the reader has, so it must send it. Thus, the total time to collect one piece of parity check information from a tag is $(ID_i \times t_{bit} + x \times t_{bit})$, and the optimal total time for collecting all parity check information from a group is $m \times (ID_i \times t_{bit} + x \times t_{bit})$. The advantage of this protocol is that the request and reply is a one-to-one mapping. In other words, collisions cannot occur in the communication between the reader and the tags. On the other hand, the reader has to transmit the tag ID in order to collect related tag information, which increases communication costs because the tag ID is 96 bits. Consequently, the time is significantly above the lower bound value of $m \times x \times t_{bit}$.

9.4.2 ID Collection Protocol

As presented in subsection 3.5.4 of Chapter 3, the RFID tag anti-collision protocols using TDMA techniques are mainly classified into Aloha-based and tree-based protocols. Using these protocols, the reader can collect tag IDs in its interrogation zone. If these ID collection protocols are borrowed to collect redundant tag information, the collection time is high, because each tag has to send all its information. In addition, the protocol has to consider the entire tag group n each time when collecting tag information. In the enhanced version of ALOHA-based protocols, as presented in Lee *et al.* (2005), the optimal time for collecting n tag information is $e \times n \times j \times x \times t_{bit}$, where e is the natural constant and is approximately equal to 2.72. This means that each tag resends its information nearly 2.72 times, on average, which is the theoretically ideal number. Experiments and simulation results demonstrated that the best performance of tree-based protocols is equivalent to that of the ALOHA-based ones (Chen *et al.*, 2011).

9.4.3 Multi-Hash Information Collection Protocol

Chen *et al.* (2011) presented the SIC and MIC protocols for collecting tag information in sensor-based RFID systems. Only the MIC protocol is considered here, because it is an improved one, which is performed stage by stage. In each stage, the reader links tags to time slots using k hash functions. Then, it uses a hash selection vector to notify the tags about the links. Each item in the vector is related to a time slot at the same index location. The reader sets the item to 0, if no tag is linked to a slot. If a tag is linked to a slot with the z -th hash function, where $1 \leq z \leq k$, then the reader sets the related item to z , which is of size $\lceil \log_2(k+1) \rceil$. After receiving the vector, each tag only requires checking the items in the vector that it is mapped to by using the k hash functions. Let T_z , $1 \leq z \leq k$, be the item that the tag is linked to by the z -th hash function. Each tag checks the items in the order from T_1 to T_k . If an item T_z has the value of z , the tag concludes that it must be allocated to a slot using the z -th hash function. The above process iterates stage after stage until all tags have sent their information. The first stage considers n tags for slot allocation and the size of its frame size is equal to n . Each successive stage considers a fewer number of tags and thus, its frame size is smaller. Figure 9.2 gives an illustrative example of the MIC protocol where $k = 2$. The arrows denote the links from the tags to the slots based on the results of the hash functions. The allocations of the tags to the slots are represented by thick arrows. In the first round of the protocol when $H[1]$ is applied, tags with ID_1 and ID_5 are allocated to slots. When $H[2]$ is applied in the second round, tag 3 and tag 4 are allocated. In part (c), a hash selection vector is built by the reader based on the slot allocation. Upon receiving the vector, each tag checks the items in the vector that it is linked to. For example, the third tag finds that the value of the item linked by $H[2]$ is equal to 2 and thus, it concludes that it must be allocated to the related slot.

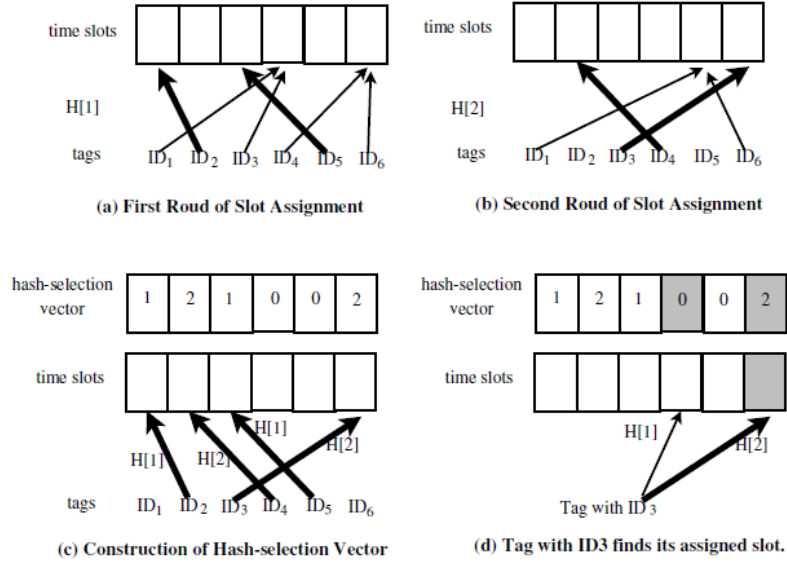


Figure 9.2: An illustrative example of the MIC protocol (Chen *et al.*, 2011)

The expected total collection time of the MIC protocol is:

$$\frac{n}{32P_k} \times ID_i \times t_{bit} + \frac{n}{P_k} \times j \times x \times t_{bit} \quad (9.1)$$

where, P_k is the probability that a tag is linked to one time slot in every stage when the k hash function is used. It has been proven that when $k = 7$, the collection time reaches the optimal value of $0.036 \times n \times ID_i \times t_{bit} + 1.16 \times n \times j \times x \times t_{bit}$, where $P_7 = 86.1\%$. Similar to the BC protocols, when the MIC is used for collecting redundant information, each tag does not have knowledge about the information that other tags have sent, so it must send its information. Thus, the optimal total time for collection m parity check information from a group is:

$$0.036 \times m \times ID_i \times t_{bit} + 1.16 \times m \times x \times t_{bit} \quad (9.2)$$

9.5 Redundant Information Collection Protocol

This section presents the novel RIC protocol that utilises a BF to filter redundant tag information from a group of tags efficiently. The designed protocol aims to avoid the redundant transmissions of c_i , as well as the corresponding s_i . The process of the RIC protocol consists of several rounds that are repeated until all c_i have been read. In each round,

the reader sends a request, and then the tags reply with their information in the successive slotted time frame. Each tag must check whether its information has been sent previously by other tags before it sends any information. The reader maintains a list of all collected c_i and its s_i . Reporting the list to the tags in order to prevent transmitting redundant information in the subsequent rounds is too costly, especially when the set of tags in the group is large. To accomplish a high level of filtering efficiency, the collected parity check values are compressed into a BF, which is then sent instead of the actual parity check values. In other words, the BF is used as a tool to carry the aggregated c_i and filter the tag's information at the latter's side.

9.5.1 Protocol Description

The RIC protocol consists of several rounds. The communication between the tags and the reader uses a framed slotted Aloha, which follows the RTF mode based on the EPCglobal Class-1 Generation-2 standard. In each round of the communication, the reader sends a request message containing two parameters, r and f , where the former is a random number and the latter is the frame size, that is, the number of slots in the frame. Upon receiving a request, each interrogated tag is randomly mapped to a slot in the frame at the index $h(r, c_i) \bmod f$, where $h(\cdot)$ is a hash function shared by all tags with a range of $[0, \dots, f-1]$. As each tag takes its c_i as the hash seed, those having the same parity check values c_i choose the same slot. Then, they send their identical parity check information x , and thus, the signals can be decoded by the reader. In this case, the slot can be called a successful slot. On the other hand, tags with different parity check values c_i may respond at the same slot, and the slot here is treated as a collision slot. Hence, the reader cannot decode the signals encoded from a set of unidentical parity check information. The reader stores the collected parity check values c_i in a list denoted as $D = \{d_1, d_2, d_3, \dots, d_a\}$. Then, it constructs a BF vector by mapping the collected parity check values to b bits array using k hash functions, as described in

Algorithm 9.1. Given a desired false positive rate P_{FP} and the number of elements in D , the optimal values of the hash functions and the optimal length of the BF constructed in the RIC protocol can be computed using Equations (8.8) and (8.9), respectively.

The reader again sends another request to collect a new set of parity check values c_i . It also sends the constructed BF and corresponding parameters b and k . Before sending any parity check information, each tag must check whether its c_i has been sent previously by other tags, and here is where the BF plays an important role by meeting this requirement. Each tag performs membership tests for all c_i it contains by using Algorithm 9.2. For each one, it performs k hash functions, which are identical to those used to construct the BF at the reader's side. It then tests whether the bit $h_z(c_i)$ is set to 1 for $1 \leq z \leq k$. If so, the tag will treat the tested c_i as redundant information and will not send it to the reader, otherwise, the tested c_i and all its s_i are sent to the reader. After receiving the tag information, the reader updates its list and reconstructs the BF. The process of filtering and collecting information will be repeated until all the tags have reported all their information. The processes involved in all rounds are identical, except that at the beginning of the first round the list of the reader is empty, and thus, b is equal to zero, which means that the BF is not sent. Algorithm 9.3 outlines the designed protocol.

Algorithm 9.1: Constructing the BF

Input: D, P_{FP}

Output: b, k, BF

- 1: Calculate b and k
- 2: $BF =$ allocate b bits initialised to 0
- 3: **for each** d_i in D :
- 4: **for** $z=1$ to k **do**

```

5:       $BF[h_z(d_i)] = 1$ 
6:  end for
7: end for each

```

Algorithm 9.2: Membership testing

Input: elm, BF, k

Output: Yes/No

```

1: for  $j=1$  to  $k$  do
2:   if  $BF[h_j(elm)] \neq 1$  then
3:     return No
4:   end if
5: end for
6: return Yes

```

Algorithm 9.3: The RIC protocol

Input: P_{FP}

Output: D containing all c_i and its s_i in the interrogated region

```

1 :  $D = \phi$ 
2 : Repeat
3 :   Constructing BF ( $D, P_{FP}$ ) return ( $b, k, BF$ )
4 :   The reader sends  $\{r, f, b, k, BF\}$ 
5 :   for each  $c_i$  in  $tag_i$ :
6 :     membership testing ( $c_i, BF, k$ ) return Yes/ No
7 :     if No then
8 :        $tag_i$  sends its  $c_i$  and the corresponding  $s_i$  at index  $h(r, c_i)$ 

```

-
- 9** : $D = D \cup c_i$ sent by tag_i
10 : go to step (13) \triangleright tag is allowed to send only once in a frame
11 : **end if**
12 : **end for each**
13 : **Until** all tags send their information
-

9.5.2 Performance Analysis

In this section, the expected collection time of the RIC protocol and the optimal value of the frame size f are derived. The expected collection time T_i of the i -th round is composed of that needed by the reader to send the BF vector and that needed by the tags to send the information. The reader broadcasts a request message, including r, f , the BF vector and its parameters. The transmissions from the reader, except for the BF vector, are very small and thus, can be ignored. Note that the BF vector may be too long, so it can be split into multiple segments of 96 bits, each being sequentially transmitted, as in Chen *et al.* (2011) and Qiao *et al.* (2016). Thus, the expected time to send b bits vector of the BF is calculated, as:

$$\frac{b}{96} \times t_{bit} \quad (9.3)$$

From Equation (8.9), b can be expressed, as:

$$- \frac{|D| \times \ln P_{FP}}{(\ln 2)^2} \quad (9.4)$$

The time for the tags to test the set of parity check values from the BF is also ignored. Recall that one parity check information is denoted by x , then the expected time for the tags to send their x information can be calculated, as:

$$E_{succ} \times x \times t_{bit} \quad (9.5)$$

where, E_{succ} is the expected number of successful slots in the frame. Therefore, the expected collection time T_i of the i -th round is:

$$T_i = \frac{b_i}{96} \times t_{bit} + E_{succ,i} \times x \times t_{bit} \quad (9.6)$$

In the ID collection protocols of such as Vogt (2002a), Lee *et al.* (2005), and Cha and Kim (2006), when the reader uses a frame of size f and the number of replying tags is n and from Equations (3.3) and (3.4), the expected number of read tags during one read cycle can be expressed, as:

$$\lambda = f \binom{n}{1} \left(\frac{1}{f}\right) \left(1 - \frac{1}{f}\right)^{n-1} \quad (9.7)$$

In the RIC protocol, each tag uses its c_i to choose one slot and so the tags having the same c_i must share the same slot, which is called a successful one. By treating this group of tags as a single tag, the successful slot can be seen as a singleton. Hence, the expected number of successful slots can be calculated, as:

$$\begin{aligned} E_{succ,i} &= f_i \binom{m_i}{1} \left(\frac{1}{f_i}\right) \left(1 - \frac{1}{f_i}\right)^{m_i-1} \\ &= m_i \left(1 - \frac{1}{f_i}\right)^{m_i-1} \\ &\approx m_i \cdot e^{-\frac{m_i-1}{f_i}} \approx m_i \cdot e^{-\frac{m_i}{f_i}} \quad \text{as } m_i, f_i \rightarrow \infty \end{aligned} \quad (9.8)$$

where, m_i is the number of x to be collected before the i -th round. By letting the first derivative of T_i be zero, the minimum value of T_i can be found, as:

$$\frac{d(T_i)}{df_i} = \frac{d(E_{succ,i})}{df_i} \times x \times t_{bit} = 0 \quad (9.9)$$

where, $\frac{d(E_{succ,i})}{df_i}$ can be obtained from Equation (9.8), as:

$$\frac{d(E_{succ,i})}{df_i} \approx \frac{m_i^2 e^{-\frac{m_i}{f_i}}}{f_i^2} \quad (9.10)$$

when f_i is large. Using Taylor series, Equation (9.10) can be written, as:

$$\frac{d(E_{succ,i})}{df_i} \approx \frac{m_i^2(1-\frac{m}{f_i})}{f_i^2} \quad (9.11)$$

By solving Equation (9.9) numerically, the optimal value of f_i that minimises T_i is approximately equal to m_i .

9.5.3 Cardinality Estimation

The reader can estimate the number of the target parity check values m before running the RIC protocol. To accomplish the estimation, the reader transmits a random number r and a frame size f . Each interrogated tag sends a short-response at a time slot $h(r, c_i) \bmod f$. Some tags having the same c_i will respond at the same slot, whilst others, having different parity check values c_i , may respond at the same slot. According to the EPCglobal Class-1 Generation-2 standard, only one bit is required to distinguish an empty slot from a nonempty one. For each received signal at the reader's side, if the channel is idle, the received signal is set to 0, whilst if it is busy, which indicates that at least one tag has sent, the received signal is set to 1. The tag replies a short response of one bit at the corresponding time slot. After receiving the responses, the RFID reader measures the state of the slots and consequently, by counting the number of empty slots, m can be estimated. The additional time overhead for estimating m of the interrogated tags is measured under various group sizes n . Table 9.1 demonstrates the estimated time of the RIC protocol, which is very small. In subsection 9.6.2 below, it is shown that the RIC protocol outperforms other information collection protocols. Therefore, taking into account the estimation overhead will not affect the performance of the RIC protocol.

n	1000	2000	3000	5000
Estimation time	0.32	0.64	0.96	1.6

Table 9.1: Estimation time comparison (in second) under different group sizes

9.5.4 Hash Functions

The problem on how to simplify the implementation of hash functions on RFID tags in order to decrease the complexity of a tag's circuit has been discussed in Li *et al.* (2010) and Chen *et al.* (2011). In general, the hash value can be obtained from a ring of pre-stored random bits. A random number generator is implemented offline with the tag ID as a seed to produce a string of random bits. This string is then pre-stored as a logical ring in the tag before deployment and when k hash values are required, k portions of the string are stored instead. For example, to obtain the hash value of $h_z(TID, r)$, where $1 \leq z \leq k$, a tag obtains a portion of bits from the first z rings after the r -th bit. Another way is to start from the r -th bit and select one bit after each r bits. The final hash value is then computed as the number represented by these bits modulo the length of the BF or the frame size depending on the application. Li *et al.* (2015) also simplified the implementation of three hash functions by pre-storing a 32-bits random number on each tag. The reader produces three random seeds in the binary form and sends them to the tags in its region. Each tag then calculates the three hash values using:

$$h(TID) = \text{getlbit}(RN \oplus RS(i), 13:1) \quad (9.12)$$

where, *getlbit* is a function used to obtain the lowest 13 bits from the XOR results, RN is a random number in the binary form, and $RS(i)$ where $i \in 1, 2, 3$, is the random seeds in the binary form. With the improvement in RFID tags, the hash functions are expected to be feasible at even more lightweight passive tags (Hutter *et al.*, 2012; Yang, 2017).

9.6 Simulation Results

In this section, the performance of the RIC protocol is evaluated with Matlab R2018b. As no existing method is aimed at collecting redundant tag information, three protocols, including the BC, MIC with seven hash functions, and the enhanced version of the ALOHA-based

(EDFSA) protocols, as presented in Lee *et al.* (2005), are implemented. Their collection times are measured and compared with those of the RIC protocol.

9.6.1 Simulation Settings

The simulation settings in Matlab follow the specifications of the EPCglobal Class-1 Generation-2 standard. A waiting time of 302 μs is used to separate any two successive communications between the reader and the tags, with the transmission rate of a tag being 53 Kb/s. A tag needs 18.87 μs to send one bit. The length of time slot a tag needs to send its information is obtained as the addition of the time for sending the information and a waiting time. For instance, if the tag information is 600 bits, the length of a time slot is around 11,623 μs . The transmission rate of the reader is 26.5 Kb/s. The reader needs 37.74 μs to send one bit. Thus, it takes nearly 3925 μs (including the waiting time) to send a message of length 96 bits. For all the implemented protocols, the total number of parity check values m is assumed to be known a priori in order to derive a realistic baseline performance comparison. In the RIC protocol, the frame size will change based on the number of parity check values to be collected. The first round considers collecting m parity check values, and its frame has m slots. Each consequent round considers a smaller value of m and consequently, has a smaller frame size. All the presented results are obtained by averaging over 100 simulation runs in order to obtain an accurate value of the statistics.

9.6.2 Collection Time Comparison Under Different Numbers of Tags and Information Lengths

The performance of the RIC protocol is evaluated under different numbers of group sizes n . The group sizes vary from 1,000 to 5,000. Each tag in a group stores the same number of parity check values j that is set to 3 and 4. The value of P_{FP} is set to 1×10^{-4} to achieve the accuracy of 99.99%. Table 9.2 presents the results of the simulated protocols for different

values of m within the same group, where the parity check information size x is the same. The collection times of all the protocols increase as the number of tags n or the number of parity check values m increases. This is intuitive, because the tags need to transmit more information. The RIC protocol obviously outperforms the other protocols by having a minimum time, followed by MIC protocol, BC and, finally, EDFSA. For example, when the number of tags in a group is 3,000 and the number of parity check values is 1,800, the collection time of the EDFSA protocol is 138.31 s, which is around 24 times the lower bound. The BC protocol follows with 47.32 s, and the MIC protocol further minimises the time to 33.63 s. The RIC protocol considerably reduces the time of the MIC protocol by around 30% to 23.56 s, with its collection time being about four times the lower bound.

Examining the second columns of $n = 3,000$, where the number of parity check values is increased to 2,400, shows that the EDFSA protocol needs 183 s. The BC protocol reduces the collection time by nearly 62% to 68.83 s, whilst the MIC protocol requires 45.32 s, which is around six times the lower bound. The RIC protocol also considerably reduces the collection time to a minimum value of 32.06 s. Again, the collection time of the RIC protocol is about four times the lower bound, and this conclusion can also be drawn from all columns of Table 9.2.

n	1,000		2,000		3,000		5,000	
m	600	800	1,200	1,600	1,800	2,400	3,000	4,000
j	3	4	3	4	3	4	3	4
x	146		151		156		161	
Total tag information	438	584	453	604	468	624	483	644
EDFSA	30.31	40.1	76.86	101.6	138.31	183	278.11	367.84
BC	15.36	22.34	31.13	45.28	47.32	68.83	80	116.23
MIC	10.58	14.3	21.78	29.4	33.63	45.32	57.57	77.71
RIC	6.71	8.93	14.68	20.1	23.56	32.06	41.94	57.75
Lower bound	1.83	2.45	3.78	5.04	5.84	7.79	10.02	13.36

Table 9.2: Collection time comparison (in seconds) for different parity check values m

Table 9.3 presents the collection times when the amount of parity check values m is fixed for each group and the parity check information size x is changed. Again, similar conclusions can be drawn. For example, when the number of tags in a group is 3,000 and $j=3$, the collection time of the RIC protocol outperforms the other simulated ones. Its collection time is 18.29 s which is 51% of the time required by the MIC protocol, 38% of the time required by the BC protocol, and just 12.3% of the time required by the EDFSA protocol. Increasing j to 4, causes an increase in the collection times of the MIC, BC, and EDFSA protocols. On the other hand, the collection time of the RIC protocol is slightly better than that with $j=3$. When further scrutinising their average number of rounds, the RIC protocol with $j=4$ needs an average of 9.37 round while the protocol with $j=3$ needs 10.9 round on average. This behaviour is due to the increase in the row weight l of the parity check matrix, which causes an increase in the amount of short IDs stored on tags. Maximising the distribution of the parity check values among the tags has the effect of enhancing the process of reporting tag information in each round. In addition, eliminating the transmission of the redundant tag information with the BF reduces the communication cost and therefore, speeds up the RIC protocol. On the other hand, the value of l should be carefully chosen as it can affect the performances of the decoding algorithms, as depicted in Figure 5.6 and Figure 5.7 in Chapter 5.

n	1,000		2,000		3,000		5,000	
m	500		1,000		1,500		2,500	
j	3	4	3	4	3	4	3	4
x	156	176	162	184	168	192	174	200
Total tag information	468	704	486	736	504	768	522	800
EDFSA	32.31	48.07	82.27	123.24	148.6	224.04	299.85	454.79
BC	15.54	23.58	31.57	48.1	48.07	73.59	81.36	125
MIC	11.21	16.82	23.16	34.98	35.86	54.47	61.63	94.19
RIC	5.28	4.53	11.58	10.35	18.29	16.75	33.03	31.07
Lower bound	1.62	1.81	3.36	3.77	5.21	5.89	8.96	10.19

Table 9.3: Collection time comparison (in seconds) for the same parity check values m

9.6.3 Collection Time Comparison Under Different Settings of the False Positive Rate

The relationship between the collection time of the RIC protocol and P_{FP} is also investigated. Table 9.4 compares those required by the RIC under different values of P_{FP} ranging from 1×10^{-2} to 1×10^{-6} , where the group size is set to $n = 2,000$ and the length of one piece of parity check information x is 151 bits. Generally, the collection time of the RIC protocol keeps increasing with a decrease in P_{FP} . For example, when P_{FP} is set to 1×10^{-2} in order to achieve accuracy of 99 %, the collection time of the RIC reaches 10.19 s when $j=3$. When P_{FP} is reduced to 1×10^{-3} in order to achieve accuracy of 99.9%, the time of the RIC protocol increases to 12.48 s. This behaviour is due to the fact that the relation between P_{FP} and b is inversely proportional, as presented in Equation (8.9). That is, a low amount of P_{FP} causes a larger b . Consequently, a larger b in the RIC protocol increases the communication overhead and thus, the time needed for transmitting the BF vector between the reader and the tags. The collection time of the RIC protocol reaches a higher value equal to 19.45 s when P_{FP} is set to the lowest tested value, which is 1×10^{-6} , in order to achieve accuracy of 99.9999 %. However, the RIC protocol is still faster than the collection times of the other simulated protocols as shown in the column of $n=2,000$ with $j=3$ of Table 9.2 and the same conclusion can also be drawn when j is set to 4. In all cases of P_{FP} , the small amount of unreported parity check information would be mitigated with the spread of tag IDs to the parity check constraints. In other words, increasing the column weight would compensate the loss in parity check information; however, the value of P_{FP} could be tuned based on the missing amount. For example, when the missing amount is high, the value of P_{FP} should be decreased in order to minimise its effect on the recovery performance of the decoding process. Thus, the RIC protocol is applicable for collecting redundant tag information for the group integrity checking and decoding processes as long as the probability of false positives is sufficiently small and controlled.

P_{FP}	1×10^{-2}	1×10^{-3}	1×10^{-4}	1×10^{-5}	1×10^{-6}
Collection time when $j = 3$	10.19	12.48	14.68	17	19.45
Collection time when $j = 4$	14	17.01	20.1	22.83	26.26

Table 9.4: Collection time comparison (in second) under different values of P_{FP} , where $n = 2,000$

9.7 Conclusions

The study presented in this chapter has been aimed at efficiently collecting redundant information from a group of tags for the group integrity checking and decoding processes, thus enhancing the complete system of group integrity applications. Extant solutions to general and different problems are not efficient since they do not distinguish the redundancy among tags, which results in long collection times. To achieve time efficiency, a novel protocol called the RIC protocol has been designed for this research. In this protocol, a BF is utilised as a tool to carry aggregated information in order to filter redundant tag information at the tag's side efficiently and thus, save collection time. The performance lower bound for collecting redundant information has been provided to assess the performance of the designed protocol and the expected collection time has also been derived. Extensive simulations have been conducted to evaluate the performance of the designed protocol as well as the existing possible solutions. The results demonstrate that the designed protocol outperforms other existing possible solutions by saving between 37% and 84% of the collection time, which is also around four times the lower bound. This makes the RIC protocol a promising candidate for collecting redundant tag information for the group integrity of tags as long as the probability of false positives is sufficiently small and controlled.

10 Conclusions and Future Work

This chapter concludes the thesis by first highlighting the contributions and achievements that have been made through the research. This is followed by outlining the limitations and obstacles encountered during it, and finally, there is identification of potential areas for further research work.

10.1 Contributions and Achievements of the Research

This research has been devoted to the development of group integrity application in RFID systems. The first part of the thesis focused on improving the performance in recovering missing tag IDs with low memory consumption and decoding complexity. In the second part, the research was focused mainly on designing a novel protocol to read redundant tag information from a group of tags with low communication overheads. During the research programme, there several achievements that have contributed to the field, which are as follows.

- 1) Motivated by the properties of Tanner graphs, or equivalently, parity check matrices constructed using PEG methods, extended grouping via the PEG method was designed. The PEG method was used to construct the parity check matrix of LDPC codes in order to increase the missing recovery capabilities of the group integrity application. Different matrices were constructed with different parameters. A group of RFID tag IDs is treated as packet symbols and encoded through the constructed parity check matrix. The constructed PEG-based LDPC codes are decoded under the IT and GE decoding algorithms. The recovery performances of the two decoding algorithms were analysed and evaluated, then being compared with the performance of other existing LDPC-based methods. The properties of the constructed PEG Tanner graphs were also analysed and

compared with the Tanner graphs of other codes, which were shown to have higher girths.

It was elicited that the PEG-based LDPC codes achieve significant missing recovery enhancements compared to other existing LDPC-based codes, with either the same or less memory overheads. (Chapter 5)

- 2) In order to strike a balance between the decoding complexities and performances of the IT and GE decoding algorithms, improved HB decoding was designed. This HB decoding algorithm includes an early stopping criterion to avoid unnecessary iterations of the IT decoding for undecodable blocks and thus, speeds up the decoding time. The practical performance of the early stopping criterion was evaluated and compared with the conventional IT decoding algorithm. The designed stopping criterion greatly reduces the average number of decoding iterations for undecodable blocks and therefore, reduces the decoding time when compared to the conventional IT decoding algorithm. (Chapter 6)
- 3) The recovery performance of the improved HB decoding algorithm was analysed and evaluated with different parameters. It achieved the optimal missing recovery capabilities of the full GE decoding algorithm. The decoding complexity of the improved HB decoding algorithm was extensively analysed and evaluated, both in terms of the number of operations required and the decoding time. It was demonstrated that the improved HB decoding algorithm considerably reduces the operational complexity and also, the time of the full GE decoding algorithm for small to medium amounts of missing RFID tags up to a certain threshold value, which depends on the missing recovery capabilities of the IT decoding algorithm. (Chapter 6)
- 4) The joint use of the two decoding components of the improved HB decoding algorithm was also adapted based on the missing amounts of RFID tags in order to avoid IT decoding when the missing amount is larger than a threshold and thus, save more decoding time. The optimum value of the threshold value was investigated for different missing amounts of tags and different parameters of the PEG method through empirical

analysis. Various simulations were conducted in order to analyse and evaluate the impact of the threshold value on the improved HB decoding time. It was elicited that the adaptive decoding algorithm is very efficient in decreasing the average decoding time of the improved HB decoding, thus saving more decoding time of up to 10% for large amounts of missing RFID tags, where the IT decoding fails to recover any missing tags. (Chapter 7)

5) Many simulations were carried out to analyse and evaluate the missing recovery performance of various short-length irregular PEG-based LDPC codes constructed with different variable degree sequences. The influence of low and high degree variable nodes on the performance of recovering missing tag IDs was also examined. It was demonstrated that the irregular PEG-based LDPC codes exhibit significant missing recovery enhancements compared to the regular PEG-based LDPC ones in the region where IT decoding is successful. However, their performances are degraded in the region where IT decoding can recover some missing tag IDs. It was empirically found that for half rate short block lengths, the density evolution method is good for irregular PEG construction. Simulation results also show that as the fraction of low degree variable nodes increases, the performance of the IT decoding in recovering missing tag IDs also increases in the two regions. On the other hand, increasing the fraction of the high degree variable nodes degrades the recovery performance in these regions. In addition, the recovery performance of the code that has a maximum variable node degree of 7 outperforms other simulated codes, with a maximum variable node degree of 9, 11, 13, and 15 in both regions. (Chapter 7)

6) A novel protocol called the Redundant Information Collection (RIC) Protocol was designed to filter and collect redundant information from a group of tags in group integrity applications with low communication overheads. To the best of this researcher's knowledge, there has been no prior work on how to collect and filter redundant tag

information at the tag's side efficiently. In the RIC protocol, A Bloom filter was constructed for the reader to filter the redundant tag information efficiently, which significantly decreases the communication overheads. The performance lower bound for collecting redundant information was provided to assess the performance of the designed protocol. The expected collection time and the cardinality estimation method were also derived. (Chapter 9)

- 7) Three existing possible solutions to general and different problems that could be applied to collect redundant tag information were implemented, analysed and examined. It was shown how all of them are not efficient at solving the redundant tag information collection problem since they do not distinguish redundancy among tags, which results in long collection times. (Chapter 9)
- 8) The performance of the RIC protocol was implemented, analysed and evaluated with different parameters and then, compared with the existing possible solutions. It was shown that the RIC protocol outperforms the existing solutions by saving between 37% and 84% of the collection time, which is nearly four times the lower bound. This characteristic makes the RIC protocol a promising candidate for collecting redundant tag information in the group integrity of tags as long as the probability of false positives is sufficiently small and controlled. (Chapter 9)

10.2 Limitations of the Research

Whilst the objectives of this research have been met, a number of issues have arisen, which may have imposed limitations upon the work progress and findings in one way or another.

The key limitations of the research are as follows.

- 1) The focus of the research was only on the widely used passive RFID tags. With this restriction, the efforts of improving the application of group integrity of RFID tags were

limited to the characteristics of this type of tags. On the other hand, the features of the other types of RFID tags may open a wider area of improvements.

- 2) The proposed mechanisms and protocol were not evaluated on real RFID systems. It would be desirable to conduct a series of experimental evaluations involving different numbers of RFID tags to confirm the validity of the numerical simulations and to appraise the practical usefulness of the proposed approaches. However, it is contended that having already established the empirical analysis have been useful and provided a fair insight about the performance.

Despite these aforementioned limitations, it is maintained that the research has made valid contributions to knowledge and provided sufficient proof of concept for the ideas proposed.

10.3 Further work

A number of suggestions for future work outside the scope of this study have been identified and they are as follows:

- 1) *The encoding process complexity*: A new method needs to be developed in order to reduce the relative complexities of encoding a group of tag IDs through the parity check matrix both in terms of the number of operations required and the encoding time;
- 2) *Average error rate bounds*: lower and upper bounds for the IT and GE decoding average error rates for the PEG-based LDPC codes in group integrity applications need to be derived theoretically;
- 3) *Dynamic Bloom filter constructions*: The construction of the BF in the RIC protocol could be implemented dynamically. To enable this feature, further development needs to be accomplished where the length of the BF is adapted in each round of the protocol instead of reconstruction the filter;

- 4) *Security features*: Further research and development is required in providing some security aspects such as protecting the information in a tag's memory and the transmitted information between the reader and tags.
- 5) *Channel error*: This is an important implementation issue, which may corrupt the information transmitted between the reader and the tags and thus, interrupting the process of group integrity checking and the RIC protocol as well. Hence, more work needs to be carried out to overcome the effect of channel errors. The group integrity method and the RIC protocol may need to be modified accordingly;
- 6) *Multi reader RFID systems*: Some large scale RFID systems include more than one reader. In contrast to the one reader deployed in small RFID system, in multi reader ones, each reader has to know which tags exist in its area in order to collect information from them. The readers must communicate with each other to read and recover the missing tag IDs. Consequently, research and software developments are required to enable such a system;
- 7) *Hashing of tags*: Due to the development of cheap and lightweight RFID tags that have limited resources, the addition of hash-based technique forms very interesting research area. That is, additional investigations and developments are needed in the area of lightweight hash functions in order to reduce the complexity of the tag's circuit even on more constrained passive tags.

References

Ahson, S. and Ilyas, M. (2008) *RFID Handbook Applications, Trchnology, Security, and Privacy*. New York: CRC Press.

Alleyne, D. and Sodha, J. (2008) ‘On Stopping Criteria for Low-Density Parity-Check Codes’, in: *6th International Symposium on Communication Systems, Networks and Digital Signal Processing*. Graz, Austria 25 July: IEEE, pp. 633–637.

Almeida, P. S., Baquero, C., Preguiça, N. and Hutchison, D. (2007) ‘Scalable Bloom Filters’, *Information Processing Letters*, 101 (6), pp. 255–261.

Banâtre, M., Allard, F. and Couderc, P. (2009) ‘Ubi-Check: A Pervasive Integrity Checking System’, *Smart Spaces and Next Generation Wired/Wireless Networking*, 5764, pp. 89–96.

Banâtre, M., Allard, F. and Couderc, P. (2010) ‘A Spatial Computing Approach for Integrity Checking of Objects Groups’, in: *4th IEEE International Conference on Self-Adaptive and Self-Organizing Systems Workshop*. Budapest, Hungary 27–28 September: IEEE, pp. 80–84.

Bashir, A. K., Park, M.-S., Lee, S.-I., Park, J., Lee, W. and Shah, S. C. (2013) ‘In-Network RFID Data Filtering Scheme in RFID-WSN for RFID Applications’, in: *6th International Conference on Intelligent Robotics and Applications*. Busan, South Korea 25–28 September: Springer, pp. 454–465.

Bloom, B. (1970) ‘Space/Time Trade-offs in Hash Coding with Allowable Errors’, *Communications of the ACM*, 13 (7), pp. 422–426.

Bocharova, I. E., Kudryashov, B. D., Skachek, V., Rosnes, E. and Ytrehus, Ø. (2017) ‘ML and Near-ML Decoding of LDPC Codes Over the BEC: Bounds and Decoding Algorithms’, in: *IEEE International Symposium on Information Theory*. Aachen, Germany 25–30 June: IEEE, pp. 1–21.

Bocharova, I. E., Kudryashov, B. D., Skachek, V., Rosnes, E. and Ytrehus, Ø. (2018) ‘ML and Near-ML Decoding of LDPC Codes Over the BEC: Bounds and Decoding Algorithms’, *IEEE Transactions on Communications*, pp. 1–16.

Bolic, M., Simplot-Ryl, D. and Stojmenovic, I. (2010) *RFID Systems: Research Trend and Challenges*. New York: Wiley.

Bonomi, F., Mitzenmacher, M., Panigrahy, R., Singh, S. and Varghese, G. (2006) ‘An Improved Construction for Counting Bloom Filters’, in: *14th Annual European Symposium on Algorithms*. Zurich 11-15 September: Springer, pp. 684–695.

Bose, P., Guo, H., Kranakis, E., Maheshwari, A., Morin, P., Morrison, J., *et al.* (2008) ‘On the False-Positive Rate of Bloom Filters’, *Information Processing Letters*, 108 (4), pp. 210–213.

Broder, A. and Mitzenmacher, M. (2004) ‘Network Applications of Bloom Filter: a Survey’, *Internet Mathematics*, 1 (4), pp. 485–509.

Brown, D. (2007) *RFID Implementation*. India: McGraw-Hill.

Bruck, J., Gao, J. and Jiang, A. (2006) ‘Weighted Bloom Filter’, in: *IEEE International Symposium on Information Theory*. Seattle, USA 9–14 July: IEEE, pp. 2304–2308.

Burmester, M. and Munilla, J. (2016) ‘An Anonymous RFID Grouping-Proof with Missing Tag Identification’, in: *IEEE International Conference on RFID*. Orlando 3–5 May: IEEE, pp. 1–7.

Burshtein, D. and Miller, G. (2004) ‘An Efficient Maximum Likelihood Decoding of LDPC Codes over the Binary Erasure Channel’, *IEEE Transactions on Information Theory*, 50 (11), pp. 1–8.

Cai, Z., Hao, J. and Wang, L. (2008) ‘An efficient Early Stopping Scheme for LDPC Decoding’, in: *13th NASA Symposium on VLSI Design*. Guangzhou, China 19–21 November: IEEE, pp. 1325–1329.

Capetanakis, J. I. (1979) ‘Tree Algorithms for Packet Broadcast Channels’, *IEEE Transaction on Information Theory*, 25 (5), pp. 505–515.

Cha, J.-R. and Kim, J.-H. (2006) ‘Dynamic Framed Slotted ALOHA Algorithms Using Fast Tag Estimation Method for RFID System’, in: *IEEE Consumer Communications & Networking Conference*. Las Vegas, USA 8–10 January: IEEE, pp. 768–772.

Chabanne, H., Urien, P. and Susini, J.-F. (2011) *RFID and the Internet of Things*. Wiley.

-
- Chaves, L., Schwuchow, M., Schmitz, A. and Taherivand, A. (2013) 'Radio Frequency Identification Reading by Using Error Correcting Codes on Sets of Tags', *United State Patent*. USA.
- Chen, H., Jin, H., Chen, L., Liu, Y. and Ni, L. M. (2012) 'Optimizing Bloom Filter Settings in Peer-to-Peer Multikeyword Searching', *IEEE Transactions on Knowledge and Data Engineering*, 24 (4), pp. 692–706.
- Chen, M., Luo, W., Chen, S. and Fang, Y. (2016) 'An Efficient Tag Searching Protocol in Large-Scale RFID Systems', *IEEE/ACM Transactions on Networking*, 24 (2), pp. 703–716.
- Chen, S., Zhang, M. and Xiao, B. (2011) 'Efficient Information Collection Protocols for Sensor-Augmented RFID Networks', in: *International Conference on Computer Communications*. Shanghai, China 10–15 April: IEEE, pp. 3101–3109.
- Chen, T. (2012) 'An Early Stopping Criterion for LDPC Decoding Based on Average Weighted Reliability Measure', in: *Cross Strait Quad-Regional Radio Science and Wireless Technology Conference*. Harbin, China 23–27 July: IEEE, pp. 123–126.
- Chen, W.-T. and Kao, W. (2011) 'A Novel Q-algorithm for EPCglobal Class-1 Generation-2 Anti-collision Protocol', *International Journal of Electronics and Communication Engineering*, 5 (6), pp. 801–804.
- Chung, S.-Y., Richardson, T. J. and Urbanke, R. L. (2001) 'Analysis of Sum-Product Decoding of Low-Density-Parity-Check Codes Using a Gaussian Approximation', *IEEE Transaction on Information Theory*, 47 (2), pp. 657–670.
- Coppersmith, D., Odlyzko, A. and Schroepel, R. (1986) 'Discrete logarithms in $GF(p)$ ', *Algorithmica*, 1 (1), pp. 1–15.
- Coresonant (2014) 'RFID Tags for Solar Module India'. Available from: <https://coresonant.appspot.com/html/rfid-tags-for-solar-module-india.html> [Accessed 23 January 2018].
- Couderc, P., Banâtre, M. and Allard, F. (2011) 'Pervasive Integrity Checking With Coupled Objects', *Procedia Computer Science*, 5, pp. 320–327.
- Cunche, M. and Roca, V. (2008) 'Improving the Decoding of LDPC Codes for the Packet Erasure Channel with a Hybrid Zyablov Iterative Decoding/Gaussian Elimination Scheme',
-

Research Report, INRIA, (March), pp. 1–19.

Cunche, M., Savin, V. and Roca, V. (2010) ‘Analysis of Quasi-Cyclic LDPC Codes Under ML Decoding Over the Erasure Channel’, in: *International Symposium on Information Theory and Its Applications*. Taichung, Taiwan 17–20 October: IEEE, pp. 861–866.

Datta, D. B. (2016) ‘Radio Frequency Identification Technology: An Overview of its Components , Principles and Applications’, *International Journal of Science, Engineering and Technology Research*, 5 (2), pp. 565–574.

Di, C., Proietti, D., Telatar, I. E., Richardson, T. J. and Urbanke, R. L. (2002) ‘Finite-Length Analysis of Low-Density Parity-Check Codes on the Binary Erasure Channel’, *IEEE Transactions on Information Theory*, 48 (6), pp. 1570–1579.

Ding, D., PEI., D. and Salomaa, A. (1996) *Chinese Remainder Theorem: Applications in Computing, Coding, Cryptography*. River Edge, NJ, USA: World Scientific.

Dutta, S., Narang, A. and Bera, S. K. (2013) ‘Streaming Quotient Filter: A Near Optimal Approximate Duplicate Detection Approach for Data Streams’, in: *39th International Conference on Very Large Data Bases*. Trento, Italy 26–30 August: ACM, pp. 589–600.

Elias, P. (1955) ‘Coding for Two Noisy Channels’, in: *3rd London Synposiain on Infonnation Theory*. London: Academic Press, pp. 61–76.

EPCglobal (2015) *EPC™ Radio-Frequency Identity Protocols Generation-2 UHF RFID Specification for RFID Air Interface*.

Fan, L., Cao, P., Almeida, J. and Broder, A. Z. (2000) ‘Summary Cache: A Scalable Wide-Area Web Cache Sharing Protocol’, *IEEE/ACM Transactions on Networking*, 8 (3), pp. 281–293.

Ficara, D., Giordano, S., Procissi, G. and Vitucci, F. (2008) ‘MultiLayer Compressed Counting Bloom Filters’, in: *27th Conference on Computer Communications*. Phoenix, AZ, USA: IEEE, pp. 933–941.

Finkenzeller, K. (2010) *RFID Handbook Fundamentals and Applications in Contactless Smart Cards, Radio Frequency Identification and Near-Field Communication*. Third Edit. Chichester: Wiley.

-
- Fujitsu (2014) *World's Largest-Capacity 64KByte FRAM Metal Mount RFID Tag*. Japan.
- Gallager, R. G. (1962) 'Low-Density Parity-Check Codes', *IRE Transactions on Information Theory*, 18 (1), pp. 21–28.
- Geravand, S. and Ahmadi, M. (2013) 'Bloom Filter Applications in Network Security: A State-of-the-Art Survey', *Computer Networks*, 57 (18), pp. 4047–4064.
- Glouche, Y. and Couderc, P. (2012) 'An Autonomous Traceability Mechanism for a Group of RFID Tags', in: *6th International Conference on Mobile Ubiquitous Computing, System, Service, and Technology*. Barcelona 23–28 September: IARIA, pp. 161–168.
- Goldreich, O., Ron, D. and Sudan, M. (2000) 'Chinese Remaindering with Errors', *IEEE Transactions on Information Theory*, 46 (4), pp. 1330–1338.
- Gravano, S. (2001) *Introduction to Error Control Codes*. UK: Oxford University Press.
- Gremillion, L. L. (1982) 'Designing a Bloom filter for Differential File Access', *Communications of the ACM*, 25 (9), pp. 600–604.
- Guo, D. and Li, M. (2013) 'Set Reconciliation via Counting Bloom Filters', *IEEE Transactions on Knowledge and Data Engineering*, 25 (10), pp. 2367–2380.
- Guo, D., Wu, J., Chen, H., Yuan, Y. and Luo, X. (2010) 'The Dynamic Bloom Filters', *IEEE Transactions on Knowledge and Data Engineering*, 22 (1), pp. 120–133.
- Guoqiong, L., Jun, Z., Ni, H., Xiaomei, H., Zhiwei, H., Changxuan, W., *et al.* (2017) 'Approximately Filtering Redundant Data for Uncertain RFID Data Streams', in: *18th IEEE International Conference on Mobile Data Management*. Daejeon, South Korea 29 May–1 June: IEEE, pp. 56–61.
- Guoqiong, L., Rui, W., Guoqiang, D., Zhen, S. and Changxuan, W. (2016) 'Approximate Filtering of Redundant RFID Data Streams in Mobile Environment', *Tehnicky Vjesnik*, 23 (2), pp. 415–423.
- Han, G. and Liu, X. (2010) 'A Unified Early Stopping Criterion for Binary and Nonbinary LDPC Codes Based on Check-Sum Variation Patterns', *IEEE Communications Letters*, 14 (11), pp. 1053–1055.
- Hu, X.-Y. (2008) 'Source Code for Progressive Edge Growth Parity-Check Matrix
-

Construction'. Available from: http://www.inference.org.uk/mackay/PEG_ECC.html [Accessed 10 March 2016].

Hu, X.-Y., Eleftheriou, E. and Arnold, D.-M. (2001) 'Progressive Edge-Growth Tanner Graphs', in: *IEEE Global Telecommunications Conference*. San Antonio, TX, USA 25–29 November: IEEE, pp. 995–1001.

Hu, X.-Y., Eleftheriou, E. and Arnold, D.-M. (2002) 'Irregular Progressive Edge-Growth (PEG) Tanner Graphs', in: *IEEE International Symposium on Information Theory*. Lausanne, Switzerland 30 June–5 July: IEEE, pp. 8803.

Hu, X.-Y., Eleftheriou, E. and Arnold, D. M. (2005) 'Regular and Irregular Progressive Edge-Growth Tanner Graphs', *IEEE Transaction on Information Theory*, 51 (1), pp. 386–398.

Huang, W., Member, S., Li, H. and Dill, J. (2011) 'Fountain Codes with Message Passing and Maximum Likelihood Decoding over Erasure Channels', in: *IEEE Wireless Telecommunication Symposium*. New York 13–15 April: IEEE, pp. 1–5.

Huang, X. and Le, S. (2007) 'Efficient Dynamic Framed Slotted ALOHA for RFID Passive Tags', in: *9th International Conference on Advanced Communication Technology*. Kobe, Japan 12–14 February: IEEE, pp. 94–97.

Huffman, W. and Pless, V. (2003) *Fundamentals of Error Correcting Codes*. New York: Cambridge University Press.

Hunt, V., Puglia, A. and Puglia, M. (2007) *A Guide to Radio Frequency Identification*. New Jersey: Wiley.

Hush, D. and Wood, C. (1998) 'Analysis of Tree Algorithms for RFID Arbitration', in: *IEEE International Symposium on Information Theory*. Cambridge, USA 16–21 August: IEEE, pp. 87131.

Hutter, M., Wenger, E., Pelnar, M. and Pendl, C. (2012) 'Elliptic Curve Cryptography on WISPs UHF RFID Tag', in: *International Workshop on Radio Frequency Identification: Security and Privacy Issues*. Hong Kong, China 30 November– 2 December: Springer, pp. 32–47.

Jia, X., Feng, Q., Fan, T. and Lei, Q. (2012) 'RFID Technology and its Applications in

-
- Internet of Things (IoT)', in: *2nd International Conference on Consumer Electronics, Communications and Networks*. Yichang, China 21–23 April: IEEE, pp. 1282–1285.
- Jiang, W., Wang, Y. and Zhang, G. (2012) 'A Two-Layer Duplicate Filtering Approach for RFID Data Streams', in: *Internet of Things*. Changsha, China 17–19 August: Springer, pp. 226–233.
- Jones, E., Chung, C. (2007) *RFID in Logistics: A Practical Introduction*. CRC Press.
- Johnson, S. J. (2009) *Introducing Low-Density Parity-Check Codes*. Australia.
- Juels, A. (2004) "' Yoking-Proofs " for RFID Tags', in: *IEEE Annual Conference on Computing and Communications Workshops*. Orlando 14–17 March: IEEE, pp. 1–6.
- Kaewsirisin, S., Supanakoon, P., Promwong, S., Sukutamanti, N. and Ketprom, U. (2008) 'Performance Study of Dynamic Framed Slotted ALOHA for RFID Systems', in: *5th International Conference on Electrical Engineering/Electronics, Computer, Telecommunications and Information Technology*. Krabi, Thailand 14–17 May: IEEE, pp. 413–416.
- Kamaludin, H., Mahdin, H. and Abawajy, J. H. (2016) 'Filtering Redundant Data from RFID Data Streams', *Journal of Sensors*, 2016, pp. 1–8.
- Karmakar, N. (2010) *Handbook of Smart Antennas for RFID Systems*. New Jersey: Wiley.
- Kienle, F. and Wehn, N. (2005) 'Low Complexity Stopping Criterion for LDPC Code Decoders', in: *Vehicular Technology Conference*. Stockholm, Sweden 30 May– 1 June: IEEE, pp. 25–28.
- Klair, D. K., Chin, K.-W. and Raad, R. (2007) 'On the Accuracy of RFID Tag Estimation Functions', in: *International Symposium on Communications and Information Technologies*. Sydney 17–19 October: IEEE, pp. 1401–1406.
- Knospe, H. and Pohl, H. (2004) 'RFID security', *Information Security*, 9 (4), pp. 39–50.
- Kou, Y., Lin, S. and Fossonier, M. P. C. (2001) 'Low-density Parity-Check Codes Based on Finite Geometries: A Rediscovery and New Results', *IEEE Transactions on Information Theory*, 47 (7), pp. 2711–2736.
- Kumar, A., Xu, J., Li, L. and Wang, J. (2006) 'Space-Code Bloom Filter for Efficient Traffic
-

Flow Measurement', *IEEE Journal on Selected Areas in Communications*, 24 (12), pp. 167–172.

LaMacchia, B. A. and Odlyzko, A. M. (1990) 'Solving Large Sparse Linear Systems over Finite Fields', in: *10th Annual International Cryptology*. Santa Barbara, California 11–15 August: Springer, LNCS 537, pp. 109–133.

Lan, L., Zeng, L., Tai, Y. Y., Chen, L., Lin, S. and Abdel-Ghaffar, K. (2007) 'Construction of Quasi-Cyclic LDPC Codes for AWGN and Binary Erasure Channels: A Finite Field Approach', *IEEE Transactions on Information Theory*, 53 (7), pp. 2429–2458.

Law, C., Lee, K. and Siu, K.-Y. (2000) 'Efficient Memoryless Protocol for Tag Identification', in: *4th International Workshop on Discrete Algorithms and Methods for Mobile Computing and Communications*. Massachusetts, USA 11 August: ACM, pp. 75–84.

Lee, C.-H. and Chung, C.-W. (2011) 'An Approximate Duplicate Elimination in RFID Data Streams', *Data and Knowledge Engineering*, 70 (12), pp. 1070–1087.

Lee, S., Joo, S.-D. and Lee, C. (2005) 'An Enhanced Dynamic Framed Slotted ALOHA Algorithm for RFID Tag', in: *2nd Annual International Conference on Mobile and Ubiquitous Systems: Networking and Services*. San Diego, USA 17–21 July: IEEE, pp. 1–7.

Li, B., He, Y. and Liu, W. (2015) 'Towards Constant-Time Cardinality Estimation for Large-Scale RFID Systems', in: *The International Conference on Parallel Processing*. Beijing, China 1–4 September: IEEE, pp. 809–818.

Li, J., You, X. H. and Li, J. (2006) 'Early Stopping for LDPC Decoding: Convergence of Mean Magnitude (CMM)', *IEEE Communications Letters*, 10 (9), pp. 667–669.

Li, T., Chen, S. and Ling, Y. (2010) 'Identifying the Missing Tags in a Large RFID System', in: *International Symposium on Mobile Ad Hoc Networking and Computing*. Chicago, USA 20–24 September: ACM, pp. 1–10.

Liu, H., Ning, H., Zhang, Y., He, D., Xiong, Q. and Yang, L. (2013) 'Grouping-Proofs-Based Authentication Protocol for Distributed RFID Systems', *IEEE Transactions on Parallel and Distributed Systems*, 24 (7), pp. 1321–1330.

Liu, J., Chen, M., Xiao, B., Zhu, F., Chen, S. and Chen, L. (2016) 'Efficient RFID Grouping Protocols', *IEEE/ACM Transactions on Networking*, 24 (5), pp. 3177–3190.

-
- Liu, J., Chen, S., Xiao, B., Wang, Y. and Chen, L. (2017) ‘Category Information Collection in RFID Systems’, in: *International Conference on Distributed Computing Systems*. Atlanta, USA 5–8 June: IEEE, pp. 2220–2225.
- Liu, L. and Lai, S. (2006) ‘RFID System’, in: *International Conference on Wireless Communications, Networking and Mobile Computing*. Wuhan, China 22–24 September: IEEE, pp. 1–4.
- Liva, G., Matuz, B., Paolini, E. and Chiani, M. (2009) ‘Pivoting Algorithms for Maximum Likelihood Decoding of LDPC Codes over Erasure Channels’, in: *IEEE Global Telecommunications Conference*. Honolulu, Hawaii 30 November–4 December: IEEE, pp. 1–6.
- Luby, M. G., Mitzenmacher, M., Shokrollahi, M. A., Spielman, D. A. and Stemann, V. (1997) ‘Practical Loss-Resilient Codes’, in: *29th Annual ACM Symposium on Theory of Computing*. El Paso, Texas, USA 4–6 May: ACM, pp. 150–159.
- Luby, M. G., Mizenmacher, M., Shokrollahi, M. A. and Spielman, D. A. (2001a) ‘Efficient Erasure Correcting Codes’, *IEEE Transactions on Information Theory*, 47 (2), pp. 569–584.
- Luby, M. G., Mizenmacher, M., Shokrollahi, M. A. and Spielman, D. A. (2001b) ‘Improved low-Density Parity-Check Codes Using Irregular Graphs’, *IEEE Transaction on Information Theory*, 47 (2), pp. 585–598.
- Luo, L., Guo, D., Ma, R. T. B., Rottenstreich, O. and Luo, X. (2018) ‘Optimizing Bloom Filter: Challenges, Solutions, and Comparisons’, *ArXiv*, pp. 1–34.
- Luo, L., Guo, D., Wu, J., Rottenstreich, O., He, Q., Qin, Y., *et al.* (2017) ‘Efficient Multiset Synchronization’, *IEEE/ACM Transactions on Networking*, 25 (2), pp. 1190–1205.
- Mackay, D. J. C. (2005) *Information Theory , Inference , and Learning Algorithm*. Fourth Edi. Cambridge University Press.
- MacKay, D. J. C. (1999) ‘Good Codes based on Very Sparse Matrices’, *IEEE Transaction on Information Theory*, 45 (2), pp. 399–431.
- Mahdin, H. and Abawajy, J. (2011) ‘An Approach for Removing Redundant Data from RFID Data Streams’, *Sensors*, 11 (10), pp. 9863–9877.
-

-
- Mattoussi, F. and Roca, V. (2012) ‘Design of Small Rate , Close to Ideal , GLDPC-Staircase AL-FEC Codes for the Erasure Channel’, in: *IEEE Global Communications Conference*. Anaheim, USA 3–7 December: IEEE, pp. 2143–2149.
- Mezzi, N. and Akaichi, J. (2013) ‘Supply Chain Duplicate Transportation RFID Data Stream Filtering’, *International Journal of Application or Innovation in Engineering & Management*, 2 (5), pp. 484–493.
- Mohsenin, T., Shirani-Mehr, H. and Baas, B. (2011) ‘Low power LDPC Decoder with Efficient Stopping Scheme for Undecodable Blocks’, in: *IEEE International Symposium on Circuits and Systems*. Rio de Janeiro, Brazil 15–18 May: IEEE, pp. 1780–1783.
- Mullin, J. (1983) ‘A Second Look at Bloom Filters’, *Communications of the ACM*, 26 (8), pp. 570–571.
- Mullin, J. (1990) ‘Optimal Semijoins for Distributed Database Systems’, *IEEE Transactions on Software Engineering*, 16 (5), pp. 558–560.
- Mullin, J. and Margoliash, D. (1990) ‘A Tale of Three Spelling Checkers’, *Journals of Software: Practice and Experience*, 20 (6), pp. 625—630.
- Nambiar, A. N. (2009) ‘RFID Technology: A Review of its Applications’, in: *Proceedings of the World Congress on Engineering and Computer Science*. San Francisco 20–22 October: Newswood Limited, pp. 1253–1259.
- Odlyzko, A. M. (1985) ‘Discrete logarithms in Finite Fields and Their Cryptographic Significance’, in: *Advances in Cryptology: Proceedings of Eurocrypt ’84*. Berlin: Springer, pp. 224–314.
- Olmos, P. M., Murillo-Fuentes, J. J. and Pérez-Cruz, F. (2010) ‘Tree-structure Expectation Propagation for Decoding LDPC Codes over Binary Erasure Channels’, in: *IEEE International Symposium on Information Theory Proceedings*. Austin, TX, USA 13–18 June: IEEE, pp. 799–803.
- Orlitsky, A., Urbanke, R., Viswanathan, K. and Zhang, J. (2002) ‘Stooping Sets and the Grith of Tanner Graph’, in: *IEEE International Symposium on Information Theory*. Lausanne, Switzerland 30 June–5 July: IEEE, pp. 1–2.
- Orlitsky, A., Viswanathan, K. and Zhang, J. (2005) ‘Stopping Set Distribution of LDPC Code
-

Ensembles’, *IEEE Transactions on Information Theory*, 51 (3), pp. 929–953.

Paolini, E., Liva, G., Matuz, B. and Chiani, M. (2008) ‘Generalized IRA Erasure Correcting Codes for Hybrid Iterative/Maximum Likelihood Decoding’, *IEEE Communications Letters*, 12 (6), pp. 450–452.

Paolini, E., Liva, G., Matuz, B. and Chiani, M. (2012) ‘Maximum Likelihood Erasure Decoding of LDPC Codes: Pivoting Algorithms and Code Design’, *IEEE Transactions on Communications*, 60 (11), pp. 3209–3220.

Potdar, V., Hayati, P. and Chang, E. (2007) ‘Improving RFID Read Rate Reliability by a Systematic Error Detection Approach’, in: *Annual RFID Eurasia*. Istanbul, Turkey 5–6 September: IEEE, pp.1–5

Pishro-Nik, H. and Fekri, F. (2004) ‘On Decoding of Low-Density Parity-Check Codes over the Binary Erasure Channel’, *IEEE Transaction on Information Theory*, 50 (3), pp. 439–454.

Qian, Y., He, Z. and Zhang, D. (2016) ‘TIP : Time-Efficient Identification Protocol for Unknown RFID Tags using Bloom Filters’, in: *22nd International Conference on Parallel and Distributed Systems*. Wuhan, China 13–16 December: IEEE, pp. 151–158.

Qiao, Y., Chen, S., Li, T. and Chen, S. (2011) ‘Energy-Efficient Polling Protocols in RFID Systems’, in: *12th ACM International Symposium on Mobile Ad Hoc Networking and Computing*. Paris, France 17–19 May: ACM, pp. 1–9.

Qiao, Y., Chen, S., Li, T. and Chen, S. (2016) ‘Tag-Ordering Polling Protocols in RFID Systems’, *ACM Transactions on Networking*, 24 (3), pp. 1548–1561.

Rabin, M. O. (1981) *Fingerprinting by Random Polynomials*, Center for Research in Computing Technology.

Richardson, T. J., Shokrollahi, M. A. and Urbanke, R. L. (2001) ‘Design of Capacity-Approaching Irregular Low-Density Parity-Check Codes’, *IEEE Transactions on Information Theory*, 47 (2), pp. 619–637.

Richardson, T. J. and Urbanke, R. L. (2001) ‘Efficient Encoding of Low-Density Parity-Check Codes’, *IEEE Transactions on Information Theory*, 47 (2), pp. 638–656.

Richardson, T. J. and Urbanke, R. L. (2008) *Modern Coding Theory*. Cambridge: Cambridge

University Press.

Roberti, M. (2011) 'RFID Journal'. Available from: <http://www.rfidjournal.com/blogs/experts/entry?8134> [Accessed 23 January 2018].

Rothenberg, C. E., Macapuna, C. A. B., Verdi, F. L. and Magalhaes, M. F. (2010) 'The Deletable Bloom Filter', *IEEE Communication Letters*, 14 (6), pp. 1–3.

Ryan, W. E. (2003) 'An Introduction to LDPC Codes', in: *CRC Handbook for Coding and Signal Processing for Magnetic Recording Systems*. Florida: CRC Press, pp. 1–23.

Ryan, W. E. and Lin, S. (2009) *Channel Codes Classical and Modern*. New York: Cambridge University Press.

Saito, J. and Sakurai, K. (2005) 'Grouping proof for RFID tags', in: *International Conference on Advanced Information Networking and Applications*. Taipei, Taiwan 25 April: IEEE, pp. 621–624.

Sankaranarayanan, S. and Vasić, B. (2005) 'Iterative Decoding of Linear Block Codes: A Parity-Check Orthogonalization Approach', *IEEE Transactions on Information Theory*, 51 (9), pp. 3347–3353.

Sarangan, V., Devarapalli, M. R. and Radhakrishnan, S. (2008) 'A Framework for Fast RFID Tag Reading in Static and Mobile Environments', *Computer Networks*, 52 (5), pp. 1058–1073.

Saravanan, K. and Senthilkumar, A. (2015) 'An Insight Review on Bloom Filter and Its Variants with Applications: An Emerging Hash Based Membership Querying Technique', *Journals of Discrete Mathematical Sciences and Cryptography*, 18 (3), pp. 247–263.

Sato, Y., Igarashi, Y., Mitsugi, J., Nakamura, O. and Murai, J. (2012) 'Identification of Missing Objects with Group Coding of RF Tags', in: *IEEE International Conference on RFID*. Orlando 3–5 April: IEEE, pp. 95–101.

Sato, Y., Mitsugi, J., Nakamura, O. and Murai, J. (2011) 'Group Coding of RF Tags to Verify the Integrity of Group of Objects', in: *IEEE International Conference on RFID*. Orlando 12–14 April: IEEE, pp. 200–206.

Sato, Y., Mitsugi, J., Nakamura, O. and Murai, J. (2012) 'Theory and Performance

Evaluation of Group Coding of RFID Tags’, *IEEE Transaction on Automation Science and Engineering*, 9 (3), pp. 458–466.

Sayers, C., Deolaikar, V. and Pradhan, S. (2010) ‘Self-Referential Integrity Checking System and Method’, *United States Patent*. USA.

Schwartz, M. and Vardy, A. (2006) ‘On the Stopping Distance and The Stopping Redundancy of Codes’, *IEEE Transaction on Information Theory*, 52 (3), pp. 975–979.

Shedsale, R. and Sarwade, N. (2012) ‘A Review of Construction Methods for Regular Ldpc’, *Indian Journal of Computer Science and Engineering*, 3 (2), pp. 380–385.

Shen, J., Tan, H., Chang, S., Ren, Y. and Liu, Q. (2015) ‘A lightweight and Practical RFID Grouping Authentication Protocol in Multiple-Tag Arrangements’, in: *International Conference on Advanced Communication Technology*. Seoul, South Korea 1–3 July: IEEE, pp. 681–686.

Shih, D.-H., Sun, P.-L., Yen, D. C. and Huang, S.-M. (2006) ‘Taxonomy and Survey of RFID Anti-Collision Protocols’, *Computer Communications*, 29 (11), pp. 2150–2166.

Shin, D., Heo, K., Oh, S. and Ha, J. (2007) ‘A Stopping Criterion for Low-Density Parity-Check Codes’, in: *Vehicular Technology Conference*. Dublin, Ireland 22–25 April: IEEE, pp. 1529–1533.

Sinha, A., Glouche, Y. and Couderc, P. (2014) ‘Distributed Tree Structure for Composite Physical Objects’, in: *5th International Conference on Ambient Systems, Networks and Technologies*. Hasselt, Belgium 2–5 June: Elsevier, 32, pp. 587–595.

Skachek, V. and Rabbat, M. G. (2014) ‘Subspace Synchronization: A Network-Coding Approach to Object Reconciliation’, in: *IEEE International Symposium on Information Theory*. Honolulu, USA 29 June–4 July: IEEE, pp. 2301–2305.

Su, Y. (2014) ‘Extended Grouping of RFID Tags Based on Resolvable Transversal Designs’, *IEEE Signal Processing Letters*, 21 (4), pp. 488–492.

Su, Y., Lin, J. and Tonguz, O. K. (2013) ‘Grouping of RFID Tags via Strongly Selective Families’, *IEEE Communication Letters*, 17 (2), pp. 1–4.

Su, Y. and Tonguz, O. K. (2013) ‘Using the Chinese Remainder Theorem for the Grouping of

-
- RFID Tags', *IEEE Transaction on Communications*, 61 (11), pp. 4741–4753.
- Su, Y. and Wang, C. (2015) 'Design and Analysis of Unequal Missing Protection for the Grouping of RFID Tags', *IEEE Transaction on Communications*, 63 (11), pp. 4474–4489.
- Su, Y., Wang, C. and Siao, H.-Y. (2015) 'On Unequal Missing Protection of the Grouping of RFID Tags', in: *IEEE International Symposium on Information Theory*. Hong Kong 14–19 June: IEEE, pp. 2994–2998.
- Sundaresan, S., Doss, R., Member, S., Zhou, W. and Member, S. (2014) 'A Robust Grouping Proof for RFID EPC C1G2 Tags', *IEEE Transaction on Information Forensics and Security*, 64 (10), pp. 2994–3008.
- Tanner, R. M. (1981) 'A Recursive Approach to Low Complexity Codes', *IEEE Transaction on Information Theory*, 27 (5), pp. 533–547.
- Tarkoma, S., Rothenberg, C. E. and Lagerspetz, E. (2012) 'Theory and Practice of Bloom Filters for Distributed Systems', *IEEE Communications Surveys & Tutorials*, 14 (1), pp. 131–155.
- Teitelbaum, J. (1998) 'Euclid's Algorithm and the Lanczos Method over Finite Fields', *Mathematics of Computation*, 67 (224), pp. 1665–1678.
- Tian, T., Jones, C., Villasenor, J. D. and Wesel, R. D. (2003) 'Construction of Irregular LDPC Codes with Low Error Floors', in: *IEEE International Conference on Communications*. Anchorage, AK, USA 11–15 May: IEEE, pp. 3125–3129.
- Tian, T., Jones, C., Villasenor, J. D. and Wesel, R. D. (2004) 'Selective Avoidance of Cycles in Irregular LDPC Code Construction', *IEEE Transactions on Communications*, 52 (8), pp. 1242–1247.
- Tjhai, C. (2007) *A Study of Linear Error Correcting Codes*. The University of Plymouth.
- Tomlinson, M., Cai, J., Tjhai, C., Ambroze, M. and Ahmed, M. (2004) 'System for Correcting Deleted or Missing Symbols'. UK Patent application number 0428042.6.
- Tomlinson, T., Tjhai, C., Ambroze, M., Ahmed, M. and Jibril, M. (2017) *Error-Correction Coding and Decoding*. Springer.
- Tomlinson, T., Tjhai, C., Cai, J. and Ambroze, M. (2007) 'Analysis of the Distribution of the
-

Number of Erasures Correctable by a Binary Linear Code and the Link to Low-Weight Codewords', *IET Communications*, 1 (3), pp. 539–548.

Vellambi, B. N. and Fekri, F. (2007) 'Results on the Improved Decoding Algorithm for Low-Density Parity-Check Codes over the Binary Erasure Channel', *IEEE Transactions on Information Theory*, 53 (4), pp. 1510–1520.

Vogt, H. (2002a) 'Efficient Object Identification with Passive RFID Tags', in: *International Conference on Pervasive Computing*. Zurich, Switzerland 26–28 August: Berlin: Springer, pp. 98–113.

Vogt, H. (2002b) 'Multiple Object Identification With Passive RFID Tags', in: *IEEE International Conference on Systems, Man and Cybernetics*. Yasmine Hammamet, Tunisia 6–9 October: IEEE, pp. 1–6.

Wang, X., Qiang, Z. and Jia, Y. (2008) 'Efficiently Filtering Duplicates over Distributed Data Streams', in: *International Conference on Computer Science and Software Engineering*. Wuhan, China 12–14 December: IEEE, 4, pp. 631–634.

Ward, M. and Kranenburg, V. (2006) *RFID: Frequency, Standards, Adoption and Innovation*, *JISC Technology and Standards Watch*.

Wiedemann, D. (1986) 'Solving Sparse Linear Equations over Finite Fields', *IEEE Transaction on Information Theory*, 32 (1), pp. 54–62.

Xiao, H. and Banihashemi, A. H. (2004) 'Improved Progressive-Edge-Growth (PEG) Construction of Irregular LDPC Codes', *IEEE Communications Letters*, 8 (12), pp. 715–717.

Xie, X., Liu, X., Li, K., Xiao, B. and Qi, H. (2017) 'Minimal Perfect Hashing-Based Information Collection Protocol for RFID Systems', *IEEE Transactions on Mobile Computing*, 16 (10), pp. 2792–2805.

Yaacob, S. S. and Mahdin, H. (2016) 'An Overview on Various RFID Data Filtering Techniques Based on Bloom Filter Approach', *Universiti Tun Hussein Onn Malaysia*, 8 (41), pp. 1–5.

Yang, G. (2017) *Optimized Hardware Implementations of Lightweight Cryptography*. Waterloo University.

-
- Yang, L., Ambroze, M. and Tomlinson, M. (2008) ‘Decoding Turbo Gallager Codes for the Erasure Channel’, *IEEE Communication Letters*, 1 (2), pp. 1–3.
- Yongsheng, H. A. O. and Zhijun, G. E. (2013) ‘Redundancy Removal Approach for Integrated RFID Readers with Counting Bloom Filter’, *Journal of Computational Information Systems*, 9 (5), pp. 1917–1924.
- Yu, J., Chen, L., Zhang, R. and Wang, K. (2017) ‘Finding Needles in a Haystack: Missing Tag Detection in Large RFID Systems’, *IEEE Transactions on Communications*, 65 (5), pp. 2036–2047.
- Yue, H., Member, S., Zhang, C. and Pan, M. (2014) ‘Unknown-Target Information Collection in Sensor-Enabled RFID System’, *IEEE/ACM Transactions on Networking*, 22 (4), pp. 1164–1175.
- Yue, H., Zhang, C., Pan, M., Fang, Y. and Chen, S. (2012) ‘A Time-Efficient Information Collection Protocol for Large-Scale RFID Systems’, in: *International Conference on Computer Communications*. Orlando, USA 25–30 March: IEEE, pp. 2158–2166.
- Zhen, B., Kobayashi, M. and Shimizu, M. (2005) ‘Framed ALOHA for Multiple RFID Objects Identification’, *IEICE Transaction on Communication*, E88–B (3), pp. 991–999.

Appendices

Appendix A-Some Source Codes of the Simulations

MainPEG.C

```

#include <stdlib.h>
#include <stdio.h>
#include <string.h>
#include <iostream>
#include <iomanip>
#include <fstream>
#include <math.h>
#include "BigGirth.h"
#include "Random.h"
#include "CyclesOfGraph.h"

#define EPS 1e-6
using namespace std;
int main(int argc, char * argv[]){
    int i, j, m, N, M;
    int sglConcent=1; // default to non-strictly concentrated parity-check distribution
    int targetGirth=100000; // default to greedy PEG version
    char codeName[100], degFileName[100];
    int *degSeq, *deg;
    double *degFrac;
    BigGirth *bigGirth;
    CyclesOfGraph *cog;

    int numArgs=(argc-1)/2;
    if (argc<9) {
        USE:

cout<<"*****
*****" <<endl;
        cout<<" Usage Reminder: MainPEG -numM M -numN N -codeName CodeName -
degFileName DegFileName " <<endl;
        cout<<"    option:    -sglConcent SglConcent                " <<endl;
        cout<<"                sglConcent==0 ----- strictly concentrated parity-check    " <<endl;
        cout<<"                degree distribution (including regular graphs)" <<endl;
        cout<<"                sglConcent==1 ----- Best-effort concentrated (DEFAULT)    "
<<endl;

```

```

cout<<" option: -tgtGirth TgtGirth " <<endl;
cout<<" TgtGirth==4, 6 ...; if very large, then greedy PEG (DEFAULT) "
<<endl;
cout<<" IF sglConcent==0, TgtGirth is recommended to be set relatively small"
<<endl;
cout<<" " <<endl;
cout<<" Remarks: File CodeName stores the generated PEG Tanner graph. The first line
contains"<<endl;
cout<<" the block length, N. The second line defines the number of parity-checks,
M."<<endl;
cout<<" The third line defines the number of columns of the compressed parity-check
"<<endl;
cout<<" matrix. The following M lines are then the compressed parity-check matrix.
"<<endl;
cout<<" Each of the M rows contains the indices (1 ... N) of 1's in the compressed
"<<endl;
cout<<" row of parity-check matrix. If not all column entries are used, the column
"<<endl;
cout<<" is filled up with 0's. " <<endl;
cout<<" " <<endl;
cout<<" File DegFileName is the input file to specify the degree distribution (node
"<<endl;
cout<<" perspective). The first line contains the number of various degrees. The
second"<<endl;
cout<<" defines the row vector of degree sequence in the increasing order. The
vector"<<endl;
cout<<" of fractions of the corresponding degree is defined in the last line.
"<<endl;
cout<<" " <<endl;
cout<<" A log file called 'leftHandGirth.dat' will also be generated and stored in
the"<<endl;
cout<<" current directory, which gives the girth of the left-hand subgraph of j,
where"<<endl;
cout<<"  $1 \leq j \leq N$ . The left-hand subgraph of j is defined as all the edges emanating
from"<<endl;
cout<<" bit nodes { 1 ... j } and their associated nodes. " <<endl;
cout<<" " <<endl;
cout<<" The last point is, when strictly concentrated parity-check degree
distribution"<<endl;
cout<<" is invoked, i.e. sglConcent==0, the girth might be weakened to some extent as
"<<endl;
cout<<" compared to the generic PEG algorithm. " <<endl;

cout<<"*****"
*****"<<endl;

```

```

    exit(-1);
}else {
    for(i=0;i<numArgs;i++){
        if (strcmp(argv[2*i+1], "-numM")==0) {
            M=atoi(argv[2*i+2]);
        } else if(strcmp(argv[2*i+1], "-numN")==0) {
            N=atoi(argv[2*i+2]);
        } else if(strcmp(argv[2*i+1], "-codeName")==0) {
            strcpy(codeName, argv[2*i+2]);
        } else if(strcmp(argv[2*i+1], "-degFileName")==0) {
            strcpy(degFileName, argv[2*i+2]);
        } else if(strcmp(argv[2*i+1], "-sglConcent")==0) {
            sglConcent=atoi(argv[2*i+2]);
        } else if(strcmp(argv[2*i+1], "-tgtGirth")==0) {
            targetGirth=atoi(argv[2*i+2]);
        } else{
            goto USE;
        }
    }
    if(M>N) {
        cout<<"Warning: M must be samller than N"<<endl;
        exit(-1);
    }
}

degSeq=new int[N];
ifstream infn(degFileName);
if (!infn) {cout << "\nCannot open file " << degFileName << endl; exit(-1); }
infn >>m;
deg=new int[m];
degFrac=new double[m];
for(i=0;i<m;i++) infn>>deg[i];
for(i=0;i<m;i++) infn>>degFrac[i];
infn.close();
double dtmp=0.0;
for(i=0;i<m;i++) dtmp+=degFrac[i];
cout.setf(ios::fixed, ios::floatfield);
if(fabs(dtmp-1.0)>EPS) {
    cout.setf(ios::fixed, ios::floatfield);
    cout <<"\n Invalid degree distribution (node perspective): sum != 1.0 but
"<<setprecision(10)<<dtmp<<endl; exit(-1);
}
for(i=1;i<m;i++) degFrac[i]+=degFrac[i-1];
for(i=0;i<N;i++) {
    dtmp=(double)i/N;

```

```

for(j=m-1;j>=0;j--) {
    if(dtmp>degFrac[j]) break;
}
if(dtmp<degFrac[0]) degSeq[i]=deg[0];
else degSeq[i]=deg[j+1];
}
bigGirth=new BigGirth(M, N, degSeq, codeName, sglConcent, targetGirth);
(*bigGirth).writeToFile_Hcompressed();

//computing local girth distribution
if(N<10000) {
    cout<<" Now computing the local girth on the global Tanner graph setting. "<<endl;
    cout<<"    might take a bit long time. Please wait ...          "<<endl;
    (*bigGirth).loadH();
    cog=new CyclesOfGraph(M, N, (*bigGirth).H);
    (*cog).getCyclesTable();
    (*cog).printCyclesTable();
    delete cog;
    cog=NULL;
}

delete [] degSeq; degSeq=NULL;
delete [] deg; deg=NULL;
delete [] degFrac; degFrac=NULL;
delete bigGirth;
}

```

Iterative Decoding

```

function [erasure_vec, avg_error] = get_iterative(fname)
addpath './lib/'
% the max word size of word in Matlab
max_word_size = 64;
alist_params = readalist_peg(fname);
H = alist2parity(alist_params);
[~, nc] = size(H);
[newH] = H;
G_s = full((newH));
[m, n] = size(G_s);
data_word = [];
while length(unique(data_word))~=n
    data_word = round((2^max_word_size-2)*rand(1, n)) + 1;
end
D_de_rep = repmat(data_word, m, 1).*G_s;
parity_words = zeros(m, 1);

```

```

for i=1:n
    parity_words = bitxor(D_de_rep(:, i), parity_words);
end
disp('Input Data Values');
disp(data_word);
disp('Generator Matrix');
disp(G_s);
disp('Parity Values');
disp(parity_words);
maxFrames = 100000;
erasure_vec = (1:nc);
avg_error = zeros(1, length(erasure_vec));
[nCheck, nBit] = size(newH);
nEdge = nnz(newH);
indexLinear = find(newH);
[indexCheck, indexBit] = find(newH); % For sparse matrix, find() is fast.
% The following initialization of the check nodes takes ONE TnewHIRD of the running
time!
checkNode = struct('indexBitConnected', 0);
check = repmat(checkNode, nCheck, 1);
for iCheck = 1:nCheck
    check(iCheck).indexBitConnected = indexBit(indexCheck == iCheck); % Connections to
check nodes
end % for iCheck
nIterationMax = 80;
for erasure_index=1:length(erasure_vec)
    cFrame = 1;
    while cFrame < maxFrames,
        y = randperm(n, erasure_vec(erasure_index));
        missing_index = false(1, n);
        missing_index(y) = true;
        % iterative decoding
        data_word_rx = data_word.*(~missing_index);
        [messageBit, nIteration] = bpdecfast(data_word_rx, parity_words, nIterationMax,
indexLinear, indexCheck, indexBit, check, nCheck, nBit, nEdge, 0);
        avg_error(erasure_index) = avg_error(erasure_index) +
sum(messageBit~=data_word)/erasure_index;
        cFrame = cFrame + 1;
    end
    avg_error(erasure_index) = avg_error(erasure_index)/cFrame;
end

```

Gaussian Decoding

```
function [erasure_vec, avg_error] = getgaussian(fname)
```

```

addpath './lib/'
% the max word size of word in Matlab
max_word_size = 64;
alist_params = readalist_peg(fname);
H = alist2parity(alist_params);
[nr, nc] = size(H);
[newH] = H;
G_s = full(fliplr(newH));
[m, n] = size(G_s);
data_word = round((2^max_word_size-1)*rand(1, n)) + 1;
D_de_rep = repmat(data_word, m, 1).*G_s;
parity_words = zeros(m, 1);
for i=1:n
    parity_words = bitxor(D_de_rep(:, i), parity_words);
end
maxFrames = 100000;
erasure_vec = (1:nc);
avg_error = zeros(1, length(erasure_vec));
for erasure_index=1:length(erasure_vec)
    cFrame = 1;
    while cFrame < maxFrames,
        y = randperm(n, erasure_vec(erasure_index));
        missing_index = false(1, n);
        missing_index(y) = true;
        % Making system of equation for unknown words.
        bprep = [parity_words D_de_rep.*repmat(~missing_index, m, 1)];
        % Computation of b in Ax = b form of the equation.
        b = zeros(m, 1);
        for k=1:n+1
            b = bitxor(bprep(:, k), b);
        end
        % Computation of A in Ax = b form of the equation.
        A = G_s(:, missing_index);
        % Using Gauss elimination to solve the system of equations.
        x = bin_gauss_solve(A, b);
        avg_error(erasure_index) = avg_error(erasure_index) ...
            + (erasure_index-sum(x==data_word(missing_index)))/erasure_index;
        cFrame = cFrame + 1;
    end
    avg_error(erasure_index) = avg_error(erasure_index)/cFrame;
end

```

Hybrid Decoding

```

function [erasure_vec, avg_error_hyb] = get_hybrid_early(fname)
addpath './lib/'

```

```

% the max word size of word in Matlab
max_word_size = 64;
alist_params = readalist_peg(fname);
H = alist2parity(alist_params);
[nr, nc] = size(H);
[newH] = H;
G_s = full((newH));
[m, n] = size(G_s);
N = n;
M = m;
data_word = [];
while length(unique(data_word))~n
    data_word = round((2^max_word_size-2)*rand(1, n)) + 1;
end
D_de_rep = repmat(data_word, m, 1).*G_s;
parity_words = zeros(m, 1);
for i=1:n
    parity_words = bitxor(D_de_rep(:, i), parity_words);
end
maxFrames = 100000;
erasure_vec = (1:nc);
avg_error_it = zeros(1, length(erasure_vec));
avg_error_hyb = avg_error_it;
[nCheck, nBit] = size(newH);
nEdge = nnz(newH);
indexLinear = find(newH);
[indexCheck, indexBit] = find(newH); % For sparse matrix, find() is fast.
% The following initialization of the check nodes takes ONE TnewHIRD of the running
time!
checkNode = struct('indexBitConnected', 0);
check = repmat(checkNode, nCheck, 1);
for iCheck = 1:nCheck
    check(iCheck).indexBitConnected = indexBit(indexCheck == iCheck); % Connections to
check nodes
end % for iCheck
nIterationMax = 80;
Hi = -1*ones(m, max(sum(H, 2)));
Hj = -1*ones(max(sum(H, 1)), n);
for i=1:m
    Hi(i, 1:sum(H(i, :))) = find(H(i, :));
end
for i=1:n
    Hj(1:sum(H(:, i)), i) = find(H(:, i));
end
Hi = int32(Hi-1);

```

```

Hj = int32(Hj-1);
for erasure_index=1:length(erasure_vec)
    cFrame = 1;
    while cFrame < maxFrames,
        y = randperm(n, erasure_vec(erasure_index));
        missing_index = false(1, n);
        missing_index(y) = true;
        % iterative decoding
        data_word_rx = data_word.*(~missing_index);
        time1 = tic;
        [messageBit, nIteration] = bpd_early(Hi(:), Hj(:), int32(data_word_rx(:)),
int32(parity_words(:)), m, n, nIterationMax, max(sum(H, 2)), max(sum(H, 1)));
        errt_index = sum(messageBit==0);
        if errt_index>0
            % if unable to decode using iterative, use Gaussian.
            mi = false(1, N);
            mi(messageBit==0) = true;
            missing_index = mi;
            D_de_rep = repmat(messageBit, M, 1).*G_s;
            % Making system of equation for unknown words.
            bprep = D_de_rep.*repmat(~missing_index, M, 1);
            % Computation of b in Ax = b form of the equation.
            b = zeros(M, 1);
            for k=1:N
                b = bitxor(bprep(:, k), b);
            end
            b = bitxor(b, parity_words);
            % Computation of A in Ax = b form of the equation.
            A = G_s(:, missing_index);
            % Using Gauss elimination to solve the system of equations.
            x = bin_gauss_solve(A, b);
            messageBit(missing_index) = x;
        end
        avg_error_hyb(erasure_index) = avg_error_hyb(erasure_index) +
sum(messageBit~=data_word)/erasure_index;
        cFrame = cFrame + 1;
    end
    avg_error_it(erasure_index) = avg_error_it(erasure_index)/cFrame;
    avg_error_hyb(erasure_index) = avg_error_hyb(erasure_index)/cFrame;
end

```

RIC Protocol

```

close all; clear all; clc;
addpath('libs');

```

```

case_no = 1;
m = 1000; % number of values
maxframes = 100; % maximum number of frames.
%n = 2*m; % number of tags
n=2000;
rate_t2r = 53e3;
rate_r2t = 26.5e3;
twait = 302e-6;
falseprob = 10^-4;
if case_no==1
    nbits = 162; % number of bits
    H = get_tags_vals(m, n, [0 1]);
else
    nbits = 184; % number of bits
    H = get_tags_vals(m, n, [0 0 1]);
end
Hmat = H;
tottime = 0;
round=0
for k=1:maxframes,
    f = m;
    H = Hmat;
    T = [];
    while f~=0
        rval = randi(1000, 1);
        % Bloom filter parameters
        b = ceil(- (m-f)*log(falseprob)/log(2)^2);
        k = ceil(log(2)*b/(m-f));
        tottime = tottime + ceil(b/96)*(twait+96/rate_r2t);
        tottime = tottime + f*(twait + nbits/rate_t2r);
        tagsloc = zeros(n, 1);
        tagsval = zeros(n, 1);
        for q=1:n,
            % for each tag, find its first value
            v_val = find(H(:, q), 1);
            % if the tag is not empty, find its slot.
            if ~isempty(v_val)
                tagsval(q) = v_val;
                tagsloc(q) = hashfunc_tags(v_val, rval, f);
            end
        end
        end
        M = bsxfun(@eq, tagsloc, (1:f));
        Q = sum(M);
        T = find(sum(M(:, Q==1), 2));
        c1 = length(T);

```

```
for q=2:max(Q),
    P = find(Q==q);
    for t=1:length(P),
        Z = find(M(:, P(t)));
        if sum(tagsval(Z) == tagsval(Z(1)))==length(Z)
            T = [T; Z];
            c1 = c1 + 1;
        end
    end
end
end
vvalvec = [];
for q=1:length(T),
    vval = find(H(:, T(q)), 1, 'first');
    vvalvec =[vvalvec; vval];
    H(vval, :) = 0;
end
round=round+1;
f = f-length(unique(vvalvec));
end

end
round=round/maxframes;
disp('average round');
disp(round);
fprintf('Average Time %6.4f seconds...\n', tottime/maxframes);
```

Appendix B-Some Constructed LDPC-Based Codes

(25, 3, 5) PEG-based	(49, 3, 7) PEG-based	(121, 3, 11) PEG-based
1 6 11 17 22	1 9 16 24 31 39 45	1 12 23 35 46 57 67 79 91 101 110 0
2 7 12 18 23	2 10 17 21 31 37 46	2 13 24 36 47 58 68 80 92 102 112 0
2 8 13 19 22	2 11 18 25 32 40 47	2 14 25 33 48 59 67 81 93 103 113 0
3 9 11 19 20	3 10 19 26 33 40 48	3 14 26 35 49 60 69 82 94 100 114 0
1 9 13 16 21	4 11 19 23 30 41 46	4 15 23 37 50 61 70 81 95 102 114 0
4 10 12 16 22	5 12 20 27 32 42 46	5 16 27 38 49 62 71 83 96 101 115 121
5 6 13 20 23	1 12 19 25 34 37 49	6 17 26 39 50 63 72 84 97 104 116 0
3 7 14 17 23	6 8 21 24 35 42 49	7 18 28 40 51 63 73 85 92 101 117 0
5 9 12 17 24	7 11 22 27 31 38 0	8 13 29 35 48 51 72 86 98 105 118 0
4 8 15 20 21	3 8 20 25 36 43 0	1 19 30 41 48 60 70 77 96 104 119 0
4 6 14 18 25	8 13 14 27 33 44 0	9 20 30 37 47 62 69 79 93 105 117 0
3 8 16 18 24	6 9 22 28 33 41 47	10 21 31 42 52 57 74 86 93 106 112 0
1 7 15 19 25	7 12 21 28 30 43 45	10 17 24 43 46 64 75 87 96 107 114 0
2 10 11 15 24	4 14 17 28 32 39 0	3 20 31 44 53 59 71 78 90 104 120 0
5 10 14 21 25	5 14 18 24 34 43 48	6 22 29 45 46 65 71 88 99 103 112 0
	4 9 20 26 35 38 0	8 19 32 42 53 58 69 83 91 107 116 0
	3 15 22 29 37 42 45	11 21 33 44 54 65 70 87 98 108 121 0
	1 15 17 30 36 44 48	8 20 25 39 45 61 73 80 89 109 121 0
	2 13 16 26 34 41 0	7 16 34 39 47 54 76 88 94 106 119 0
	5 10 16 29 35 44 47	9 16 23 42 55 65 75 85 97 109 118 120
	7 13 23 29 36 40 49	4 22 32 44 56 62 75 89 92 106 113 0
	6 15 18 23 38 39 0	11 18 26 41 55 58 76 79 90 103 115 0
		5 14 28 37 54 64 77 86 99 110 116 0
		4 18 25 36 38 64 78 84 94 108 0 0
		10 15 29 34 41 66 68 84 85 111 113 0
		3 15 27 40 55 57 72 80 99 107 0 0
		1 21 28 36 50 59 76 82 89 105 111 0
		5 22 30 43 52 63 68 82 91 98 120 0
		2 12 32 34 51 60 74 78 95 109 115 0
		9 17 33 40 52 61 77 83 88 100 111 0
		6 12 31 38 56 66 73 87 100 102 119 0
		11 13 27 43 53 66 74 81 97 110 117 0
		7 19 24 45 49 56 67 90 95 108 118 0

(169, 3, 13) PEG-based	(200, 3, 6) PEG-based
1 14 27 42 54 67 79 92 106 119 132 145 156 0	1 35 69 103 137 170 0
2 14 28 43 55 68 80 93 107 120 133 146 158 0	2 36 70 104 138 171 0
3 15 29 43 56 69 81 94 108 121 134 147 159 0	3 37 71 105 139 172 0
2 16 30 41 56 70 82 95 109 122 135 144 160 0	4 37 72 106 140 173 0
4 17 31 44 53 71 83 96 110 118 132 148 158 0	5 38 73 107 141 169 0
5 18 32 45 57 68 83 97 111 123 136 149 160 0	6 39 74 103 142 174 0
6 19 30 46 58 72 84 96 106 124 137 142 159 166	7 40 75 108 143 175 0
7 20 32 47 59 73 85 98 104 120 135 147 161 0	8 34 72 109 144 176 0
8 21 33 46 60 68 86 98 112 121 138 150 162 0	9 40 64 106 145 177 0
9 22 34 47 60 72 87 99 109 125 134 145 163 0	10 39 76 110 127 178 0
10 19 31 48 60 67 88 94 113 123 139 143 161 0	3 41 77 111 146 179 0
1 17 35 49 55 72 89 98 114 123 140 151 164 0	11 42 78 111 147 173 0
10 23 36 41 57 74 84 100 115 126 141 152 162 0	12 43 76 112 139 180 0
11 24 37 39 61 75 90 101 109 117 142 149 165 0	13 44 79 107 134 175 0
12 19 27 45 59 76 89 102 110 122 141 153 157 165	5 45 80 113 138 181 196
3 25 36 50 62 73 89 96 116 119 139 146 163 0	14 46 81 105 148 171 0
6 26 34 49 63 71 86 95 115 127 133 149 161 0	1 37 82 114 149 182 0
12 22 38 43 64 77 85 100 117 128 138 154 166 0	15 47 71 115 150 183 0
8 23 29 42 63 73 83 102 117 129 140 155 167 0	12 48 83 116 151 184 0
8 16 39 50 59 74 87 103 111 128 143 156 168 0	10 44 84 117 152 167 0
9 16 35 45 53 78 88 93 112 119 142 147 154 167	9 35 85 118 153 185 0
13 24 32 48 62 78 86 103 105 118 141 145 166 0	7 49 86 109 136 178 0
7 26 38 51 65 74 79 101 114 129 137 157 158 0	16 50 83 110 146 186 0
4 24 30 42 51 69 80 97 113 126 138 151 169 0	5 51 87 119 148 187 0
13 14 34 50 66 76 82 101 112 126 136 148 159 0	17 52 88 97 154 175 0
13 23 38 44 58 75 81 92 116 125 131 151 168 0	18 53 77 117 155 171 0
5 25 33 52 56 66 91 100 118 125 133 157 164 0	8 54 80 120 156 168 0
4 21 28 40 58 62 79 99 108 122 130 154 164 0	19 55 89 121 145 181 0
11 15 27 44 57 78 91 95 107 128 137 150 163 0	12 56 70 122 142 188 0

9 15 40 48 65 77 90 102 116 120 132 152 160 0
 1 18 37 40 63 64 91 93 113 121 135 153 168 0
 3 20 35 51 64 67 82 103 107 124 131 152 165 0
 5 22 31 39 54 76 81 104 115 129 144 146 0 0
 2 25 37 47 65 71 84 94 105 130 140 156 169 0
 10 20 28 52 54 69 90 105 110 127 136 150 167 0
 11 26 33 53 55 70 85 97 106 130 143 155 0 0
 6 18 29 52 61 70 80 99 114 131 139 148 162 0
 12 21 41 49 66 75 88 104 111 124 134 155 0 0
 7 17 36 46 61 77 87 92 108 127 144 153 169 0

20 56 75 123 155 189 0
 21 57 82 124 146 180 0
 22 41 90 118 141 190 0
 14 58 91 113 157 191 0
 17 42 87 125 152 192 0
 23 55 83 120 140 193 0
 24 47 92 102 158 174 0
 18 49 88 122 141 194 0
 25 59 82 126 159 185 0
 26 36 92 127 137 195 0
 10 60 93 113 159 188 0
 18 61 94 101 149 193 0
 27 48 95 126 144 196 0
 19 41 87 103 160 183 0
 28 62 72 121 143 197 0
 29 51 70 126 134 190 0
 24 63 88 106 161 198 0
 22 62 84 123 156 182 0
 30 64 81 128 135 176 199
 23 49 69 119 147 197 0
 15 39 96 129 162 194 0
 31 56 96 130 154 179 0
 32 65 77 131 140 199 0
 24 58 89 132 153 187 0
 9 38 78 129 157 182 0
 23 57 81 107 123 200 0
 6 53 67 116 128 198 0
 30 36 86 114 151 192 0
 16 62 97 104 153 199 0
 11 60 86 120 155 183 0
 25 61 91 115 151 189 0
 21 47 84 130 163 191 0
 31 50 79 105 156 174 0
 16 40 91 117 139 190 0
 17 66 98 121 163 170 0
 15 64 95 119 164 186 0
 2 58 98 128 149 169 0
 14 34 99 118 142 167 195
 29 46 74 115 131 177 0
 33 63 90 124 165 172 0
 20 67 85 112 152 168 0
 33 35 93 108 150 200 0
 27 52 99 110 166 177 200
 19 59 75 129 167 172 0
 21 51 94 99 143 198 0
 1 43 97 133 165 191 0
 30 52 80 111 158 185 0
 6 54 100 134 145 189 0
 33 54 95 104 163 178 0
 26 55 78 133 166 0 0
 22 46 101 112 144 170 0
 25 38 76 132 154 0 0
 7 66 74 135 138 193 0
 11 50 94 132 137 176 0
 4 60 100 130 164 166 0
 31 63 73 135 147 195 0
 32 43 100 108 148 194 0
 32 57 98 127 160 196 0
 3 66 93 116 162 187 0
 8 59 102 122 164 192 0
 29 68 85 102 160 197 0
 13 45 101 124 162 173 0
 13 65 89 114 168 0 0
 26 67 90 109 159 186 0
 4 61 68 125 165 181 0
 27 68 79 136 161 188 0
 28 53 73 136 150 0 0
 20 45 71 133 161 184 0
 28 48 92 125 157 179 0
 34 42 65 96 169 184 0
 2 44 69 131 158 180 0

(502, 3) PEG-based

1 85 170 256 339 424 0
 2 86 171 257 340 425 0
 3 87 172 258 333 390 0
 4 88 173 259 341 426 0
 5 89 174 260 342 427 0
 6 89 175 261 343 428 0
 7 90 176 262 344 429 0
 8 91 170 263 345 430 0
 9 92 177 264 346 428 0
 10 93 178 257 347 431 0
 2 88 179 265 348 432 0
 11 94 180 266 349 433 0
 12 95 181 267 350 434 0
 13 96 182 268 351 427 0
 14 93 183 269 352 434 0
 13 97 184 270 353 419 0
 15 98 185 271 354 434 0
 16 98 186 272 355 435 0
 17 99 187 273 356 365 0
 10 100 186 274 357 436 0
 18 101 184 275 358 437 0
 19 102 180 257 359 438 0
 20 103 188 276 343 439 0
 21 104 189 277 360 440 0
 19 105 190 278 361 441 0
 22 106 191 279 362 442 0
 23 107 192 280 363 443 0
 24 108 193 281 364 444 0
 25 109 194 282 365 368 0
 26 110 195 283 366 445 0
 27 111 179 284 346 446 0
 28 112 196 261 367 447 0
 29 113 197 285 368 448 0
 30 114 198 258 369 433 0
 31 115 199 286 370 433 0
 32 116 200 287 371 414 0
 29 111 201 263 372 449 0
 33 100 202 288 358 450 0
 33 117 203 289 373 451 0
 28 118 198 290 352 452 0
 34 119 195 291 360 438 0
 33 84 168 292 339 443 0
 35 120 195 270 374 453 0
 36 121 204 266 375 454 0
 37 96 205 293 355 455 0
 38 122 206 294 376 456 0
 39 123 207 295 377 452 0
 40 103 208 294 374 429 0
 21 124 209 285 369 427 0
 41 92 210 296 345 457 0
 12 97 211 297 378 458 0
 42 95 212 298 379 446 0
 43 94 213 299 380 459 0
 20 125 214 281 381 460 0
 18 126 174 300 347 461 0
 22 127 215 275 366 462 0
 44 98 216 301 381 420 0
 43 95 207 291 363 463 0
 45 128 217 252 382 463 0
 21 129 218 298 383 464 0
 46 130 171 302 377 465 0
 47 127 170 303 384 455 0
 39 131 206 304 385 431 0
 48 132 219 273 378 442 0
 32 91 220 283 340 466 0
 47 133 221 305 350 460 0
 42 103 202 306 386 424 0
 49 118 211 307 364 467 0
 50 134 181 308 344 468 0
 1 102 169 309 336 450 0
 16 135 191 282 370 469 0
 51 136 199 310 387 470 0
 52 137 222 271 359 448 0
 22 114 223 311 388 471 0
 53 138 224 303 389 472 0

(502, 3) ACE-based

6 29 93 158 195 247 271 417 420 0 0 0 0
 96 152 177 220 248 384 0 0 0 0 0 0 0
 44 62 77 169 241 295 482 492 0 0 0 0 0
 271 326 492 0 0 0 0 0 0 0 0 0
 17 188 407 0 0 0 0 0 0 0 0 0
 227 439 481 0 0 0 0 0 0 0 0 0
 7 12 92 93 98 315 327 0 0 0 0 0 0
 308 326 454 0 0 0 0 0 0 0 0 0
 58 65 118 202 276 496 0 0 0 0 0 0
 85 110 153 194 236 267 372 414 477 0 0 0 0
 21 50 109 123 159 163 227 384 403 496 0 0 0
 67 232 284 411 467 0 0 0 0 0 0 0
 86 216 217 255 336 344 0 0 0 0 0 0 0
 11 20 90 130 256 337 368 0 0 0 0 0 0
 248 0 0 0 0 0 0 0 0 0 0 0
 9 91 138 193 342 426 0 0 0 0 0 0 0
 38 75 101 138 249 433 0 0 0 0 0 0 0
 11 403 421 0 0 0 0 0 0 0 0 0
 29 198 208 230 252 335 494 499 0 0 0 0 0
 51 357 385 404 407 416 0 0 0 0 0 0 0
 26 79 99 187 235 243 455 0 0 0 0 0 0
 39 185 188 358 362 366 367 401 409 0 0 0 0
 18 80 95 143 175 192 333 372 410 465 0 0 0
 22 74 217 223 337 343 353 0 0 0 0 0 0
 175 306 452 0 0 0 0 0 0 0 0 0
 138 186 195 0 0 0 0 0 0 0 0 0
 277 331 373 416 429 462 0 0 0 0 0 0
 211 282 366 374 441 0 0 0 0 0 0 0
 55 203 344 0 0 0 0 0 0 0 0 0
 59 76 112 226 435 0 0 0 0 0 0 0
 35 107 314 0 0 0 0 0 0 0 0 0
 103 408 423 430 0 0 0 0 0 0 0 0
 79 147 291 320 368 442 465 0 0 0 0 0 0
 21 30 102 150 203 284 293 320 420 429 0 0 0
 24 28 121 221 427 0 0 0 0 0 0 0 0
 9 156 457 0 0 0 0 0 0 0 0 0
 74 108 256 286 299 415 458 0 0 0 0 0 0
 253 292 387 464 0 0 0 0 0 0 0 0
 56 201 206 239 270 485 0 0 0 0 0 0 0
 243 346 390 0 0 0 0 0 0 0 0 0
 78 117 174 312 374 0 0 0 0 0 0 0
 334 432 0 0 0 0 0 0 0 0 0 0
 71 127 128 310 371 400 436 463 466 0 0 0 0
 242 328 0 0 0 0 0 0 0 0 0 0
 67 73 116 150 0 0 0 0 0 0 0 0
 242 294 300 341 363 410 0 0 0 0 0 0 0
 27 168 214 243 279 316 322 326 0 0 0 0 0
 199 219 265 340 428 447 473 0 0 0 0 0 0
 3 41 163 284 0 0 0 0 0 0 0 0
 107 255 375 498 0 0 0 0 0 0 0 0
 3 51 72 152 185 297 324 391 393 404 419 455 0
 291 355 414 0 0 0 0 0 0 0 0 0
 94 104 219 237 277 346 430 466 0 0 0 0 0
 3 45 113 189 272 371 0 0 0 0 0 0 0
 36 92 145 176 272 283 311 406 0 0 0 0 0
 38 406 0 0 0 0 0 0 0 0 0 0 0
 125 375 440 485 0 0 0 0 0 0 0 0
 65 109 139 155 335 363 0 0 0 0 0 0 0
 8 11 166 0 0 0 0 0 0 0 0 0
 42 83 122 149 167 440 474 475 0 0 0 0 0
 120 126 131 154 307 356 0 0 0 0 0 0 0
 38 57 244 413 0 0 0 0 0 0 0 0
 47 63 96 258 263 276 334 381 0 0 0 0 0
 41 44 64 88 306 411 0 0 0 0 0 0 0
 34 322 357 377 394 427 488 0 0 0 0 0 0
 121 245 304 352 422 0 0 0 0 0 0 0
 177 182 379 438 0 0 0 0 0 0 0 0
 186 402 490 0 0 0 0 0 0 0 0 0
 18 45 112 255 266 0 0 0 0 0 0 0 0
 23 84 90 154 237 302 397 436 462 0 0 0 0
 4 14 169 261 314 0 0 0 0 0 0 0 0
 7 42 98 338 438 0 0 0 0 0 0 0 0
 100 104 316 364 434 0 0 0 0 0 0 0 0
 50 134 262 292 296 386 0 0 0 0 0 0 0
 53 172 253 278 316 325 349 447 0 0 0 0 0

54 99 204 305 390 473 0	105 156 185 288 460 496 0 0 0 0 0 0 0
55 111 208 312 370 474 0	82 267 381 437 0 0 0 0 0 0 0 0 0
56 121 199 313 361 445 0	160 182 484 0 0 0 0 0 0 0 0 0 0
57 139 220 314 391 470 0	97 246 308 495 0 0 0 0 0 0 0 0 0
40 140 225 310 377 475 0	85 136 240 283 337 352 491 0 0 0 0 0 0
58 141 197 299 353 476 0	2 33 63 147 297 300 384 0 0 0 0 0 0
59 142 201 295 392 461 0	94 151 223 313 324 328 382 501 0 0 0 0 0
60 143 226 312 340 477 0	47 108 127 144 197 239 246 354 412 438 450 0 0
61 139 188 286 383 478 0	197 251 268 451 495 0 0 0 0 0 0 0 0
47 124 202 315 348 461 0	19 30 87 263 309 427 454 0 0 0 0 0 0
3 144 205 243 367 456 0	132 229 303 317 0 0 0 0 0 0 0 0 0
62 145 227 290 393 479 0	26 83 128 329 431 436 0 0 0 0 0 0 0
6 100 228 302 394 418 0	79 81 137 140 159 180 224 381 0 0 0 0 0
63 146 182 251 359 480 0	39 118 157 164 206 254 387 391 395 421 0 0 0
56 143 229 295 355 447 0	170 193 278 290 420 483 0 0 0 0 0 0 0
64 105 187 267 351 481 0	35 87 105 158 214 370 397 458 0 0 0 0 0
32 147 191 316 395 482 0	218 339 354 0 0 0 0 0 0 0 0 0 0
51 148 215 317 386 476 0	41 87 222 269 323 425 0 0 0 0 0 0 0
25 122 230 269 348 483 0	152 177 231 383 388 487 0 0 0 0 0 0 0
62 124 187 316 394 425 0	22 109 133 307 330 485 0 0 0 0 0 0 0
65 136 224 277 356 460 0	108 165 221 227 237 239 453 0 0 0 0 0 0
38 149 177 317 373 484 0	122 135 301 351 367 479 0 0 0 0 0 0 0
41 134 200 292 396 485 0	184 229 240 247 442 451 472 0 0 0 0 0 0
8 150 196 300 397 486 0	62 306 368 412 474 498 502 0 0 0 0 0 0
66 151 225 318 381 449 0	76 143 0 0 0 0 0 0 0 0 0 0 0
24 152 176 319 362 455 0	32 37 191 195 324 394 0 0 0 0 0 0 0
67 153 227 298 398 458 0	260 434 467 0 0 0 0 0 0 0 0 0
19 107 231 317 399 487 0	165 389 418 0 0 0 0 0 0 0 0 0
25 153 200 274 397 488 0	10 24 73 0 0 0 0 0 0 0 0 0
68 121 218 311 400 489 0	213 226 286 470 0 0 0 0 0 0 0 0
23 154 205 283 380 449 0	189 319 422 0 0 0 0 0 0 0 0 0
69 131 203 267 401 435 0	8 56 184 200 212 238 301 315 385 500 0 0 0
70 117 232 284 402 478 0	206 457 469 470 0 0 0 0 0 0 0 0
50 128 215 261 403 490 0	67 126 340 355 370 444 445 459 0 0 0 0 0
71 155 207 289 404 491 0	27 202 205 236 241 257 312 380 493 0 0 0 0
9 155 197 272 405 464 0	331 386 0 0 0 0 0 0 0 0 0 0 0
53 156 233 320 371 492 0	97 157 190 364 425 0 0 0 0 0 0 0
34 131 234 315 332 436 0	81 132 145 155 171 248 280 287 366 380 447 491 0
42 86 167 321 406 490 0	47 91 153 214 223 257 272 285 329 446 489 0 0
23 150 189 308 364 491 0	225 0 0 0 0 0 0 0 0 0 0 0 0
72 157 235 277 339 474 0	90 154 191 211 373 377 0 0 0 0 0 0 0
58 119 230 301 394 490 0	57 59 111 142 170 276 298 0 0 0 0 0 0
73 132 236 319 407 489 0	273 281 295 350 490 497 0 0 0 0 0 0 0
8 115 237 322 408 441 0	78 141 181 197 254 499 0 0 0 0 0 0 0
59 158 235 323 382 476 0	35 69 100 140 148 163 236 267 361 0 0 0 0
74 122 217 297 409 454 0	33 52 187 228 249 274 377 459 0 0 0 0 0
75 159 210 306 385 493 0	19 142 183 240 261 396 405 0 0 0 0 0 0
69 146 227 264 374 470 0	23 303 319 463 502 0 0 0 0 0 0 0 0
76 90 234 318 400 480 0	235 317 476 0 0 0 0 0 0 0 0 0
36 101 238 263 404 475 0	66 106 200 204 245 254 310 321 409 0 0 0 0
52 104 223 244 372 465 0	32 36 74 153 187 204 285 325 433 448 453 456 0
72 135 225 299 337 438 0	114 218 275 0 0 0 0 0 0 0 0 0 0
46 160 209 313 410 428 0	15 59 207 477 0 0 0 0 0 0 0 0 0
27 112 186 266 411 467 0	53 133 176 228 300 356 482 491 0 0 0 0 0
62 144 213 314 412 487 0	13 224 302 330 398 424 0 0 0 0 0 0 0
57 108 239 253 413 429 0	34 36 101 141 286 317 344 401 408 488 0 0 0
36 154 173 282 386 478 0	77 94 103 173 264 308 318 393 0 0 0 0 0
44 99 232 309 405 452 0	58 72 84 91 354 378 500 0 0 0 0 0 0
63 88 240 324 387 494 0	380 417 423 451 0 0 0 0 0 0 0 0
58 127 241 325 361 495 0	37 75 232 303 0 0 0 0 0 0 0 0 0
38 129 193 326 349 423 0	66 72 113 151 229 315 442 445 0 0 0 0 0
77 151 242 297 342 474 0	147 160 323 352 386 0 0 0 0 0 0 0 0
45 160 216 321 393 495 0	5 127 321 327 0 0 0 0 0 0 0 0 0
77 101 190 304 414 432 0	1 12 234 273 371 418 0 0 0 0 0 0 0
70 144 194 322 385 477 0	17 30 269 305 418 0 0 0 0 0 0 0 0
78 161 182 325 406 488 0	43 149 207 234 290 422 456 472 0 0 0 0 0
16 97 234 296 415 432 0	46 201 274 439 480 0 0 0 0 0 0 0 0
79 107 233 260 405 467 0	173 359 452 0 0 0 0 0 0 0 0 0
7 126 243 325 349 471 0	60 151 159 219 281 347 388 389 392 0 0 0 0
4 158 244 327 351 483 0	1 111 129 169 305 323 428 474 0 0 0 0 0
71 126 221 250 387 459 0	25 362 443 450 453 0 0 0 0 0 0 0 0
44 162 240 255 379 481 0	244 360 405 471 493 0 0 0 0 0 0 0 0
30 163 203 328 343 479 0	13 31 110 210 238 250 334 0 0 0 0 0 0
15 142 236 326 396 496 0	4 21 119 132 412 0 0 0 0 0 0 0 0
80 137 166 318 369 483 0	136 402 445 487 0 0 0 0 0 0 0 0
74 161 196 329 410 453 0	7 173 230 233 301 0 0 0 0 0 0 0 0
57 163 173 330 406 416 0	148 198 232 353 361 378 0 0 0 0 0 0 0
68 164 172 331 358 497 0	69 157 279 332 435 0 0 0 0 0 0 0 0

29 162 245 287 367 373 0	68 216 279 398 437 0 0 0 0 0 0 0
80 148 246 312 389 457 0	46 99 351 0 0 0 0 0 0 0 0 0
60 120 209 320 416 494 0	96 265 382 390 452 469 479 0 0 0 0 0
26 164 231 265 401 475 0	299 345 376 414 443 0 0 0 0 0 0 0
54 138 212 272 410 431 0	230 234 0 0 0 0 0 0 0 0 0 0
14 152 210 280 337 437 0	49 92 199 359 428 478 483 0 0 0 0 0
65 142 242 262 379 462 0	61 125 415 439 0 0 0 0 0 0 0 0
30 136 247 319 417 466 0	77 81 130 231 258 307 361 483 0 0 0 0 0
49 149 248 271 418 462 0	53 126 130 166 299 484 0 0 0 0 0 0
45 93 172 286 384 498 0	89 167 298 331 360 425 0 0 0 0 0 0
78 147 248 322 338 499 0	17 64 313 0 0 0 0 0 0 0 0 0 0
41 163 216 268 366 500 0	110 115 358 473 0 0 0 0 0 0 0 0
81 130 193 260 345 472 0	205 260 345 385 395 0 0 0 0 0 0 0
39 87 241 255 411 482 0	76 93 123 175 196 280 383 0 0 0 0 0
35 85 185 316 342 451 0	5 139 205 252 398 0 0 0 0 0 0 0
65 116 178 276 409 451 0	28 46 56 133 180 365 441 490 0 0 0 0 0
48 102 249 275 391 486 0	31 64 150 203 325 0 0 0 0 0 0 0
49 140 174 332 365 439 0	26 52 57 63 66 120 146 172 289 365 432 0 0
59 109 233 258 419 435 0	40 139 253 322 335 348 359 0 0 0 0 0 0
4 165 214 274 363 472 0	75 221 268 305 423 435 473 0 0 0 0 0 0
50 120 250 309 372 423 0	62 102 112 348 502 0 0 0 0 0 0 0
61 156 251 300 415 450 0	40 68 102 161 393 466 478 480 0 0 0 0 0
43 161 223 273 371 444 0	116 179 309 426 494 0 0 0 0 0 0 0
79 166 181 324 415 445 456	13 161 218 247 424 475 0 0 0 0 0 0 0
71 116 246 256 420 501 0	60 225 318 429 0 0 0 0 0 0 0 0
5 159 230 279 383 487 0	6 16 32 82 176 207 241 370 399 401 0 0 0
82 148 176 333 421 479 0	9 71 86 89 98 192 264 265 298 0 0 0 0
15 145 171 331 368 502 0	2 107 134 156 215 263 415 419 0 0 0 0 0
10 166 239 279 404 496 0	104 124 168 181 250 289 333 343 449 0 0 0 0
82 123 189 265 353 473 0	113 141 202 251 383 497 0 0 0 0 0 0 0
9 86 237 281 375 440 0	128 190 338 339 494 0 0 0 0 0 0 0 0
55 87 222 259 403 430 0	172 332 469 480 0 0 0 0 0 0 0 0
48 155 198 294 338 494 0	116 259 262 349 374 0 0 0 0 0 0 0 0
64 119 178 284 400 500 0	61 271 318 351 426 448 454 0 0 0 0 0 0
17 90 220 289 419 447 0	52 135 367 409 430 437 0 0 0 0 0 0 0
14 133 244 328 411 463 0	215 224 413 471 0 0 0 0 0 0 0 0 0
52 167 194 303 420 426 0	174 259 288 347 391 424 459 0 0 0 0 0 0
61 123 185 334 422 477 0	70 101 275 294 0 0 0 0 0 0 0 0 0
73 125 184 330 402 464 0	124 209 304 358 0 0 0 0 0 0 0 0 0
83 113 175 304 422 481 0	10 129 208 282 297 304 311 0 0 0 0 0 0 0
78 113 239 296 310 473 0	24 43 178 275 465 0 0 0 0 0 0 0 0
5 94 240 331 389 486 0	136 244 468 0 0 0 0 0 0 0 0 0 0
3 92 242 327 399 488 0	125 282 295 343 417 431 0 0 0 0 0 0 0
1 108 252 293 421 499 0	1 114 131 166 309 484 486 501 0 0 0 0 0
67 114 238 301 344 502 0	193 312 355 362 403 0 0 0 0 0 0 0 0
35 165 245 321 388 497 0	16 103 233 288 0 0 0 0 0 0 0 0 0
46 118 251 262 395 459 493	146 174 190 210 268 340 410 461 0 0 0 0 0
60 140 183 288 399 493 0	48 131 283 320 341 394 446 501 0 0 0 0 0
18 104 252 264 407 469 0	119 162 194 285 476 0 0 0 0 0 0 0 0
20 164 248 254 392 458 0	114 149 209 468 0 0 0 0 0 0 0 0 0
55 153 169 329 375 437 0	65 171 196 302 460 0 0 0 0 0 0 0 0
80 96 237 291 391 426 0	25 43 170 338 461 0 0 0 0 0 0 0 0
11 160 208 334 414 443 0	48 250 260 266 348 0 0 0 0 0 0 0 0
76 141 226 292 390 484 0	27 49 80 106 188 209 217 273 280 350 489 0 0
75 137 204 287 382 500 0	78 257 356 363 450 476 497 0 0 0 0 0 0
74 139 221 278 346 492 0	61 118 140 178 404 448 0 0 0 0 0 0 0
2 157 243 328 378 501 0	50 54 180 208 242 287 330 360 464 0 0 0 0
28 110 235 334 402 468 0	158 270 408 413 0 0 0 0 0 0 0 0 0
82 151 228 323 408 444 0	84 124 162 179 213 472 498 0 0 0 0 0 0
64 149 229 329 413 482 0	8 51 73 353 372 478 0 0 0 0 0 0 0 0
84 132 222 276 393 499 0	31 34 89 115 264 277 321 329 0 0 0 0 0 0
37 130 247 315 403 485 0	10 37 189 222 225 296 336 395 421 431 444 0 0
27 159 249 254 417 440 0	164 481 0 0 0 0 0 0 0 0 0 0 0 0
11 106 228 293 350 448 0	60 69 70 161 213 216 293 357 365 369 376 440 495
66 134 219 335 347 454 0	16 28 71 142 228 294 296 350 387 392 499 0 0
79 145 241 330 397 501 0	23 48 178 181 198 341 449 463 471 479 0 0 0
54 146 183 308 392 424 0	20 55 105 129 183 212 269 461 477 0 0 0 0
81 147 212 335 416 489 0	33 106 259 379 389 493 0 0 0 0 0 0 0
6 109 218 256 380 485 0	54 95 134 392 0 0 0 0 0 0 0 0 0
84 156 238 327 423 425 0	12 165 328 342 488 0 0 0 0 0 0 0 0
26 138 175 307 412 502 0	39 42 55 160 186 245 290 468 0 0 0 0 0
53 106 177 259 352 497 0	100 274 399 433 470 0 0 0 0 0 0 0 0
40 150 232 311 357 495 0	6 123 0 0 0 0 0 0 0 0 0 0 0 0
77 112 226 336 360 362 0	45 162 192 204 400 444 467 0 0 0 0 0 0
81 117 190 333 354 436 0	82 235 251 379 0 0 0 0 0 0 0 0 0
12 152 201 314 357 453 0	15 220 378 402 449 0 0 0 0 0 0 0 0
83 154 249 326 401 439 0	14 29 80 85 171 246 342 0 0 0 0 0 0
31 89 236 305 341 0 0	49 215 411 419 462 0 0 0 0 0 0 0

56 168 217 332 398 442 0	191 249 281 311 327 0 0 0 0 0 0 0
13 169 224 306 354 471 0	95 117 146 179 256 405 464 0 0 0 0 0
66 115 231 290 413 466 0	2 144 196 212 278 291 434 458 482 0 0 0 0
70 165 211 246 417 484 0	5 88 155 347 406 481 0 0 0 0 0 0
34 167 253 323 395 498 0	115 168 201 210 287 319 369 390 400 443 0 0 0
17 128 179 337 408 465 0	314 345 407 456 0 0 0 0 0 0 0 0
69 91 214 313 418 468 0	22 25 120 135 137 145 0 0 0 0 0 0 0
75 85 247 278 398 496 0	15 44 83 99 122 143 183 220 310 346 364 396 460
68 135 250 268 376 422 0	58 261 388 399 475 0 0 0 0 0 0 0
76 158 180 307 407 430 0	20 137 184 270 373 375 397 432 0 0 0 0 0
51 125 213 269 336 480 0	86 117 121 199 349 486 487 0 0 0 0 0 0
63 129 219 280 412 469 0	70 455 0 0 0 0 0 0 0 0 0 0 0
67 143 192 253 356 376 0	182 194 258 293 376 457 500 0 0 0 0 0 0
31 157 206 320 421 491 0	18 68 144 148 222 313 446 0 0 0 0 0
7 168 254 285 341 492 0	19 238 252 266 336 441 0 0 0 0 0 0
37 141 188 324 388 446 0	40 97 164 167 231 339 369 382 489 0 0 0 0
73 162 192 302 384 441 0	262 289 332 416 486 0 0 0 0 0 0 0
72 105 245 338 396 0 0	14 54 88 119 200 333 396 0 0 0 0 0 0
24 110 255 288 409 457 0	226 233 492 0 0 0 0 0 0 0 0 0
83 133 229 270 335 498 0	4 111 211 292 0 0 0 0 0 0 0 0

(512, 3, 6) PEG-based	(512, 3, 19) PEG-based
1 87 173 260 345 432 0	1 29 57 86 112 141 168 195 221 248 275 302 330 357 384 411 439 466 494
2 88 174 261 346 433 0	2 30 58 87 113 142 170 196 222 249 276 303 331 358 385 412 440 467 495
3 89 175 262 347 434 0	3 29 59 88 114 143 170 187 223 250 277 304 332 359 386 413 441 468 496
4 89 176 263 348 435 0	4 28 59 89 115 144 171 197 224 251 278 305 333 360 387 414 442 469 494
5 90 177 264 349 436 0	2 31 60 90 114 145 172 198 225 252 279 306 334 361 388 411 443 470 497
6 91 178 265 350 437 0	5 32 58 91 116 146 173 199 226 248 280 307 335 362 389 415 444 471 498
7 92 179 266 351 438 0	6 33 61 92 117 147 169 200 227 253 281 308 336 363 389 416 445 472 499
8 87 180 267 352 439 0	7 33 62 81 115 136 174 201 222 252 282 309 337 362 390 417 446 473 500
9 93 181 268 353 440 0	8 33 63 93 118 148 175 178 228 254 274 310 330 360 385 418 447 474 501
10 94 182 269 354 441 0	9 34 63 94 119 149 176 202 229 255 283 311 333 364 391 419 448 475 502
2 95 183 270 355 442 0	10 35 64 95 120 150 177 203 224 253 284 312 331 365 392 420 449 476 503
11 92 184 265 356 443 0	11 36 65 91 121 151 171 203 230 256 285 309 338 366 393 421 450 477 504
12 96 185 268 357 444 0	12 37 64 91 108 152 178 204 231 252 286 313 339 359 394 422 439 478 505
13 97 186 271 358 445 0	10 38 62 96 119 146 179 196 232 257 281 304 329 367 395 423 451 479 501
14 97 187 272 359 446 0	13 32 66 94 114 153 180 205 233 258 287 314 340 368 396 424 452 469 499
13 98 188 273 360 447 0	13 39 62 97 122 151 170 199 229 259 288 315 341 369 397 425 438 480 506
15 99 189 274 344 435 0	14 40 67 98 123 154 181 206 234 260 287 316 342 370 392 426 445 474 495
16 100 190 259 361 445 0	15 41 64 94 124 147 156 206 222 261 289 302 328 371 398 427 450 470 507
17 101 191 275 350 400 0	16 39 68 99 120 144 182 207 235 262 290 317 343 372 394 417 443 466 508
10 102 192 276 361 432 0	17 42 66 100 125 154 177 208 227 263 291 306 332 373 399 428 446 480 509
18 103 182 277 362 448 0	18 43 69 101 126 149 171 209 236 261 282 310 344 374 400 429 453 481 495
19 104 193 278 363 449 0	12 44 67 90 127 155 183 210 237 262 275 318 332 374 385 419 454 482 510
20 105 194 279 364 450 0	19 45 70 97 128 156 184 211 221 260 292 319 345 359 388 424 455 483 511
21 106 195 280 365 451 0	1 32 71 102 115 157 185 212 238 264 293 320 343 373 386 418 455 479 504
19 107 173 281 366 452 0	19 46 57 98 126 142 182 205 237 265 294 315 334 375 398 423 456 484 498
22 108 196 282 367 453 0	20 47 58 99 117 158 186 198 233 251 295 321 346 369 393 429 454 485 512
23 109 189 280 368 454 0	21 48 66 103 112 159 176 196 235 259 289 305 347 363 383 413 449 482 512
24 110 183 283 369 389 0	18 38 67 99 124 160 187 200 239 249 283 322 348 368 401 411 444 486 0
25 111 197 284 370 455 0	22 40 72 87 129 161 187 208 232 266 295 317 349 376 396 430 457 473 502
26 112 172 285 353 456 0	3 49 73 104 130 156 163 213 230 253 286 316 350 357 402 429 458 487 506
27 113 198 286 371 457 0	16 50 74 105 128 153 155 214 231 257 293 321 336 377 401 431 442 488 493
28 114 184 287 372 450 0	6 46 74 103 110 150 167 197 226 264 279 310 341 367 403 432 459 475 496
29 115 186 288 373 458 0	23 42 75 87 131 162 188 211 240 267 289 313 343 378 395 433 456 488 510
30 116 199 285 371 459 0	20 34 74 82 129 163 189 201 234 265 284 301 351 379 404 427 441 466 492
31 117 200 289 374 454 0	8 48 76 105 124 162 183 199 236 268 277 323 327 372 405 434 446 489 0
32 118 201 290 375 460 0	21 36 72 81 132 145 179 206 241 265 277 318 352 377 406 433 458 490 508
29 111 202 291 376 461 0	21 43 73 106 116 164 184 210 218 250 278 308 337 373 404 435 452 486 497
33 119 197 292 377 462 0	24 51 55 86 123 139 173 203 242 269 282 324 350 367 398 418 448 478 511
33 120 203 293 378 463 0	9 36 57 84 130 165 183 186 243 266 279 320 353 358 407 435 460 491 505
28 100 204 294 379 437 0	8 52 69 88 120 161 190 201 238 267 296 308 335 380 408 436 454 487 0
34 121 205 295 380 448 0	22 47 77 104 112 138 191 209 225 264 297 324 354 381 405 419 461 492 0
33 122 196 296 381 464 0	19 38 78 102 121 133 161 214 243 254 291 313 355 371 389 434 462 468 508
35 95 206 297 367 434 0	22 41 59 107 122 166 173 215 234 254 298 320 356 368 403 422 451 476 512
36 123 190 298 382 464 0	25 51 68 84 129 164 180 204 244 270 276 323 352 361 399 432 463 483 494
37 124 183 286 383 465 0	26 30 79 93 133 150 180 212 240 269 295 307 353 363 388 419 464 492 0
38 96 177 279 384 466 0	27 49 63 100 127 158 181 194 224 256 293 319 334 376 403 425 463 481 507
39 125 193 299 385 467 0	7 29 56 108 134 164 192 197 202 256 298 325 349 377 409 426 462 472 510
40 126 207 300 376 468 0	16 43 60 86 133 147 193 216 220 271 284 325 345 362 395 437 459 480 0
21 94 176 301 372 469 0	4 44 80 96 131 159 192 217 243 272 288 323 344 375 410 417 441 477 0

41 92 208 302 374 470 0
 42 127 209 303 386 471 0
 12 103 210 299 359 472 0
 43 94 211 304 387 473 0
 20 128 212 305 388 474 0
 18 129 213 302 389 475 0
 44 130 214 306 364 408 508
 22 131 215 307 390 473 0
 43 98 216 299 391 476 0
 45 95 217 305 392 477 0
 46 132 218 308 393 446 0
 21 133 219 309 364 478 0
 47 118 188 252 356 435 0
 39 102 220 310 365 479 0
 48 134 221 311 394 480 0
 32 91 217 274 349 481 0
 47 133 222 312 395 474 0
 42 135 223 300 357 482 0
 49 102 198 313 396 483 0
 50 136 224 309 366 484 0
 51 137 225 314 367 485 0
 1 138 226 271 387 486 0
 16 134 227 306 375 428 0
 52 110 228 288 397 481 488
 53 114 229 264 385 487 0
 22 130 193 208 324 488 0
 54 129 203 315 398 489 0
 55 139 219 282 300 490 0
 56 140 213 301 345 472 0
 57 125 212 289 343 491 0
 58 99 229 316 399 492 0
 40 120 230 317 400 471 0
 59 141 231 281 347 457 0
 60 133 232 262 355 445 0
 61 132 233 310 379 493 0
 62 142 181 318 389 438 0
 47 143 215 292 383 431 0
 63 99 221 319 369 476 0
 3 144 221 294 388 494 0
 56 145 192 320 401 449 0
 6 146 196 285 402 495 0
 64 104 194 273 403 491 0
 51 147 234 263 404 496 0
 32 148 204 272 405 461 0
 62 149 235 280 406 480 0
 25 150 190 286 407 497 0
 65 151 171 321 408 486 489
 66 145 175 322 360 430 484
 41 141 205 323 358 498 0
 38 106 236 324 386 499 0
 67 152 237 291 409 430 0
 8 153 235 291 378 449 0
 24 136 218 325 410 439 0
 68 128 238 317 410 415 0
 25 154 180 282 411 436 0
 19 155 204 297 348 500 0
 69 121 200 319 412 501 0
 70 156 239 326 398 499 0
 23 132 175 261 362 483 0
 71 147 179 327 368 436 0
 50 126 220 298 413 502 0
 72 142 240 297 371 447 0
 53 157 215 305 376 459 0
 9 157 241 328 414 453 0
 73 158 242 269 414 466 0
 34 86 211 258 415 479 0
 42 117 176 329 378 503 0
 23 159 243 271 416 453 0
 58 155 219 330 350 475 0
 74 135 201 233 403 464 0
 75 155 202 276 353 504 0
 8 124 243 265 417 489 0
 59 159 238 301 396 505 0
 69 131 233 331 370 506 0
 76 152 230 287 384 440 486
 72 103 222 332 418 452 0
 52 90 188 333 381 468 0
 36 101 226 331 397 431 0

15 30 81 88 135 155 172 191 239 255 294 326 344 360 404 437 449 489 505
 24 49 78 103 135 166 192 208 225 270 299 312 346 364 394 421 464 491 499
 23 53 61 109 121 143 177 218 238 249 287 319 349 364 410 414 439 482 500
 14 39 79 109 132 157 163 219 232 236 297 311 335 382 401 416 459 484 0
 23 41 68 110 127 141 179 209 230 272 292 303 340 379 386 434 442 484 0
 25 35 76 100 113 165 174 215 245 267 297 326 333 366 406 424 443 479 493
 25 47 70 96 132 148 167 193 231 250 300 303 347 378 390 426 438 470 0
 4 45 82 93 116 154 193 205 242 273 299 311 352 383 384 436 461 485 506
 15 46 80 109 125 140 175 216 246 251 298 317 340 361 405 413 445 465 503
 5 53 69 111 122 159 181 214 242 263 292 304 338 381 387 412 457 492 497
 14 52 54 110 136 152 184 217 235 273 283 306 330 356 393 423 458 467 0
 9 53 77 83 113 144 152 219 247 248 300 327 348 374 408 420 447 488 0
 10 54 73 85 137 153 174 195 246 263 285 315 347 376 391 432 460 485 0
 17 37 70 89 92 141 160 213 229 258 301 309 355 382 408 430 451 474 503
 3 50 83 98 118 146 191 220 221 258 290 328 331 366 397 428 457 481 0
 1 35 82 90 111 140 190 218 247 270 280 322 342 378 409 416 448 473 496
 5 28 78 95 125 148 168 202 244 257 285 326 339 369 402 430 456 486 0
 28 48 79 108 117 137 172 211 228 272 296 312 350 356 407 412 463 471 0
 18 42 56 107 130 167 194 204 241 268 288 307 351 380 384 437 465 493 504
 2 54 84 89 118 166 188 216 223 255 296 318 348 357 400 425 452 477 511
 27 40 71 101 137 165 169 207 233 269 299 322 337 382 387 433 450 487 0
 11 55 75 111 136 158 178 212 223 271 281 316 341 372 406 415 465 491 509
 20 56 85 102 123 145 175 217 227 259 294 327 354 365 402 422 440 471 502
 11 31 76 92 119 135 157 194 247 261 290 324 345 383 399 431 462 476 500
 6 51 71 104 131 151 176 198 246 271 280 302 339 365 400 436 464 489 0
 26 44 61 85 138 149 186 207 244 273 291 305 351 370 397 431 455 478 0
 27 45 60 95 134 138 162 210 219 274 301 321 342 375 396 438 444 467 0
 12 34 75 97 106 168 182 200 226 245 274 325 355 380 407 428 461 469 0
 13 55 80 83 134 160 189 190 228 241 275 329 336 381 390 435 453 468 0
 17 52 65 106 139 142 185 195 239 266 300 328 354 370 409 414 453 475 501
 26 50 65 107 140 169 189 213 237 260 276 314 346 371 410 420 460 490 0
 7 31 77 101 128 139 188 220 245 268 286 329 353 379 391 421 440 490 498
 24 37 72 105 126 143 185 215 240 262 278 314 338 358 392 427 447 483 509

77 149 244 264 402 507 0
 63 156 206 284 354 433 0
 46 111 234 295 419 508 0
 27 151 217 334 401 462 0
 57 139 241 277 420 429 0
 62 108 245 269 421 446 0
 44 98 246 316 379 509 0
 36 149 212 313 418 508 0
 58 88 247 293 419 497 0
 77 119 201 326 352 457 0
 38 151 202 277 422 469 0
 78 160 227 263 423 447 0
 45 115 244 302 407 471 0
 70 100 248 335 374 442 0
 79 161 230 309 390 510 0
 80 154 249 325 375 485 0
 71 107 211 318 417 477 0
 16 143 250 336 424 469 0
 81 121 178 303 385 433 0
 7 162 240 247 421 444 0
 4 163 248 332 425 504 0
 44 159 185 326 392 511 0
 80 97 242 329 395 459 0
 30 164 180 261 408 465 0
 15 165 182 337 411 509 0
 68 166 192 316 418 470 0
 74 125 251 270 400 512 0
 57 147 199 336 369 463 493
 29 142 200 256 347 482 0
 78 122 191 283 358 487 0
 60 167 197 338 405 476 0
 54 123 252 308 373 451 0
 26 166 245 339 403 0 0
 65 127 253 337 382 429 0
 14 140 235 319 426 460 0
 49 146 223 318 409 492 0
 30 136 254 294 423 467 0
 45 168 195 295 381 460 0
 82 168 184 276 427 480 0
 83 169 222 323 397 502 0
 41 93 254 274 383 506 0
 65 131 255 330 360 512 0
 59 101 206 325 422 0 0
 35 86 194 267 427 492 0
 39 154 247 323 392 507 0
 48 119 220 279 348 495 0
 49 169 234 311 391 0 0
 50 168 250 315 359 505 0
 4 108 224 257 405 474 0
 61 162 207 278 355 451 0
 79 115 227 339 343 0 0
 43 120 218 259 349 458 0
 71 166 252 284 384 478 0
 82 128 228 335 377 0 0
 84 150 251 281 351 463 0
 5 161 240 321 388 505 0
 73 123 208 262 352 472 0
 10 161 243 340 412 495 0
 15 138 251 306 342 501 0
 9 87 195 275 428 442 0
 55 124 253 332 394 0 0
 48 153 231 334 387 493 0
 64 116 237 292 428 438 0
 17 118 256 304 407 0 0
 52 89 249 260 429 511 0
 14 170 254 296 420 443 0
 61 113 210 328 406 500 0
 85 163 236 293 412 455 0
 80 171 189 341 391 482 0
 78 157 246 340 351 488 0
 67 93 174 304 404 450 0
 5 170 173 314 424 0 0
 3 91 241 315 370 504 0
 1 113 245 335 419 487 0
 60 107 255 289 393 498 0
 35 163 213 333 368 414 0
 46 104 253 268 372 484 0
 55 145 205 342 377 456 0

18 112 249 317 363 466 0
 20 146 187 337 413 496 0
 82 127 246 290 430 448 0
 76 150 257 320 423 475 0
 11 96 232 342 410 496 0
 75 122 210 322 415 481 0
 74 160 242 334 409 497 0
 84 172 207 311 416 478 0
 2 158 169 287 426 462 0
 28 109 258 343 401 455 0
 64 117 229 298 362 510 0
 81 129 232 273 313 502 0
 79 141 223 328 424 499 0
 37 130 258 329 422 512 0
 66 105 225 340 373 490 0
 11 144 216 288 421 452 0
 27 137 216 312 346 491 0
 86 143 162 341 386 510 0
 54 170 209 270 399 441 0
 85 139 186 344 427 467 0
 83 109 203 290 425 432 444
 6 138 239 310 312 461 0
 26 148 225 341 420 494 0
 53 112 231 308 425 506 0
 40 156 181 272 380 503 0
 81 152 214 296 411 500 0
 77 165 179 322 395 473 0
 12 153 228 266 399 507 0
 84 106 187 331 346 494 0
 31 158 250 344 402 483 0
 56 116 191 324 393 479 0
 13 88 257 327 357 441 0
 66 167 226 336 363 443 477
 85 114 198 275 417 434 0
 69 164 238 314 356 440 0
 34 160 177 338 382 416 0
 17 171 224 266 361 509 0
 70 90 199 307 394 498 0
 68 134 174 333 366 503 0
 75 144 209 307 413 439 454
 63 135 214 260 431 470 0
 51 126 178 320 406 511 0
 73 137 237 330 380 458 0
 67 167 248 321 365 501 0
 31 148 185 283 390 468 0
 7 140 239 338 404 490 0
 37 172 256 327 398 485 0
 76 110 255 267 396 456 0
 72 105 259 303 345 465 0
 24 165 236 339 426 437 0
 83 164 244 278 354 0 0

(512, 3, 2) CRT-based

1 24 47 70 93 116 139 162 185 208 231 254 277 300 323 346 369 392 415 438 461 484 507
 2 25 48 71 94 117 140 163 186 209 232 255 278 301 324 347 370 393 416 439 462 485 508
 3 26 49 72 95 118 141 164 187 210 233 256 279 302 325 348 371 394 417 440 463 486 509
 4 27 50 73 96 119 142 165 188 211 234 257 280 303 326 349 372 395 418 441 464 487 510
 5 28 51 74 97 120 143 166 189 212 235 258 281 304 327 350 373 396 419 442 465 488 511
 6 29 52 75 98 121 144 167 190 213 236 259 282 305 328 351 374 397 420 443 466 489 512
 7 30 53 76 99 122 145 168 191 214 237 260 283 306 329 352 375 398 421 444 467 490 0
 8 31 54 77 100 123 146 169 192 215 238 261 284 307 330 353 376 399 422 445 468 491 0
 9 32 55 78 101 124 147 170 193 216 239 262 285 308 331 354 377 400 423 446 469 492 0
 10 33 56 79 102 125 148 171 194 217 240 263 286 309 332 355 378 401 424 447 470 493 0
 11 34 57 80 103 126 149 172 195 218 241 264 287 310 333 356 379 402 425 448 471 494 0
 12 35 58 81 104 127 150 173 196 219 242 265 288 311 334 357 380 403 426 449 472 495 0
 13 36 59 82 105 128 151 174 197 220 243 266 289 312 335 358 381 404 427 450 473 496 0
 14 37 60 83 106 129 152 175 198 221 244 267 290 313 336 359 382 405 428 451 474 497 0
 15 38 61 84 107 130 153 176 199 222 245 268 291 314 337 360 383 406 429 452 475 498 0
 16 39 62 85 108 131 154 177 200 223 246 269 292 315 338 361 384 407 430 453 476 499 0
 17 40 63 86 109 132 155 178 201 224 247 270 293 316 339 362 385 408 431 454 477 500 0
 18 41 64 87 110 133 156 179 202 225 248 271 294 317 340 363 386 409 432 455 478 501 0

19 42 65 88 111 134 157 180 203 226 249 272 295 318 341 364 387 410 433 456 479 502 0
 20 43 66 89 112 135 158 181 204 227 250 273 296 319 342 365 388 411 434 457 480 503 0
 21 44 67 90 113 136 159 182 205 228 251 274 297 320 343 366 389 412 435 458 481 504 0
 22 45 68 91 114 137 160 183 206 229 252 275 298 321 344 367 390 413 436 459 482 505 0
 23 46 69 92 115 138 161 184 207 230 253 276 299 322 345 368 391 414 437 460 483 506 0
 1 30 59 88 117 146 175 204 233 262 291 320 349 378 407 436 465 494 0 0 0 0 0
 2 31 60 89 118 147 176 205 234 263 292 321 350 379 408 437 466 495 0 0 0 0 0
 3 32 61 90 119 148 177 206 235 264 293 322 351 380 409 438 467 496 0 0 0 0 0
 4 33 62 91 120 149 178 207 236 265 294 323 352 381 410 439 468 497 0 0 0 0 0
 5 34 63 92 121 150 179 208 237 266 295 324 353 382 411 440 469 498 0 0 0 0 0
 6 35 64 93 122 151 180 209 238 267 296 325 354 383 412 441 470 499 0 0 0 0 0
 7 36 65 94 123 152 181 210 239 268 297 326 355 384 413 442 471 500 0 0 0 0 0
 8 37 66 95 124 153 182 211 240 269 298 327 356 385 414 443 472 501 0 0 0 0 0
 9 38 67 96 125 154 183 212 241 270 299 328 357 386 415 444 473 502 0 0 0 0 0
 10 39 68 97 126 155 184 213 242 271 300 329 358 387 416 445 474 503 0 0 0 0 0
 11 40 69 98 127 156 185 214 243 272 301 330 359 388 417 446 475 504 0 0 0 0 0
 12 41 70 99 128 157 186 215 244 273 302 331 360 389 418 447 476 505 0 0 0 0 0
 13 42 71 100 129 158 187 216 245 274 303 332 361 390 419 448 477 506 0 0 0 0 0
 14 43 72 101 130 159 188 217 246 275 304 333 362 391 420 449 478 507 0 0 0 0 0
 15 44 73 102 131 160 189 218 247 276 305 334 363 392 421 450 479 508 0 0 0 0 0
 16 45 74 103 132 161 190 219 248 277 306 335 364 393 422 451 480 509 0 0 0 0 0
 17 46 75 104 133 162 191 220 249 278 307 336 365 394 423 452 481 510 0 0 0 0 0
 18 47 76 105 134 163 192 221 250 279 308 337 366 395 424 453 482 511 0 0 0 0 0
 19 48 77 106 135 164 193 222 251 280 309 338 367 396 425 454 483 512 0 0 0 0 0
 20 49 78 107 136 165 194 223 252 281 310 339 368 397 426 455 484 0 0 0 0 0
 21 50 79 108 137 166 195 224 253 282 311 340 369 398 427 456 485 0 0 0 0 0
 22 51 80 109 138 167 196 225 254 283 312 341 370 399 428 457 486 0 0 0 0 0
 23 52 81 110 139 168 197 226 255 284 313 342 371 400 429 458 487 0 0 0 0 0
 24 53 82 111 140 169 198 227 256 285 314 343 372 401 430 459 488 0 0 0 0 0
 25 54 83 112 141 170 199 228 257 286 315 344 373 402 431 460 489 0 0 0 0 0
 26 55 84 113 142 171 200 229 258 287 316 345 374 403 432 461 490 0 0 0 0 0
 27 56 85 114 143 172 201 230 259 288 317 346 375 404 433 462 491 0 0 0 0 0
 28 57 86 115 144 173 202 231 260 289 318 347 376 405 434 463 492 0 0 0 0 0
 29 58 87 116 145 174 203 232 261 290 319 348 377 406 435 464 493 0 0 0 0 0
 1 31 61 91 121 151 181 211 241 271 301 331 361 391 421 451 481 511 0 0 0 0 0
 2 32 62 92 122 152 182 212 242 272 302 332 362 392 422 452 482 512 0 0 0 0 0
 3 33 63 93 123 153 183 213 243 273 303 333 363 393 423 453 483 0 0 0 0 0
 4 34 64 94 124 154 184 214 244 274 304 334 364 394 424 454 484 0 0 0 0 0
 5 35 65 95 125 155 185 215 245 275 305 335 365 395 425 455 485 0 0 0 0 0
 6 36 66 96 126 156 186 216 246 276 306 336 366 396 426 456 486 0 0 0 0 0
 7 37 67 97 127 157 187 217 247 277 307 337 367 397 427 457 487 0 0 0 0 0
 8 38 68 98 128 158 188 218 248 278 308 338 368 398 428 458 488 0 0 0 0 0
 9 39 69 99 129 159 189 219 249 279 309 339 369 399 429 459 489 0 0 0 0 0
 10 40 70 100 130 160 190 220 250 280 310 340 370 400 430 460 490 0 0 0 0 0
 11 41 71 101 131 161 191 221 251 281 311 341 371 401 431 461 491 0 0 0 0 0
 12 42 72 102 132 162 192 222 252 282 312 342 372 402 432 462 492 0 0 0 0 0
 13 43 73 103 133 163 193 223 253 283 313 343 373 403 433 463 493 0 0 0 0 0
 14 44 74 104 134 164 194 224 254 284 314 344 374 404 434 464 494 0 0 0 0 0
 15 45 75 105 135 165 195 225 255 285 315 345 375 405 435 465 495 0 0 0 0 0
 16 46 76 106 136 166 196 226 256 286 316 346 376 406 436 466 496 0 0 0 0 0
 17 47 77 107 137 167 197 227 257 287 317 347 377 407 437 467 497 0 0 0 0 0
 18 48 78 108 138 168 198 228 258 288 318 348 378 408 438 468 498 0 0 0 0 0
 19 49 79 109 139 169 199 229 259 289 319 349 379 409 439 469 499 0 0 0 0 0
 20 50 80 110 140 170 200 230 260 290 320 350 380 410 440 470 500 0 0 0 0 0
 21 51 81 111 141 171 201 231 261 291 321 351 381 411 441 471 501 0 0 0 0 0
 22 52 82 112 142 172 202 232 262 292 322 352 382 412 442 472 502 0 0 0 0 0
 23 53 83 113 143 173 203 233 263 293 323 353 383 413 443 473 503 0 0 0 0 0
 24 54 84 114 144 174 204 234 264 294 324 354 384 414 444 474 504 0 0 0 0 0
 25 55 85 115 145 175 205 235 265 295 325 355 385 415 445 475 505 0 0 0 0 0
 26 56 86 116 146 176 206 236 266 296 326 356 386 416 446 476 506 0 0 0 0 0
 27 57 87 117 147 177 207 237 267 297 327 357 387 417 447 477 507 0 0 0 0 0
 28 58 88 118 148 178 208 238 268 298 328 358 388 418 448 478 508 0 0 0 0 0
 29 59 89 119 149 179 209 239 269 299 329 359 389 419 449 479 509 0 0 0 0 0
 30 60 90 120 150 180 210 240 270 300 330 360 390 420 450 480 510 0 0 0 0 0

